

A Thesis Submitted for the Degree of PhD at the University of Warwick

Permanent WRAP URL:

<http://wrap.warwick.ac.uk/113445/>

Copyright and reuse:

This thesis is made available online and is protected by original copyright.

Please scroll down to view the document itself.

Please refer to the repository record for this item for information to help you to cite it.

Our policy information is available from the repository home page.

For more information, please contact the WRAP Team at: wrap@warwick.ac.uk

Interactions of monoclonal antibodies with an influenza A virus

by

Matthew J. Edwards

B.Sc. (Hons) *Microbiology* (University of Wales, College of Cardiff)

M.Sc. *Virology* (London School of Hygiene and Tropical Medicine)

A thesis presented for the degree of Doctor of Philosophy,
submitted to the University of Warwick.

Department of Biological Sciences,

University of Warwick

UK.

September 1999.

Contents

1	INFLUENZA VIRUS	1
1.1	OVERVIEW :	2
1.2	INFLUENZA A VIRUS INFECTION AND DISEASE IN HUMANS.....	2
1.2.1	<i>Influenza – the disease</i> :	2
1.2.2	<i>Epidemiology</i> :	3
1.2.3	<i>Antigenic variation of influenza A virus</i>	4
1.2.3.1	Antigenic drift –.....	4
1.2.3.2	Antigenic shift :	5
2	STRUCTURE OF INFLUENZA A VIRUS	9
2.1	OVERVIEW	10
2.2	INFLUENZA GENES AND THE PROTEINS:.....	12
2.2.1	<i>RNA segments 1, 2, and 3 encode polymerase proteins PA, PB1 and PB2</i>	12
2.2.2	<i>RNA segment 4 – Haemagglutinin (HA)</i>	13
2.2.2.1	Antigenic sites on the H1 HA (influenza A/PR/8/34 H1N1 virus) –	14
2.2.2.2	Comparison of antigenic sites on the H1 and H3 HAs –.....	15
2.2.3	<i>RNA segment 5 – Nucleoprotein (NP)</i>	18
2.2.4	<i>RNA segment 6 – neuraminidase (NA)</i>	19
2.2.5	<i>RNA segment 7 : matrix proteins M1 and M2</i>	21
2.2.5.1	M1 protein.....	21
2.2.5.2	M2 protein.....	21
2.2.6	<i>RNA segment 8 : non-structural proteins NS1 and NS2</i>	22
2.2.6.1	NS1 protein	22
2.2.6.2	NS2 protein	24
3	INFECTIOUS CYCLE OF INFLUENZA A VIRUS	25
3.1	OVERVIEW	26
3.2	VIRUS ATTACHMENT TO TARGET CELL RECEPTORS.....	26
3.3	VIRUS ENTRY (INTERNALISATION).....	28
3.4	VIRUS UNCOATING	29
3.4.1	<i>Primary uncoating</i>	29
3.4.2	<i>Secondary Uncoating</i>	37
3.5	PRIMARY TRANSCRIPTION OF vRNA TO mRNA.....	37
3.6	REPLICATION OF vRNA.....	38
3.7	TRANSLATION OF VIRAL PROTEINS	40
3.8	ASSEMBLY AND RELEASE OF PROGENY VIRUS	41

4	ANTIBODIES AND THE HUMORAL RESPONSE TO INFLUENZA A VIRUS	43
4.1	ANTIBODIES : STRUCTURE AND FUNCTION	44
4.1.1	<i>Overview</i>	44
4.1.2	<i>Immunoglobulin isotypes</i>	46
4.1.2.1	IgG (murine) – subtypes IgG1, IgG2a, IgG2b and IgG3.....	46
4.1.2.2	IgA.....	46
4.1.2.3	IgM.....	48
4.1.2.4	IgD.....	48
4.1.2.5	IgE	48
4.2	HUMORAL IMMUNE RESPONSE TO INFLUENZA A	49
4.2.1	<i>Overview</i>	49
4.2.2	<i>The role of antibody in the recovery from influenza A virus infection</i>	49
4.2.3	<i>The role of antibody in the protective from re-infection by influenza virus</i>	51
4.3	MECHANISMS OF NEUTRALIZATION OF INFLUENZA A VIRUS.....	52
4.3.1	<i>Neutralization without involvement of the cell</i>	52
4.3.1.1	Aggregation of virions –.....	52
4.3.2	<i>Neutralization in the context of the cell</i>	53
4.3.2.1	Inhibition of virus-cell interactions (attachment) –	53
4.3.2.2	Neutralization of virus after it has attached to cells (post-attachment neutralization).....	55
4.3.2.3	Inhibition of virus internalisation into cells	56
4.3.2.4	Inhibition of virus –cell fusion (primary uncoating).....	56
4.3.2.5	Inhibition of events which occur after primary uncoating.....	57
5	MATERIALS AND METHODS.....	59
5.1	GENERAL METHODS.....	60
5.1.1	<i>Haemagglutination assay</i>	60
5.1.2	<i>Haemagglutination-inhibition assay</i>	60
5.1.3	<i>Total protein quantitation</i>	60
5.1.4	<i>SDS PAGE analysis of proteins</i>	61
5.2	CELL CULTURE.....	61
5.2.1	<i>Madin-Darby canine kidney (MDCK) and Baby hamster kidney (BHK) cell culture and maintenance</i>	61
5.2.2	<i>Hybridoma cell culture and maintenance (monoclonal antibody production)</i>	62
5.3	ANTIBODIES	63
5.3.1	<i>Monoclonal antibodies</i>	63
5.3.2	<i>Antibody Purification</i>	63
5.3.3	<i>Production of Fabs by proteolytic digestion of IgG</i>	64
5.3.4	<i>Production of F(ab)₂ by proteolytic digestion of IgG</i>	66
5.4	VIRUSES AND VIROLOGICAL METHODS	66
5.4.1	<i>Influenza A virus and production</i>	66

5.4.2	<i>Assessment of titre of influenza A</i>	66
5.4.3	<i>Purification of influenza A</i>	67
5.4.4	<i>Influenza A neutralization assay</i>	68
5.4.4.1	Neutralization assay by reduction of cytopathic effect	68
5.4.4.2	Neutralization Enzyme-Linked Immunosorbent assay (ELISA)	68
5.4.5	<i>Post-attachment neutralization (PAN) assay</i>	69
5.4.5.1	PAN by plaque reduction	69
5.4.5.2	Post-attachment neutralization ELISA	69
5.5	MECHANISMS OF NEUTRALIZATION ASSAYS.....	70
5.5.1	<i>Influenza attachment detection ELISA</i>	70
5.5.2	<i>Endosomal internalisation detection ELISA</i>	71
5.5.3	<i>Fusion assays</i>	72
5.5.3.1	Inhibition of hemolysis of CRBCs by influenza virus	72
5.5.3.2	Analysis of fusion inhibition by MAbs with octadecyl rhodamine-B-choride (R18) labelled virus	72
5.6	ASSAYS TO INVESTIGATE THE NATURE OF THE INHIBITION OF FUSION BY MAB AND FAB FRAGMENTS	73
5.6.1	<i>Inhibition of hemolysis of CRBCs by influenza virus at a pre-fusion intermediate stage</i>	73
5.6.2	<i>Low pH conformational change detection ELISA</i>	74
5.6.3	<i>Proteinase-K digestion resistance assay</i>	75
5.6.4	<i>Determination of acid sensitivity of MAb binding by ELISA</i>	75
5.7	KINETIC ANALYSIS OF THE MAbs AND THEIR FAB FRAGMENTS USING THE BIACORE 2000... ..	76
5.7.1	<i>Surface immobilisation</i>	76
5.7.2	<i>Virus capture</i>	77
5.7.3	<i>Measurement of kinetic binding</i>	77
5.7.4	<i>Data evaluation</i>	77
5.8	REVERSIBILITY OF NEUTRALIZATION AND HI WITH AMMONIUM HYDROXIDE (AMOH)	78
5.8.1	<i>Reversibility of neutralization and HI of virus neutralized in solution</i>	78
5.8.2	<i>Reversibility of neutralization and HI of virus attached to a cell receptor</i>	78
5.8.3	<i>Kinetics of the reversibility of HI and neutralization of virus attached to CRBCs</i>	79
5.8.4	<i>Quantitation of the removal of virus from the CRBCs by bacterial neuraminidase</i>	80
5.8.4.1	Biotinylated virus detection ELISA.....	80
5.8.5	<i>Neuraminidase assay</i>	80
5.8.6	<i>Reversibility of HI and neutralization of virus attached to CRBCs and then treated with low pH at 4°C</i>	81
5.9	LIST OF REAGENT SUPPLIERS.....	81

6 RESULTS: COMPARISON OF THE MECHANISM OF NEUTRALIZATION OF INFLUENZA A/PR/8/34 VIRUS BY MONOCLONAL IGGs AND THEIR FRAGMENTS. ... 83

6.1	INTRODUCTION.....	84
6.2	MAB H36-4.5-2.....	86
6.2.1	<i>Comparison of the neutralization by plaque reduction by H36 IgG, F(ab)₂ and Fab fragments.</i>	86
6.2.2	<i>Analysis of the inhibition of attachment of A/PR8 to both MDCK and BHK cells by MAb H36.</i>	88
6.2.3	<i>Analysis of the relationship between A/PR8 infectivity and internalisation in MDCK cells as a function of H36 IgG concentration.</i>	90
6.2.4	<i>Analysis of the relationship between A/PR8 infectivity and endosomal fusion of virus to MDCK and BHK cells as a function of H36 concentration.</i>	92
6.3	FAB H36.....	95
6.3.1	<i>Analysis of the inhibition of attachment of influenza A to MDCK and BHK cells by Fab H36.</i>	95
6.4	REAL-TIME KINETIC BINDING ANALYSIS OF H36 IgG AND ITS FAB FRAGMENT TO VIRUS PARTICLES USING SURFACE PLASMON RESONANCE.	97
6.4.1	<i>Comparison of the kinetics of binding of H36 IgG and its Fab fragment to whole virus particles.</i>	97
6.5	H36 F(AB) ₂	101
6.5.1	<i>Analysis of the relationship between attachment and infectivity of A/PR/8 to MDCK cells as a function of H36 F(ab)₂ concentration.</i>	101
6.6	SUMMARY : COMPARISON OF THE CHARACTERISTICS OF NEUTRALIZATION OF H36 IgG AND ITS ANTIBODY FRAGMENTS.	101
6.7	MAB H37-45-5R3.....	103
6.7.1	<i>Comparison of the neutralization of A/PR/8 by H37 IgG and its Fab fragment by plaque reduction.</i>	103
6.7.2	<i>Analysis of the relationship between A/PR/8 virus infectivity and attachment to both MDCK and BHK cells as a function of H37 IgG concentration.</i>	103
6.7.3	<i>Analysis of the relationship between A/PR/8 virus infectivity and the internalisation in MDCK cells as a function of H37 IgG concentration.</i>	106
6.7.4	<i>Analysis of the relationship between A/PR/8 virus infectivity and endosomal fusion in both MDCK and BHK cells as a function of H37 IgG concentration.</i>	106
6.8	FAB H37.....	110
6.8.1	<i>Analysis of the relationship between attachment and infectivity of A/PR/8 virus to both MDCK and BHK cells as a function Fab H37</i>	110
6.9	REAL-TIME KINETIC ANALYSIS OF H37 IgG AND ITS FAB TO VIRUS PARTICLES USING SURFACE PLASMON RESONANCE.	110
6.9.1	<i>Comparison of the kinetics of binding of H37 IgG and its Fab fragment to whole virus particles.</i>	110
6.10	SUMMARY: COMPARISON OF THE MECHANISM OF NEUTRALIZATION OF INFLUENZA BY H37 IgG AND FAB H37.	115
6.11	MAB H9-D3-4R2.....	115

6.11.1	<i>Comparison of the neutralization by plaque reduction by H9 IgG and Fab.</i>	115
6.11.2	<i>Analysis of the relationship between A/PR8 virus infectivity and attachment to both MDCK and BHK cells as a function of H9 IgG concentration.</i>	117
6.11.3	<i>Analysis of the relationship between A/PR/8 virus infectivity and internalisation as a function of H9 IgG concentration.</i>	117
6.11.4	<i>Analysis of the effect of H37 IgG on endosomal fusion of A/PR/8 virus in cells</i>	120
6.12	FAB H9-D3-4R2	120
6.12.1	<i>Analysis of the relationship between A/PR/8 virus infectivity and attachment to both MDCK and BHK cells as a function of Fab H9 concentration.</i>	120
6.12.2	<i>Analysis of the relationship between A/PR/8 virus infectivity and internalisation as a function of H9 Fab concentration.</i>	124
6.12.3	<i>Analysis of the relationship between A/PR/8 virus infectivity and endosomal fusion in both MDCK and BHK cells as a function of H9 Fab concentration.</i>	126
6.13	REAL-TIME KINETIC ANALYSIS OF H9 IgG AND ITS FAB TO VIRUS PARTICLES USING SURFACE PLASMON RESONANCE.	126
6.13.1	<i>Comparison of the kinetics of binding of H9 IgG and its Fab fragment to whole virus particles.</i>	126
6.14	SUMMARY: COMPARISON OF THE MECHANISM OF NEUTRALIZATION OF INFLUENZA A VIRUS BY H9 IgG AND FAB.	129
6.15	DISCUSSION :	133
6.15.1	<i>Comparison of the characteristics of neutralization of A/PR/8 virus by the IgGs and their Fabs.</i>	133
6.15.2	<i>Comparison of the neutralization activity of H36, H37 and H9 IgGs and Fabs.</i>	135
6.15.3	<i>Comparison of the mechanism of neutralization of A/PR/8 virus by the IgGs and their antibody fragments.</i>	137
6.15.4	<i>Neutralization of influenza and other animal viruses by Fab fragments.</i>	142
6.15.5	<i>Critique of the techniques used in this chapter</i>	146
6.15.5.1	Preparation of Fabs -	146
6.15.5.2	Attachment and infectivity ELISA assays -	146
6.15.5.3	Virus internalisation ELISA -	147
6.15.5.4	Virus-cell fusion assay -	147
7	RESULTS : INVESTIGATION OF THE POST-ATTACHMENT NEUTRALIZATION (PAN) OF INFLUENZA A/PR/8/34 VIRUS BY MONOCLONAL IGGs AND THEIR FABS.	149
7.1	INTRODUCTION.	150
7.2	COMPARISON OF THE STANDARD NEUTRALIZATION (STAN) AND PAN AT 4°C AND 37°C OF THE IGGs AND THEIR FABS.	151
7.2.1	<i>STAN and PAN at 4 °C and 37 °C by H36 IgG.</i>	151
7.2.2	<i>STAN and PAN at 4 °C and 37 °C of A/PR/8 by H36 Fab.</i>	152
7.2.3	<i>STAN and PAN at 4 °C and 37 °C of A/PR/8 virus by H37 IgG.</i>	153

7.2.4	<i>STAN and PAN at 4 °C and 37 °C of A/PR/8 virus by H37 Fab.</i>	154
7.2.5	<i>STAN and PAN at 4 °C and 37 °C of A/PR/8 virus by H9 IgG.</i>	155
7.2.6	<i>STAN and PAN at 4 °C and 37 °C of A/PR/8 virus by H9 Fab.</i>	156
7.3	KINETICS OF PAN OF A/PR/8 VIRUS BY H36 IgG AND FAB.	157
7.3.1	<i>Comparison of the kinetics of PAN of A/PR/8 virus by H36 IgG and Fab at 4 °C and 37 °C in MDCK cells.</i>	157
7.4	MECHANISM OF PAN BY IGGs AND THEIR FABs	158
7.4.1	<i>Analysis of the relationship between A/PR/8 virus internalisation in MDCK cells and PAN as a function of H36 IgG concentration.</i>	158
7.4.2	<i>Analysis of the relationship between A/PR/8 virus internalisation in MDCK cells and PAN as a function of H36 Fab.</i>	160
7.4.3	<i>Analysis of the relationship between A/PR/8 virus PAN and the virus-cell fusion in MDCK cells as a function of H36 IgG concentration.</i>	162
7.4.4	<i>Analysis of the relationship between A/PR/8 virus PAN and the virus-cell fusion in MDCK cells as a function of H36 Fab concentration.</i>	162
7.4.5	<i>Analysis of the relationship between A/PR/8 virus PAN and virus-cell fusion as a function of H9 Fab concentration.</i>	165
7.4.6	<i>Analysis of the effect of H36 IgG on haemolysis of chick red blood cells (CRBCs) by attached A/PR/8 virus.</i>	165
7.4.7	<i>Analysis of the effect of H36 Fab on haemolysis of CRBCs by pre-attached A/PR/8 virus.</i>	167
7.4.8	<i>Analysis of the effect of H9 Fab on haemolysis of CRBCs by pre-attached A/PR/8 virus.</i>	168
7.4.9	<i>Summary of the mechanism of PAN by the antibodies and their Fabs.</i>	169
7.5	INVESTIGATION OF INHIBITION OF FUSION DURING PAN BY THE ANTIBODIES.	171
7.5.1	<i>Analysis of the sensitivity of MAbs binding to conformational changes of the HA induced by low pH.</i>	171
7.5.2	<i>Analysis of the effect of H36 IgG and Fab on haemolysis of CRBCs by the pre-fusion intermediate of A/PR/8 virus.</i>	172
7.5.3	<i>Analysis of the effect of the Fabs on the low pH induced conformational change of the HA of pre-attached virus (in PAN-like format).</i>	173
7.6	DISCUSSION :	178
7.6.1	<i>Comparison of the STAN and PAN of A/PR/8 virus by the antibodies.</i>	178
7.6.2	<i>Mechanism of PAN by the IgGs and their Fabs.</i>	180
7.6.3	<i>Investigation of inhibition of fusion during PAN.</i>	181
7.6.3.1	<i>Characteristics of the pre-fusion intermediate of A/PR/8 virus.</i>	181
7.6.3.2	<i>Analysis of the process of fusion-inhibition during PAN.</i>	184
7.6.4	<i>PAN of other animal viruses.</i>	186

8 ANALYSIS OF THE REVERSIBILITY OF THE HAEMAGGLUTINATION-INHIBITION AND NEUTRALIZATION OF INFLUENZA A/PR/8 VIRUS BY MABS.....	189
8.1 INTRODUCTION.....	190
8.2 ANALYSIS OF THE REVERSIBILITY OF HAEMAGGLUTINATION-INHIBITION (HI) AND NEUTRALIZATION OF VIRUS IN SOLUTION BY MABS.	191
8.2.1 <i>Investigation of the reversibility of HI and neutralization of virus in solution by the monoclonal IgA (H37-66) at 4 °C and 37 °C.</i>	<i>191</i>
8.2.2 <i>Investigation of the reversibility of HI and neutralization of virus in solution by the monoclonal H36 IgG at 4 °C and 37 °C.</i>	<i>193</i>
8.2.3 <i>Investigation of the reversibility of HI and neutralization of virus in solution by the monoclonal H37 IgG at 4 °C and 37 °C.</i>	<i>195</i>
8.2.4 <i>Investigation of the reversibility of HI and neutralization of virus in solution by the monoclonal H9 IgG at 4 °C and 37 °C.</i>	<i>197</i>
8.3 DETERMINATION OF WHETHER ANTIBODY BOUND TO VIRUS IS COMPLETELY REMOVED BY TREATMENT WITH AMOH.	197
8.3.1 <i>Investigation of whether some antibody remains bound to virus after AmOH treatment by reactivity with anti-Fab antiserum.</i>	<i>197</i>
8.4 ANALYSIS OF THE REVERSIBILITY OF HI AND NEUTRALIZATION OF VIRUS ATTACHED TO CHICKEN RED BLOOD CELLS (CRBCs).	199
8.4.1 <i>Investigation of the reversibility at 4 °C and 37 °C of HI and neutralization of virus pre-attached to CRBCs: IgA (H37-66).</i>	<i>199</i>
8.4.2 <i>Investigation of the reversibility at 4 °C and 37 °C of HI and neutralization of virus pre-attached to CRBCs: IgGs.</i>	<i>200</i>
8.5 ANALYSIS OF THE POOR REVERSIBILITY AT 37°C OF HI AND NEUTRALIZATION OF VIRUS ATTACHED TO CELLS: IGA MAB.	203
8.5.1 <i>Investigation of the effect of temperature on the reversibility of HI and neutralization of virus attached to CRBCs: IgA MAb.</i>	<i>203</i>
8.5.2 <i>Analysis of the kinetics of the recovery of HA and infectivity of virus that was attached to CRBCs and then neutralized by 10 µg/ml IgA MAb.....</i>	<i>203</i>
8.5.3 <i>Analysis of the reversibility of HI and neutralization of virus attached to cells, other than CRBCs: IgA MAb.....</i>	<i>206</i>
8.5.3.1 <i>Investigation of the reversibility of HI and neutralization of virus attached to fixed MDCK cell: 10µg/ml of IgA MAb.....</i>	<i>206</i>
8.5.3.2 <i>Investigation of the reversibility of HI and neutralization of virus attached to fixed H9 T-cells 10 µg/ml of IgA MAb.</i>	<i>206</i>
8.5.3.3 <i>Investigation of the reversibility of HI and neutralization of virus bound to a soluble receptor, fetuin: 10 µg/ml of IgA MAb.....</i>	<i>209</i>
8.5.4 <i>Quantitation of the removal of virus from the CRBC by bacterial neuraminidase after neutralization by MAbs.</i>	<i>209</i>

8.5.4.1	Analysis of the effect of temperature on the recovery of virus from the CRBC after neutralization by MAbs.	209
8.5.4.2	Analysis of the effect of MAb concentration on the recovery of neutralized virus from the CRBC.....	211
8.5.5	<i>Investigation of whether IgA MAb could sterically inhibit the viral neuraminidase activity.</i>	213
8.6	ANALYSIS OF THE REVERSIBILITY OF HI AND NEUTRALIZATION OF VIRUS ATTACHED TO THE CRBC TREATED AT PH 5, 4°C: IGA MAB.	215
8.7	DISCUSSION :	217
8.7.1	<i>Reversibility of HI and neutralization of virus in solution by MAbs.</i>	217
8.7.2	<i>Reversibility of HI and neutralization of virus attached to CRBCs by MAbs</i>	218
8.7.2.1	Analysis of the low reversibility of HI and neutralization of attached virus: at 37°C	218
8.7.3	<i>Reversibility of HI and neutralization of virus attached to CRBCs after incubation at low pH and 4 °C: IgA MAb</i>	222
9	SUMMARY OF RESULTS / DISCUSSION	224
9.1	OVERVIEW	225
9.2	THE EFFICIENCY OF NEUTRALIZATION	225
9.3	THE MECHANISM OF NEUTRALIZATION OF INFLUENZA A VIRUS	227
9.4	PAN OF INFLUENZA A VIRUS	228
9.5	REVERSIBILITY OF HI AND NEUTRALIZATION OF INFLUENZA A VIRUS	228
9.6	DOES THE INFLUENZA VIRUS HA UNDERGO CONFORMATIONAL OR ORIENTATIONAL CHANGES AFTER BINDING TO THE CELL RECEPTOR?.....	230

List of Figures

Figure 2.1 A schematic diagram of the structure of the type A influenza.....	11
Figure 2.2 Schematic representation of the H3 HA crystal structure. Shaded areas show the H1 HA antigenic sites superimposed onto the H3 structure	16
Figure 2.3 A comparison of the antigenic sites on the H1 HA (A/PR/8/34) and the H3 HA (A/Hong Kong/1/68).....	17
Figure 3.1 The influenza A virus infectious cycle. Steps 1 to 3.....	27
Figure 3.2 The low pH-induced conformational change in HA. (A) The structure of the TBHA ₂ monomer in schematic form at neutral pH, and (B) the corresponding region of the TBHA ₂ monomer following the low pH conformational rearrangements.....	31
Figure 3.3 Schematic model for the conformational changes and rearrangements of the HAs involved in the fusion process.....	34
Figure 3.4 Mechanism for priming of influenza viral RNA transcription by capped cellular RNAs..	39
Figure 3.5 The post-translational processing of the HA	41
Figure 4.1 Schematic diagram of an IgG molecule, including its modes of flexibility.....	45
Figure 4.2 Schematic representation of the structure of the four murine IgG subclasses.....	47
Figure 5.1 PAGE gel analysis to show level of contaminating IgG in (A) a H36 Fab preparation and (B) a H36 F(ab) ₂ preparation.	65
Figure 6.1 Neutralization of A/PR8 by H36 IgG, F(ab) ₂ and Fab in MDCK cells.	87
Figure 6.2 Analysis of the relationship between A/PR8 infectivity and attachment as a function of H36 concentration.....	89
Figure 6.3 Analysis of the relationship between A/PR8 infectivity and the internalisation in MDCK cells as a function of H36 IgG concentration.....	91
Figure 6.4 Analysis of the relationship between A/PR8 infectivity and fusion of virus to MDCK cells as a function of H36 concentration.	93
Figure 6.5 Analysis of the relationship between A/PR8 infectivity and fusion of virus to BHK cells as a function of H36 concentration.....	94
Figure 6.6 Analysis of the relationship between A/PR8 infectivity and attachment as a function of Fab H36 concentration.....	96
Figure 6.7 The binding of H36 IgG at five concentrations to captured whole influenza virus particles.....	98
Figure 6.8 The binding of H36 Fab at four concentrations to captured whole influenza virus particles.	99

Figure 6.9 Analysis of the relationship between A/PR8 infectivity and attachment to MDCK cells as a function of H36 F(ab) ₂ concentration.....	102
Figure 6.10 Neutralization of A/PR8 by H37 IgG and Fab in MDCK cells.	104
Figure 6.11 Analysis of the relationship between A/PR8 infectivity and attachment as a function of H37 concentration.....	105
Figure 6.12 Analysis of the relationship between A/PR8 infectivity and the internalisation in MDCK cells as a function of H37 IgG concentration.....	107
Figure 6.13 Analysis of the relationship between A/PR8 infectivity and fusion of virus to MDCK cells as a function of H37 concentration.	108
Figure 6.14 Analysis of the relationship between A/PR8 infectivity and fusion of virus to BHK cells as a function of H37 concentration.	109
Figure 6.15 Analysis of the relationship between A/PR8 infectivity and attachment as a function of Fab H37 concentration.....	111
Figure 6.16 The binding of H37 IgG at five concentrations to captured whole influenza virus particles.	112
Figure 6.17 The binding of H37 Fab at four concentrations to captured whole influenza virus particles.	113
Figure 6.18 Neutralization of A/PR8 by H9 IgG and Fab.....	116
Figure 6.19 Analysis of the relationship between A/PR8 infectivity and attachment as a function of H9 IgG concentration.....	118
Figure 6.20 Analysis of the relationship between A/PR8 infectivity and the internalisation in MDCK cells as a function of H9 IgG concentration.	119
Figure 6.21 Analysis of the relationship between A/PR8 infectivity and fusion of virus to MDCK cells as a function of H9 concentration.	121
Figure 6.22 Analysis of the relationship between A/PR8 infectivity and fusion of virus to MDCK cells as a function of H9 concentration.	122
Figure 6.23 Analysis of the relationship between A/PR8 infectivity and attachment as a function of Fab H37 concentration.....	123
Figure 6.24 Analysis of the relationship between A/PR8 infectivity and the internalisation in MDCK cells as a function of H9 Fab concentration.	125
Figure 6.25 Analysis of the relationship between A/PR8 infectivity and fusion of virus to MDCK cells as a function of H9 Fab concentration.....	127
Figure 6.26 Analysis of the relationship between A/PR8 infectivity and fusion of virus to BHK cells as a function of H9 Fab concentration.....	128
Figure 6.27 The binding of H9 IgG at five concentrations to captured whole influenza virus particles.	130
Figure 6.28 The binding of H9 Fab at four concentrations to captured whole influenza virus particles.	131
Figure 6.29 Diagrammatic representation of a monomer of the H1 haemagglutinin, based on the H3 crystal structure.....	136

Figure 7.1 Comparison of the standard neutralization (STAN) and post-attachment neutralization (PAN) of A/PR/8 virus by H36 IgG in MDCK cells.....	152
Figure 7.2 Comparison of the STAN and PAN of A/PR/8 virus by H36 Fab in MDCK cells.....	153
Figure 7.3 Comparison of the STAN and PAN of A/PR/8 virus by H37 IgG in MDCK cells.	154
Figure 7.4 Comparison of the STAN and PAN of A/PR/8 virus by H37 Fab in MDCK cells.	155
Figure 7.5 Comparison of the STAN and PAN of A/PR/8 virus by H9 IgG in MDCK cells.....	156
Figure 7.6 Comparison of the STAN and PAN of A/PR/8 virus by H9 Fab in MDCK cells.	157
Figure 7.7 Analysis of the kinetics of PAN by H36 IgG and Fab at 4 °C and 37 °C in MDCK cells. (A) PAN with H36 IgG at 55nM and (B) PAN with H36 Fab at 100nM.....	158
Figure 7.8 Analysis of the relationship between A/PR/8 virus internalisation in MDCK cells and PAN as a function of H36 IgG.	159
Figure 7.9 Analysis of the relationship between A/PR/8 virus internalisation in MDCK cells and PAN as a function of H36 Fab.	161
Figure 7.10 Analysis of the relationship between A/PR/8 virus PAN and virus-cell-fusion as a function of H36 IgG concentration.....	163
Figure 7.11 Analysis of the relationship between A/PR/8 virus PAN and virus-cell-fusion as a function of H36 Fab concentration.	164
Figure 7.12 Analysis of the relationship between A/PR/8 virus PAN and virus-cell-fusion as a function of H9 Fab concentration.	166
Figure 7.13 Analysis of the effect of H36 IgG concentration on the haemolysis of CRBCs by pre-attached A/PR/8 virus.....	167
Figure 7.14 Analysis of the effect of H36 Fab concentration on the haemolysis of CRBCs by pre-attached A/PR/8 virus.....	168
Figure 7.15 Analysis of the effect of H9 Fab concentration on the haemolysis of CRBCs by pre-attached A/PR/8 virus.....	169
Figure 7.16 Analysis of the effect of low pH on MAbs binding to captured virus.	172
Figure 7.17 Analysis of the effect of H36 IgG and Fab on haemolysis by the cold-fusion intermediate of A/PR/8 virus.....	174
Figure 7.18 Analysis of the affect of H36 Fab on the low pH-induced conformational change of the HA of A/PR/8 virus (in PAN-like format).....	176
Figure 8.1 Analysis of the reversibility of HI and neutralization of virus free in solution: IgA MAbs (H37-66).	192
Figure 8.2 Analysis of the reversibility of HI and neutralization of virus free in solution: H36 IgG.	194
Figure 8.3 Analysis of the reversibility of HI and neutralization of virus free in solution: H37 IgG.	196
Figure 8.4 Analysis of the reversibility of HI and neutralization of virus free in solution: H9 IgG.....	198

Figure 8.5 Analysis of the reversibility of HI and neutralization of virus pre-attached to CRBCs: IgA MAb (H37-66).....	201
Figure 8.6 Analysis of the reversibility of HI and neutralization of virus pre-attached to CRBCs: H36 IgG.....	202
Figure 8.7 Investigation of the effect of temperature on the reversibility of HI and neutralization of virus attached to CRBCs: 10 µg/ml of IgA MAb.....	204
Figure 8.8 Kinetics of the reversibility of HI and neutralization of virus attached to CRBCs: 10 µg/ml IgA.....	205
Figure 8.9 The reversibility of HI and neutralization of virus attached to fixed MDCK cells: 10 µg/ml of IgA.....	207
Figure 8.10 The reversibility of HI and neutralization of virus attached to fixed H9 T-cells: 10 µg/ml of IgA.....	208
Figure 8.11 Reversibility of HI and neutralization of virus bound to a soluble receptor, fetuin: the IgA MAb.....	210
Figure 8.12 Standard curve of the optical density (OD) at 405nm against HAU of biotinylated virus.....	212
Figure 8.13 The effect of temperature on the recovery of neutralized virus bound to CRBCs.....	212
Figure 8.14 The effect of concentration of neutralizing MAb on the recovery of virus from the surface of CRBCs.....	213
Figure 8.15 The reversibility of HI of virus attached to CRBCs treated at pH 5, 4 °C: IgA MAb.....	216
Figure I.1 Analysis of the relationship between A/PR/8 virus internalisation in MDCK cells and PAN as a function of H37 IgG.....	236
Figure I.2 Analysis of the relationship between A/PR/8 virus internalisation in MDCK cells and PAN as a function of H37 Fab.....	237
Figure I.3 Analysis of the relationship between A/PR/8 virus internalisation in MDCK cells and PAN as a function of H9 IgG.....	238
Figure I.4 Analysis of the relationship between A/PR/8 virus internalisation in MDCK cells and PAN as a function of H9 Fab.....	239
Figure I.5 Analysis of the relationship between A/PR/8 virus PAN and virus-cell-fusion as a function of H37 IgG concentration.....	240
Figure I.6 Analysis of the relationship between A/PR/8 virus PAN and virus-cell-fusion as a function of H37 Fab concentration.....	241
Figure I.7 Analysis of the relationship between A/PR/8 virus PAN and virus-cell-fusion as a function of H9 IgG concentration.....	242
Figure I.8 Analysis of the effect of H37 IgG concentration on the haemolysis of CRBCs by pre-attached A/PR/8 virus.....	243
Figure I.9 Analysis of the effect of H37 Fab concentration on the haemolysis of CRBCs by pre-attached A/PR/8 virus.....	244

Figure I.10 Analysis of the effect of H9 IgG concentration on the haemolysis of CRBCs by pre-attached A/PR/8 virus.....	245
Figure I.11 Analysis of the effect of H37 IgG and Fab on haemolysis of CRBCs by the cold-fusion intermediate of A/PR/8 virus.....	246
Figure I.12 Analysis of the effect of H9 IgG and Fab on haemolysis of CRBCs by the cold-fusion intermediate of A/PR/8 virus.....	247
Figure I.13 Analysis of the affect of H37 Fab on the low pH-induced conformational change of the HA of A/PR/8 virus (in PAN-like format).....	248
Figure I.14 Analysis of the affect of H37 Fab on the low pH-induced conformational change of the HA of A/PR/8 virus (in PAN-like format).....	249
Figure I.15 Susceptibility to proteinase-K digestion following low pH treatment of neutralized or non-neutralized virus.....	250
Figure I.16 Reversibility of HI by ammonium hydroxide: IgA.....	251
Figure I.17 Analysis of the reversibility of HI and neutralization of virus pre-attached to CRBCs: H37 IgG.....	252
Figure I.18 Analysis of the reversibility of HI and neutralization of virus pre-attached to CRBCs: H9 IgG.....	253

List of Tables

Table 2.1 Influenza A RNA coding assignments for A/PR/8/34 strain.....	11
Table 2.2 A comparison of antigenic sites on H1 and H3.....	17
Table 6.1 Comparison of the neutralizing activities of H36 IgG and its Fab fragments	87
Table 6.2 Analysis of the internalisation of non-neutralized (N_0) and 50% neutralized (N_{50}) virus under the negative control conditions.	91
Table 6.3 Analysis of the fusion of non-neutralized (N_0) virus under the negative control conditions.	93
Table 6.4 Analysis of the fusion of non-neutralized (N_0) virus under the negative control conditions.	94
Table 6.5 Local fits of association and dissociation curves for H36 IgG and H36 Fab.	100
Table 6.6 Comparison of the neutralizing activities of H37 IgG and its Fab fragments	104
Table 6.7 Analysis of the internalisation of non-neutralized (N_0) and N_{50} virus under the negative control conditions.....	107
Table 6.8 Analysis of the fusion of non-neutralized virus under the negative control conditions.....	108
Table 6.9 Analysis of the fusion of non-neutralized virus under the negative control conditions	109
Table 6.10 Local fits of association and dissociation curves for H37 IgG and Fab.....	114
Table 6.11 Comparison of the neutralizing activities of H9 IgG and its Fab fragments.	116
Table 6.12 Analysis of the internalisation of non-neutralized (N_0) and N_{50} virus under the negative control conditions.....	119
Table 6.13 Analysis of the fusion of non-neutralized virus under the negative control conditions	121
Table 6.14 Analysis of the fusion of non-neutralized virus under the negative control conditions.	122
Table 6.15 Analysis of the internalisation of non-neutralized (N_0) and N_{50} virus under the negative control conditions.....	125
Table 6.16 Analysis of the fusion of non-neutralized virus under the negative control conditions	127
Table 6.17 Analysis of the fusion of non-neutralized virus under the negative control conditions	128
Table 6.18 Local fits of association and dissociation curves for H9 IgG and Fab.	132
Table 6.19 Summary of the mechanism of neutralization by H36, H37 and H9 IgGs and their antibody fragments in MDCK cells.	134
Table 7.1 Analysis of the internalisation of non-neutralized (N_0) virus under the negative control conditions.	159

Table 7.2 Analysis of the internalisation of non-neutralized (N_0) virus under the negative control conditions.....	161
Table 7.3 Analysis of the fusion of non-neutralized virus under the negative control conditions.....	163
Table 7.4 Analysis of the fusion of non-neutralized virus under the negative control conditions.....	164
Table 7.5 Analysis of the fusion of non-neutralized virus under the negative control conditions.....	166
Table 7.6 Summary of the mechanism of PAN by the antibodies and their Fabs.....	170
Table 7.7 Characteristics of the conformation-specific MAbs.....	175
Table 7.8 Comparison of the binding of the low pH conformation specific MAbs to A/PR/8 virus in different stages of fusion.....	177
Table 7.9 The relative difference between PAN and STAN by the IgGs at 50% PAN (PAN_{50}) and 90% PAN (PAN_{90}).....	178
Table 8.1 The affect of the addition of anti-Fab antiserum to virus neutralized by the MAbs at 37 °C following treatment by AmOH.....	199
Table 8.2 Inhibition of viral neuraminidase activity by IgA MAb.....	214
Table I.1 Analysis of the internalisation of non-neutralized (N_0) virus under the negative control conditions.....	236
Table I.2 Analysis of the internalisation of non-neutralized (N_0) virus under the negative control conditions.....	237
Table I.3 Analysis of the internalisation of non-neutralized (N_0) virus under the negative control conditions.....	238
Table I.4 Analysis of the internalisation of non-neutralized (N_0) virus under the negative control conditions.....	239
Table I.5 Analysis of the fusion of non-neutralized virus under the negative control conditions.....	240
Table I.6 Analysis of the fusion of non-neutralized virus under the negative control conditions.....	241
Table I.7 Analysis of the fusion of non-neutralized virus under the negative control conditions.....	242

Acknowledgements

I am very grateful to my supervisor Prof. Nigel Dimmock for his support throughout this project. I am also indebted to other members of the influenza and HIV groups for their advice and support, especially Stuart Dimes and Lesley McLain. I would also like to thank Dheeraj Khiytani for the use of his laptop through times of need and help with scanning.

I am extremely grateful to Dr Ian Campbell, (Biacore AB) for his support and advice in the experiments using the Biacore 2000 instrument and analysis of the kinetics data.

I also wish to thank Leonie Clemo, who put up with a lot while I wrote this, for all her love and support.

Finally, I wish to thank my parents and grandparents for their invaluable encouragement and financial assistance, without which none of this would have been possible.

Work in this thesis was supported by the B.B.S.R.C.

Declaration

I hereby declare that this thesis has been composed by myself and has not been accepted in any previous application for a degree. The work presented was carried out by myself, with the exception of those instances where the collaboration of others has been acknowledged. All sources of information have been specifically acknowledged by reference.

Matthew J. Edwards.

Abbreviations

Abbreviations are defined at the first moment in the text. The following list defines key abbreviations used in this thesis:

AmOH	Ammonium hydroxide
BHK	Baby hamster kidney
cDNA	Complementary deoxyribonucleic acid
CDR	Complementarity determining region
CRBC	Chick red blood cells
ELISA	Enzyme-linked immunosorbant assay
F(ab) ₂	Bivalent antigen binding fragment
Fab	Monovalent antigen binding fragment
Fc	Crystallisable fragment
FcR	Fc Receptor
FCS	Foetal calf serum
FPV/R	Influenza A/fowl plague/Rostock/34 (H7N1)
HA	Haemagglutinin
HAU	Haemagglutination units
HBS	HEPES-buffered saline
HI	Haemagglutination inhibition
HIU	Haemagglutination inhibition units
HIV-1	Human immunodeficiency virus type 1
Ig	Immunoglobulin
IgA	Immunoglobulin A
IgG	Immunoglobulin G
IgM	Immunoglobulin M
k_a	Association rate constant
KA	Equilibrium association constant
k_d	Dissociation rate constant
KD	Equilibrium dissociation constant
MAb	Monoclonal antibody
MDCK	Madin-Darby canine kidney cells
Mr	Relative molecular weight

N ₅₀	50% neutralization
N ₉₀	90% neutralization
NA	Neuraminidase
NP	Nucleoprotein
p.f.u.	Plaque forming unit
PAGE	Polyacrylamide gel electrophoresis
PAN	Post-attachment neutralization
PBS	Phosphate-buffered saline
PCR	Polymerase chain reaction
PEG	Polyethylene glycol
A/PR/8	Influenza A/Puerto Rico/8/34 (H1N1) virus
RNA	Ribonucleic acid
SDS	Sodium dodecyl sulphate
SEM	Standard error of the mean
sIgA	Secretory IgA
SPR	Surface plasmon resonance
STAN	Standard neutralization of free (unattached) virus
TBS	Tris-buffered saline
v/v	volume:volume
w/v	weight:volume
X:31	Reassortant influenza A virus (H3N2)

Amino Acids:

A	Ala	Alanine
C	Cys	Cysteine
D	Asp	Asparatic acid
E	Glu	Glutamic acid
F	Phe	Phenylalanine
G	Gly	Glycine
H	His	Histidine
I	Ile	Isoleucine
K	Lys	Lysine
L	Leu	Leucine
M	Met	Methionine

N	Asn	Asparagine
P	Pro	Proline
Q	Gln	Glutamine
R	Arg	Arginine
S	Ser	Serine
T	Thr	Threonine
V	Val	Valine
W	Trp	Tryptophan
Y	Tyr	Tyrosine

Summary

This investigation examines the efficiency and mechanism of neutralization of influenza A/PR/8/34 virus by three haemagglutinin (HA)-specific monoclonal IgGs (H36, H37 and H9) and their Fabs. The efficiency of neutralization by the Fabs was lower than that of their IgGs. This was concentration-dependent: 50% neutralization (N_{50}) required 104- to 375-fold more Fab than IgG, and at N_{90} required 15- to 208-fold more Fab than IgG. Affinities of the IgGs and Fabs were very similar and thus did not contribute to the difference in their neutralization efficiencies. The mechanism of neutralization of influenza virus by the IgGs was complex. At N_{90} , the majority of the loss of infectivity was attributable to inhibition of virus attachment to cells, whilst at N_{50} inhibition of attachment accounted for only a minority of the infectivity loss, with the majority attributed to inhibition of fusion. In between N_{50} and N_{90} both mechanisms operate simultaneously. In contrast, inhibition of attachment by the H36 and H37 Fabs was the dominant mechanism of neutralization throughout the range of concentrations studied. The H9 Fab did not inhibit virus-attachment, but inhibited virus-cell fusion. Therefore, it was concluded that the difference between the IgGs and their Fabs was the ability of the IgGs to display simultaneous neutralization mechanisms.

Post-attachment neutralization (PAN) provides compelling evidence of the ability of antibodies to neutralize by mechanisms other than inhibition of attachment. H36, H37 and H9 IgGs and their Fabs gave PAN at 4°C and 37°C. Efficiency of PAN by the IgGs was lower than the standard neutralization of free virus (STAN). The efficiency of PAN and STAN by the Fabs was similar, except for H9 Fab whose PAN activity was significantly greater than its STAN activity. The mechanism of PAN by both IgGs and their Fabs was inhibition of fusion.

The HA of influenza A/PR/8/34 virus goes through a series of conformational intermediates in the fusion process. Examination of the pre-fusion intermediate (created by treating at pH 5 and 4°C) using conformation-specific MAbs detected changes in the viral HA, but these were less extensive than in virus treated at pH 5 and 37°C (post-fusion conformation). The pre-fusion intermediate does not cause fusion, but is a fusion-committed state, as it can subsequently undergo fusion at high efficiency at pH 7.5 when the temperature is raised to 37°C. IgGs and Fabs did not inhibit the haemolysis of CRBCs by the pre-fusion intermediate, nor did they inhibit the conformational changes of the HA that trigger the fusion process. It was concluded that these antibodies interfere sterically with events that occur prior to the formation of the pre-fusion intermediate.

The point at which neutralization becomes irreversible was investigated using the three IgGs and a monoclonal IgA. Neutralization of virus in solution was shown to be reversible by removing antibody from the virus with ammonium hydroxide (pH 11.5) (AmOH). The reversibility of neutralization was also examined under conditions designed to mimic the early steps in the virus infectious cycle, (1) virus attachment to cells and (2) low pH-induced virus-cell fusion. Neutralization could be reversed by removal of antibody with AmOH, after neutralization of (1) virus attached to cells and (2) after low pH treatment of virus attached to cells. This suggested that these MAbs do not trigger a permanent loss of virus infectivity, but are required to be bound to the virus for the duration of the neutralization process.

1 Influenza virus

1.1 Overview :

Influenza viruses belong to the family Orthomyxoviridae, which are enveloped viruses with a segmented negative sense, single stranded RNA genome (Lamb and Krug, 1996). The three types of influenza viruses A, B and C can be distinguished on the basis of the antigenicity of their nucleocapsid (NP) and matrix (M1) proteins. The influenza A viruses are also assigned to specific subtypes based on the antigenicity of their major surface glycoproteins, haemagglutinin (HA) and neuraminidase (NA). Currently there are 15 known HA subtypes (H1 to H15) and 9 NA subtypes (N1 to N9) (WHO Memorandum, 1980; Rohm *et al.*, 1996). The entire spectrum of subtypes are found in aquatic birds, considered to be the natural reservoir of influenza A. However, a restricted number are capable of infecting mammals, including humans, swine, horses and marine mammals (Webster *et al.*, 1992).

The current nomenclature system of influenza A viruses includes the type of virus, the animal from which it was isolated if not human, the place of isolation, the strain number, the year and the subtype of HA and NA (WHO Memorandum, 1980). For example, A/Puerto Rico/8/34 (H1N1) is a human influenza A virus, isolated in Puerto Rico in 1934, is strain number 8, and has H1 subtype HA and N1 subtype NA.

1.2 Influenza A virus infection and disease in humans.

1.2.1 Influenza – the disease :

Influenza viruses are primarily respiratory pathogens, and are transmitted primarily via the aerosol route (Moser *et al.*, 1979). The clinical outcome of the infection is dependent both on the virus strain and a number of host factors, such as age, physiological state and previous immunological exposure (reviewed in Kilbourne, 1987). As a result of these factors the disease can have a spectrum of clinical outcomes ranging from asymptomatic to lethal due to viral pneumonia, but more frequently infection causes an acute debilitating febrile illness (Murphy and Webster,

1996). The incubation period is variable, ranging from 24 hours to 5 days and ends with an abrupt onset of illness that may include cough, myalgia, malaise, headache, high fever and nasal and conjunctival discharge (Kilbourne, 1987). In individuals with uncomplicated influenza disease symptoms normally resolve after 1 to 2 weeks. Influenza is mainly associated with the upper respiratory tract, but there can be involvement of the lung, or blood and can occasionally be associated with gastrointestinal and neurological symptoms (reviewed in Sweet and Smith, 1980). Secondary bacterial infections are common and in the pre-antibiotic era was a major contributor to mortality (Bisno *et al.*, 1971). The risk of mortality is increased in the elderly (>65 years) and those with chronic diseases, such as diabetes, asthma, and diseases of the kidneys and heart (Kilbourne, 1987).

1.2.2 Epidemiology :

Influenza epidemics occur almost yearly during the winter months. Epidemics occur simultaneously along the same lines of latitude, for example, October to March north of the equator and from April to September south of the equator (Hope-Simpson, 1981). Influenza disease is perpetuated by two types of antigenic variations, (1) antigenic drift and (2) antigenic shift. Both allow escape from the protective immunity in the population generated by infection by previous strains. Antigenic drift involves minor antigenic changes in the HA and NA and variants cause epidemics of disease, whereas world wide pandemics are caused by antigenic shifts, involving major antigenic changes of the HA and sometimes NA resulting from replacement of gene segments (Murphy and Webster, 1996).

It is generally accepted that influenza disease spreads via direct contact between infected individuals and non-immune individuals (Webster, 1998). However, this mode of transmission does not explain how an antigenic drift variant can cause simultaneous disease outbreaks in two geographically separate locations without a discernible connection. A controversial hypothesis to explain this phenomenon proposed that acute infection with influenza virus forms a persistent non-infectious state in the host. The host is then an asymptomatic carrier for 1 to 2 years until seasonal changes, such as solar irradiation reactivate the infectious state and infect non-immune individuals (Hope-Simpson and Golubev, 1987; Hope-

Simpson, 1992). At present no direct evidence exists that latent influenza infections can occur in humans or other animals, although a number of studies have demonstrated persistent infections in cell culture (Robinson *et al.*, 1979; De and Nayak, 1980; Frielle *et al.*, 1984). Alternatively, it has recently been appreciated that influenza circulates during inter-epidemic periods at a much reduced incidence. Therefore, this could also account for separate geographically distinct outbreaks during the winter months (Webster *et al.*, 1992).

1.2.3 Antigenic variation of influenza A virus.

1.2.3.1 Antigenic drift –

Antigenic drift in the HA occurs by the accumulation of point mutations leading to amino acid changes which alter the antigenic sites such that they escape immune surveillance (Webster *et al.*, 1982). Antigenic variation in the HA occurs rapidly with new epidemiologically important drift variants possessing four or more antigenic substitutions in two or more antigenic sites. For example, six amino acid changes located in sites B, D, and E were found in the H1 epidemic strain of influenza A/Chile/83 compared to the previous circulating H1 strain (Wilson and Cox, 1990). In fact amino acid substitutions occur throughout the HA sequence with only a few stretches of conserved residues, indicating the plasticity and evolutionary potential of the HA (Both *et al.*, 1983). Two hypotheses have been proposed to explain the high rate of variation in the HA:

- (1) the mutation rate of the HA gene is higher than the other segments. Hence, the rate of neutral changes (silent mutations) is higher and results in a higher frequency of incorporation of these changes in the virus strain (Gojobori *et al.*, 1990; Sugita *et al.*, 1991; Cox and Bender, 1995).
- (2) the high mutation rate of the HA is driven by the selective pressure of the host immune response (Palese and Young, 1982).

The structure of the influenza A evolutionary tree has been determined as cactus-like, with only one lineage (trunk) extending to the top, whilst all other lineages (branches) are short representing lineages that died out. The viruses that constitute the trunk of the evolutionary tree contain a higher frequency of amino acid

substitutions in its HA than the viruses on the side branches. This supports the second hypothesis that the influenza A virus is undergoing positive Darwinian evolution due to the strong selective pressure of the immune response and that its primary immune evasion strategy is to “outrun” its immune system “pursuers” through new mutations (Fitch *et al.*, 1991). Further strong support comes from studies of viral isolates from severely immunocompromised patients showing that the HA or NP of the viruses had not undergone any changes (Rocha *et al.*, 1991; Klimov *et al.*, 1995).

Antigenic drift can be reproduced in the laboratory by growth of influenza A with monoclonal antibodies (MAbs) to a single antigenic site. The escape mutants usually possess one amino acid change that prevents binding of the selecting MAb. These mutants occur at a frequency of approximately 10^{-5} (Yewdell *et al.*, 1979; Webster and Laver, 1980). However, escape mutations do not arise when virus is grown in the presence of MAbs to two antigenic sites as the frequency of producing double escape mutants is 10^{-10} . Infection with influenza produces a polyclonal antibody response with mixtures of antibodies to each antigenic site; hence it is difficult to envisage how antigenic drift mutants arise under these selection pressures (Wang *et al.*, 1986). Studies of mouse and rabbit antisera to whole inactivated influenza have shown that some were able to select escape mutants, indicating that the polyclonal response was biased to a single antigenic site (Lambkin and Dimmock, 1995; Cleveland *et al.*, 1997). This suggested that infection of previously immunologically naïve individuals with influenza virus, such as young children, may produce a biased antibody response and drive antigenic drift. However, as changes in two antigenic sites are required to generate an epidemiologically important virus, then selection of variants may be sequential involving different hosts.

1.2.3.2 Antigenic shift :

Since the first human influenza A virus (H1N1) was isolated in 1933, antigenic shifts have occurred in 1957 with the emergence of the H2N2 (Asian influenza) virus, in 1968 when the H3N2 (Hong Kong influenza) appeared and then in 1977 when the H1N1 virus re-emerged. However, the 1977 virus was not strictly speaking an antigenic shift as the virus had re-emerged, but it will be grouped as an antigenic shift, as it caused a pandemic in the younger members of the population that had

been born since the initial outbreak. Seroarcheological evidence has suggested that influenza viruses of the H1, H2 and H3 subtypes have infected humans since the mid-nineteenth century and there has been a cyclical alternation in their appearance (Masurel and Marine, 1973; Webster *et al.*, 1992).

One of the questions central to influenza research to date is where the novel strains that cause pandemics come from? Phylogenetic evidence has suggested that pandemic strains were derived from avian influenza viruses (Fang *et al.*, 1981; Kida *et al.*, 1987). As a result three mechanisms for the introduction of new human pandemic strains have been proposed:

- (1) Pandemic strains are derived from the reassortment of an avian strain with a circulating human strain. Molecular studies have provided convincing genetic evidence that the 1957 and 1968 strains arose by genetic reassortment. The 1957 H2N2 virus HA, NA and PB1 genes were derived from an avian origin, whilst the remaining five internal genes were conserved from the circulating H1N1 strain at that time. Also the 1968 H3N2 virus contained an avian virus-like H3 HA and PB1 genes, whilst all other genes were retained from the circulating H2N2 strain (Scholtissek *et al.*, 1978b; Gething *et al.*, 1980; Fang *et al.*, 1981; Kawaoka *et al.*, 1989; Bean *et al.*, 1992). Other studies have provided strong evidence for genetic reassortment *in vivo*, both between human and animal strains and in humans (Webster *et al.*, 1971; Nishikawa and Sugiyama, 1983).
- (2) Pandemic strains emerge by direct transmission to the human population of an avian strain or strain from another mammal that has become infectious for humans. Phylogenetic evidence has indicated that this mechanism may explain the appearance of the H1N1 1918 "Spanish influenza" (Gorman *et al.*, 1991). Until recently it was considered that this mechanism would probably work by an avian to swine, swine to human transmission route as even though in volunteer experiments limited infection of humans with large doses of avian influenza had been achieved, there had been no report of natural infection of humans with avian strains (Beare and Webster, 1991). In contrast, swine to human transmission had been described in Fort Dix in America (Rota *et al.*, 1989). However, recently numerous reports have demonstrated direct transmission of avian influenza strains to humans. For example, influenza genes obtained from a woman with conjunctivitis

was found to have an extremely high homology (98.2%) with a H7N7 virus isolated from turkeys (Banks *et al.*, 1998). Also most strikingly 18 cases of human influenza from multiple transmissions of H5N1 viruses from infected chickens were reported from Hong Kong (Claas *et al.*, 1998; Subbarao *et al.*, 1998). The human H5N1 virus was extremely similar to an avian H5N1 virus that had caused an outbreak in chickens in Hong Kong in March / May in 1997. Distinguishing features of the human and avian H5N1 strains included (a) a multiple polybasic amino acid cleavage site, a motif associated with high pathogenicity in avian viruses, (b) binding to NeuAc α 2,3-Gal containing receptors, not NeuAc α 2,6-Gal containing receptors, (c) a carbohydrate at position 158 on the HA which decreased affinity for cell receptors and (d) a 19 amino acid deletion in the stalk of the NA which resulted in a decreased ability to release virus from cells (Shortridge *et al.*, 1998; Subbarao *et al.*, 1998; Bender *et al.*, 1999; Matrosovich *et al.*, 1999). However, as with other direct transmissions of avian-like influenza virus, the human H5N1 virus showed no capacity for secondary transmissions to humans. Therefore, if the 1918 pandemic virus was a direct transmission of an avian-like virus then the feature it possessed to allow human to human transmission remains a mystery. A possible explanation is that the H1 strain spread from avian to human some years prior to 1918, and adapted to its new mammal host before causing widespread disease (Reid *et al.*, 1999).

- (3) Pandemic strains which have caused epidemics previously may hide in an unchanged form before re-establishing infection. Evidence for this comes from the reappearance in 1977 of a H1N1 virus that was genetically identical to a virus that caused a human epidemic in 1950 (Nakajima *et al.*, 1978; Scholtissek *et al.*, 1978a). Possible hiding places for this virus included preservation in frozen storage, preservation in an animal reservoir or integration into a host. As integration into a host has not been detected and virus from an animal reservoir would contain some changes, it is generally thought that the 1977 virus escaped from frozen storage, possibly from a laboratory (Webster *et al.*, 1992).

As the most recent pandemic influenza strains of 1957 and 1968 have been shown to be reassortants between human influenza and non-human influenza

viruses, the question arises as to where this reassortment takes place? The pig has been the prime candidate for this role as it can be host for both avian and human influenza strains (Scholtissek *et al.*, 1983). Serological and genetic studies of influenza virus (H3N2) isolated from children in the Netherlands indicated that they were human-avian reassortants and that they were generated and still circulating in European swine (Claas *et al.*, 1994). Also recent molecular characterisation of host cell receptor specificity has shown that receptors for both human and avian influenza strains were present in the pig tracheas and that avian-like swine viruses acquired the ability to recognise the human virus receptors after continued replication (Ito *et al.*, 1998). However, the recent outbreak of H5N1 virus in humans implicates man as a possible “intermediate”, as the avian-like virus could mix with a currently circulating human influenza virus to form a new pandemic strain (Claas and Osterhaus, 1998). However, conclusive evidence must await the arrival of the next pandemic influenza virus.

2 Structure of influenza A virus

2.1 Overview

Electron microscopy of influenza A viruses grown in eggs or tissue culture cells (laboratory-adapted) showed that they are mainly spherical particles of between 80-120nm in diameter (Figure 2.1) (Nermut and Frank, 1971). In contrast, influenza viruses isolated from clinical samples are pleomorphic and may be spherical, elongated or filamentous (Horne *et al.*, 1960).

The lipid envelope of the virus is derived from the host cell plasma membrane (Kates *et al.*, 1961) and contains 3 types of viral transmembrane proteins, the HA, NA and M2. The HA and NA glycoproteins project radially outward to approximately 14 nm from the surface of the virus and there are estimated to be between 400 and 1200 spikes on influenza viruses (Tiffany and Blough, 1970; Wrigley, 1979; Taylor *et al.*, 1987). The M2 protein is an ion channel protein and is present on the virion surface in only a few copies (Zebedee and Lamb, 1988; Jackson *et al.*, 1991; Hughey *et al.*, 1992). Internal to the lipid bilayer is the viral matrix protein (M1), which is 3 to 4nm thick and encloses the ribonucleoprotein (RNP) complexes (Reginster and Nermut, 1976; Ruigrok *et al.*, 1989). The RNP complexes can be separated into different size classes and contain 4 types of proteins with 8 different segments of ssRNA (Pons, 1971; Rees and Dimmock, 1981). The proteins include the nucleoprotein (NP) and three polymerase (P) proteins (PB1, PB2 and PA). Electron microscopic examination has shown that the RNPs are flexible rods with terminal loops and helical mid-section (Pons *et al.*, 1969). The RNP comprises the RNA-dependent transcriptase complex, and purified cores carry out cap binding, endonuclease, RNA synthesis and polyadenylation reactions (Bishop *et al.*, 1971a; Bishop *et al.*, 1971b; Bishop *et al.*, 1972; Compans and Caligiuri, 1973; Plotch *et al.*, 1979; Plotch *et al.*, 1981; Pritlove *et al.*, 1998). The NS2 protein is an integral component of the virion associating with the M1 protein and present in approximately 130-200 copies (Richardson and Akkina, 1991; Yasuda *et al.*, 1993). The genome is composed as 8 negative sense RNA segments, which encode 10 gene products (Table 2.1) (Lamb and Choppin, 1983).

Figure 2.1 A schematic diagram of the structure of the type A influenza virion (adapted from Lambkin, 1994).

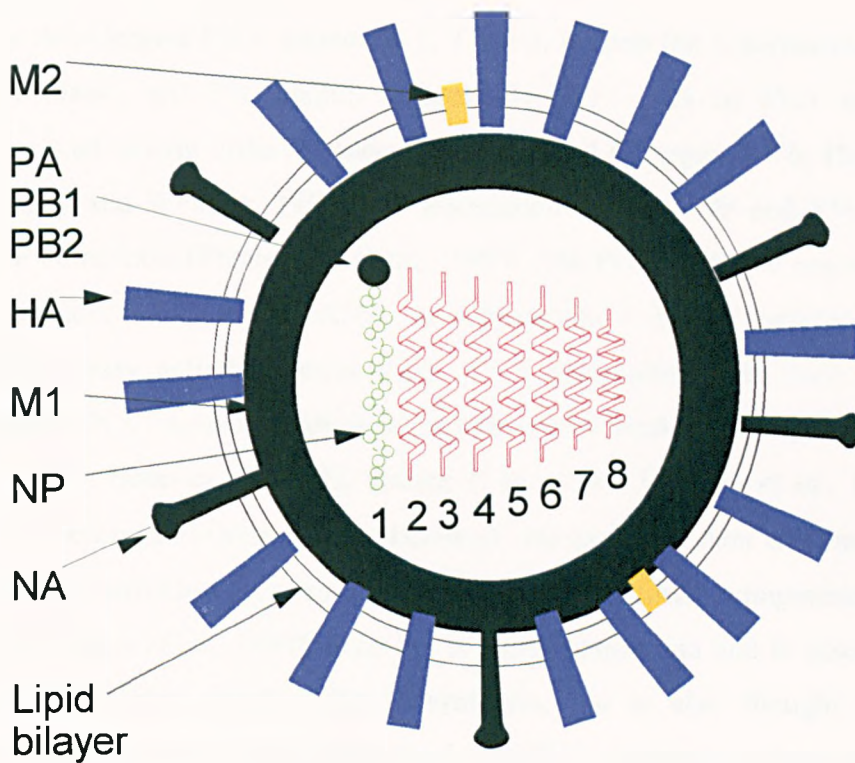


Table 2.1 Influenza A RNA coding assignments for A/PR/8/34 strain (from Lamb and Choppin, 1983)

<i>RNA segment</i>	<i>Length (nucleotides)</i>	<i>Predicted Polypeptide length (amino acids)</i>	<i>Encoded polypeptide</i>
1	2341	759	PB2
2	2341	757	PB1
3	2233	716	PA
4	1778	566	HA
5	1565	498	NP
6	1413	454	NA
7	1027	252	M1
8	890	97	M2
		230	NS1
		121	NS2

2.2 Influenza genes and the proteins:

2.2.1 RNA segments 1, 2, and 3 encode polymerase proteins PA, PB1 and PB2

The three largest RNA segments, 1, 2 and 3, encode the 3 polymerase proteins PB2, PB1 (basic) and PA (acidic) respectively (Mr – 82k to 95k), which are highly conserved among different subtypes (Lamb and Choppin, 1976; Horisberger, 1980; Murphy and Webster, 1996). In association with the NP and RNA they form the RNP complexes (Perales and Ortín, 1997). The PB2 subunit is required for initiation of transcription of viral mRNA, as it binds the 5' cap of cellular mRNAs and its endonuclease activity cleaves them 10-13 nucleotides from their 5' ends. These capped RNA fragments then serve as primers for viral mRNA synthesis (Ulmanen *et al.*, 1981; Blaas *et al.*, 1982; Braam *et al.*, 1983; Licheng *et al.*, 1995; Shi *et al.*, 1996; Perales and Ortín, 1997). However, the cap-dependent endonuclease and RNA synthesis activities does require all 3 polymerase protein components (Hagen *et al.*, 1994; Cianci *et al.*, 1995). The PA is a phosphoprotein and is essential for cRNA-dependent virion RNA (vRNA) synthesis, but is also thought to regulate the synthesis of viral proteins at the level of mRNA expression (Herget and Scholtissek, 1993; Nakagawa *et al.*, 1996; Perales and Ortín, 1997; Sanz-Ezquerro *et al.*, 1998). Expression of PA by transfection induces degradation of co-expressed proteins and this function has been mapped to the amino terminal region of the protein. However, the biological significance of this activity is not understood (Sanz-Ezquerro *et al.*, 1995; Sanz-Ezquerro *et al.*, 1996). The PB1 proteins harbours the polymerase activity and is involved in elongation of viral mRNA synthesis, template RNA and vRNA synthesis (Braam *et al.*, 1983; Ulmanen *et al.*, 1983; Nakagawa *et al.*, 1995; Kobayashi *et al.*, 1996; Toyoda *et al.*, 1996). Recently the RNA binding domain has been mapped to two sites on PB1 (Li *et al.*, 1998). Characterisation of the RNA binding has found that the N-terminus and C-terminus appear to be involved in binding to the 5' and 3' arm of the panhandle (González and Ortín, 1999). Nuclear localisation signals (NLS) have been found in both the PB1 and PA proteins (Nath and Nayak, 1990; Nieto *et al.*, 1994). The functional polymerase complexes PB1, PB2 and PA are localised to the nucleus of the cell, where all virus RNA synthesis occurs (Jones *et al.*, 1986; Shapiro *et al.*, 1987; Mukaigawa and Nayak, 1991).

2.2.2 RNA segment 4 – Haemagglutinin (HA)

The HA is synthesised as a single polypeptide HA0 (Mr ~ 76k). The HA spike glycoprotein is a homotrimer of non-covalently linked monomers (Wiley *et al.*, 1977; Wilson *et al.*, 1981) and is evenly distributed over the virus surface (Murthi and Webster, 1986). An important determinant of infectivity is the cleavage of the HA0 into two disulphide-linked chains HA1 (Mr ~47kD) and HA2 (Mr ~29kD) (Lazarowitz and Choppin, 1975; Tashiro and Rott, 1996). The HA has four major roles–

- (1) responsible for virus attachment to target cells via interaction with sialic acid bearing host cell receptors (Lazarowitz and Choppin, 1975)
- (2) is responsible for virus-cell fusion virus, which causes release of the core of the virus into the cytoplasm (White *et al.*, 1982; Wharton *et al.*, 1986)
- (3) is a major determinant of virulence (reviewed by Webster and Rott, 1987)
- (4) is the major viral antigen to which neutralizing antibodies are directed (Wilson and Cox, 1990).

Cleavage of the HA liberates the hydrophobic N-terminus end of HA2 (fusion peptide) which is vital for the virus fusion activity. Increased pathogenicity has been associated with the structure of the cleavage site as virulent avian H5 and H7 subtypes possess a multi-basic residue cleavage site, whereas avirulent strains only possess a single arginine residue (Kawaoka and Webster, 1987; Vey *et al.*, 1992).

The cleavage of avirulent strains is restricted to a limited number of proteases such as trypsin (Kido *et al.*, 1992), but the polybasic cleavage site of the virulent strains allows cleavage by proteases ubiquitously distributed among many cell types. This allows replication in many different organs, resulting in increased pathogenicity (Kawaoka and Webster, 1988; Steineke-Gröber *et al.*, 1992; Vey *et al.*, 1992; Horimoto and Kawaoka, 1994; Steinhauer, 1999). It is interesting that the H5N1 virus that recently infected humans in Hong Kong possessed the multi-basic cleavage site, but its infection was confined to the respiratory tract (Subbarao *et al.*, 1998).

The X-ray crystallographic structure of bromelain-released HA from a H3 subtype has been determined (Wilson *et al.*, 1981). The trimer protein extends 135Å from the viral envelope and has two distinct domains. A 76Å fibrous stem formed from triple-stranded coiled-coil of α -helices derived from HA1 and HA2 residues extends from the envelope to a globular head domain, which consists mainly of anti-parallel β -sheets. The hydrophobic fusion peptides released by proteolytic cleavage of the HA0 are buried between the subunit interfaces approximately 100Å from the top of the globular head. Recent determination of the X-ray crystallographic structure of recombinant vaccinia-expressed mutant HA0 (H3N2) indicated that most of the structure is superimposable on that of the cleaved HA (Chen *et al.*, 1998). However, the cleavage site forms a prominent loop that protrudes away from the surface of the trimer allowing accessibility to proteases. The trimer is stabilised by the fibrous stem region, with the globular heads forming a loose association. The globular head domain contains the HA receptor-binding site surrounded by the five major highly variable antigenic sites. The receptor-binding site consists of a pocket inaccessible to antibody, formed by residues of tyr98, trp153, his183, glu190 and leu194 in most subtypes (Wilson *et al.*, 1981; Wilson and Cox, 1990). Also the type of amino acid at residue 226 has been shown to alter receptor specificity for sialic acid linked to galactose by either NeuAca-2,6- or NeuAca-2,3- linkages (Rogers *et al.*, 1983; Weis *et al.*, 1988). The HA trimer is glycosylated during maturation and transportation to plasma membrane of host cell. The function of the carbohydrate chains are currently unknown, but it has been suggested that they could have an influence on tropism (Shortridge *et al.*, 1998; Bender *et al.*, 1999) and immune evasion by masking antigenic sites (Caton *et al.*, 1982; Skehel *et al.*, 1984; Wiley and Skehel, 1987).

2.2.2.1 Antigenic sites on the H1 HA (influenza A/PR/8/34 H1N1 virus) –

There are four major antigenic sites on the H1 HA; Sa, Sb, Ca and Cb (Figure 2.2) (Caton *et al.*, 1982). Sites Sa and Sb lie at the top of the globular head near the receptor-binding pocket (Figure 2.3). They are in close proximity, separated by a polypeptide loop consisting of residues 156-160. The Sa site includes residues 128, 129, 158, 160, 162 and 167. The Sb site lies to the rear of the Sa site on the globular

head and includes residues 156, 159, 192, 193, 196, and 198. The Sa site incorporates the “front-facing” residues of the separating polypeptide chain, 158 and 160, whilst the Sb site utilises the “rear-facing” residues 156 and 159.

The antigenic site, Ca, can be differentiated into two sub-sites, Ca1 and Ca2. These two sub-sites are in close proximity in the trimer, as they span the monomer-monomer interface; hence in the trimer they are opposite each other. Site Ca1 contains residues 169, 173, 207 and 240. Site Ca2 consists of two loops containing residues 140, 143, 145, 224 and 225.

The fourth antigenic site, Cb, includes residues 78 to 83 (excluding residue 80) and 122, at the bottom of the globular head of the HA.

2.2.2.2 *Comparison of antigenic sites on the H1 and H3 HAs –*

It is possible to compare the antigenic sites of the H1 and H3 HAs as structurally important amino acids are conserved between both subtypes, indicating a similar overall 3-dimensional structure (Caton *et al.*, 1982). However, the HA1 units of the H1 and H3 HAs show a low overall homology of only 35% (Winter *et al.*, 1981).

A comparison of the H1 and H3 antigenic sites are shown diagrammatically in Figure 2.3 and in Table 2.1 (reviewed by Lambkin, 1994).

Figure 2.2 Schematic representation of the H3 HA crystal structure. Shaded areas show the H1 HA antigenic sites superimposed onto the H3 structure (adapted from Dimmock, 1993).

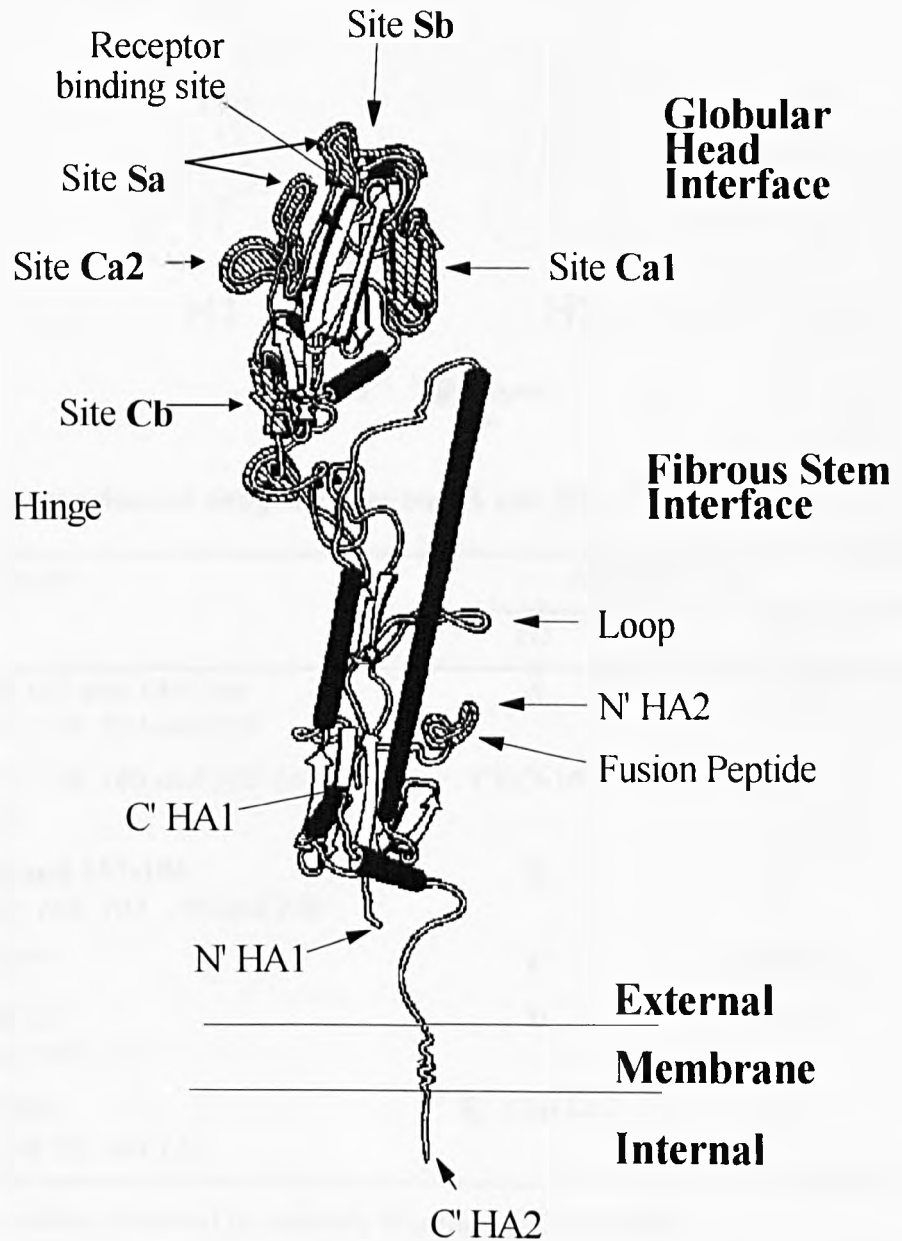


Figure 2.3 A comparison of the antigenic sites on the H1 HA (A/PR/8/34) and the H3 HA (A/Hong Kong/1/68) (Caton *et al.*, 1982; taken from Schofield, 1996).

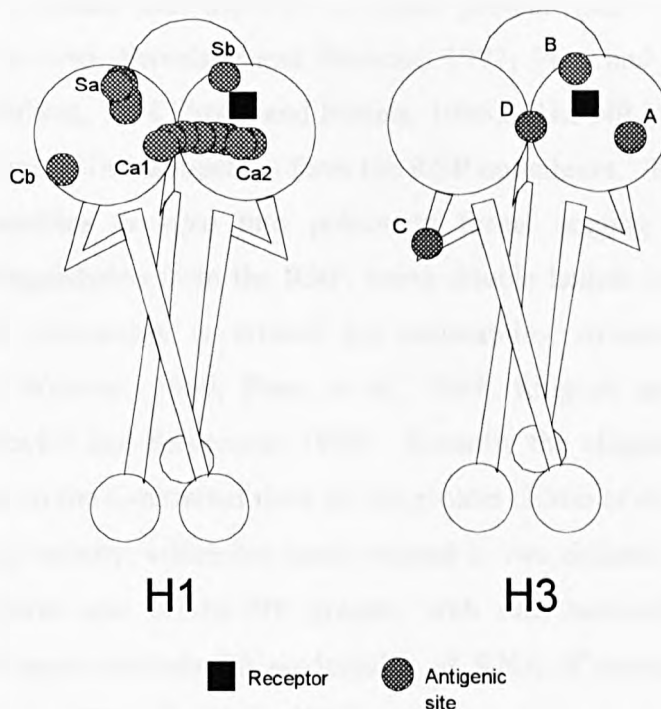


Table 2.2 A comparison of antigenic sites on H1 and H3.

Amino Acids	Antigenic Site	
	H3	H1
133 and 137 and 140-148 <i>140, 143, 145, 224 and 225</i>	A	<i>Ca2</i>
<i>128, 129, 158, 160 and 162-167</i> <i>(not 164)</i>	CHO-165	<i>Sa</i>
155-160 and 187-196 <i>156, 159, 192, 193, 196 and 198</i>	B	<i>Sb</i>
52 and 277	C	CHO-271
201 and 217 <i>169, 173, 207, 240</i>	D	<i>Ca1</i>
(63, 78, 83) <i>78-83 (not 80) and 122</i>	E / CHO-81	<i>Cb</i>

Bold type - residues involved in antibody binding in H3 structure.

Italic type - residues involved in antibody binding in H1 structure (these are given as their relative H3 position for ease of comparison)

CHO - glycosylated

2.2.3 RNA segment 5 – Nucleoprotein (NP)

RNA segment 5 codes for the NP, a basic protein ($M_r \sim 56k$) which is phosphorylated *in vivo* (Privalsky and Penhoet, 1977; Petri and Dimmock, 1981; Privalsky and Penhoet, 1981; Arese and Portela, 1996). The NP interacts with itself and with the 8 viral RNA segments to form the RNP complexes. The purified virion NP protein assembles *in vitro* into polymeric forms ranging from trimers to structures indistinguishable from the RNP, being double helical hairpins indicating that the NP-NP interaction is critical for maintaining structure of the RNPs (Kingsbury and Webster, 1969; Pons *et al.*, 1969; Ruigrok and Baudin, 1995; Prokudinakantorovich and Semenova, 1996). Recently the oligomerization domain has been mapped to the C-terminal third of the protein (Elton *et al.*, 1999). The NP has RNA-binding activity, which has been mapped to two distinct regions of the N-terminal 180 amino acid of the NP protein, with one molecule of NP protein interacting with approximately 20 nucleotides of RNA (Compans and Chopin, 1975; Baudin *et al.*, 1994; Albo *et al.*, 1995).

The NP protein accumulates in the nucleus due to the action of two independent nuclear localisation signals (NLS) at the C-terminal and N-terminal and their ability to interact with importin- α in the nuclear pore (Davey *et al.*, 1985; O'Neill *et al.*, 1995; Wang *et al.*, 1997; Weber *et al.*, 1998). It has also been suggested that phosphorylation plays a role in nucleocytoplasmic transport of NP (Neumann *et al.*, 1997). Also recently an interaction between NP and actin filaments has been shown to cause cytoplasmic accumulation of the NP protein (Digard *et al.*, 1999).

The RNP complexes are the functional templates for the replication and transcription of the genome and it has been found that NP in the complexes also interacts with the PB1 and PB2 proteins (Biswas *et al.*, 1998). Recently, it has been suggested that this NP-polymerase interaction is responsible for making vRNPs switch from mRNA to cRNA synthesis (Mena *et al.*, 1999). It is evident that the NP is a multifunctional protein of pivotal importance to influenza replication.

2.2.4 RNA segment 6 – neuraminidase (NA)

The neuraminidase (NA) is a type II membrane glycoprotein with an uncleaved hydrophobic amino-terminal signal/membrane anchor domain and a 6 amino acid tail (Air and Laver, 1989). The NA represents approximately 20% of the spikes on the virus and has been described as mushroom-like in appearance, with a large oblong head domain supported by a thin stalk region (Laver and Valentine, 1969; Taylor *et al.*, 1987). Analysis of the distribution of spikes on the virus surface by immunoelectron microscopy revealed a uniform distribution of the HA, whilst the NA occur in discrete patches (Murthi and Webster, 1986).

The NA has a number of functions:

- (1) It prevents self-aggregation of the virions by removing sialic acids residues from infected cells during both entry and release (Palese *et al.*, 1974; Basak *et al.*, 1985). The neuraminidase enzyme (acylneuraminyl hydrolase) catalyses the cleavage of the α -ketosidic linkage between terminal sialic acid and an adjacent D-galactose (Gottschalk, 1957; Lamb and Krug, 1996).
- (2) It facilitates passage of virus through the protective mucin-covered target cells in the respiratory tract, by desialylation of the sialomucoproteins (Colman and Ward, 1985; Klenk and Rott, 1988).
- (3) It removes sialic acid from newly synthesised HA0 polypeptide which allows proteolytic cleavage to occur (Schulman and Palese, 1977).
- (4) It facilitates virus envelope-cell membrane fusion (Huang *et al.*, 1980; Huang *et al.*, 1985). However, the exact role, if any, the NA plays during fusion has not been elucidated and it has been shown the HA alone can mediate fusion (White *et al.*, 1982).

It has also been suggested that the length of the NA stalk can confer host range specificity (Castrucci and Kawaoka, 1993; Luo *et al.*, 1993). It is interesting that the avian H5N1 virus that infected humans in Hong-Kong possessed a 19 amino acid deletion in its NA stalk (Subbarao *et al.*, 1998).

There are 9 known NA subtypes of influenza viruses and X-ray crystallographic structure of pronase released N2 neuraminidase has been determined (Assad *et al.*, 1980; Varghese *et al.*, 1983). The NA exists as a tetrameric spike. Each of the monomers are held together in the tetramer by disulphide linkages and consist of six topologically identical, four stranded, anti-parallel β -sheets, arranged in

a propeller-like formation. The box-shaped head domain contains four enzyme active (catalytic) sites and has a circular 4-fold symmetry stabilised in part by calcium ions. The substrate binding site has been located to a large pocket on the surface of each subunit ringed by highly conserved charged residues which are important in enzymatic activity (Varghese *et al.*, 1983; Lentz *et al.*, 1987; Varghese *et al.*, 1995). Specificity for either NeuAc α 2-3Gal or NeuAc α 2-6Gal sialic acid substrates is determined by the residues 275 and 431 which are located in the framework region of the enzymatic site, but not in the site itself (Kobasa *et al.*, 1999). The authors suggested that amino acid substitutions in these residues altered the conformation of the enzymatic site facilitating binding of different species of sialic acid. A mutant resistant to the new anti-neuraminidase drug zanamivir (4,guanidino-Neu5Ac2en) also had a mutation in framework residue, 119, again indicating the importance of the framework residues in the enzymatic activity (von Itzstein *et al.*, 1993; Blick *et al.*, 1995; McKimm-Breschkin *et al.*, 1996; Sahasrabudhe *et al.*, 1998). Studies with zanamivir-resistant mutants with changes only in their HA and with reassortant viruses, have indicated the critical importance of a balance between the affinity of the HA for sialic acid receptors and the extent of the removal of the sialic acid residues by NA, in the infectivity of influenza viruses (Gubareva *et al.*, 1996; Kaverin *et al.*, 1998).

Neuraminidase activity can be blocked by anti-NA antibody (Jackson and Webster, 1982). This inhibition is substrate size-dependent indicating that the antibodies act by steric hindrance. Four antigenic sites on the neuraminidase have been mapped. They form a continuous circle around the catalytic site of a monomer and can inhibit binding of substrates (Colman *et al.*, 1983; Webster *et al.*, 1984). The antibodies to NA are not neutralizing, but can decrease plaque size when added to the overlay (Kilbourne *et al.*, 1968).

The 6 amino acid cytoplasmic tail is highly conserved in all 9 subtypes of NA, suggesting that it has an important function. Using reverse genetics techniques, it has been suggested that the cytoplasmic tail affects the NA incorporation into virions, virion morphology, and virulence in mice (Bilsel *et al.*, 1993; Mitnaul *et al.*, 1996). However, this has been contradicted by other studies suggesting that NA mutants lacking the cytoplasmic tail can be incorporated in virions and are infectious (Liu *et al.*, 1995).

2.2.5 RNA segment 7 : matrix proteins M1 and M2

RNA segment 7 of influenza encodes two proteins, M1 and M2. A co-linear transcript yields the mRNA for M1 protein and splicing of the co-linear mRNA gives rise to M2 protein (Lamb and Lai, 1982).

2.2.5.1 M1 protein

M1 (Mr ~ 28k) is the most abundant protein in the virion (Skehel and Schild, 1971). The M1 is type-specific although some antigenic differences have been demonstrated between subtypes with MAbs (Schild, 1972; Le Comte and Oxford, 1981).

The M1 forms a shell beneath the lipid envelope and numerous studies have found an interaction between M1 and the membranes (Bucher *et al.*, 1980; Gregoriades and Frangione, 1981; Ruigrok *et al.*, 1989; Fujiyoshi *et al.*, 1994). Investigation using membrane fractionation has also shown that a proportion of M1 associates with the plasma membrane in infected cells, and it has been suggested that it also interacts with the cytoskeleton (Kretzschmar *et al.*, 1996; Zhang and Lamb, 1996). An interaction between M1 and RNA has been demonstrated using immune electron microscopy, filter binding assays and blotting (Wakefield and Brownlee, 1989; Ye *et al.*, 1989; Murti *et al.*, 1992). The X-ray crystal structure of the N-terminal portion of M1 (residues 2-158) at pH 4 has recently been determined (Sha and Luo, 1997). This M1 fragment structure forms dimers and binds single stranded RNA non-specifically via 10 positively charged residues (95-105). The authors also propose that a conformational change facilitates interaction of the hydrophobic N-domain with the membrane. The electrostatic interaction of the M1 with viral RNA allows encapsidation of the RNP complexes and also inhibits transcription and replication (Zvonarjev and Ghendon, 1980; Ye *et al.*, 1989). M1 is the main regulatory of RNP nuclear transport, promoting export, but inhibiting import (Martin and Helenius, 1991a; Martin and Helenius, 1991b; Whittaker *et al.*, 1995; Whittaker *et al.*, 1996; Bui *et al.*, 1996).

2.2.5.2 M2 protein

M2 is a 92 amino acid type III integral membrane protein (Mr ~ 15k) (Lamb *et al.*, 1985; Hull *et al.*, 1988). It is expressed abundantly on the apical surface of polarised epithelial cells, but only a small number of M2 molecules are incorporated into

virion particles (14-68) (Lamb *et al.*, 1985; Zebedee and Lamb, 1988; Hughey *et al.*, 1992). M2 exists as a disulphide bond-linked homotrimer on the cell surface and is post-translationally modified by phosphorylation and palmitoylation (Lamb *et al.*, 1985; Sugrue *et al.*, 1990b); Holsinger *et al.*, 1994).

Extensive studies have revealed a role for the M2 protein in the early and late stages of virus infection. Using the anti-viral drugs amantadine and rimantadine, it has been determined that when the M2 protein is expressed in cells and in planar lipid bilayers, it has ion channel activity allowing the transport H⁺ ions (Duff and Ashley, 1992; Pinto *et al.*, 1992; Wang *et al.*, 1994). Amantadine inhibits ion transport by binding to the transmembrane domain and blocking the ion channel. Resistant mutants possess changes that do not allow interaction with the drug (Hay *et al.*, 1985; Duff and Ashley, 1992; Schroeder *et al.*, 1994). From these studies it was suggested that the M2 channel allows passage of H⁺ ions into the interior of the virus, and hence acidification of the core during virus uncoating (reviewed by Hay, 1992). Acidification of the core influences the rate of fusion and be necessary for the dissociation of M1 from the RNP (Martin and Helenius, 1991b; Martin and Helenius, 1991a; Bron *et al.*, 1993; Wharton *et al.*, 1994; Bui *et al.*, 1996).

M2 also plays a critical role in later stages of infection by modulating the pH of intracellular compartments. This prevents the newly synthesised HA0 being exposed to low pH that would trigger a premature conformational change and result in the production of non-infectious particles (Sugrue *et al.*, 1990a; Ruigrok *et al.*, 1991; Ciampor *et al.*, 1992; Grambas and Hay, 1992).

2.2.6 RNA segment 8 : non-structural proteins NS1 and NS2

RNA segment 8 encodes two proteins, NS1 and NS2. NS1 is encoded by a co-linear mRNA transcript, whilst NS2 is encoded by a spliced mRNA.

2.2.6.1 NS1 protein

NS1 is a phosphorylated protein (Mr ~ 26k) and is abundantly expressed in infected cells being associated with polysomes, the nucleus and nucleolus (Lazarowitz *et al.*, 1971; Privalsky and Penhoet, 1981; Krug and Etkind, 1973). The protein is directed

to the nucleus by two independent nuclear localisation signals (Greenspan *et al.*, 1988).

NS1 is a multi-functional protein that interacts with a plethora of cellular factors. Functions recently identified include - (1) stimulation of the rate of translation of viral mRNAs (Enami *et al.*, 1994; de la Luna *et al.*, 1995), (2) regulation of nuclear export of mRNA (Fortes *et al.*, 1994; Qiu and Krug, 1994), (3) inhibition of pre-mRNA splicing (Fortes *et al.*, 1994), (4) inhibition of the activation of double-stranded RNA-activated protein kinase mechanism (Lu *et al.*, 1995), and (5) host gene expression shut-off by down-regulation of cellular mRNA maturation at the point of polyadenylation site cleavage (Shimizu *et al.*, 1999). Two functional domains have been identified in the NS1 protein: an N-terminal RNA-binding domain and an effector domain in the carboxy-half (Qian *et al.*, 1994). The inhibition of the nuclear export of mRNA is due to the interaction of two host cell proteins with the effector domain of NS1. The NS1 interacts with the 30kD sub-unit of the host cell cleavage and polyadenylation factor (CPSF) and the poly(A)-binding protein II (PAB II) (Chen *et al.*, 1999). This interaction means that 3' cleavage of cellular RNAs, followed by poly(A) polymerase (PAP) catalysed addition of a short poly(A) tail is inhibited. This results in the accumulation of cellular pre-mRNAs with short poly(A) tails that can be used as primers for viral mRNA synthesis. The RNA binding domain has been implicated in the inhibition of pre-mRNA splicing (Fortes *et al.*, 1994; Lu *et al.*, 1994). The NS1 interaction with the U6 small nuclear ribonucleoprotein (snRNP), a key component of the catalytic core within the spliceosome disrupts its function and inhibits splicing (Lu *et al.*, 1994; Qiu *et al.*, 1995). Recently, it has been suggested that NS1 also interacts with a novel 70Kda human protein, designated as NS1-binding protein (NS1-BP) which also seems to have a role in inhibition of splicing (Wolff *et al.*, 1998). Collectively, the functions of the NS1 protein may allow it to regulate the switch from early to late protein synthesis by retaining late viral mRNAs in nucleus until the appropriate time. This would require the NS1 protein at some point losing its functions, and this may be brought about by inhibition of post-translational modification, such as phosphorylation (Lu *et al.*, 1994; Vogle *et al.*, 1994).

2.2.6.2 *NS2 protein*

NS2 (Mr ~ 11k) is a structural protein present in the virion, in association with the M1 protein, at approximately 130-200 copies, (Richardson and Akkina, 1991; Yasuda *et al.*, 1993). The NS2 protein facilitates nuclear export of viral RNPs by acting as an adapter between the RNPs and the cellular nucleoporins of the nuclear transport machinery (O'Neill *et al.*, 1998). It has recently been renamed as the nuclear export protein (NEP) based on its function and its newly identified structural role.

3 Infectious cycle of influenza A virus

3.1 Overview

The infectious cycle of influenza A can be divided into the following 8 steps:

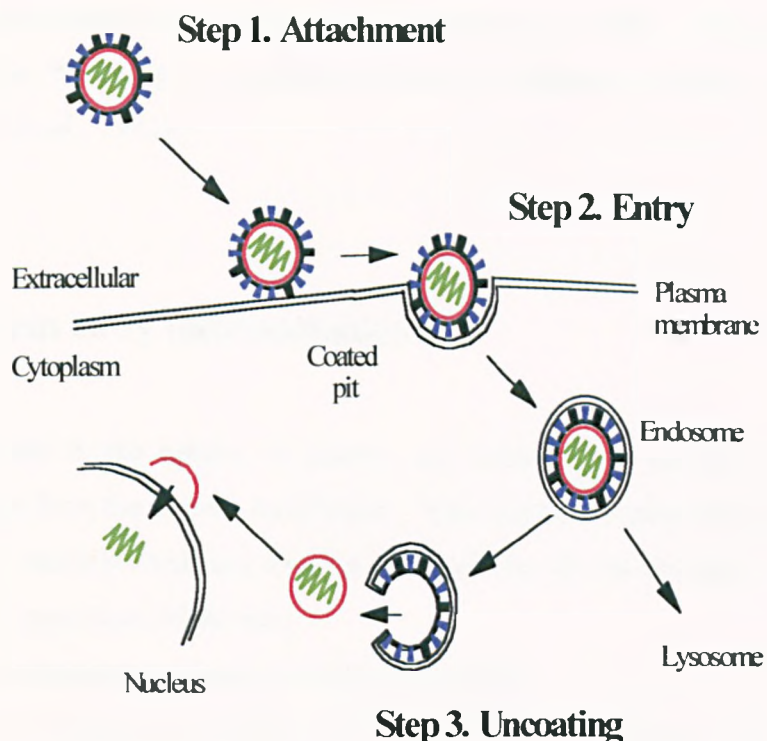
- (1) Attachment
- (2) Entry (internalisation)
- (3) Uncoating
- (4) Primary transcription of input vRNA
- (5) Replication of vRNA and secondary transcription
- (6) Translation of mRNA to produce viral proteins
- (7) Post-translational modification of viral proteins
- (8) Assembly of virus structural components and release of progeny virus

Steps 1 to 3 are shown in Figure 3.1.

3.2 Virus attachment to target cell receptors

Influenza A virus infection is initiated by attachment of the HA to N-terminal acetylneuraminic acid residues (sialic acid) present on cell surface glycoproteins or glycolipids (Gottschalk, 1957). The sialic acid residues are ubiquitous on a diverse number of cell types. This allows influenza virus to attach to a wide range of cells, but not all cells are permissive for infection. Influenza viruses differ in their recognition of NeuA α -2,3-Gal or NeuA α -2,6-Gal linkages (Rogers and Paulson, 1983). Human strains generally show a specificity for NeuA α -2,6-Gal linkages, whilst avian strains recognise NeuA α -2,3-Gal linkages, but this can be sub-type specific (Pritchett *et al.*, 1987). The HA-sialic acid interaction is of low affinity $2 \times 10^{-3} \text{M}$, but a high avidity is achieved by multi-valent interactions (Pritchett and Paulson, 1989; Sauter *et al.*, 1989; Glick and Knowles, 1991). The binding kinetics of influenza virus attachment to MDCK cells has recently been analysed. More virions can bind at lower temperature (4°C) compared to physiological temperatures, but there is a higher affinity binding at 37°C (Nunes-Correia *et al.*, 1999).

Figure 3.1 The influenza A virus infectious cycle. Steps 1 to 3 (taken from Outlaw and Dimmock, 1993).



The receptor binding site on the H3 HA is a pocket at the distal end of the HA1 molecule and its constitutive residues are highly conserved (Wiley *et al.*, 1981). The base of the pocket is formed by a phenolic hydroxyl residue, Tyr 98 and the aromatic ring from Trp 153. The rear of the pocket is formed by residues Glu 190, Leu 194, His 183 and Thr 155, whilst the left hand side and right hand sides of the pocket are formed by residues 134 to 138 and 224 to 228 respectively. Single amino acid substitutions correlate with alterations of receptor specificity. A change from leucine to glutamine at position 226 correlates with a change in linkage specificity from NeuAc α -2,6- to NeuAc α -2,3-, while the opposite mutation reverses this effect (Rogers *et al.*, 1983; Rogers *et al.*, 1985). However, position 226 is not an exclusive determinant of receptor linkage specificity, as in H1 strains position 226 does not appear significant, and also a study of a large number of H3 isolates indicated receptor linkage specificity correlated with position 226 in concert with changes at position 228 (Daniels *et al.*, 1987; Connor *et al.*, 1994).

Recent studies have suggested a role for the cellular protein annexin V, in influenza virus attachment, perhaps as a secondary receptor after the initial sialic acid contact. However, a definitive role of annexin V in the influenza infectious cycle has not been elucidated (Otto *et al.*, 1994; Huang *et al.*, 1996). Also anti-HA antibodies can cause Fc receptor mediated uptake of influenza viruses into macrophages (Tamura *et al.*, 1991).

3.3 Virus entry (internalisation).

Endocytosis is the uptake of ligands and solutes into vesicles that bud into the cytoplasm from the plasma membrane. There are four distinct types of endocytosis:

- (1) clathrin-mediated endocytosis, (vesicles of 100-150 nm)
- (2) caveolae (50-80 nm)
- (3) macropinocytosis (500-2000 nm), and
- (4) micropinocytosis (95-100 nm) (reviewed by Bishop, 1997)

Internalisation of influenza A virus occurs by receptor-mediated endocytosis via clathrin-coated pits (Matlin *et al.*, 1981; Marsh, 1984; Patterson and Oxford, 1986). These specialised vesicles have a layer of the protein, clathrin, on the cytoplasmic side of the plasma membrane. The coat forms from lattices of hexagons and pentagons of the clathrin protein made from the functional unit called the triskelion. This complex event is triggered when clathrin is recruited to the plasma membrane by the AP-2 adapter complex, forming clathrin coated pits where virus-receptor complexes accumulate (AP-2 also recruits the membrane bound receptors to the coated pits). These pits eventually expand inwards and pinch off into the cytoplasm forming coated vesicles (reviewed by Mellman, 1996). Following internalisation virus containing vesicles are uncoated and fuse with endosomes.

Receptor-mediated endocytosis can be inhibited by a number of treatments including (1) potassium ion depletion, (2) treatment with a hypertonic medium and (3) cytosol acidification (Heuser and Anderson, 1989; Heuser, 1989; Hansen *et al.*, 1993). These treatments inhibit different stages of the endocytosis pathway. The K⁺ ion depletion and hypertonic treatments are thought to remove membrane-associated clathrin lattices so that they form abnormal empty microcages in the cytoplasm,

whilst cytosol acidification interferes with the clathrin-coated pit budding from the membranes (Hansen *et al.*, 1993). Endocytosis is also temperature-dependent, being inhibited at 4°C (Matlin *et al.*, 1981; Richman *et al.*, 1986).

Virus entry into cells is rapid with a halftime of approximately 10 minutes, but this is virus strain and cell-type specific (Matlin *et al.*, 1981; Yoshimura *et al.*, 1982). There has also been one report that influenza can be internalised via non-clathrin coated vesicles in MDCK cells (Marsh and Helenius, 1989). However, it is unknown whether this represents a significant entry pathway for influenza virus.

3.4 Virus uncoating

Influenza A virus undergoes a two-stage uncoating process involving:

- (1) Primary uncoating in which viral envelope fuses with endosomal vesicle membrane
- (2) Secondary uncoating in which matrix protein is removed from the RNPs.

3.4.1 Primary uncoating

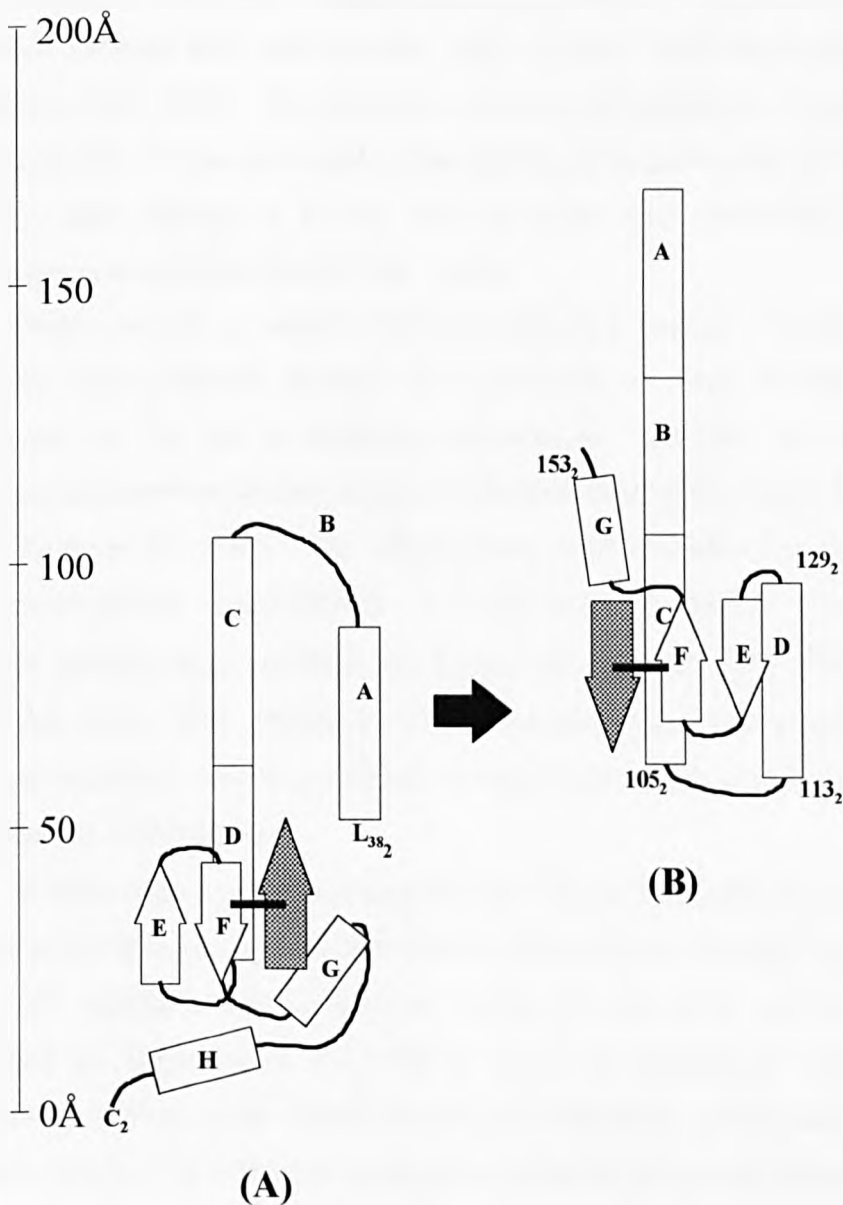
Primary uncoating involves the fusion of the virus envelope with the host cell endosomal membrane and release of the viral core into the cytoplasm. Fusion of the virus and endosome is mediated by the viral HA and is low pH-dependent. Acidification of the endosome occurs via the action of V-ATPase proton pumps in the endosomal membrane and results in an irreversible conformational change of the viral HA which triggers fusion (Wiley and Skehel, 1987; Stegmann *et al.*, 1989; Bullough *et al.*, 1994; Guinea and Carrasco, 1995). The ultimate mechanism of fusion of two membranes, remains obscure. However, many years of research, have elucidated many of the key steps.

The low pH-induced conformational changes of the HA are required to release the hydrophobic fusion peptides which are buried into the trimer structure at pH 7 (Wilson *et al.*, 1981; Bullough *et al.*, 1994). The crucial role of the fusion peptide in the fusion process has been demonstrated by site-specific mutations in the peptide, which modified or abolished fusion activity (Daniels *et al.*, 1985; Gething *et al.*, 1986a). Dissociation to some extent of the HA1 globular heads of the HA trimer is

required for exposure of the previously cryptic fusion peptides and the fusion process itself, as demonstrated in studies which engineered intermonomer disulphide bonds to crosslink the HA1 domains (Godley *et al.*, 1992; Kemble *et al.*, 1992). Biochemical, biophysical and immunological studies also provided support for dissociation of the globular heads being a requirement for fusion (Doms, 1993; Gaudin *et al.*, 1995). This was also correlated with a disordered spike morphology of the HA at low pH and 37°C in cryo-electron microscopic studies (Puri *et al.*, 1990). However, studies with the HAs of X:31 (H3 subtype) at 0°C and A/Japan (H2 subtype) at 37°C indicated that dissociation of the globular heads was not required for fusion (Puri *et al.*, 1990; Stegmann *et al.*, 1990). In fact, as fusion was found to be more efficient at 0°C with the X:31 HA than at 37°C, it was suggested that the HA with maximal separation/dissociation of the globular heads was fusion-inactive and that the fusion-active conformation was an intermediate. It was proposed that the fusion-active intermediate HA, possesses a rearranged HA2 stem domain with exposure of the fusion peptides to the sides of the trimer, but maintains its native state globular head domain (i.e. no dissociation) ((Stegmann *et al.*, 1990; Stegmann and Helenius, 1993). However, alternative studies proposed a two-stage model of the low pH-induced conformational changes of the X:31 strain HA, based on immunological probing (White and Wilson, 1987; Kemble *et al.*, 1992). Stage I of the model consisted of a partial dissociation of the globular head domains and exposure of the fusion peptide, and this was followed by stage II represented by complete (maximal) dissociation of the headgroups (Kemble *et al.*, 1992). Recently, this model has been revised to a 3-state model, which describes the pH-driven transition from the native tense (T) state to a relaxed fusion-active (R) state, followed by the desensitised (D) state (Korte *et al.*, 1999).

A leap forward in the understanding of the conformational changes that occur during fusion came with the determination of the X-ray crystallographic structure of a derivative of the low pH HA, called TBHA2 (Bullough *et al.*, 1994) (Figure 3.2 B). The TBHA2 fragment was constructed by incubating bromelain-released HA (BHA) at low pH, followed by digestion with trypsin to cleave off the globular heads and finally by digestion with thermolysin to digest the fusion peptides. The crystal structure of the fragment revealed massive rearrangements of the HA2. The most

Figure 3.2 The low pH-induced conformational change in HA. (A) The structure of the TBHA₂ monomer in schematic form at neutral pH, and (B) the corresponding region of the TBHA₂ monomer following the low pH conformational rearrangements (Bullough *et al.*, 1994; taken from Schofield, 1996). The regions of the HA2 chain are labelled A-H. The first strand of the HA1 chain is also shown (grey arrow). The disulphide bond between 14₁ and 137₂ is shown as a black line. The two structures are aligned upon the C region, which is unaffected by the conformational change. Arrow structures represent β -sheet domains and rectangles represent α -helical domains.



striking change was that a loop, designated B (Figure 3.2 A and B), had been transformed into an α -helix. This connected to existing α -helical regions A and C and probably acts to project the fusion peptide approximately 100Å away from the virus surface. Also residues 106-112 convert from a helical configuration to an extended loop which causes the D helix to be flipped by 180°C. Interestingly, approximately 20 C-terminal amino acids which should not be present in the TBHA2 fragment were not resolved indicating that they possessed a disordered or flexible conformation and suggested that they may form the connection to the transmembrane region. (Bullough *et al.*, 1994; Hernandez *et al.*, 1996). Electron microscopic study of HA containing virosomes which had been pre-treated at low pH and reacted with an antibody that binds to residues surrounding HA2 107 indicated that this region had been inverted 180° and was now approximately 110Å from the viral envelope (Wharton *et al.*, 1995). The inverted structure is supported by a study that showed that treatment of virus at low pH in the absence of target membrane released fusion peptides that inserted in to the viral envelope and resembled its own HA2 transmembrane domain (Weber *et al.*, 1994).

Fusion activity is variable between influenza strains. H1, H2 and H3 HA subtypes have different kinetics of inactivation of their fusion activity after incubation at low pH at different temperatures, and this has correlated with differences in conformational changes in the HAs (Puri *et al.*, 1990; Stegmann *et al.*, 1990; Korte *et al.*, 1999). The subtypes also show differences in the temperature-dependence of their fusion activity. X:31 HA is fusion active at 0°C, whilst A/PR/8 HA (H1 subtype) does not show any fusion activity below 15°C (Tsurudome *et al.*, 1992; Pak *et al.*, 1994). However, most fusion studies have concentrated on the X:31 HA and numerous models to explain HA-mediated membrane fusion are based on observations of this strain.

In this review I will concentrate on only one of the numerous proposed models, as this in my opinion, has been afforded the most support through experimental data, but I will highlight major differences compared with other models. This model, proposed by Stegmann *et al* (1990) is based on observations of X:31 HA and suggests a pathway to the fusion of the two membranes without dissociation of the globular heads. The individual steps of the fusion model are described below (Figure 3.3):

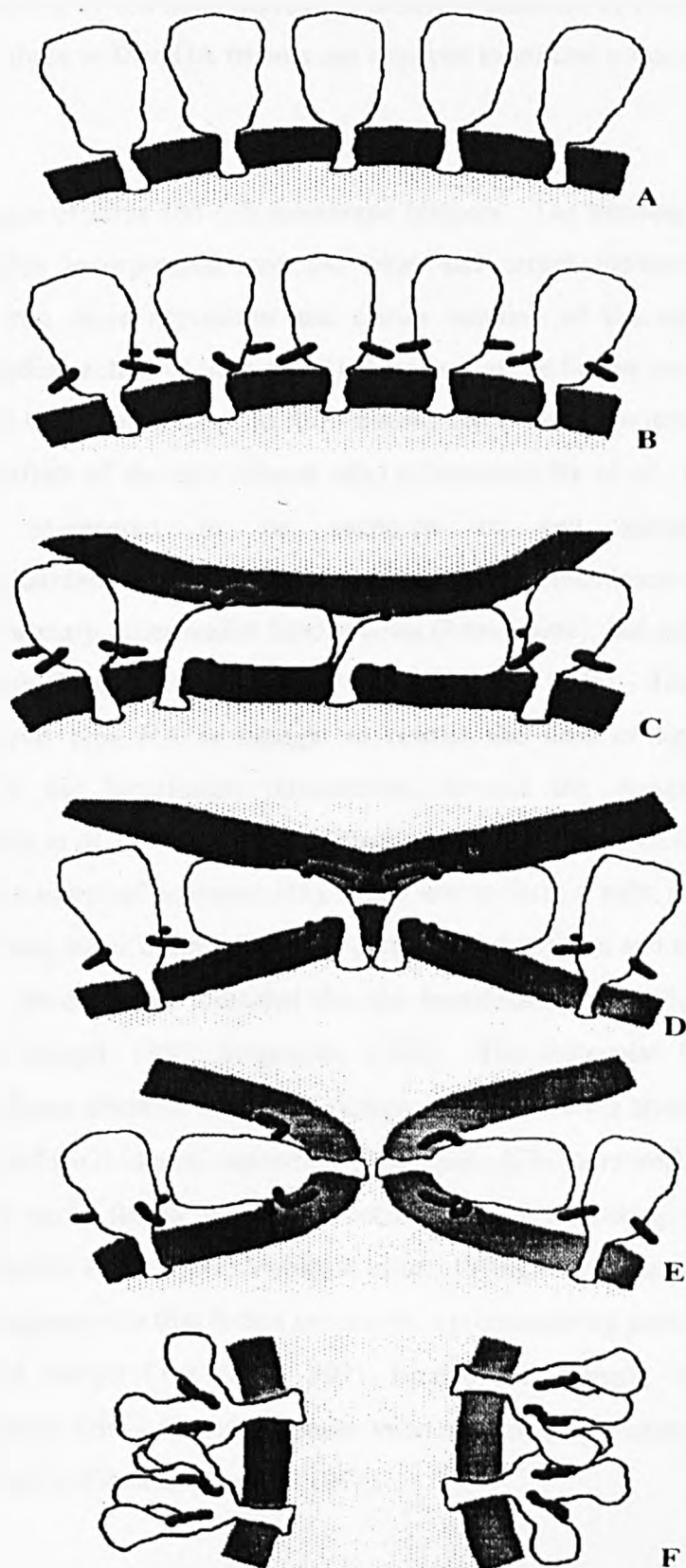
Step A: Schematic of the HA in its native conformation at pH 7.

Step B: The primary conformational change occurs rapidly after exposure to the low pH. This involves conformational changes in the HA2 stem region resulting in exposure of the fusion peptide. The globular heads do not dissociate and hence the fusion peptides are released to the side of the HA. An alternative model proposed by Hernandez *et al* (1996) disagreed and suggested that partial dissociation of the globular heads allow the spring loaded conformational change, seen in the X-ray crystal structure, to propel the fusion peptides towards the top of the HA.

Step C: Exposure of the fusion peptides leads to hydrophobic attachment of some of the HA molecules to the external bilayer leaflet of the target membrane. As the globular heads do not dissociate, it was suggested that a tilting of the HA allows insertion of the fusion peptide into both the target and viral membrane (Harter *et al.*, 1989; Stegmann *et al.*, 1990; Stegmann *et al.*, 1991; Tsurudome *et al.*, 1992; Weber *et al.*, 1994). Recent studies with isolated HA incorporated into model planar bilayers have shown that HA can tilt by approximately 80° at low pH and that this tilting is reversible upon return to pH 7 unless the HA is bound to a target membrane (Tatulian *et al.*, 1995; Tatulian and Tamm, 1996). An alternative model suggested that tilting of the HA does not occur, but that the released fusion peptide on the sides of the HAs provide a hydrophobic surface that pulls lipid into the gap between the membranes forming a lipidic stalk intermediate that eventually breaks into a fusion pore (Bentz *et al.*, 1990; Bentz *et al.*, 1993; Lee and Lentz, 1997).

Step D: Formation of the fusion complex. After insertion of the fusion peptides into the target membranes there is a lag period in the fusion process that varies in length with temperature and virus strain (Spruce *et al.*, 1989; Stegmann *et al.*, 1990; Clague *et al.*, 1991; Spruce *et al.*, 1991; Stegmann *et al.*, 1991). In fact it has been demonstrated that if the fusion process is interrupted at this point by return to pH 7, then the virus will remain in a fusion-committed state for times exceeding 60 minutes and will then undergo fusion at high efficiency when the temperature is elevated (Schoch *et al.*, 1992). It has been suggested that during the lag phase clustering and

Figure 3.3 Schematic model for the conformational changes and rearrangements of the HAs involved in the fusion process (taken from Stegmann *et al*, 1990).



orientational changes occur in the trimers in the viral envelope, and these form a rosette-like fusion complex (Doms and Helenius, 1986; Morris *et al.*, 1989; Ellens *et al.*, 1990; Clague *et al.*, 1991). The clustering of the HAs depends on their rotational and lateral mobility (Junankar and Cherry, 1986; Gutman *et al.*, 1993). A study of the fusion activity of cell lines expressing different densities of HAs indicated that a minimum of three to four HA trimers are required to initiate a fusion event (Danieli *et al.*, 1996).

Step E: Merger of virus and cell membrane bilayers. The bending of the HA with fusion peptides incorporated into the viral and target membranes brings the membranes into close apposition and causes bending of the membranes. The concerted bending action of the ring of HA trimers at the fusion site drives the outer leaflets of the bilayer to interact to form a restricted hemifusion intermediate (where only outer leaflets of the lipid bilayer mix) (Chernomordik *et al.*, 1998). HAs that had been engineered to be anchored in cell membranes via a glycosylphosphatidylinositol (GPI) tail instead of the transmembrane domain, induced unrestricted primary outer leaflet lipid mixing (hemifusion), but not pore formation and full fusion (Kemble *et al.*, 1994; Melikyan *et al.*, 1995). The transmembrane domain of wild type HA is thought to restrict the flow of lipids and prevent expansion of the hemifusion intermediate beyond the proteinaceous 'fence' (Chernomordik *et al.*, 1998). This is dependent on the number of HAs at the fusion site as if the number of activated HAs is too low to form a tight ring-like complex, then the growing hemifusion intermediate can break the fence and cause unrestricted hemifusion. Studies have indicated that the hemifusion intermediate consists of a lipidic stalk (Siegel, 1993; Stegmann, 1993). The molecular fence of HAs is proposed to focus attention within the fusion site to cause the transformation of the restricted hemifusion into an expanding fusion pore (Chernomordik *et al.*, 1998). A flickering of early fusion pores has been observed indicating that this step is reversible (Spruce *et al.*, 1991; Melikyan *et al.*, 1993a; Melikyan *et al.*, 1993b). An alternative suggestion is that fusion occurs via a proteinaceous pore whose expansion leads to lipid merger (Tse *et al.*, 1993; Lindau and Almers, 1995). However, argument against this is the recent observation of flickering fusion pores in protein-free lipid bilayers (Chanturiya *et al.*, 1997).

Step F: Dilation of fusion pore and dissociation of the ectodomains. This step of the pathway is very poorly understood. It is known that the initial pore undergoes a progressive widening with small aqueous contents being able to move through before large ones (Zimmerberg *et al.*, 1994). However, what drives the irreversible pore dilation is unknown. It has been suggested the further conformational change of the HA ectodomain desensitised (D) state, could drive this reaction, but at present there is no evidence for this (Stegmann *et al.*, 1990; Hernandez *et al.*, 1996).

An important question, still unanswered, about the HA-driven fusion process is whether the HAs that attach to cell receptors are responsible for the fusion activity. Numerous studies have provided evidence that receptor binding may facilitate fusion (Niles and Cohen, 1993; Stegmann *et al.*, 1995). However, other studies contradict this, and indicate that attached HAs are not involved in fusion (Ellens *et al.*, 1990; Alford *et al.*, 1994). One of these studies analysed the fusion activity of A/PR/8 virus (H1N1) to liposomes containing different amounts of ganglioside receptors (GDIa). It was shown that fusion with liposomes containing 5 mol % ganglioside was greater than with liposomes containing two or three times more receptor (Alford *et al.*, 1994). The authors suggested that if the receptor bound HAs were of primary importance in the fusion process, then higher fusion efficiency should be seen with liposomes containing the greater number of receptors. In a recent study, the fusion of virosomes containing two antigenically distinct HAs that were activated to fuse at different pHs, with liposomes containing lipid-associated anti-HA monoclonal Fab fragments used as surrogate receptors, was analysed (Millar *et al.*, 1999). Using liposomes containing Fabs that bind to only one HA, the fusion capacities of bound or unbound HAs were analysed at different pH. The results showed that bound HA mediated fusion and secondly that a high density of non-specific Fab actually inhibited fusion by a process they termed “molecular overcrowding”. This study represents the strongest evidence yet that fusion is mediated by receptor-bound HA, and this in turn suggests that the attachment of receptor to HA may alter the fusion pathway, perhaps by altering the extent or rate of conformational changes (Tsurudome *et al.*, 1992). However, it should be stressed that the Fab surrogate receptors may not behave like sialic acid containing receptors, and that HAs can drive the fusion of receptor-free liposomes (Millar *et al.*, 1999).

3.4.2 Secondary Uncoating

Secondary uncoating involves the dissociation of the M1 from the RNP. The dissociation is necessary for nuclear import of the RNP complexes (Martin and Helenius, 1991; Whittaker *et al.*, 1996). This has also been strongly supported by studies of the anti-influenza drugs amantadine and rimantadine, which inhibit M1 dissociation from vRNP during virus entry and inhibit vRNP transport to the nucleus (Bukrinskaya *et al.*, 1982; Martin and Helenius, 1991). These drugs inhibit the acid-activated M2 ion channel which is thought to permit flow of H⁺ ions into the virus interior channel (Hay *et al.*, 1985; Pinto *et al.*, 1992), indicating that acidification of the virus core was required for M1 dissociation. Acidification of vRNPs *in vitro* and *in vivo* has been shown to cause M1 dissociation (Zhirnov, 1990; Bui *et al.*, 1996). These studies have shown that acidification is the switch that allows the M1 to carry out its uncoating, nuclear transport and vRNP assembly functions. Transport of RNP to the nucleus after M1 dissociation is rapid (50% of total input NP antigen accumulated in nucleus in approximately 10 minutes in CHO cells), with the import of NP into the nucleus via nuclear pores being an active process dependent on ATP (Martin and Helenius, 1991; Kemler *et al.*, 1994). However, acidification of the viral core is not required for transcription of vRNP as purified RNPs treated at either neutral or acidic pH were transcribed (Kemler *et al.*, 1994).

3.5 Primary transcription of vRNA to mRNA

The RNA transcriptase and replicase functions of the virus are carried out by proteins PB1, PB2 and PA in association with the NP protein, which form the RNP complex. This complex transcribes the vRNA into mRNAs that are capped at the 5' end and polyadenylated at the 3' end (Glass *et al.*, 1975; Plotch and Krug, 1977). Transcription occurs by a unique cap-snatching process, in which the PB2 component of the polymerase complex acts as an endonuclease and cleaves capped cellular RNAs 10 to 13 nucleotides from their 5' ends, preferentially at a purine

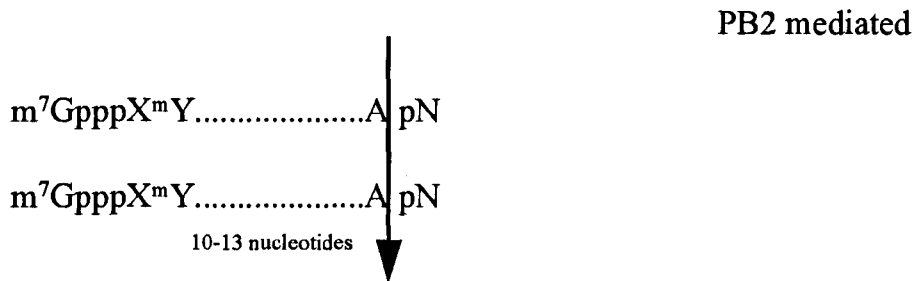
residue (Plotch *et al.*, 1981) (Figure 3.4). The 5' methylated cap fragments prime the transcription process by causing an allosteric modification of the polymerase complex (Kawakami *et al.*, 1985). Transcription is initiated by the incorporation of a guanidine (G) residue onto the 3' end of the resulting fragments and is then elongated by the PB1 subunit of the polymerase protein until a stretch of 5 to 7 uridine (U) residues is reached, 15 to 22 nucleotides before the 5' ends of the vRNA. Termination occurs by stuttering at the stretch of U residues causing the addition of poly(A) tail to the 3' end (Plotch *et al.*, 1981; Kitson *et al.*, 1991; Zheng *et al.*, 1999). The polyadenylation reaction has recently been shown to require a hairpin loop at the 5' end of the vRNA (Pritlove *et al.*, 1999). The 3' and 5' ends of each of the RNA segments have a conserved 12 and 13 residues respectively that show inverted complementarity and form a panhandle structure (Desselberger *et al.*, 1980; Hsu *et al.*, 1987). This structure may have a regulatory role in transcription, replication, the endonuclease activity of the polymerase complex, and packaging of the RNA into virus particles (Hsu *et al.*, 1987; Hagen *et al.*, 1994).

3.6 Replication of vRNA

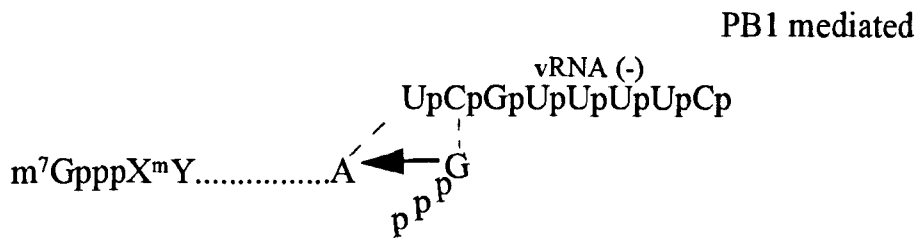
The synthesis of vRNA is dependent upon the production of viral proteins (Hay, 1982). Replication of the vRNA occurs by initial synthesis of full length copies of vRNAs to form template RNAs, which are then copied into vRNA. The template RNAs are complete copies of the vRNA and lack the polyadenylated tail. As a result a change in the properties of the polymerase complex is required so that they switch from mRNA to cRNA synthesis. This involves changing from capped RNA-primed initiation on unprimed initiation and to anti-terminate at the poly(A)-site (Beaton and Krug, 1984). It has been determined that free NP interacts with the polymerase complex and is responsible for the switch to cRNA and anti-termination (Beaton and Krug, 1986; Shapiro and Krug, 1988; Mena *et al.*, 1999). The NP is thought to bind to the RNA phosphate sugar backbone, and possibly melts the RNA secondary structure responsible for termination (Baudin *et al.*, 1994).

Figure 3.4 Mechanism for priming of influenza viral RNA transcription by capped cellular RNAs (taken from Lambkin, 1994).

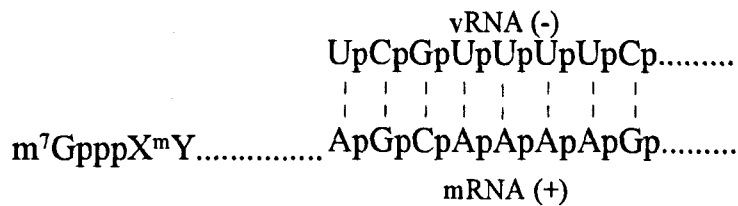
1. Cleavage of primer



2. Initiation on primer of mRNA synthesis.



3. Elongation of chain



3.7 Translation of viral proteins

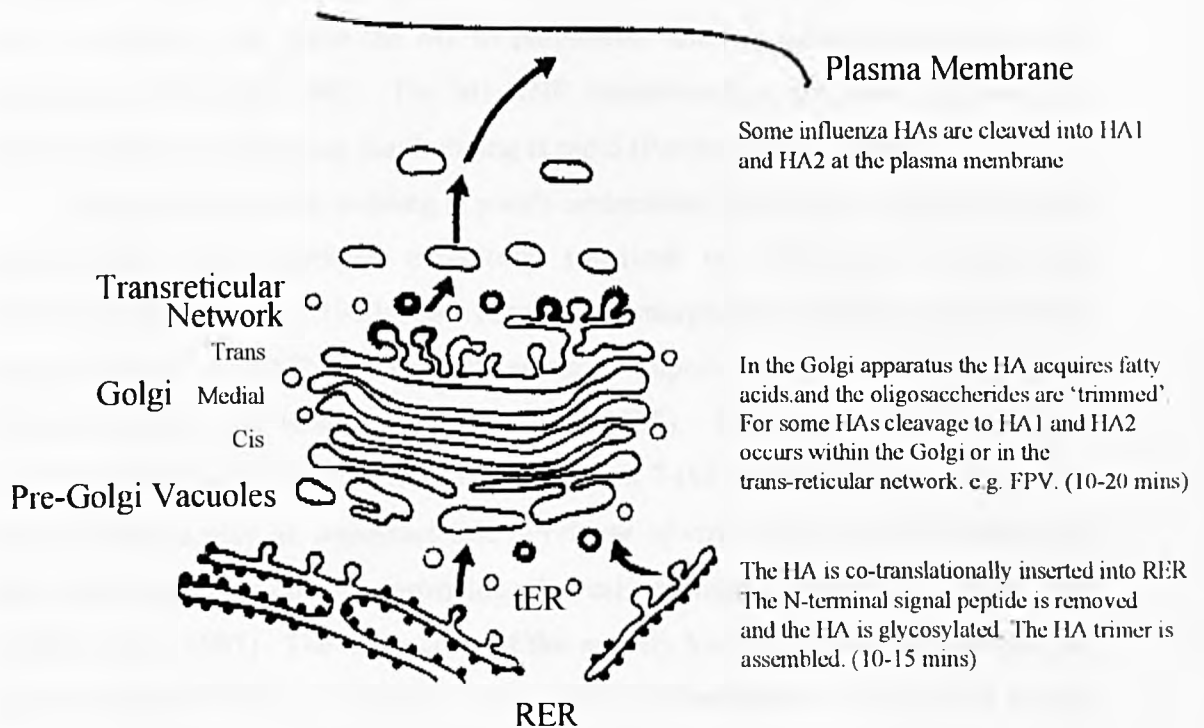
Production of new viral proteins is detected in infected cells after one hour of infection and is associated with a decrease in host cell protein synthesis which is complete after approximately 3 hours (Skehel, 1972; Skehel, 1973; Katze *et al.*, 1986). Translation of viral proteins is temporally regulated with NP and NS1 proteins predominantly synthesised in the early stage of infection, whilst during late stages the NS1 production decreases and M1, HA and NA production increases (Skehel, 1973; Meier-Ewert and Compans, 1974; Avery and Dimmock, 1975; Lamb and Choppin, 1976; Inglis and Mahy, 1979). The production of NS1 is thought to be important in host cell shut-off and in translation of viral gene products. Two different mechanisms have been proposed to explain shut-off of cellular protein synthesis:

- (1) Degradation of pre-existing cellular mRNAs (Inglis, 1982; Beloso *et al.*, 1992). It is thought that the degradation is initiated by cleavage of the 5' methylated caps of cellular mRNAs which leaves them more susceptible to cellular nucleases.
- (2) NS1 down-regulates cellular mRNA maturation at the point of polyadenylation-site cleavage (Shimizu *et al.*, 1999). Inhibition of cellular pre-mRNA maturation results in a lack of export to the cytoplasm.

The level of translation in cells is dependent on the phosphorylation of the α -subunit of the initiation factor eIF-2. Influenza virus infection induces the phosphorylation of eIF-2 by an TNA-activated P68 kinase, (PKR) which suppresses translation (Katze *et al.*, 1986). However, NS1 protein is able to circumvent this host defence mechanism by binding to and preventing activation of the PKR (Lu *et al.*, 1995; Hatada *et al.*, 1999).

A number of the viral proteins undergo post-translational modification. The HA and NA are co-translationally inserted into the rough endoplasmic reticulum (RER) and the transported to the golgi complex for further post-translation processing (reviewed in Lamb and Choppin, 1983) (Figure 3.5). The HA trimer is formed in the RER before transit to the Golgi apparatus (Copeland, 1986; Gething, 1986).

Figure 3.5 The post-translational processing of the HA (taken from Schofield, 1996).



The M2 protein has a critical role in the maturation of the HA trimer as it regulates the intracompartamental pH in the trans-Golgi network and associated transport vesicles. This maintains the pH above the threshold at which the conformational changes of the HA occur that are responsible for fusion, and hence maintains infectivity of budding virus (Sugrue *et al.*, 1990; Ciampor *et al.*, 1992).

3.8 Assembly and release of progeny virus

Influenza A viruses bud from the plasma membrane. Host cell proteins are excluded from the virions indicating the existence of unknown selection processes (Wang *et al.*, 1976). The selection process is further apparent with some viral proteins, such as the M2 which is greatly underrepresented in the virion compared to its plasma membrane expression (Lamb *et al.*, 1985; Zebedee and Lamb, 1988). It has recently

been demonstrated that incorporation of the HA is affected by the length of its cytoplasmic tail, with mutant HAs possessing elongated tails being excluded from virions (Zhou *et al.*, 1998). The M1 proteins form a layer beneath the plasma membrane and are associated with RNPs (Patterson *et al.*, 1988). Interaction of M1 with the RNPs, may cause the M1 to polymerise and the membrane to bulge out (Simons and Garoff, 1980). The M1-RNP interaction has not been detected near budding viruses, suggesting that budding is rapid (Patterson *et al.*, 1988).

The process of viral budding is poorly understood. Influenza viruses are highly pleomorphic, with particles exhibiting spherical or filamentous morphology (Kilbourne and Murphy, 1960). The filamentous morphology depends on interaction between the M1 and M2 proteins, suggesting an important role for these proteins in virion assembly and budding (Roberts *et al.*, 1998). High virus yields have also previously been associated with the RNA segment 7 (M proteins) (Baez *et al.*, 1980). The NA spikes play an important role in release of virus from the cell surface and preventing aggregation by destroying the cell membrane-associated sialic acid (Griffin *et al.*, 1983). The importance of this activity has been underlined recently by the new anti-viral drug Zanamivir that inhibits neuraminidase activity and causes aggregation of virions at the cell surface (McKimm-Breschkin *et al.*, 1998).

4 Antibodies and the humoral response to influenza A virus

4.1 Antibodies : Structure and function

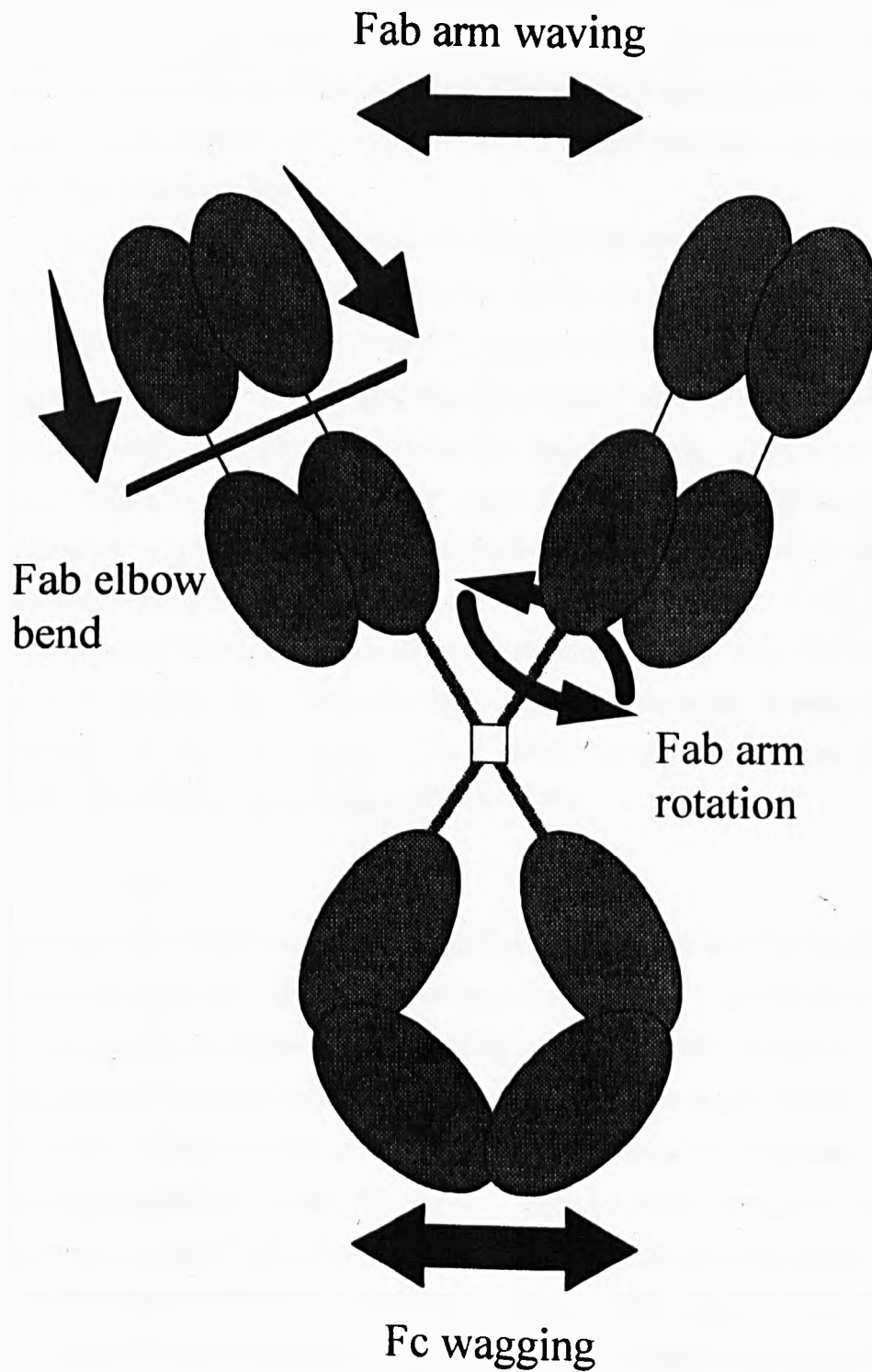
4.1.1 Overview

There are five isotypes of immunoglobulin: IgA, IgD, IgE, IgG and IgM. All antibodies have a common core structure of two identical light chains (approximately 25kD) and two identical heavy chains (approximately 50kD). The heavy chains are linked together and one light chain is attached to each heavy chain by disulphide bridges (i.e. HL+HL) forming a structure with bilateral 2-fold symmetry. All of the immunoglobulin classes have this structure, with the IgA and IgM consisting of multimers of this structure. Both types of chain consist of a series of repeating homologous units, each about 110 amino acids in length. These fold independently into a characteristic globular domain, known as an immunoglobulin domain. Many molecules of the immune system contain this globular domain and are said to belong to the Ig superfamily.

All Ig domains possess two layers of β -pleated sheet with three or four strands of anti-parallel polypeptide chain (reviewed in Abbas *et al.*, 1994). Each chain has an amino terminal variable domain (V_L and V_H) and a carboxy-terminal constant domain (C_L and C_H). Each variable domain has three regions of hypervariability, called complementarity-determining regions (CDR) surrounded by framework regions. The pairing of the V_L and V_H domains form the antibody paratope that recognises the epitope of the antigen. The framework regions hold the CDRs in the correct position for epitope binding, although they have in some cases been found to contribute to epitope binding (Wilson and Stanfield, 1993). In both V_H and V_L regions there are three CDRs, but generally the heavy chain CDRs have most involvement, particularly the CDR-H3.

The C_H region has 3 or 4 domains and the first of these domains are separated by a hinge region (Figure 4.1). This structure can be cleaved at the hinge region can be cleaved by the proteolytic enzyme papain, producing 3 separate pieces. Two pieces are identical, consisting of the complete light chain and the V_H - C_{H1} heavy chain fragment, is capable of binding antigen and are called the Fab fragments (approximately 50kD). The remaining piece is the Fc fragment consisting of the $C_{H2-3/4}$ domains. Alternatively, the enzyme pepsin cleaves neat the C_{H2} domain, so the Fab regions retain the hinge and the fragment is known as $F(ab)_2$.

Figure 4.1 Schematic diagram of an IgG molecule, including its modes of flexibility (taken from Burton, 1990).



4.1.2 Immunoglobulin isotypes

4.1.2.1 IgG (murine) – subtypes IgG1, IgG2a, IgG2b and IgG3.

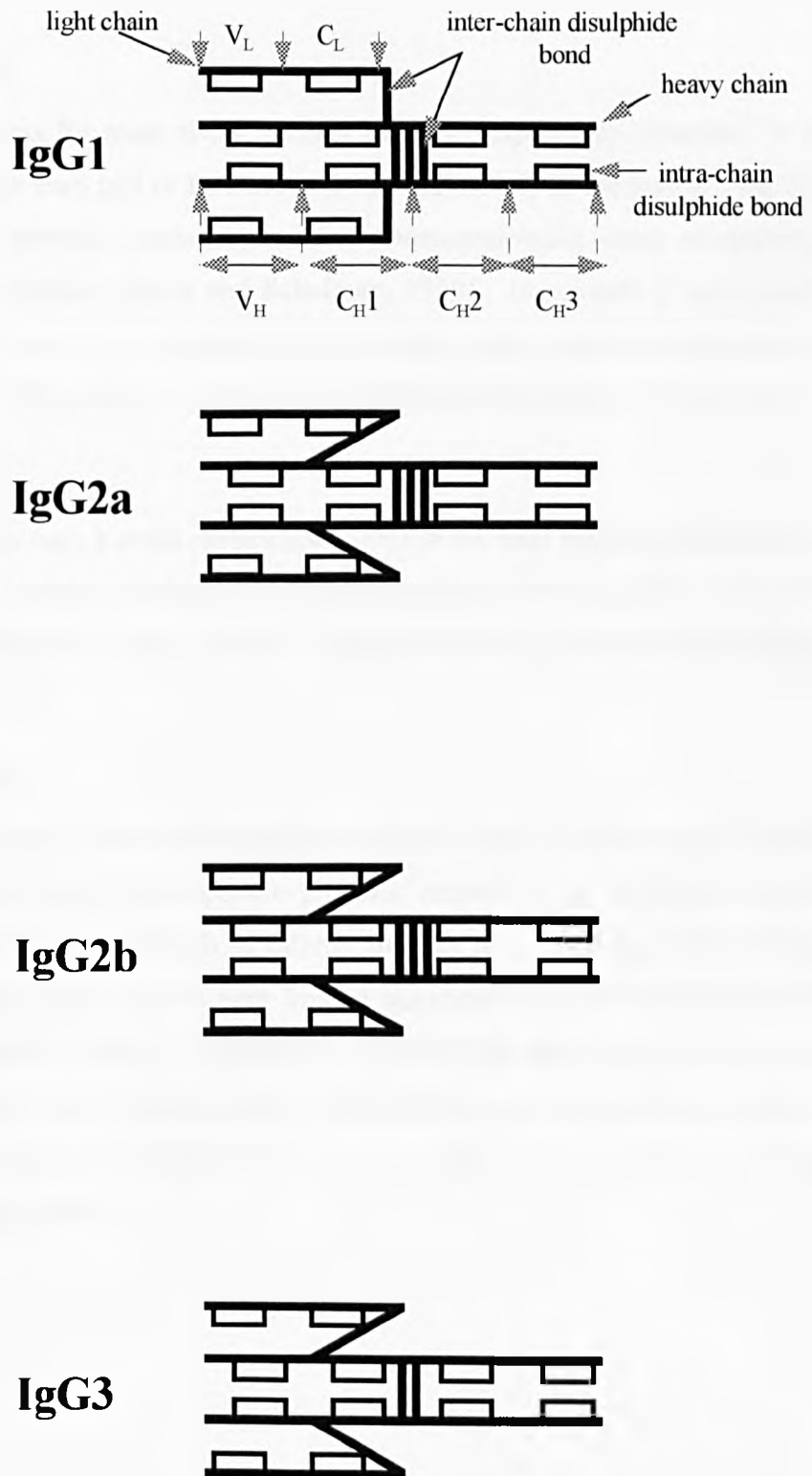
IgGs are monomeric antibodies (approximately 160kD), constituting approximately 70-75% of the plasma pool. They play a major role in the secondary response to infection. Murine IgG (used exclusively in this thesis) are segregated into 4 isotypes, IgG1, IgG2a, IgG2b and IgG3, based on differences in their sequence, carbohydrate content and disulphide bonding (Figure 4.2). Humans also have 4 subtypes of IgG, IgG1, IgG2, IgG3 and IgG4.

IgG possesses a large degree of structural flexibility (Figure 4.1). The Fab arms are capable of bending at the elbow region, and the angle of bend has been determined to range from 127.2° to 175.1° (reviewed by Padlan, 1994). If the IgG is bound monovalently to an antigen then the second Fab unit has rotational freedom about the hinge, thus displaying a propeller-like movement. Crystal structures of a murine IgG2a MAb revealed a large degree of flexibility with Fab regions loosely tethered to a mobile Fc region (movements of the Fc region have been termed 'wagging') (Figure 4.1) (reviewed by Burton, 1990; Harris *et al.*, 1992). Flexibility of the Fc region has been correlated with activation of complement (Oi *et al.*, 1984). The IgG subtypes have different efficiencies of complement fixation, due to the flexibility of their Fc region. Their ability to fix complement are ranked IgG2b>IgG2a>IgG3>IgG1 (Nisonoff *et al.*, 1975).

4.1.2.2 IgA

IgA represents 15-20% of the immunoglobulin plasma pool and is primarily involved in mucosal immunity. The majority of IgA is dimeric and is predominantly found in the seromucous secretions, such as saliva, tracheobronchial secretions, colostrum, milk and genito-urinary secretions (reviewed by Underdown and Schiff, 1987). The IgA dimer consists of two immunoglobulin units linked by disulphide bonds to a non-immunoglobulin J-chain (Mr = 15k). The IgA found in external secretions is known as secretory IgA (sIgA) and contains an additional polypeptide, called the secretory component (Mr = 70k). The secretory component is initially part of the IgA receptor on epithelial cells, which the IgA binds to when it is transported to the

Figure 4.2 Schematic representation of the structure of the four murine IgG subclasses (taken from Nisonoff *et al*, 1975).



apical surface of the cell. The receptor is cleaved to form the secretory component and allows release of the antibody from the cell surface (Kühn and Kraehenbuhl, 1981).

4.1.2.3 *IgM*

The IgM accounts for most of the primary immune response to infection. It has a lower prevalence than IgG or IgA and is found exclusively in the serum. The IgM is a pentameric molecule consisting of five immunoglobulin units connected and stabilised by a J-chain (Davis and Schulman, 1989). In solution it has a star-like conformation, but can if interacting with a multivalent antigen, adopt a crab-like conformation. The IgM is very efficient at activating the complement cascade.

4.1.2.4 *IgD*

IgD accounts for only a small percentage (<1%) of the total plasma immunoglobulin. Membrane-bound IgD is found at high concentrations on the surface of circulating mature B-cells and may play a role in antigen-triggered lymphocyte differentiation (Roitt *et al.*, 1993).

4.1.2.5 *IgE*

IgE is responsible for defence against metazoan gut parasites and immediate hypersensitivity reactions to specific proteins, referred to as allergens, and cause chronic allergic conditions such as asthma and hay fever (Metzger, 1978; Mitchell, 1979). IgE are found only in very limited quantities in the serum, but are found associated with the surface of basophils and mast cells due to the presence of IgE receptors. An allergen that cross-links IgE molecules on the surface, of mast cells triggers the release of 'mediators' that are responsible for the pathology of allergic disease (Metzger, 1978).

4.2 Humoral Immune response to Influenza A

4.2.1 Overview

Infection with influenza A virus results in the production of antibodies to HA, NA, NP and M proteins (Kilbourne, 1987). However, only antibodies generated to the HA and NA glycoproteins are associated with resistance to infection (reviewed by Murphy and Clements, 1989).

Infection of immunologically naive children with a live attenuated influenza vaccine resulted in HA-specific IgA, IgM and IgG antibodies in nasal wash specimens by two weeks post-infection (Murphy *et al.*, 1982; Murphy and Clements, 1989). The IgM and IgA serum and nasal wash titres peaked at two weeks post-infection and the IgM then declined. The serum IgG response peaked between four to seven weeks and in 50% of the children this coincided with a peak of nasal IgG response. Comparison of the specific activity of antibody in the nasal wash and serum, indicated that IgA is actively secreted to the nasal mucosa, because of the secretory component-mediated active transport of immunoglobulins possessing a J chain (Brandtzaeg, 1981). However, IgG present in the nasal wash is usually a transudate from serum (Wagner *et al.*, 1987).

The secondary response to influenza is dominated by IgA and IgG, with IgM occurring variably, probably in relation to the degree of antigenic variation between viruses (Gonchoroff *et al.*, 1982). Serum HI titres gradually decrease over the first six months, but may persist due to infection with related antigenic drift variants. The secondary response generates a greater degree of cross-reactive antibodies compared to the primary response, for example, in unprimed children (reviewed by Ada and Jones, 1986).

4.2.2 The role of antibody in the recovery from influenza A virus infection

Infection results in a peak virus titre after 3 to 4 days, which then declines (Dhar and Ogra, 1985). The humoral response to HA does not peak until the second week post-infection, which suggested that immunoglobulins had only a minimal role in recovery (Mims and White, 1984). This traditional view was supported by studies

with athymic mice, which are unable to control infection and eventually succumb to it (Wells *et al.*, 1981). These studies vindicated the importance of T-cell response in influenza infection and it has since been determined that both CD8- and CD4-positive T-cells play a role in the recovery of immunocompetent mice from primary infection (reviewed by Doherty *et al.*, 1992; Topham *et al.*, 1996b). However, other work has indicated that the B-cell response is indispensable and plays an equally important role in recovery from influenza virus infection (reviewed by Gerhard *et al.*, 1997). An early investigation of B-cell deficient mice indicated that there were two phases to the recovery process – (1) a T-cell-dependent early phase (day 5-7) that resulted in a rapid decrease in virus titre and, (2) a B-cell-dependent late phase (day 7 onwards), that eventually resulted in clearance (Iwasaki and Nozima, 1977). B-cell deficient mice showed the biphasic course of infection, but could not clear the infection and a steady increase in virus titre was followed by death. Further analysis with B-cell deficient μ MT mice showed that they were more susceptible to highly pathogenic strains of influenza, such as A/PR/8/34 (H1N1) and A/Japan/305/57 (H2N2), but were as susceptible as immunocompetent mice to the low pathogenic strain X:31 (an H3N2 reassortant) (Topham *et al.*, 1996a; Gerhard *et al.*, 1997). These studies demonstrated that the B-cell antibody response was of similar, if not greater importance, for recovery of primary influenza infection than CD8 T-cells.

The specific role of antibodies in the recovery from influenza virus has been analysed by passive transfer of HA-specific MAbs into severe combined immunodeficient (SCID) mice. An initial study showed that treatment with a mixture of MAbs resulted in complete clearance of infection (Scherle *et al.*, 1992). Individual MAbs also showed a therapeutic activity which was greatly dependent on the immunoglobulin-isotype (Palladino *et al.*, 1995). Intraperitoneal administered virus-specific IgA or IgM MAbs could not cure viral pneumonia, despite having good neutralizing activity *in vitro*. Recovery from viral pneumonia was only possible by administration of IgG MAbs. It is thought that IgA and IgM antibodies have only a restricted access to the lower respiratory tract compartments hence their therapeutic activity may be restricted in a viral pneumonia (Palladino *et al.*, 1995).

IgG MAbs contribute to the resolution of influenza virus infection in two principal ways (1) cell targeting (CT) activity, in which their binding to infected cells reduces the production of progeny virus, (2) virus neutralizing (VN) activity, in which binding to progeny virus inhibits further spread of infection (Mozdzanowska

et al., 1999). Recent observations have indicated that MAbs with no VN activity *in vitro* fail to clear an influenza virus infection in SCID mice but reduce pulmonary virus titres. Therefore, CT activity is therapeutic, but MAbs resolve the infection to a greater extent by their VN activity (Mozdzanowska *et al.*, 1997).

4.2.3 The role of antibody in the protective from re-infection by influenza virus

The serum IgG response correlates closely with protection from influenza infection in humans (Couch and Kasel, 1983). Resistance to infection induced by a live attenuated virus correlated with levels of HA-specific IgG and IgA antibodies (Clements *et al.*, 1986). Resistance to infection can also be conferred by passive administration of neutralizing antibodies. This has been shown with administration of anti-HA polyclonal and monoclonal antibodies in immunologically naïve mice (Ennis, 1982; McLain and Dimmock, 1989). Protection against influenza virus challenge was also demonstrated with passively transferred anti-HA MAbs in SCID mice (Palladino *et al.*, 1995). The protective activity was found not to be isotype-dependent, unlike that seen in recovery of influenza infection, with IgA, IgM and IgG all conferring protection to subsequent challenge. Interestingly, a recent study of IgA knockout mice (IgA^{-/-}), showed that IgA is not required for prevention or recovery from influenza disease, as a control IgA^{+/+} mice showed similar levels of pulmonary virus replication and rate of clearance as the knockout IgA^{-/-} mice (Mbawuike *et al.*, 1999). This indicated that IgG and IgM responses could effectively replace IgA and protect from infection. However, passive transfer of polymeric IgA could protect from challenge, in agreement with previous studies (Palladino *et al.*, 1995). This supports the idea that protective immunity is not immunoglobulin-class specific and underlines the importance of stimulating both systemic and mucosal immunity in vaccination strategies (Mbawuike *et al.*, 1999).

4.3 Mechanisms of neutralization of influenza A virus.

Neutralization can be accomplished by either antibody alone, termed simple neutralization, or by the interaction of the antibody with a number of secondary effectors, such as complement.

Simple neutralization can be defined as the *in vitro* process in which antibody interacts with virus and results in a loss of infectivity. The mechanism of neutralization is a complex process, in which antibodies can interfere with events at various stages of the virus infectious cycle. The mechanism of neutralization is dependent on a number of variables, including intrinsic properties of the virus and neutralization epitope, the isotope of the antibody, the cell receptor and the virus:antibody ratio. As a result, depending on the conditions, neutralization may occur by only one mechanism or by two or more mechanisms that occur simultaneously (reviewed by Dimmock, 1993; Dimmock, 1995). Numerous studies with HA-specific MAbs have correlated loss of infectivity, with loss of particular viral functions essential in the initial stages of infection and these are described in the following section..

4.3.1 Neutralization without involvement of the cell

4.3.1.1 Aggregation of virions –

Aggregation is due to crosslinking of viruses by antibody, which reduces infectivity by decreasing the number of infectious units present. It is dependent on the antibody:virus ratio, as it requires antibodies to have an available paratope and crosslink two or more viruses. Saturating concentrations of antibody form minimal aggregates as there are limited free epitopes (Dimmock, 1993).

Aggregation of influenza virus has been demonstrated with IgG, IgA and IgM (Taylor and Dimmock, 1985; Taylor and Dimmock, 1985; Armstrong *et al.*, 1990; Outlaw *et al.*, 1990; Armstrong and Dimmock, 1992). Aggregates formed by either of the immunoglobulin types were unstable and could be dispersed by vortexing (Armstrong *et al.*, 1990). Aggregation of influenza A/fowl plague/Rostock/34

(H7N1) (FPV/R) by IgG was concentration-dependent (Outlaw *et al.*, 1990). For example, maximum aggregation by the HC2 antibody occurred as a sharp peak at a ratio of 0.1 HIU:1 HAU and then decreased with increasing concentration of antibody. The maximum aggregate size was 6.3 virus particles and this level could theoretically account for 79% neutralization, which correlated well with the actual percentage neutralization. However, as neutralization increased (>99%) with increasing antibody, the level of aggregation decreased indicating that the antibody was neutralizing by mechanisms other than aggregation. Similar results were also obtained for HC61 IgG, but HC10 IgG gave maximal aggregation without any loss of infectivity, suggesting that these aggregates were highly unstable.

Aggregation of influenza A/PR/8/34 virus by a polymeric IgA MAb was also concentration-dependent (Outlaw and Dimmock, 1990; Armstrong and Dimmock, 1992). Maximal aggregation by the IgA gave >50 particles/aggregate. However, the maximum theoretical neutralization was only 41% from a total of >99% neutralization of infectivity. Similar observations were made with an anti-FPV/R IgM MAb, which aggregated virus, but theoretical neutralization levels could not account for the total actual percentage neutralization of infectivity.

Collectively, these studies indicated that aggregation could only account for a small proportion of the total neutralization of influenza viruses and that other mechanisms must account for remaining neutralization. This is especially striking at >99% neutralization levels at which point virus particles are monodisperse.

4.3.2 Neutralization in the context of the cell

4.3.2.1 Inhibition of virus-cell interactions (attachment) –

Steric hindrance of the virus-cell receptor interaction has commonly been assumed to be the sole mechanism of neutralization of viruses by antibody. This mechanism has been supported by the X-ray crystallographic structure of BHA, which showed that the receptor-binding pocket was in close proximity to the major antigenic sites (Weis *et al.*, 1988). Also it has been demonstrated that an anti-A/PR/8 HA IgG, H18-L9 could inhibit the attachment of virus to a B-cell lymphoma line, A20 over a range of concentrations that correlated well with neutralization of infectivity (Eisenlohr *et al.*,

1987). However, numerous other studies with IgM, IgA and IgG have indicated that the situation is more complex and even under conditions where antibodies can inhibit attachment, this is often not of sufficient extent to account for the total neutralization observed (Taylor and Dimmock, 1985; Taylor and Dimmock, 1985; Outlaw *et al.*, 1990; Outlaw and Dimmock, 1990; Armstrong and Dimmock, 1992).

Inhibition of attachment of influenza virus by a panel of six IgGs was dependent on concentration and cell type (Outlaw *et al.*, 1990). At low concentrations, inhibition of attachment correlated relatively well with the percentage neutralization and increased with increasing IgG concentration. For example, at 63% neutralization, inhibition of attachment for the six IgGs ranged from 30 to 55%. However, as the IgG concentration was increased to give higher levels of neutralization, the inhibition of virus attachment to cells was decreased, i.e. at >99.9% neutralization, 99% of virus attached to cells. This phenomenon was observed in both murine tracheal epithelial cells and BHK cells, where maximum inhibition of attachment was 55 and 50% respectively and then decreased with increasing IgG concentration. However, this was not observed with inhibition of virus attachment to chick red blood cells (CRBCs) in which the maximum level of inhibition of virus attachment did not decrease with increasing IgG. It was suggested that high concentrations of IgG had a restricted rotational movement due to their close packing on the virus surface. Also the BHK and murine tracheal cells possess long cell receptors in contrast to the short 5 nm glycoprotein A receptors on the CRBCs, that allowed them to interdigitate with the fixed array of IgG allowing attachment (Viitala and Järnefelt, 1985; Outlaw *et al.*, 1990). Conversely, IgGs at lower concentrations are less densely packed, and so would interfere with the cell receptors due to their greater rotational freedom.

Inhibition of virus attachment by the anti-A/PR/8 polymeric IgA MAb, H37-66, was antibody concentration-dependent (Outlaw and Dimmock, 1990; Armstrong and Dimmock, 1992). At lower concentrations of IgA that caused up to 99% neutralization, no inhibition of attachment was detected (Armstrong and Dimmock, 1992). However, at higher concentrations of IgA inhibition of virus attachment to cells increased to a maximum of 90%, compared with >99% neutralization of infectivity (Outlaw and Dimmock, 1990). As seen with the IgGs, when saturating concentrations of IgA were used attachment of virus to cells was restored.

Analysis of the effect of an anti-FPV/R HA secretory IgA (sIgA) purified from rat bile, on virus attachment to cells showed that it was concentration and temperature-dependent (Taylor and Dimmock, 1985). The sIgA caused 90% inhibition of virus attachment to BHK cells and 96.5% neutralization at 4°C. However, when the temperature was increased to 25°C and 37°C, inhibition of attachment decreased to 50%, but neutralization remained high at 96.5%. The authors suggested that thermal agitation increased the probability of the virus attachment site and cell receptor interaction. Monomeric IgA, produced by differential reduction of the sIgA, gave 98.5% neutralization, but did not inhibition attachment. Inhibition of virus attachment to cells by an anti-FPV/R polyclonal IgM, was similar to the IgA, being dependent on concentration and temperature (Taylor and Dimmock, 1985). At 4°C the IgM could block >95% of virus attachment to BHK cells, but raising the temperature to 37°C decreased this level to 53%.

In summary all of the immunoglobulin-types could inhibit virus attachment to cells, but this could not account for the total neutralization of infectivity and was strictly dependent on the prevailing conditions, such as concentration of antibody, cell type and temperature.

4.3.2.2 Neutralization of virus after it has attached to cells (post-attachment neutralization)

Post-attachment neutralization (PAN) is defined as the reduction in viral infectivity achieved by antibody reacting with virus that has already attached to a target cell, but has not yet fused with the target membrane (Armstrong and Dimmock, 1996). The ability to give PAN provides the most compelling evidence that antibodies can interfere with stages of the virus infectious cycle that occur after virus-cell attachment. This area of research has been neglected with influenza virus, apart from one study that showed that an anti-PR/8 polyclonal rabbit serum gave PAN at 4°C (Ishida and Ackermann, 1956). However, antibodies have been shown to give PAN in many other viral systems (Kjellén, 1985; Gollins and Porterfield, 1986; Blumenthal *et al.*, 1987; Dietzschold *et al.*, 1987; Wohlfart, 1988; Farrell and Shellam, 1990; Vrijzen *et al.*, 1993; Osioy and Anderson, 1995; Armstrong *et al.*, 1996); Armstrong and Dimmock, 1996).

4.3.2.3 *Inhibition of virus internalisation into cells*

Inhibition of the uptake of virus into clathrin coated pits has only been observed with polymeric IgM (Taylor and Dimmock, 1985; Outlaw and Dimmock, 1990). Proteinase-K digestion of IgM-neutralized virus that had attached to BHK cells, caused the release from the cells of >80% of RNA from ³²P-labelled virions, compared to <20% of vRNA released from non-neutralized virus (Taylor and Dimmock, 1985). Bacterial neuraminidase treatment also released IgM neutralized virus-antibody complexes (Outlaw and Dimmock, 1990). These studies both demonstrate that IgM inhibited internalisation of the virus-IgM complexes into the cell. Virus attached to cells after neutralization with either IgG or IgA became progressively resistant to neuraminidase treatment during a 60 minute incubation indicating that neutralised virus was being internalised into cells (Armstrong and Dimmock, 1992; Outlaw and Dimmock, 1993)

4.3.2.4 *Inhibition of virus-cell fusion (primary uncoating)*

The fusion activity of enveloped viruses can be studied by labelling membranes of the viruses with a lipid soluble fluorescent probe, such as octadecyl rhodamine-B-chloride (R18) (Miller and Hutt-Fletcher, 1988). When R18 is present in lipid at high concentrations fluorescence is quenched, but when it is diluted by lateral diffusion following fusion with another membrane, fluorescence occurs (dequenching). This technique has been used with influenza virus to analyse the effect of neutralization by a panel of monoclonal IgGs on endosomal fusion in BHK cells (Outlaw and Dimmock, 1993). The IgGs all caused inhibition of endosomal fusion in a concentration-dependent manner. At concentrations required to give 63% neutralization, three of the IgGs, HC187, HC280 and HC19 neutralized by inhibition of fusion alone. However, at concentrations that gave >99.97% neutralization, two of the IgGs HC2 and HC61, caused partial inhibition of fusion with approximately 20% virus-cell fusion still remaining. This suggested that these antibodies were capable of inhibiting a further stage of the virus infectious cycle.

A panel of IgGs have also been shown to inhibit the fusogenic activity virus with RBCs (Kida *et al.*, 1983). In this study it was shown that when virus-antibody

complexes were pre-treated at pH 5.9 prior to attachment, and then mixed with RBCs, the virus attached but haemolysis was inhibited. The authors concluded that the IgGs were inhibiting the low pH-driven conformation change of the HA required to initiate the fusion event.

Low concentrations of a polymeric IgA MAb, H37-66, allowed virus to attach and be endocytosed even though it caused >99% neutralization (Armstrong and Dimmock, 1992). Analysis of the intracellular distribution of viral NP indicated that it remained cytoplasmic, presumable in endosomes. This suggested that the IgA was inhibiting endosomal fusion / primary uncoating and the release of the viral core into the cytoplasm. In support of this was the observation that the IgA MAb could also inhibit cell-cell fusion under low pH conditions. The authors suggested that the polymeric nature of the IgA MAb was important in the fusion-inhibition activity based on two observations :

- (1) that monomeric IgA produced by differential reduction had good neutralization activity but did not inhibit attachment or primary uncoating
- (2) that electron microscopy showed that some IgA molecules appeared to be lying over on the virus surface, suggesting interactions with HAs with both its monomeric units (Armstrong and Dimmock, 1992).

It has been proposed that by cross-linking neighbouring HA trimers that HA mobility could be restricted (Schofield, 1996). Mobility of HA has been shown to be important in fusion as co-operativity of HA trimers seems to be critical in establishing a fusion pore, which is thought to comprise of a minimum of 3 to 4 HA trimers (Junankar and Cherry, 1986; Danieli *et al.*, 1996). Hence, the IgA could inhibit HA co-operativity and mobility by cross-linking the HAs and inhibiting formation of a fusion pore (Schofield, 1996). However, analysis of the importance of valency in inhibition of fusion by IgG or IgA has not been carried out. This could be analysed by investigating the fusogenic activity of virus neutralized by monovalent Fab fragments.

4.3.2.5 *Inhibition of events which occur after primary uncoating*

70% of vRNA of virus neutralized by HC2 IgG was located in the nucleus, but no transcription took place (Possee *et al.*, 1982; Rigg *et al.*, 1989). Analysis of the RNase resistance of vRNP from neutralized virus found it to be RNase-insensitive at

37°C, compared to vRNP from non-neutralized virus which was 7-fold more susceptible to digestion (Rigg *et al.*, 1989). Susceptibility to RNase digestion has previously been correlated with active transcription of vRNPs (Koff and Knight, 1979). Therefore, it was proposed that the antibody was inhibiting a requirement for the vRNP to undergo a conformational relaxation, termed tertiary uncoating, which is required for transcription (Rigg *et al.*, 1989). This was further supported by a study with the polymeric IgA, MAb, H37-66 (Armstrong and Dimmock, 1992). The IgA inhibits virus-cell fusion at low concentration. However, when the block to fusion was artificially bypassed using acidified PEG, then immunofluorescence showed a distribution of neutralized viral NP and M1 antigens that was indistinguishable from non-neutralized virus. Hence, as NP was transported to the nucleus it was assumed that the vRNP was present in its correct location, but that transcription did not occur.

In summary, antibody-mediated neutralization of influenza virus is a complex process which can occur by a single mechanism or by two or more mechanisms acting simultaneously. However, the properties of the antibodies that give them the ability to neutralize influenza virus by different mechanisms such as inhibition of attachment or inhibition of fusion has not been elucidated and requires further investigation.

5 Materials and Methods

5.1 General Methods

5.1.1 Haemagglutination assay

Virus was diluted in PBS to a required initial dilution and then 200 µl was added to row one of a 96 well round bottom plate (Greiner). This was double diluted across the plate to a final volume of 100µl. 25µl of chicken red blood cells (CRBCs) (Serotech) at 0.66% were added to each well using a dropper. This was mixed using a vibrator and incubated for 45 minutes at 20°C. The 50% agglutination end point was estimated by interpolation between complete agglutination and no agglutination; this being 1 haemagglutination unit (HAU). The titre is expressed as HAU per ml.

5.1.2 Haemagglutination-inhibition assay

The titre of unpurified antibodies was determined by their ability to inhibit haemagglutination of the CRBCs by the virus. The antibodies were initially diluted in PBS to the required initial dilution and then 200 µl was added to row 1 of a 96 well round bottom plate (Greiner). This was double diluted across the plate to a final volume of 100 µl. 4 HAU in 25 µl of virus was then added to each well, mixed using the vibrator and incubated for 60 minutes at 20°C. 25 µl of CRBCs at 0.66% were added to each well using a dropper, mixed and incubated for 45 minutes at 20°C. The 50% end point is read as in the haemagglutination assay and the titre is expressed as Haemagglutination-inhibition units (HIU/ml).

5.1.3 Total protein quantitation

Ultra-violet absorbance

Purified protein was diluted in PBS to a final volume of 500 µl. Two quartz cuvettes were prepared, the first containing 500 µl of PBS and the second containing the 500 µl of the protein sample. The two cuvettes were placed in cells 1 and 2 of a UV Spectrophotometer set at a wavelength of 280nm and the cuvette in cell 1 was used as a reference (to determine the background absorbance of the buffer) to set the instrument to zero. The cuvette in cell 2 was then read and output recorded after

allowing to stabilise. The total protein concentration was determined by reference to the extinction coefficient of the specific protein.

Bio-Rad dye binding assay

A standard curve of known concentrations of bovine IgG antibodies was obtained by using the Bio-Rad micro protein assay (Sigma). This involved adding 20 µl of IgG with 1 ml of Bio-Rad reagent (diluted 5-fold in distilled water and filtered through Whatmann filter paper) and incubating for 10 minutes. The samples were then read on a spectrophotometer at a wavelength of 595nm, using 1 ml of Bio-Rad reagent alone as the reference. The standard curve was plotted for the range of IgG concentrations that remained linear against absorbance. Unknown antibody concentrations would then be determined using the micro protein assay and the absorbance value used to calculate the protein concentration from the standard curve.

5.1.4 SDS PAGE analysis of proteins

SDS PAGE analysis was carried out using the Bio-Rad Protean II mini-gel kit (Bio-Rad). This involved analysis of proteins on either 8, 10, or 12% polyacrylamide gels. 10x non-reducing or reducing (containing DTT) loading buffer was diluted 10-fold in the protein sample and boiled for 3 minutes. High molecular weight markers (Amersham) were treated identically. 20 µl of sample were loaded onto the gel, along with PAGE gel running buffer and run at 100 mV until dye front had just left the base of the gel. Gels were fixed with 40% methanol / 10% acetic acid for 30 minutes and then stained with Brilliant Blue Colloidal Coomassie stain (Sigma). The gels were dried on a gel dryer at 80°C for 90 minutes.

5.2 Cell culture

5.2.1 Madin-Darby canine kidney (MDCK) and Baby hamster kidney (BHK) cell culture and maintenance

MDCK cells (a kind gift from Dr W. Barclay, University of Reading) were maintained at 37°C in a humidified atmosphere of 5% CO₂ (Flow), in DMEM (Gibco) supplemented with 0.02 mM glutamine (Gibco) 5% v/v heat inactivated

foetal calf serum (Gibco) and 50 µg/ml of gentamicin (Gibco). Cells were grown in large vented tissue culture flasks (Gibco) and subcultured when a confluent monolayer had formed. The cell monolayers were treated with 15 ml of 0.2% versene for 20 minutes, followed by 5 ml of 0.25% trypsin (Sigma) for 5 minutes at 37°C. The cell suspension was pelleted by low speed centrifugation, resuspended at the appropriate dilution and aliquoted. The number of passages was recorded and the cells were discarded after passage 20.

BHK cells (ECACC) were cultured under similar conditions to the MDCKs and were maintained in GMEM (Gibco) supplemented with 0.02 mM glutamine, 10% heat inactivated FCS and 50 µg/ml gentamicin. They were sub-cultured in a similar manner to the MDCKs except that they were removed from the flask by treatment with 15 ml of 0.2% versene and 1 ml 0.25% trypsin for 5 minutes at 37°C.

5.2.2 Hybridoma cell culture and maintenance (monoclonal antibody production)

The mouse hybridoma cell lines (a kind gift from Dr W. Gerhard, Wistar Institute, Philadelphia, USA) were maintained at 37°C in a humidified atmosphere of 5% CO₂, in RPMI 1640 (Gibco) supplemented with 10% heat inactivated FCS, 2 mM glutamine and 50 µg/ml gentamicin. The cells were grown in either large vented tissue culture flasks (Gibco) or large Integra Cell 2000 flasks (Integra). The cells grown in the large vented flasks were subcultured when confluent by shaking the flasks vigorously to form a single cell suspension. The cells were pelleted by low speed centrifugation and then resuspended in an appropriate dilution and aliquoted.

Hybridoma cells secrete monoclonal antibody (MAb) into the media during growth, hence supernatant was recovered after low speed centrifugation and also harvested 14 days after subculturing. The tissue culture fluid was clarified by low speed centrifugation and the supernatant (containing MAb) was decanted and stored at -20°C.

The large Integra Cell Line 2000 system was used for production of milligram quantities of MAb. The cell compartment of the flask was seeded with 10x10⁶ hybridoma cells and maintained in 15 ml of RPMI 1640 (Gibco) supplemented with 15% FCS, 2 mM glutamine and 50 µg/ml gentamicin. The nutrient compartment contained 1 litre of RPMI 1640 supplemented with 1% FCS, 5 mM glutamine and 10

$\mu\text{g/ml}$ gentamicin and the flask was incubated in a humidified atmosphere of 5% CO_2 at 37°C . The cells were subcultured every 3 days by removing the litre of nutrient medium and then pipetting the 15 ml of cell media from the cell compartment. This was diluted 1 in 2 with fresh cell media and pipetted back into the cell compartment, followed by a fresh litre of nutrient media. The remaining volume of cell suspension was pelleted by low speed centrifugation and the cell pellet was discarded. The supernatant was stored at -20°C .

5.3 Antibodies

5.3.1 Monoclonal antibodies

The hybridoma cell lines for the anti-H1 HA of influenza A/Puerto Rico/8/34 secreting the MAbs (1) H36-4.5-2 (site Sb,IgG2a), (2) H9-D3-4R2 (site Cb, IgG3 – also secretes non-specific IgG1 heavy chains), (3) H37-45-5R3 (site Ca2, IgG3), (4) H16-S53-1 (site Sa, IgG2b – also secretes non-specific IgG1 heavy chains) and (5) H37-66-1 (site Sb, IgA) (Caton *et al.*, 1982; Staudt and Gerhard, 1983) were kindly provided by Dr W. Gerhard (Wistar Institute, Philadelphia, USA). The hybridoma cell lines for the anti-NP MAbs, HB-65 (IgG2a) and HB-67 (IgG1) were obtained from R.G. Webster (St Jude Children's Research Hospital, Tennessee).

The ascitic fluids containing the anti-H1 HA from influenza A/Puerto Rico/8/34 MAbs (1) Y8-10C2 (site Sb, low pH HA conformation), (2) H3-4C5 (site Ca2, low pH HA conformation), (3) H2-4C2 (site Cb, low pH HA conformation), (4) H18-S13 (site Cb, low pH HA conformation) and (5) H17-L2 (site Ca2, native HA conformation) (Yewdell *et al.*, 1983) were kindly supplied by Dr W. Gerhard (Wistar Institute, Philadelphia, USA). The ascitic fluids were aliquoted and stored at -20°C .

5.3.2 Antibody Purification

The tissue culture fluids containing IgG MAbs were purified by affinity chromatography, using protein A-Sepharose (Sigma) column under low salt conditions. The tissue culture fluid was adjusted to pH 8 by addition of 100 mM Tris/HCL (pH 8) and then passed through the column approximately 5 to 6 times.

The column was washed by the addition of 10 column volumes of 100 mM Tris/HCL (pH 8), followed by 10 column volumes of 10 mM Tris/HCL (pH 8). The bound IgG was eluted in 1ml fractions of 100 mM glycine (pH 3) and the pH of the fractions was raised by the addition of 100 μ l of 1M Tris/HCL (pH 8). The protein content of the fractions was then analysed by the Bio-Rad dye binding assay and the peak fractions were pooled.

The fractions were then concentrated using an Amicon 8010 stirred pressure concentrator (Amicon) with a 10 KD molecular weight cut-off filter. The final concentrated antibody was dialysed overnight in 3 changes of PBS and then quantified using A280nm analysis.

5.3.3 Production of Fabs by proteolytic digestion of IgG

Protein A purified IgG was used in 1 mg aliquots in the production of Fabs with immobilised papain (Sigma).

Reaction conditions for digestion of IgG2a MAbs

6.2 μ l fresh 0.01 M cysteine (Sigma), 20 μ l of EDTA and 1U of agarose immobilised papain (10U rehydrated with 1 ml PBS) was added to 1 mg of IgG2a and the final volume made up to 1 ml with 200 mM sodium acetate, pH 5.5. This was incubated for 3 hours in a shaking water bath at 37°C.

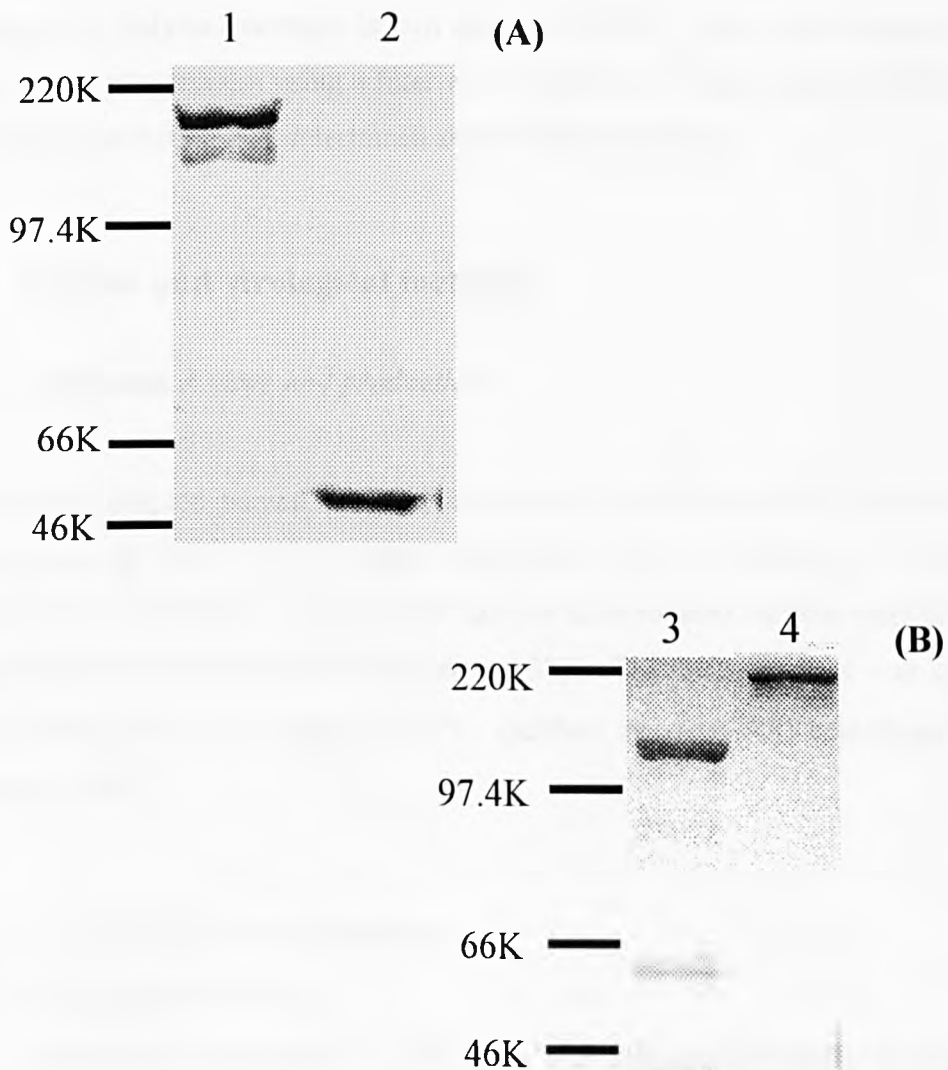
Reaction conditions for digestion of IgG3 MAbs

6.2 μ l fresh 1 M cysteine (Sigma), 20 μ l of EDTA and 1U of agarose immobilised papain (10U rehydrated with 1 ml PBS) was added to 1 mg of IgG2a and the final volume made up to 1 ml with 200 mM sodium acetate, pH 5.5. This was incubated for 1 hour in a shaking water bath at 37°C.

Both types of reactions were stopped by brief microcentrifugation to pellet immobilised papain, followed by 100 μ l of 55 mM Iodoacetamide (Sigma) and 100 μ l 1 M Tris/HCl (pH 8). The Fab samples were repeatedly passed down a protein A column to remove undigested IgG and Fc fragments, followed by dialysis overnight in two changes of PBS. The Fabs were concentrated in the Amicon concentrator using a filter with a 10KD molecular weight cut-off and the protein concentration was determined spectrophotometrically. The Fab preparation was then analysed by PAGE and stained with sensitive colloidal coomassie to check purity of sample (Figure 5.1). All Fab preparations had undetectable levels of IgG

contamination which in this system was <50 ng/ml of IgG. This was assumed to be a negligible quantity in terms of biological activity.

Figure 5.1 PAGE gel analysis to show level of contaminating IgG in (A) a H36 Fab preparation and (B) a H36 F(ab)₂ preparation. Fab was analysed on an 8% PAGE gel, whilst F(ab)₂ were run on a 10% PAGE gel. All samples were mixed with non-reducing loading buffer and stained for protein with colloidal coomassie brilliant blue G25 (Sigma). Lane 1, IgG (Mr ~ 160K); 2, Fab (Mr ~ 55K); 3, F(ab)₂ (Mr ~ 110K); 4, IgG (Mr ~ 160K).



5.3.4 Production of F(ab)₂ by proteolytic digestion of IgG

Protein A purified IgG was used in 0.5 mg aliquots in the production of F(ab)₂ with immobilised pepsin (Sigma).

Reaction conditions for digestion of IgG2a MAbs

500U of pepsin (10000U rehydrated with 5 ml PBS) was added to 0.5 mg of IgG and made up to 1 ml with 0.1 M sodium citrate, pH 3.5. This was incubated for 8 hours in a shaking water bath at 37°C.

The reaction was stopped by brief microcentrifugation to pellet immobilised pepsin, followed by 100 µl 3 M Tris/HCl (pH 8) to neutralize the pH. The F(ab)₂ samples were repeatedly passaged down a protein A column to remove undigested IgG, followed by dialysis overnight in two changes of PBS. They were concentrated in the Amicon concentrator using a filter with a 10KD molecular weight cut-off and the protein concentration was determined spectrophotometrically.

5.4 Viruses and virological methods

5.4.1 Influenza A virus and production

The mouse adapted human strain of influenza A/Puerto Rico/8/34 (H1N1) (PR/8) was grown up from the #593 stock preparation (Dr S. Armstrong, University of Warwick) in the allantoic cavity of 10 day old embryonated chicken eggs (Poynden Egg Farm) and incubated for 48 hours at 33°C. The allantoic fluid was collected after chilling the eggs overnight at 4°C, clarified by low speed centrifugation and stored at -70°C.

5.4.2 Assessment of titre of influenza A

(1) Haemagglutination assay

As described previously to determine the haemagglutination units per ml (HAU/ml) of the new virus stock (this value gives approximate virus particle

numbers, as 1 HAU = 10^6 virus particles, but does not provide any information on the infectivity of the virus preparation) (Barrett and Inglis, 1985).

(2) Plaque assay

MDCK monolayers were grown overnight on 6-well cell culture plates (Falcon) and washed with PBS. The virus was serially diluted in PBS and then 100 μ l was inoculated (in duplicate) onto the MDCK monolayers and incubated for 45 minutes at 20°C. The infected monolayers were then overlaid with 0.9% agar (Gibco) in 199 medium (buffered with 5 to 8ml of sodium bicarbonate) containing 0.2% (v/v) bovine serum albumin (BSA) in PBS (Sigma), 0.01% (v/v) DEAE dextran (Sigma) in PBS, 100 U/ml penicillin/100 μ g/ml streptomycin and 30 U/ml TPCCK trypsin (Sigma). The infected monolayers were incubated for 3 days at 33°C in a humidified atmosphere of 5% CO₂ in air before fixing with 10% formal-saline for 10 minutes and staining with 1% Toluidine blue (BDH). The infectivity was expressed as plaque forming units per ml (pfu/ml).

5.4.3 Purification of influenza A

The allantoic fluid was clarified by low speed centrifugation to remove cell debris. The virus was then pelleted in a type 19 fixed angle rotor (Beckman) at 60000-x g for 120 minutes in a Beckman ultra-centrifuge. The pellets were soaked overnight in 500 μ l of PBS, resuspended and then vigorously vortexed. This was loaded onto a 10-45% (w/v) linear sucrose gradient and centrifuged at 60000-x g for 90 minutes. The visible bands were harvested and tested by HA assay to determine peak virus band. This band was pelleted at 110000-x g for 90 minutes and pellets were soaked in 200 μ l of PBS overnight. The pellets were resuspended, vortexed vigorously and loaded onto a 20-70% (w/v) linear sucrose gradient. This was centrifuged at 60000-x g for 16 hours and the visible virus band was harvested. The harvested band was diluted in PBS and pelleted at 110000-x g for 90 minutes. The pellet was soaked in 100 μ l PBS overnight, resuspended, aliquoted and stored at -70°C.

5.4.4 *Influenza A neutralization assay*

5.4.4.1 *Neutralization assay by reduction of cytopathic effect*

100 pfu/ml of influenza A was mixed with an equal volume of dilutions of MAb for 60 minutes at 37°C to allow neutralization to occur. 100 µl of the virus/MAb mix was inoculated onto the centre of washed MDCK monolayers in 6-well plates (or BHK) (grown overnight) and incubated for 45 minutes at 20°C. The monolayers were overlaid with a 1 to 1 mix of 0.9% agar (Gibco) and 199 medium (buffered with 5 to 8ml of sodium bicarbonate), containing 0.2% (v/v) bovine serum albumin (BSA) in PBS (Sigma), 0.01% (v/v) DEAE dextran (Sigma) in PBS, 100U/ml penicillin / 100 µg/ml streptomycin and 30 U/ml TPCK trypsin (Sigma). The infected monolayers were incubated for 3 days at 33°C in a humidified atmosphere of 5% CO₂ in air before fixing with 10% formal-saline for 10 minutes and staining with 1% Toluidine blue (BDH). The number of plaques were counted for each antibody dilution and calculated as a percentage of the virus control (virus incubated with an equal volume of PBS) and subtracted from 100 to give the percentage neutralization.

5.4.4.2 *Neutralization Enzyme-Linked Immunosorbent assay (ELISA)*

This ELISA was adapted from (Benne *et al.*, 1994). Virus in 0.5% BSA/PBS was incubated with an equal volume of dilutions of MAb in 0.5% BSA/PBS for 60 minutes at 37°C to allow neutralization to occur. 100 µl of the virus/MAb mix was inoculated onto a washed MDCK monolayer in a 96 well cell culture plate (Gibco) and incubated for 25min at 4°C. The plate were washed three times by hand with DMEM and then 100 µl of warm DMEM, supplemented with 1% FCS, 2 mM glutamine and 20 µg/ml gentamicin (maintenance media) was added and the plate were incubated overnight at 37°C in an humidified atmosphere to allow one replication cycle of the attached infectious virus. The cells were washed by hand with DMEM and fixed by the addition of 100 µl of 2% paraformalehyde for 15 minutes. The fixed plates were washed using a plate washer on a fixed programme that washed the plate 4 times in TBS/tween and then the plate was blocked with 3% BSA/TBS for 90 minutes at 20°C. The *de novo* expressed HA on the cell surface was then used as a marker of virus replication and detected by the addition of 100 µl

of mouse anti-HA IgA (H37-66-1) in 1%BSA/TBS-tween for 90 minutes at 37°C. The plate was washed with the plate washer and the bound IgA was detected by the addition of 100 µl of anti-IgA alkaline phosphatase conjugate (Sigma) diluted 1 in 30000 in 1% BSA/TBS-tween for 60 minutes at 37°C. The final wash using the plate washer was followed by the addition of 100 µl of p-nitrophenyl phosphate (PNPP) alkaline phosphatase substrate tablets, diluted 2 tablets to 10 ml of diethanolamine buffer at 37°C. The plate was read every 15 minutes on a titertek Lab systems optical plate reader (Life Sciences International) with a 405nm filter until the virus control had an optical density of approximately 1.0 to 1.2.

5.4.5 Post-attachment neutralization (PAN) assay

5.4.5.1 PAN by plaque reduction

100 µl of 50 pfu/ml of cold virus was inoculated onto the centre of a washed MDCK (or BHK) monolayer, that had been pre-chilled, and incubated for 20 minutes at 4°C. The monolayer was washed 3 times with cold DMEM and then inoculated with 100 µl of a series of MAb dilutions for 60 minutes at 37°C (or 120 minutes at 4°C). The monolayers were washed 3 times with DMEM by hand and overlaid as described in section 5.5.4.1. The infected monolayers were incubated for 3 days at 33°C in a humidified atmosphere of 5% CO₂ in air before fixing with 10% formal-saline for 10 minutes and staining with 1% Toluidine blue (BDH). The number of plaques were counted for each antibody dilution and calculated as a percentage of the virus control (virus incubated with an equal volume of PBS) and subtracted from 100 to give the percentage neutralization.

5.4.5.2 Post-attachment neutralization ELISA

Virus was pre-chilled at 4°C and 100 µl was inoculated onto a MDCK (or BHK) monolayer in a 96 well cell culture plate (Gibco) for 20 minutes at 4°C. The plate was washed 3 times by hand with cold DMEM and then inoculated with 100 µl of a series of dilutions of MAb for 60 minutes (or 120 minutes at 4°C) at 37°C. The plate was washed three times by hand with DMEM and then 100 µl of warm DMEM, supplemented with 1% FCS, 2 mM glutamine and 20 µg/ml gentamicin

(maintenance media) was added and the plate were incubated overnight at 37°C in an humidified atmosphere to allow one replication cycle of the attached infectious virus. The cells were washed by hand with DMEM and fixed by the addition of 100 µl of 2% paraformaldehyde for 15 minutes. The fixed plates were washed using a plate washer on a fixed programme that washed the plate 4 times in TBS/tween and then the plate was blocked with 3% BSA/TBS for 90 minutes at 20°C. The *de novo* expressed HA on the cell surface was then used as a marker of virus replication and detected as described previously in section 5.5.4.2.

5.5 Mechanisms of neutralization assays

5.5.1 *Influenza attachment detection ELISA*

1000 HAU/ml of virus in 0.5% BSA/PBS was incubated with an equal volume of dilutions of MAb in 0.5% BSA/PBS for 60 minutes at 37°C to allow neutralization to occur. 100 µl of the virus/MAb mix was inoculated onto a washed MDCK monolayer in a 96 well cell culture plate (Gibco) and incubated for 25 minutes at 4°C. The plates were washed three times by hand with cold DMEM and then the cell monolayers and attached virus was fixed and permeabilised with 100 µl of methanol at -20°C for 20 minutes. The fixed plates were washed using a plate washer on a fixed programme that washed the plate 4 times in TBS/tween and then the plate was blocked with 3% BSA/TBS overnight at 4°C. The next stage involved detection of the internalised nucleoprotein of the attached permeabilised virus. Therefore, after the plates were washed, 100 µl of 5 µg/ml of anti-NP MAb (either HB-65, IgG2a or HB-67, IgG1, depending on the isotype of MAb used to neutralize the virus) in 1% BSA/TBS-tween was added for 90 minutes at 37°C. After a further wash using the plate washer, 100 µl of a 1 in 2000 dilution in 1% BSA/TBS-tween of either rabbit anti-mouse IgG1 or IgG2a was added and incubated for 60 minutes at 37°C. Following washing, the bound anti-species antibody was detected by the addition of 100 µl of goat anti-rabbit alkaline phosphatase conjugate (Dako) diluted 1 in 2000 in 1% BSA/TBS-tween for 60 minutes at 37°C. The final wash was followed by the addition of 100 µl of PNPP alkaline phosphatase substrate tablets diluted 2 tablets to

10 ml of diethanolamine buffer diluted five-fold in distilled water at 37°C. The plate was read every 15 minutes on a titertek Lab systems optical plate reader with a 405nm filter until the virus control had an optical density of approximately 1.0 to 1.2.

5.5.2 Endosomal internalisation detection ELISA

1500 HAU/ml of virus in 0.5% BSA/PBS was incubated with an equal volume of dilutions of MAb in 0.5% BSA/PBS for 60 minutes at 37°C to allow neutralization to occur. 100 µl of the virus/MAb mix was inoculated MDCK (or BHK) monolayer in a 96 well cell culture plate (Gibco) and incubated for 20 minutes at 4°C. The plates were washed three times by hand with cold DMEM, followed by the addition of 100 µl of warm DMEM for 30 minutes at 37°C, to allow the attached virus to internalise into the cell. The plates were again washed 3 times with cold DMEM and then in order to remove uninternalised virus they were treated with 50 µl of 0.5 U/ml of neuraminidase (from clostridium perfringens) (Sigma) in PBS for 10 minutes at 37°C. This was repeated and the cell monolayers were freeze-fractured by incubating at -20°C for 10 minutes, followed by an incubation at 37°C for 5 minutes. This was repeated twice and the cells were fixed and permeabilised by the addition of 100 µl of methanol for 30 minutes at -20°C. The fixed plates were washed using the plate washer on a fixed programme that washed the plate 4 times in TBS/tween and then the plate was blocked with 3% BSA/TBS overnight at 4°C. The plates were washed, followed by the addition of 100µl of 5µg/ml of anti-NP MAb (either HB-65, IgG2a or HB-67, IgG1) in 1%BSA/TBS-tween for 90 min at 37°C, to detect the internal nucleoprotein of internalised virus. The bound anti-NP MAb was detected as described in section 5.6.1.

Controls used in this assay to show that the signal detected was indeed internalised virus antigen included (1) incubation at 4°C so that internalisation was not permitted (Matlin *et al.*, 1981; Richman *et al.*, 1986) and (2) pre-incubating the cell monolayer with a hypertonic medium (0.45 M NaCl / HBS) for 30 minutes at 20°C before inoculation of virus as this treatment prevents formation of correct clathrin lattice and hence inhibits receptor-mediated endocytosis (Heuser and Anderson, 1989; Hansen *et al.*, 1993).

5.5.3 Fusion assays

5.5.3.1 Inhibition of hemolysis of CRBCs by influenza virus

Hemolysis and hemolysis inhibition assays were adapted from (Sato *et al.*, 1983). Neat (8%) CRBCs (Serotec) were pelleted at 2500-x g for 1 minute and washed with cold PBS. 10000 HAU/ml of virus was mixed with 200 µl of washed CRBCs and incubated for 30 minutes at 4°C on a rotating blood mixer. Unattached virus was removed by pelleting the CRBCs by brief centrifugation and washing in 1 ml of cold PBS. This was repeated and then 200 µl of a series of dilutions of MAb was mixed with the cells for 60 minutes at 37°C. The CRBCs were then pelleted and washed as described previously, followed by the addition of 250 µl of citrate buffer, pH 5 for 45 minutes at 37°C. The cells were then pelleted and 200 µl of the supernatant was placed into a 1 ml plastic cuvette. The supernatants from the hemolysed samples were diluted with 800 µl of PBS and then the OD read at 520nm on a spectrophotometer. The percentage inhibition of hemolysis was calculated by comparing the extent of hemolysis in the virus control to the reduction of hemolysis caused by the neutralizing MAb.

5.5.3.2 Analysis of fusion inhibition by MAbs with octadecyl rhodamine-B-choride (R18) labelled virus

(1) Preparation of R18 labelled virus stock –

500 µl of 250×10^5 HAU/ml of freshly prepared purified virus was mixed with 5 µl of R18 (Molecular probes, Europe) for 60 minutes at 20°C in the dark (final concentration of 85.5 µM). The virus-R18 mix was centrifuged at 10000-x g for 2 minutes to pellet precipitate. Pelleting the virus through a 20% sucrose cushion at 110,000g for 90 minutes was carried out to remove free R18 label. The remaining pellet was resuspended in 100 µl of PBS and then stored at -70°C. Solubilisation of the labelled virus in 1% Triton X-100 (BDH) led to an ~150-fold increase in fluorescence, indicating that the R18 was highly self-quenched and incorporated into the virus lipid bilayer.

(2) Fusion assay using R18 labelled virus –

100 µl of 2000 HAU/ml of non-neutralized or neutralized R18 labelled virus was inoculated onto the middle of MDCK or BHK cell monolayer in a 3 cm dish and allowed to attach for 25 minutes at 4°C. Unbound virus was removed by washing 3 times by hand with cold DMEM, followed by the addition of 200 µl of warm DMEM for 30 minutes at 37°C. After a further wash with cold DMEM 500 µl of cold versene was added to the cells for 5 minutes at 20°C. The cells were then suspended by scraping, pelleted at 2500-x g and resuspended in cold 2% paraformaldehyde on ice in the dark. Fluorescence was determined using a Perkin-Elmer fluorescence spectrophotometer, exciting at 560nm and emitting at 590nm, with a slit length of 10cm.

Negative controls used to determine that increase of fluorescent signal was due to virus-cell fusion was (1) labelled virus and cells kept at 4°C to inhibit fusion and (2) cells were pre-treated with 500 nM bafilomycin-A1 (from *Streptomyces griseus*) (Calbiochem) for 15min at 37°C prior to infection (Yoshimori *et al.*, 1991; Palokangas *et al.*, 1994; Guinea and Carrasco, 1995). The bafilomycin is a potent V-ATPase inhibitor and prevents acidification of endosomal vesicles in the cell, which inhibits low pH activated fusion.

5.6 Assays to investigate the nature of the inhibition of fusion by MAb and Fab fragments

5.6.1 Inhibition of hemolysis of CRBCs by influenza virus at a pre-fusion intermediate stage

Neat (8%) CRBCs (Serotech) were pelleted at 2500-x g for 1 minute and washed with cold PBS. 10000 HAU/ml of virus was mixed with 200 µl of washed CRBCs and incubated for 30 minutes at 4°C on a rotating blood mixer. Unattached virus was removed by pelleting the CRBCs by brief centrifugation and washing in 1 ml of cold PBS. This was repeated and followed by the addition of 200 µl cold citrate buffer, pH 5 for 30 minutes at 4°C, in order to trigger the pre-fusion intermediate (Tsurudome *et al.*, 1992; Pak *et al.*, 1994). The virus-CRBC complexes were then pelleted and washed twice with 1 ml of cold PBS, pH 8. 200 µl of a series of

dilutions of MAb in PBS, pH 7.5, were mixed with the cells for 60 minutes at 37°C. The CRBCs were then pelleted and washed as described previously, followed by the addition of 250 µl of citrate buffer, pH 5 for 45 minutes at 37°C. The cells were then pelleted and 200 µl of the supernatant was placed into a 1 ml plastic cuvette. The supernatants from the hemolysed samples were diluted with 800 µl of PBS and then the optical density read at 405nm on a spectrophotometer. The percentage inhibition of hemolysis was calculated by comparing the extent of hemolysis in the virus control to the reduction of hemolysis caused by the neutralizing MAb.

5.6.2 Low pH conformational change detection ELISA

1000 HIU/ml of anti-HA IgA (H37-66-1) in PBS was coated to an ELISA plate overnight at 4°C. This was washed using the plate washer and blocked with 3% BSA/TBS-tween for 120 minutes at 20°C. The IgA coated plate was then used to capture virus by adding 100 µl of 1000 HAU/ml of virus for 45 minutes at 4°C. This experiment was also carried out using a monolayer of paraformaldehyde-fixed MDCK cells to capture virus in order to determine if binding to the cell receptor had an influence on HA conformation. The unbound virus was removed by washing 3 times by hand with DMEM and the remaining bound virus was neutralized with 50 µl of Fab for 60 minutes at either 4°C or 37°C. This was washed 3 times by hand and then 100 µl of citrate buffer was added, with half the plate being treated with pH 5 and the other control half being treated with pH 7.5, for 30 minutes at either 4°C or 37°C. The pH was neutralized by washing 3 times with PBS, pH 8, followed by 100 µl of a series of dilutions of the conformation-specific MAbs in 1% BSA/TBS-tween for 60 minutes at 4°C. The unbound MAb was removed by washing 3 times with DMEM and then the plates were fixed with methanol for 20 minutes at -20°C. The fixed plates were blocked with 3% BSA/TBS-tween for 90 minutes at 20°C and then washed using the plate washer. The bound conformational MAbs were detected using a 1 in 30000 dilution of rabbit anti-mouse IgG Fc region alkaline phosphatase conjugate in 1% BSA/TBS-tween (Sigma) for 90 minutes at 37°C. The final wash was followed by the addition of 100 µl of PNPP alkaline phosphatase substrate

tablets diluted 2 tablets to 10 ml of diethanolamine buffer diluted five-fold in distilled water at 37°C.

5.6.3 Proteinase-K digestion resistance assay

Purified virus at 200,000 HAU/ml was neutralized with an equal volume of MAb or Fab for 60 minutes at 37°C. The pH of the neutralization mix was then either lowered to pH 5 by the addition of 0.1 M HCl, or kept at pH 7.5 (for the controls) and incubated for 30 minutes at 37°C. The pH of the neutralization mix was increased to pH 7.5 by the addition of 0.1 M Tris/HCl, pH 8. In order to determine whether the treatment had caused the virus HA to adopt its low pH conformation or whether this change had been inhibited by the antibody, an equal volume of proteinase-K was added at 1 µg/ml in PBS for 30 minutes at 37°C. The HA is only susceptible to cleavage by this enzyme in its low pH conformation and hence the ability to cleave the HA of neutralized virus can act as a marker of whether the antibody can inhibit the low pH-induced conformational changes. The digestion reaction was stopped by the addition of 10x cracking buffer and the reaction mix could then be stored at -70°C. To analyse the digestion, 25 µl of the mix was run on a 12% PAGE gel under reducing conditions and then stained with Brilliant-Blue colloidal coomassie.

5.6.4 Determination of acid sensitivity of MAb binding by ELISA

An IgA coated ELISA plate was prepared as described previously and then blocked with 3% BSA/TBS-tween for 90 minutes at 20°C. 100 µl of virus at 1000 HAU/ml was then added to the plate and incubated for 45 minutes at 37°C. Unbound virus was removed by washing 3 times by hand with DMEM, followed by 100 µl of citrate buffer at either pH 5 or pH 7.5 for 30 minutes at 37°C. The pH was then increased to pH 7.5 by washing 3 times in PBS at pH 7.5. The captured virus was neutralized with the addition of 50 µl of MAb for 60 minutes at 37°C. Following MAb binding unbound MAb was removed by washing 3 times with DMEM and then the virus – MAb complexes were fixed by the addition of methanol at -20°C. The fixed plates were blocked with 3% BSA/TBS-tween for 90 minutes at 20°C and then washed using the plate washer. The bound MAbs were detected using a 1 in 30000 dilution

of rabbit anti-mouse IgG alkaline phosphatase conjugate in 1% BSA/TBS-tween (Sigma) for 90 minutes at 37°C. The final wash using the plate washer was followed by the addition of 100 µl of PNPP alkaline phosphatase substrate tablets diluted 2 tablets to 10 ml of diethanolamine buffer diluted five-fold in distilled water at 37°C. Determination of the effect of the low pH HA conformation on MAb binding was made by comparing binding levels on pH 7 virus and pH 5 virus.

5.7 Kinetic analysis of the MAbs and their Fab fragments using the BIAcore 2000

Method for kinetic analysis of MAbs was adapted from Schofield and Dimmock, (1996).

5.7.1 Surface immobilisation

MAb H37-45-5R3 was covalently coupled to a biosensor chip, CM5, by an amine coupling procedure. Initially the chip surface was normalised by washing the surface with a 40% glycerol solution, in order to equalise the dextran polymer coating on the chip surface to reduce non-specific binding of the ligand and to equalise the responses of the 4 lanes. Activation of the bonds on the dextran polymer coated chip surface was carried out by the injection of 40 µl of a 1 to 1 mix of EDS and NHS (BIAcore) over the chip surface at a flow rate of 10 µl/min. MAb H37-45-5R3 at 50 µg/ml in sodium acetate buffer, pH 5, was injected only over lane 2 of the sensor chip at a flow rate of 10 µl/min, using the manual injection system so that the amount of MAb bound to the chip surface could be monitored and stopped at 9000 resonance units (RU). Remaining active sites on lanes 1 and 2 were blocked by the injection of 40 µl of ethanolamine buffer (BIAcore) at a flow rate of 10 µl/min, with the extraclean command which washing the flow cells with buffer at 100 µl/min for a couple of seconds. MAb bound unspecifically was removed by injecting 30 µl of 0.05 M triethylamine (Sigma) at a flow rate of 20 µl/min.

5.7.2 Virus capture

40 μl of purified virus at 8000 HAU/ml, diluted in 100 mg/ml CM5 dextran/HBS (prevents non-specific interactions with chip surface) (BIAcore) was injected over lanes 1 and 2 in the 2-1 detection mode at a flow rate of 20 $\mu\text{l}/\text{min}$. The 2-1 detection mode subtracts signal from the blank control, lane 1, from signal in lane 2, so that bulk refractive index changes are removed and the sensorgram 2-1 shows actual binding events. Following the injection the flow cells were washed using the extraclean command and the virus baseline was left to stabilise for 300 seconds. Approximately 700 RU of virus was bound and used for kinetic analysis of MAbs and Fabs.

5.7.3 Measurement of kinetic binding

Kinetic measurements for each of the MAb/Fab pairs were made simultaneously on the same chip surface (separate chip for each MAb/Fab pair) to minimise effect of surface differences on kinetics and over at least 3 different concentrations. 40 μl of the antibodies, diluted in HBS buffer, was injected over lanes 1 and 2 using the kininject command, at a flow rate of 20 $\mu\text{l}/\text{min}$ and a dissociation time of 600 seconds. After the dissociation the chip surface was regenerated back to the covalently coupled H37 baseline by 2 injections of 30 μl of 0.05 M triethylamine and 1 injection of 20 μl of 0.05 M triethylamine at a flow rate of 20 $\mu\text{l}/\text{min}$. At this stage the sensorgram cycle was stopped and before a new cycle started the Flush command was used to wash the IFC and flow cells with HBS buffer to remove any contaminating triethylamine.

5.7.4 Data evaluation

The kinetics of the binding of the MAbs and Fabs was analysed using the BIA evaluation software package (version 2.2). The data for each concentration of antibody was fitted locally to a Langmuir 1 to 1 binding model, with the dissociation and association rates being calculated separately. Initially the rate of dissociation (k_d) was calculated by selecting 300 seconds of dissociation data (kept constant to compare MAbs and Fabs) and this rate was used along with the analyte concentration in moles (M) to determine the association rate (k_a). The mean of the equilibrium

dissociation constants (K_d) for the antibody was calculated to determine the overall affinity.

5.8 Reversibility of neutralization and HI with ammonium hydroxide (AmOH)

5.8.1 Reversibility of neutralization and HI of virus neutralized in solution

The method was adapted from Schofield (1996). 100 μ l of virus at 20000 HAU/ml was incubated with an equal volume of MAb in PBS for 60 minutes at either 4 or 37°C. The virus-antibody mix was then added to an equal volume of 0.1 M AmOH, pH 11.5 for 30 minutes at 4°C. The virus and antibody were then separated by passing 100 μ l down a Sephacryl S1000 (5cm³ gel bed volume), which had previously been equilibrated with 0.1 M AmOH, pH 11.5. The virus, due to its size, was eluted in the void volume of the column and collected in 100 μ l fractions of 0.1 M AmOH, pH 11.5. The fractions were then neutralized by the addition of 25 μ l of 1 M Tris/HCl, pH 8 and the presence of virus assayed by the HA assay. The 3 peak fractions were then diluted between 100- and 10000-fold in PBS and the infectivity determined by plaque assay.

5.8.2 Reversibility of neutralization and HI of virus attached to a cell receptor

100 μ l of virus at 20000 HAU/ml was mixed with 200 μ l of CRBCs at 8% (pre-washed in PBS) for 30 minutes at 4°C on a rotary blood mixer. Unbound virus was removed by pelleting the CRBCs by brief centrifugation and washing in 1 ml of cold PBS. This was repeated twice and then the pellet of CRBCs were resuspended in 200 μ l of MAb, diluted in PBS, for 60 minutes at either 4 or 37°C. The CRBC-virus-antibody complexes were washed as described above and then resuspended with 200 μ l of 1 U/ml of neuraminidase (from *Clostridium perfringens*) (Sigma) in PBS for 60 minutes at 37°C, to elute the virus-MAb complexes from the cell surface. The CRBCs were pelleted by brief centrifugation and the supernatant containing the virus was mixed with an equal volume of 0.1 M AmOH, pH 11.5, for 30 minutes at 4°C. The virus and antibody were then separated by passing 100 μ l down a

Sephacryl S1000 (5cm³ gel bed volume), which had previously been equilibrated with 0.1M AmOH, pH 11.5. The virus due to its size was eluted in the void volume of the column and collected in 100 µl fractions of 0.1M AmOH, pH 11.5. The fractions were then neutralized by the addition of 25 µl of 1 M Tris/HCl, pH 8 and the presence of virus assayed by the HA assay. The 3 peak fractions were then diluted between 100- and 10000-fold in PBS and the infectivity determined by plaque assay.

The effect of temperature on the reversibility of HI and neutralization of virus attached to CRBCs was investigated by incubation by the CRBC-virus-antibody complexes in waterbaths set at different temperatures.

The reversibility of HI and neutralization of virus attached to different cell types and a soluble receptor was also analysed using the following –

- (1) 5x10⁶ MDCK cells/ml
- (2) 4x10⁶ H9 T-cells/ml
- (3) 4 mg/ml fetuin (Sigma)

5.8.3 Kinetics of the reversibility of HI and neutralization of virus attached to CRBCs.

Virus was attached to CRBCs at 4°C as described above. Ten individual samples were prepared to represent each of the time points. Unbound virus was removed by pelleting the CRBCs by brief centrifugation and washing in 1 ml of cold PBS. This was repeated twice and then the pellet of CRBCs were resuspended in 200 µl of MAb, diluted in PBS, for 60 minutes at either 4°C. Unbound MAb was removed by pelleting the CRBCs by brief centrifugation and washing in 1 ml of cold PBS. The CRBC-virus-MAb complexes were resuspended in warm PBS and placed in a 37°C waterbath. At 2 minute intervals a sample was removed and 200µl of 1 U/ml bacterial neuraminidase was added for 30 minutes at 37°C. The CRBCs were then pelleted and the supernatant containing the released virus was stored at 4°C. At the end of the time course each of the supernatants was mixed with an equal volume of

0.1M AmOH, pH 11.5 for 30 minutes at 4°C. The virus and MAb were separated and sampled as described above.

5.8.4 Quantitation of the removal of virus from the CRBCs by bacterial neuraminidase.

5.8.4.1 Biotinylated virus detection ELISA.

2 mg of freshly prepared and purified virus were biotinylated using the Sulfo-NHS biotinylation kit according to the manufacturer's instructions. ELISA plates were coated overnight with the HA specific H16 IgG at 10 µg/ml in PBS, followed by blocking with 3% BSA/TBS-T for 120 minutes. Biotinylated virus was used then in the reversibility of neutralization of virus attached to CRBCs as described previously. The supernatant containing released virus after treatment of the cells with bacterial neuraminidase was serially diluted in PBS and added to the ELISA plate overnight at 4°C. The plates were then washed four times using the plate washer, followed by 100 µl of a 1 in 5000 dilution in 1% BSA/TBS-T of streptavidin-alkaline phosphatase conjugate for 60 minutes at 37°C. The plate was again washed using the plate washer and then 100 µl of PNPP alkaline phosphatase enzyme substrate was added and incubated at 37°C. Quantitation of the recovery of virus from the CRBCs was made possible as known concentrations of biotinylated virus were used as positive controls and used to draw a standard curve of optical density at 405nm and HAU.

5.8.5 Neuraminidase assay.

The method was carried out as described by (Barrett and Inglis, 1985). Briefly, 100 µl of a virus sample was added to 10 mg/ml of the fetuin substrate in 0.2 M sodium phosphate buffer, pH 6 and incubated for 120 minutes at 35°C. 100 µl of periodate reagent was added for 20 minutes at 20°C, followed by 1 ml of arsenite reagent. This was followed by 2.5 ml of thiobarbituric acid reagent, which was vortexed and then placed in a boiling water bath for 15 minutes. The solution was allowed to cool on ice for 5 minutes, followed by the addition of 4 ml of acidified-butanol. This was

vortexed and then centrifuged at 913-x g for 10 minutes. Results were read on a spectrophotometer at 549nm and compared to a calibration curve.

5.8.6 Reversibility of HI and neutralization of virus attached to CRBCs and then treated with low pH at 4°C.

Virus was attached to CRBCs as described in section 5.9.2. Attached virus was neutralized with MAb for 60 minutes at 4°C. Unbound MAb was removed by pelleting the cells by brief centrifugation. The CRBC-virus-MAb complexes were then resuspended in PBS, pH 5, and incubated for 30 minutes at 4°C. The cells were then pelleted and washed three times with cold PBS, pH 7.5. The CRBC-virus-MAb complexes were then resuspended in 1 U/ml bacterial neuraminidase for 60 minutes at 4°C. The recovered virus was treated with AmOH at 4°C, separated from antibody and assayed as described in section 5.9.2.

5.9 List of reagent suppliers

(Amicon)	Amicon Ltd, Stonehouse, UK
(Amersham)	Amersham International Plc, UK
(BDH)	Merck Ltd, Lutterworth, UK
(Beckman)	Beckman-RIIC, High Wycombe, UK
(Biacore)	Biacore-AB, Uppsala, Sweden
(Bio-Rad)	Bio-Rad Life Sciences, Hemel Hempstead, UK
(Calbiochem)	Novabiochem (UK) Ltd, Beeston, UK
(Dako)	Dako Ltd, Ely, UK
(ECACC)	European Collection of Animal Cell Cultures, Porton Down, UK
(Falcon)	Fahrenheit Lab supplies, Milton Keynes, UK
(Gibco)	GibcoBRL Life Technologies, Paisley, UK
(Greiner)	Greiner, Stonehouse, UK
(Integra)	Integra Bioscience Ltd, Letchworth, UK
(Life Sciences International)	Life Sciences International, Basingstoke, UK

(Molecular probes)

Molecular Probes Europe BV, Leiden, The Netherlands

(Poynden Egg Farm)

Poynden Egg Farm, Goss Oaks, Herts, UK

(Serotech)

Serotech, Kidlington, UK

(Sigma)

Sigma, Poole, UK

6 Results: Comparison of the mechanism of neutralization of influenza A/PR/8/34 virus by monoclonal IgGs and their fragments.

6.1 Introduction

This chapter examines the relevance of antibody valency, molecular mass and affinity on the efficiency of neutralization of virus in free solution. Previous studies using Fabs from polyclonal antibodies and more recently from monoclonal antibodies (MAbs) have shown that they have a significantly lower neutralization efficiency than their parent antibodies (Lafferty, 1963; Yoden *et al.*, 1985; Kida *et al.*, 1985; Schofield *et al.*, 1997b).

A number of explanations have been proposed. For example, a study using Fabs produced from polyclonal antibodies showed that dilution of the virus-Fab mix led to a recovery of infectivity (Lafferty, 1963). Thus neutralizing Fabs are more readily dissociated from their antigen than parental MAb and it was speculated that this was due to a loss of functional affinity resulting from reduction of valency. An alternative idea for the reduction in the efficiency of Fab neutralization came from the study of the neutralization and HI ability of a panel of Fabs and their respective IgGs to 4 non-overlapping antigenic regions (I – IV) of an H7 influenza A virus (Yoden *et al.*, 1985). Fabs to groups I and II displayed a 32 to 64 fold drop neutralization titres compared with their parent IgG, whilst Fabs to groups III and IV had a >100-fold loss of neutralization and no detectable HI titre. These authors suggested that neutralization efficiency was lower with group III and IV Fabs due to the loss of bivalency, as the addition of anti-Fab anti-serum resulted in increased neutralization levels to coincide with that of the parent MAbs. However, no evidence of cross-linking of Fabs was provided and data could be also explained by an increased ability to inhibit attachment. In addition a study using a spin labelling technique indicated that an antibody to group IV (81/6), inhibited the low pH dependent conformational change of the HA (Kida *et al.*, 1985; Yoden *et al.*, 1986). A later study showed that MAb 81/6 did not inhibit attachment or internalisation, but did inhibit endosomal fusion (Imai *et al.*, 1998). In addition electron microscopy of antibody binding to HA rosettes indicated that MAb 81/6 bound to the side of an HA trimer, in contrast to the binding to the top of the globular head seen by MAbs which give HI. Together these studies suggest that neutralizing activity of MAb 81/6 requires a bivalent binding, as inhibition of fusion may be due to the inhibition of a conformational change of the HA, caused by the MAb binding to the side of the HA.

This could allow the MAb to directly crosslink monomers of the HA trimer and the resulting inhibition of the conformational changes would be analogous to that occurring in a virus with engineered intermonomer disulphide bonds (Kemble *et al.*, 1992). However, one should be cautious when making these assumptions as the conformational and binding analysis was carried out on isolated HA rosettes, which may not behave as the HA present on virus particles.

More recently, an extensive study of neutralization and HI abilities of five anti H7 (FPV) influenza A monoclonal IgGs, their monovalent Fabs and bivalent F(ab)₂ fragments was carried out by Schofield *et al.* (1997b). This study again found that neutralization required 54- to 542-fold more Fab than IgG on a molar basis. However, the bivalent F(ab)₂s showed similar neutralizing activities to their parent IgGs, only requiring 1.4- to 4-fold more to neutralize. These data strongly suggest that bivalent interaction with the virus was necessary for efficient neutralization. A comparison of functional affinities of the IgGs and Fabs using SPR showed that affinities for two of the Fabs, HC2 and HC61 were only 3 to 4 fold lower than their IgGs. This suggested that for these Fabs the difference in molecular mass was responsible for differences in neutralization ability compared to their IgGs.

A complementary study by Schofield *et al.* (1997a) looked at the relationship between efficiency of neutralization (percentage neutralization per unit concentration) and affinity. In this study the authors suggested that if antibody affinity was the sole determinant of efficiency of neutralization then the ratio of the rate of neutralization (K_{NEUT}) and the equilibrium dissociation constant (K_D) should equal 1. However, for a number of IgGs this ratio was 23 to 125 fold and it was concluded that factors other than the antibody affinity contribute to the efficiency of neutralization. One of these may have been the mechanism of neutralization.

Although there is general agreement that Fabs display a lower efficiency of neutralization of influenza A virus than their respective MAb, there seems to be little agreement over the cause of the loss of efficiency. Reductions in affinity, valency and molecular mass have all been proposed as possible causes. The aim of this section is to address this issue by comparing the mechanism of neutralization of the IgGs and their respective Fabs and by analysing their affinities. Differences found will be discussed in relation to their valency, molecular mass and affinity.

In this study I have examined the dose response relationship of neutralization, the mechanism of neutralization of influenza A virus, and the affinity of three

monoclonal IgGs, three monovalent Fabs and one F(ab)₂. All Fabs showed significantly lower neutralization efficiency than the MAbs from which they were derived. The MAbs all displayed a similar complex mechanism of neutralization in which they were able to simultaneously inhibit two stages of the influenza infectious cycle. In contrast, the Fabs all displayed a single mechanism of neutralization. Comparisons of the efficiency of neutralization were complicated by the dual mechanisms of the IgGs. However, the differences decreased with increasing concentration. The differences in affinities of IgGs and their respective Fabs were small and did not account for the reduction in neutralization efficiency.

6.2 MAb H36-4.5-2

6.2.1 Comparison of the neutralization by plaque reduction by H36 IgG, F(ab)₂ and Fab fragments.

Figure 6.1 indicates that neutralization efficiency of both the antibody fragments is reduced compared to the IgG. Table 6.1 reveals that there is a difference between the neutralization efficiency at 50% and 90% with the Fab compared to the IgG. At 50% neutralization the Fab requires a 104-fold higher concentration than the IgG, but at 90% the difference is only 15-fold. This suggests that the efficiency of neutralization by the Fab increases with increasing concentration compared to the IgG. A similar though less marked trend is seen with the F(ab)₂ as at 50% neutralization there is an 8-fold discrepancy, whereas at 90% neutralization there is only a 2.5-fold discrepancy.

Figure 6.1 Neutralization of A/PR8 by H36 IgG, F(ab)₂ and Fab in MDCK cells. Data are the mean of three experiments, measured by plaque reduction. The bar represents the SEM. Curves were generated by non-linear regression using the Graphpad Prism package ($R = >0.98$).

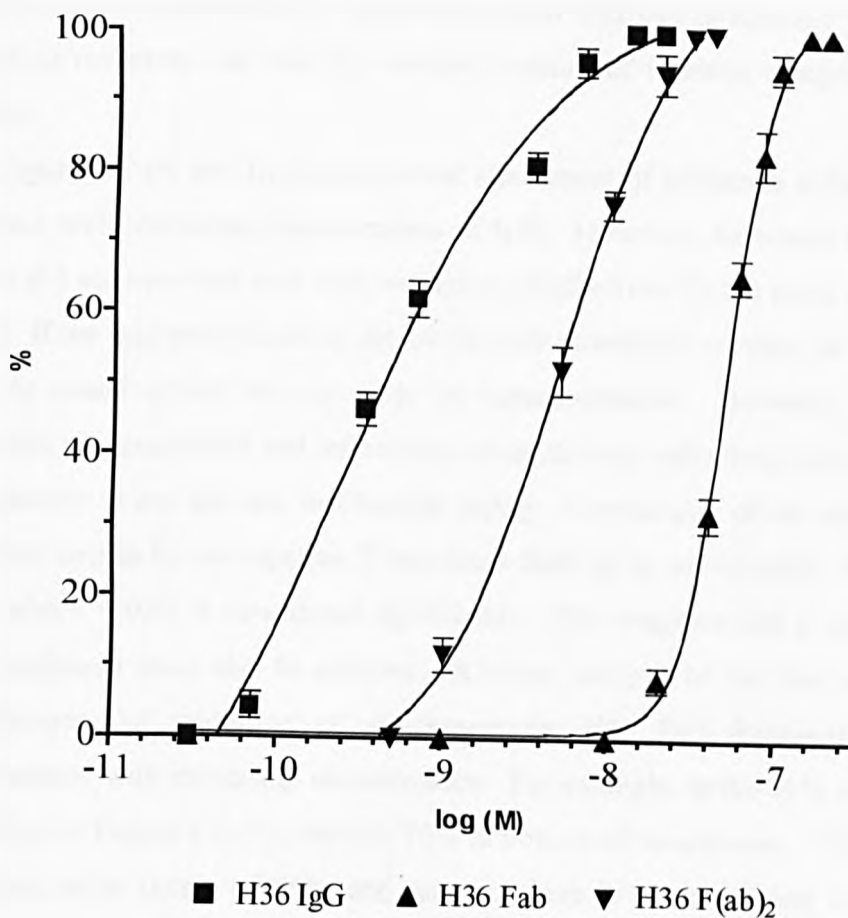


Table 6.1 Comparison of the neutralizing activities of H36 IgG and its Fab fragments. Data taken from figure 8.1.

Antibody	Concentration (nM) required to give neutralization of		Antibody fragment : IgG ratio at neutralization of	
	50%	90%	50%	90%
H36 IgG	0.5	6	-	-
Fab	52.0	90	104 : 1	15.0 : 1
F(ab) ₂	4.0	15	8 : 1	2.5 : 1

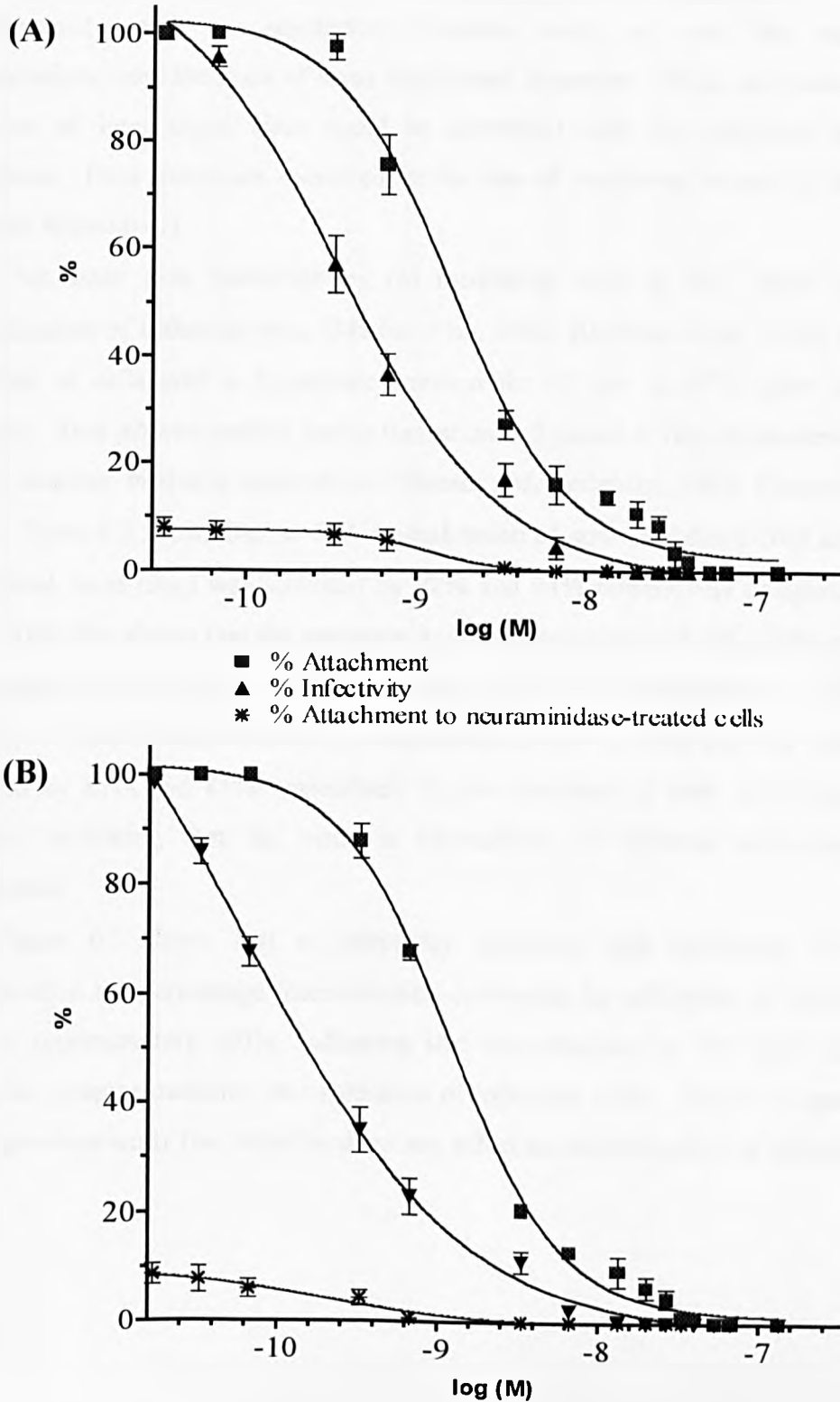
6.2.2 Analysis of the inhibition of attachment of A/PR8 to both MDCK and BHK cells by MAb H36.

The analysis of the effect of H36 IgG on virus attachment is shown in Figure 6.2 (A and B). Neuraminidase pre-treatment reduced the level of attachment of non-neutralized virus by >90% and this fell away with increasing IgG, showing that the majority of the attachment in these attachment ELISAs is specific to sialic acid containing receptors and that Fc receptor capture of immune complexes was not involved.

Figure 6.2 (A and B) indicates that attachment of influenza to both cell types decreased with increasing concentration of IgG. However, decreases in attachment of virus did not correlate well with reduction of infectivity by the same concentration of IgG. If the IgG neutralized by inhibiting only attachment of virus to cell receptor, then one would expect the curves to be superimposable. However, Figure 6.2A shows that the attachment and infectivity curves diverge indicating that the inhibition of attachment is not the sole mechanism acting. Comparison of the attachment and infectivity curves by an unpaired T-test show them to be significantly different ($P = 0.005$, where < 0.05 is considered significant). This suggests that a stage or stages after attachment must also be effected. A closer analysis of the data indicates that the efficiency of inhibition of attachment by H36 IgG increases relative to neutralization, with increasing concentration. For example, at the 90% neutralization point (N_{90}) in Figure 6.2 (A), there is 70% inhibition of attachment. This shows that at neutralization levels of 90% and greater, there is an increasing correlation of inhibition of attachment with loss of infectivity, indicating it to be the dominant mechanism acting. However, at the 50% neutralization point (N_{50}) there is only a 10% inhibition of attachment indicating that 40% of the virus must be neutralized by other mechanisms.

A comparison of Figure 6.2 (A) and (B) also reveals only minor differences in the extent to which inhibition of attachment correlates with loss of infectivity in both MDCK and BHK cells. At N_{50} in BHK cells there is a 5% inhibition of attachment, whereas at N_{90} there is a 70% inhibition of attachment. Therefore, this demonstrates that the lack of correlation of inhibition of attachment, at lower neutralization levels, with infectivity is repeatable in two different cell lines.

Figure 6.2 Analysis of the relationship between A/PR8 infectivity and attachment as a function of H36 concentration. Data with MDCK cells (A) and BHK cells (B) are shown. Infectivity and attachment were assayed by ELISA in parallel in the same batch of monolayers in 96 well plates, using the same virus-antibody mixtures. Inhibition of attachment of A/PR8 to neuraminidase-treated cells was used as the negative control. Data are the mean of five experiments. Curves were generated as in Figure 6.1 ($R = >0.98$ for all attachment and infectivity data).



6.2.3 *Analysis of the relationship between A/PR8 infectivity and internalisation in MDCK cells as a function of H36 IgG concentration.*

Since virus neutralized at low concentrations of H36 IgG attached to the cell surface, the antibody must interfere with a stage of the virus infectious cycle after attachment. This could be internalisation of virus by receptor-mediated endocytosis or fusion of virus to the endosomal vesicle. Here I analysed the effect of H36 IgG on the internalisation of virus by MDCK cells (Figure 6.3). This assay was carried out simultaneously with an attachment detection assay as over the range of concentrations used the level of virus attachment decreases. Thus, any reduction in the level of internalised virus could be correlated with the reduction in virus attachment. Data shown are corrected for the loss of attachment caused by the H36 IgG (see Appendix I).

This assay was controlled by (a) incubating cells at 4°C, which inhibits internalisation of influenza virus (Matlin *et al.*, 1981; Richman *et al.*, 1986) and (b) treatment of cells with a hypertonic solution for 15 min at 37°C prior to virus infection. This inhibits clathrin lattice formation and shows if virus is internalised by classic receptor mediated endocytosis (Heuser and Anderson, 1989; Hansen *et al.*, 1993). Table 6.2 shows that at 4°C internalisation of non-neutralized (N_0) and 50% neutralized virus (N_{50}) was inhibited by 92% and 94% respectively compared with 37°C. This also shows that the neuraminidase treatment protocol efficiently removes non-internalised virus, and that neutralized virus is not internalised by a different pathway. Table 6.2 also shows that internalisation of N_0 virus and N_{50} virus was inhibited by 81% and 85% respectively by pre-treatment of cells with hypertonic solution, indicating that the virus is internalised via clathrin lattice-mediated endocytosis.

Figure 6.3 shows that as infectivity decreases with increasing H36 IgG concentration the percentage internalisation (corrected for inhibition of attachment) stays at approximately 100%, indicating that neutralization by H36 IgG does not affect the receptor-mediated internalisation of influenza virus. This is in agreement with a previous study that failed to show any effect on internalisation of influenza

Figure 6.3 Analysis of the relationship between A/PR8 infectivity and the internalisation in MDCK cells as a function of H36 IgG concentration. Infectivity and internalisation were assayed in parallel in the same batch of monolayers in 96 well plates, using the same virus-antibody mixtures. Data are corrected for inhibition of attachment to cells measured in the same experimental system. All data are the mean of three experiments. The curve has been generated as described previously ($R \Rightarrow 0.98$).

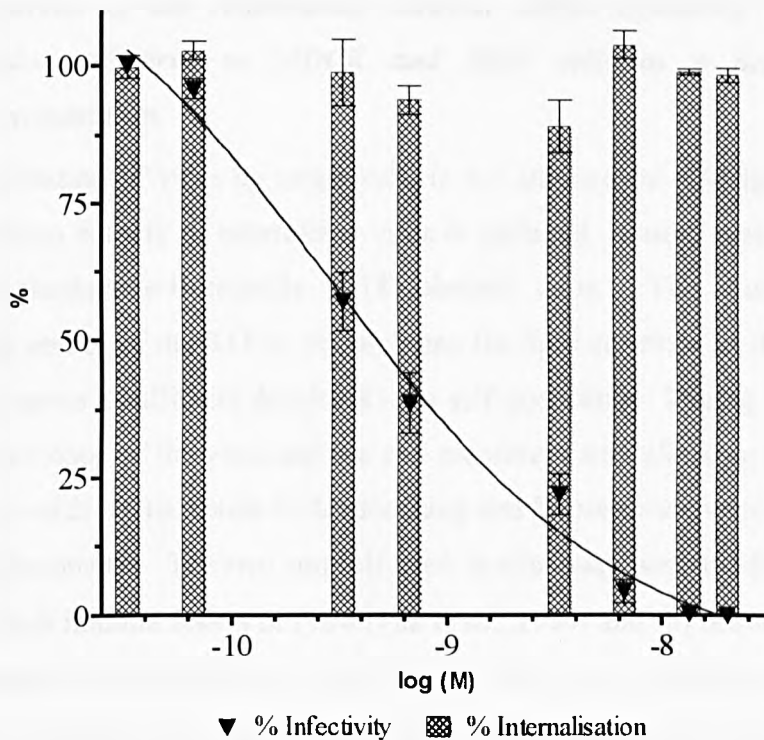


Table 6.2 Analysis of the internalisation of non-neutralized (N_0) and 50% neutralized (N_{50}) virus under the negative control conditions. Data are presented as percentage inhibition of internalisation relative to non-neutralized virus at 37°C.

<i>Control conditions</i>	<i>% inhibition of internalisation</i>
Cold (4°C) – N_0	92 (+/- 2)
Cold (4°C) – N_{50}	94 (+/- 7)
Hypertonic treated - N_0	81 (+/- 6)
Hypertonic treated – N_{50}	85 (+/- 5)

virus by a number of monoclonal IgG antibodies (Outlaw and Dimmock, 1993; Outlaw, 1989).

A similar set of experiments was performed on BHK cells (data not shown) and preliminary results also indicated that H36 IgG did not have any effect on the internalisation of neutralized virus that attached to cells.

6.2.4 Analysis of the relationship between A/PR8 infectivity and endosomal fusion of virus to MDCK and BHK cells as a function of H36 concentration.

As internalisation of virus by target cells is not affected by H36 IgG, it is possible that the fusion activity of neutralized virus is inhibited. Fusion was measured using octadecyl rhodamine-B-chloride (R18)-labelled virus. This fluorescence assay utilises the ability of the R18 to dissolve into the lipid envelope of the virus *in vitro*. When it reaches a sufficient density R18 is self-quenching. During virus-cell fusion the lipid envelope of the virus and the cell membrane mix allowing the R18-label to diffuse outwards. This results in dequenching and fluorescence which is measured in a spectrophotometer. The two controls used in this assay were (a) fusion carried out at 4°C, which inhibits fusion of PR/8 (Pak *et al.*, 1994) and (b) pre-treatment of cells with bafilomycin, an inhibitor of cellular V-ATPase, that reduces the endosomal pH required to trigger fusion of influenza virus (Palokangas *et al.*, 1994; Guinea and Carrasco, 1995). Tables 6.3 and 6.4 give the extent of fusion inhibition under control conditions in both MDCK and BHK cells respectively. At 4°C fusion was inhibited by 91% in MDCK cells and 94% in BHK cells. This indicated that the majority of the signal was due to virus-driven fusion. Inhibition of fusion caused by bafilomycin was 86% in MDCK cells and 88% in BHK cells, again demonstrating the specificity of the fluorescent signal to low pH-dependent virus-cell fusion

Figures 6.4 and 6.5 show that as infectivity decreased with increasing concentration of H36 IgG the percentage fusion also decreased. This suggested a causal relationship between inhibition of virus-cell fusion and neutralization by H36 IgG.

Figure 6.4 Analysis of the relationship between A/PR8 infectivity and fusion of virus to MDCK cells as a function of H36 concentration. Both sets of data were obtained using 3 cm monolayers. Infectivity was determined by plaque reduction and fusion was measured by fluorescence dequenching of R18-labelled virus. Data are the mean of three experiments and have been corrected for inhibition of virus attachment to cells. Curves were generated as in Figure 6.1 ($R = >0.98$ for all fusion and infectivity data).

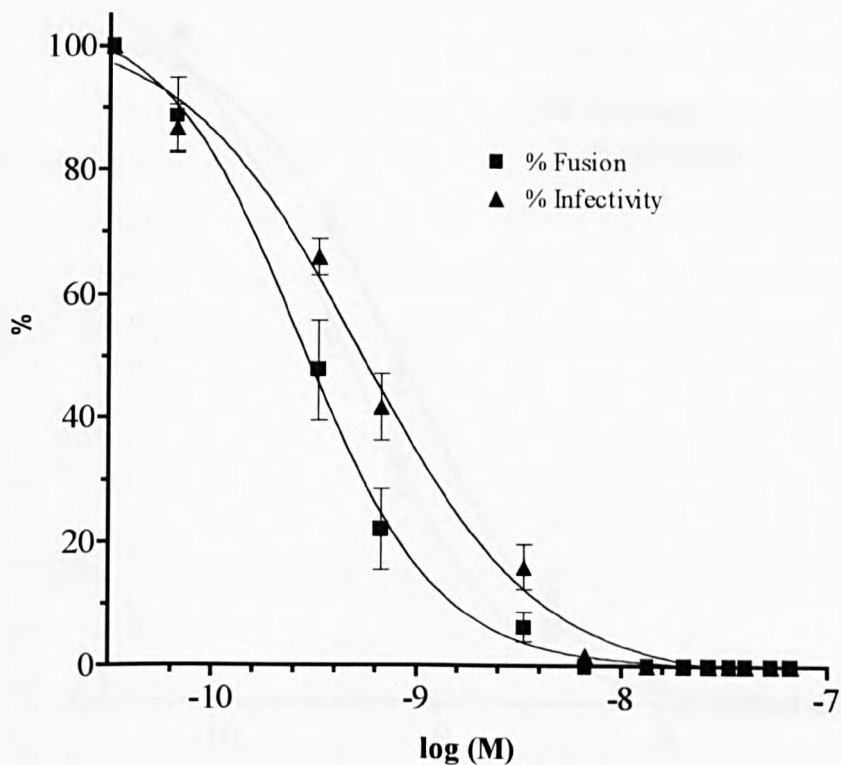


Table 6.3 Analysis of the fusion of non-neutralized (N_0) virus under the negative control conditions. Data are presented as percentage inhibition of fusion relative to non-neutralized virus at 37°C. Data are the mean of three experiments

<i>Control conditions</i>	<i>% inhibition of internalisation</i>
Cold (4°C) – N_0	91 (+/- 4)
Bafilomycin treated - N_0	86 (+/- 8)

Figure 6.5 Analysis of the relationship between A/PR8 infectivity and fusion of virus to BHK cells as a function of H36 concentration. Both sets of data were obtained using 3 cm monolayers. Infectivity was determined by plaque reduction and fusion was measured by fluorescence dequenching of R18-labelled virus. Data are the mean of three experiments and have been corrected for inhibition of virus attachment to cells. Curves were generated as in Figure 6.1 ($R = >0.99$ for all fusion and infectivity data).

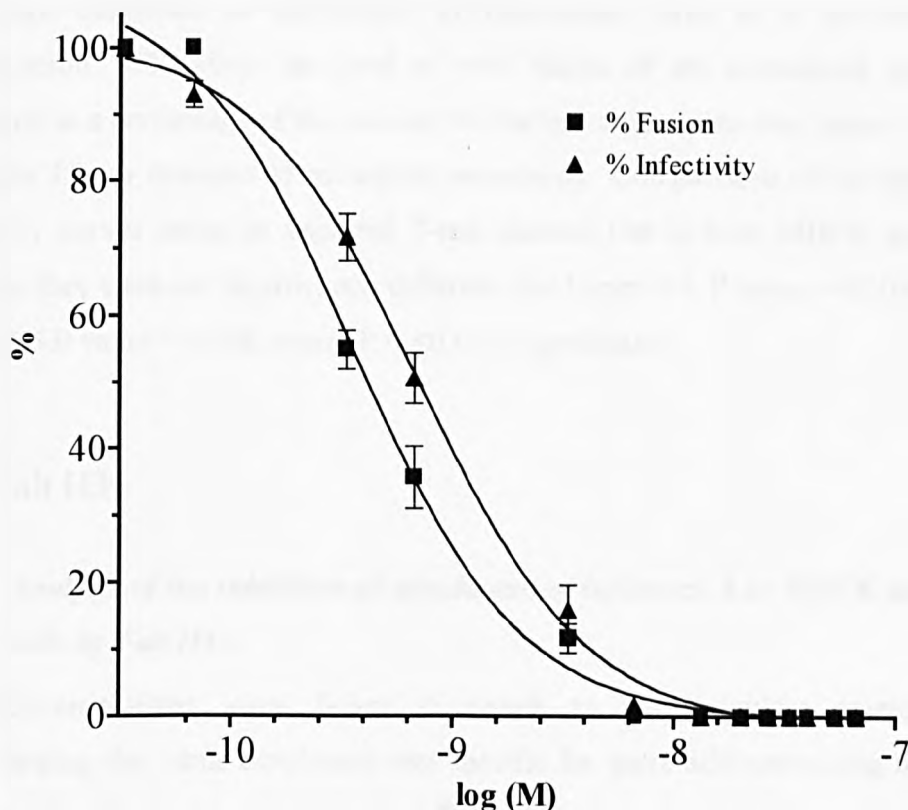


Table 6.4 Analysis of the fusion of non-neutralized (N_0) virus under the negative control conditions. Data are presented as percentage inhibition of fusion relative to non-neutralized virus at 37°C. Data are the mean of three experiments.

<i>Control conditions</i>	<i>% inhibition of internalisation</i>
Cold (4°C) – N_0	94 (+/- 3)
Bafilomycin treated - N_0	88 (+/- 5)

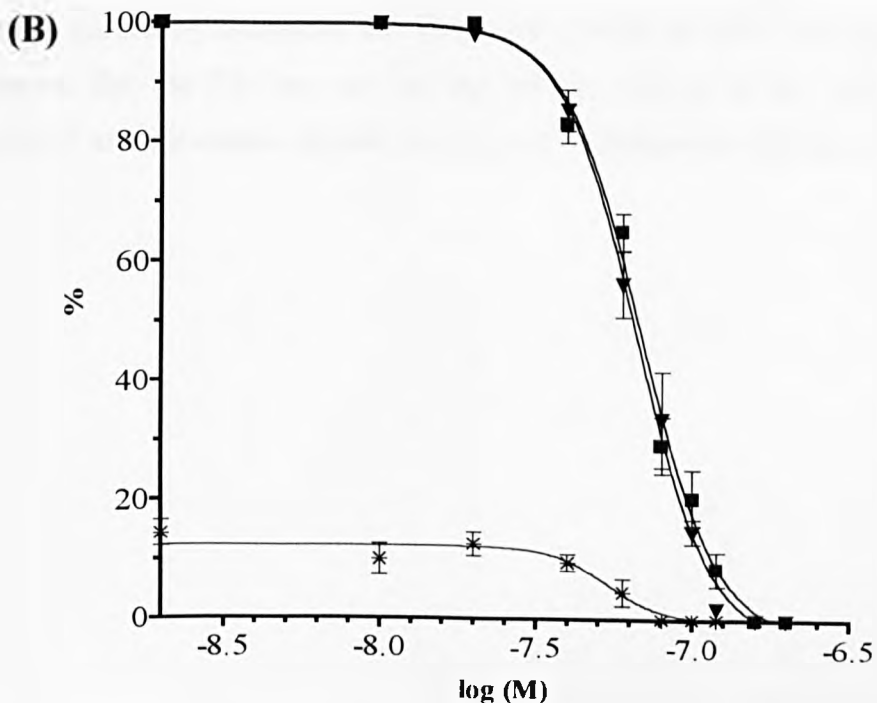
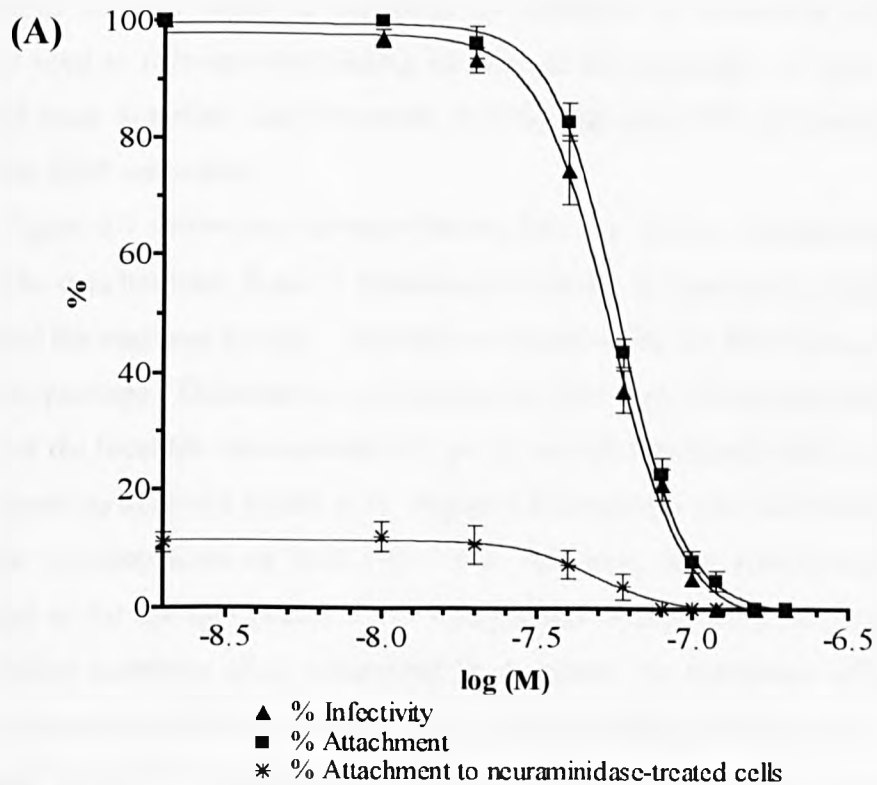
The data in Figures 6.4 and 6.5 have been corrected for inhibition of attachment of the neutralized virus caused by H36 IgG. The level of inhibition of attachment of neutralized virus to cells was analysed by treating the infected cells with Triton-X100 to solubilise the viral and cellular membranes. This results in complete diffusion of the input R18-labelled membranes and provides the maximum level of fluorescence of the input virus. Therefore, if virus attachment was inhibited by neutralizing antibody then the total level of fluorescence would be decreased compared to the non-neutralized control. This decrease was used to calculate the percentage inhibition of attachment of neutralized virus at a particular IgG concentration. Therefore, the level of viral fusion of the neutralized virus was calculated as a percentage of the amount of attached virus rather than input virus (see Appendix I.2 for example of correction procedure). Comparisons of the fusion and infectivity curves using an unpaired T-test showed that in both MDCK and BHK cells that they were not significantly different (for Figure 6.4, P value = 0.101 and for Figure 6.5 P value = 0.268, where $P < 0.05$ is significant).

6.3 Fab H36

6.3.1 Analysis of the inhibition of attachment of influenza A to MDCK and BHK cells by Fab H36.

Fab H36-neutralized virus failed to attach to neuraminidase treated cells demonstrating that virus attachment was specific for sialic acid containing receptors on the cell surface (Figure 6.6 A and B). Figure 6.6 (A) and (B) indicates that attachment of virus to both types of cell decreases with increasing concentrations of Fab. The decrease in attachment, in contrast to the situation with the MAb, correlates very closely with loss of infectivity, suggesting a causal relationship. An unpaired T-test revealed that the attachment and infectivity curves for MDCK and BHK cells were not significantly different (Figure 6.6 (A) P value = 0.620 and (B) P value = 0.856, where $P < 0.05$ is significant).

Figure 6.6 Analysis of the relationship between A/PR8 infectivity and attachment as a function of Fab H36 concentration. Data with MDCK cells (A) and BHK cells (B) are shown. Infectivity and attachment were assayed by ELISA in parallel in the same batch of monolayers in 96 well plates, using the same virus-antibody mixtures. Inhibition of attachment of A/PR8 to neuraminidase-treated cells was used as the negative control. Data are the mean of five experiments. Curves were generated as in Figure 6.1 ($R = >0.98$ for all attachment and infectivity data).



6.4 Real-time kinetic binding analysis of H36 IgG and its Fab fragment to virus particles using surface plasmon resonance.

6.4.1 Comparison of the kinetics of binding of H36 IgG and its Fab fragment to whole virus particles.

The purpose of this section was to determine the functional affinities of the H36 IgG and Fab in order to determine whether the loss of neutralization efficiency in the Fab relative to the IgG could be explained by reduction in functional affinity. The method used to calculate the binding kinetics of the antibodies to whole virus was adapted from Schofield and Dimmock, (1996) and uses SPR technology with the BIAcore 2000 instrument.

Figure 6.7 shows the real-time binding kinetics of four concentrations of H36 IgG. The data has been X and Y transformed in order to equalise the injection points ($t=0$) and the response to zero. The data was fitted using the BIAevaluation (v3.0.2) software package. Dissociation and association data were fitted individually and the means of the local fits was calculated to get an overall functional affinity (K_D) for the concentrations analysed (Table 6.5). Figure 6.8 shows the real time binding kinetics for four concentrations of H36 Fab. The data have been transformed and then analysed as for the IgG (Table 6.5). Comparison of the means of the equilibrium dissociation constants (K_D), considered to represent the functional affinity in this study, reveals that the H36 IgG and Fab are almost identical with values of 5.60×10^{-10} M and 5.55×10^{-10} M respectively. These affinities are very high, being similar to the values quoted by Schofield and Dimmock, (1996) for FPV monoclonal IgGs. This shows that the Fab has not lost any affinity relative to the IgG and hence reduction of affinity cannot explain the reduced neutralization efficiency seen in the Fab.

Figure 6.7 The binding of H36 IgG at five concentrations to captured whole influenza virus particles. Analysis was conducted in the 2-1 format, so curves show the relative response difference (Resp. Diff) between background control channel and the channel containing captured virus, measured in response units (RU) against time measured in seconds(s). Dark lines represent the area of dissociation used in the local fits.

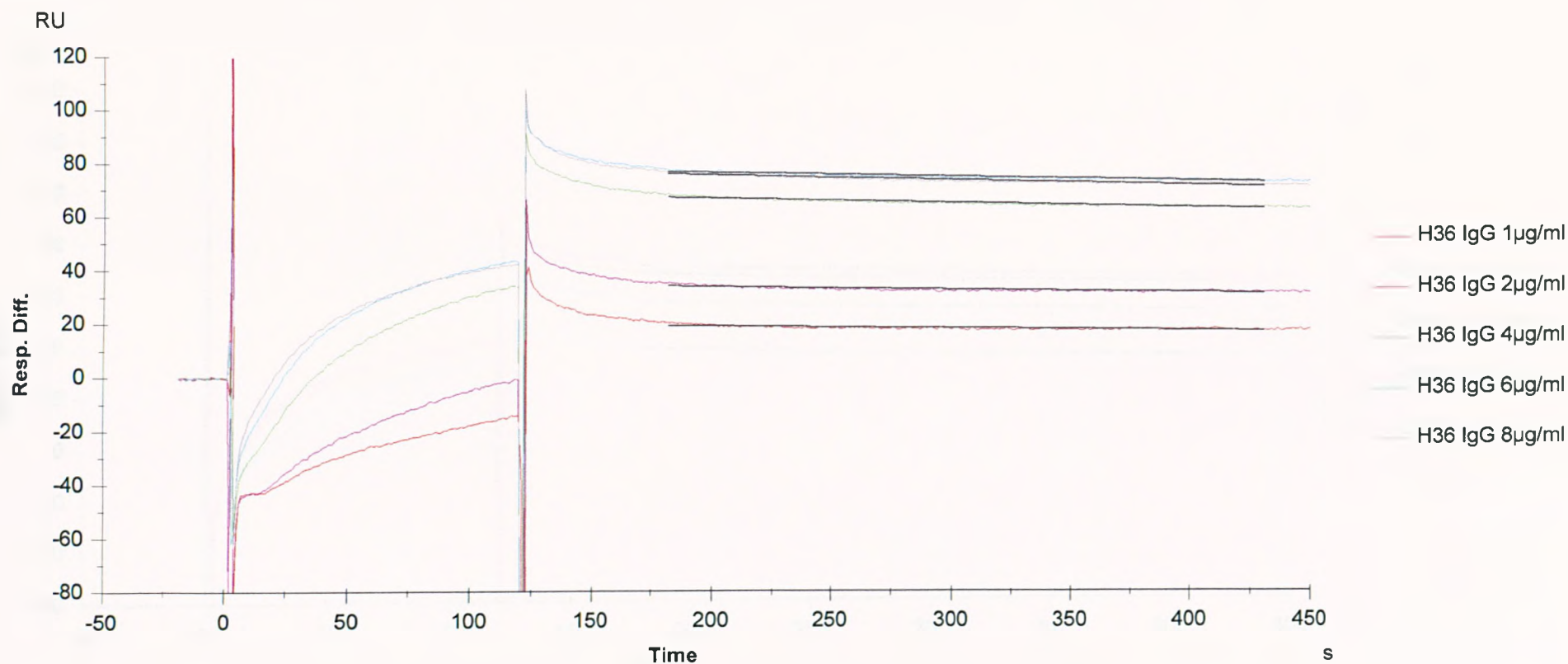


Figure 6.8 The binding of H36 Fab at four concentrations to captured whole influenza virus particles. Analysis was conducted in the 2-1 format, so curves show the relative response difference (Resp. Diff) between background control channel and the channel containing captured virus, measured in response units (RU) against time measured in seconds(s). Dark lines represent the area of dissociation used in the local fits.

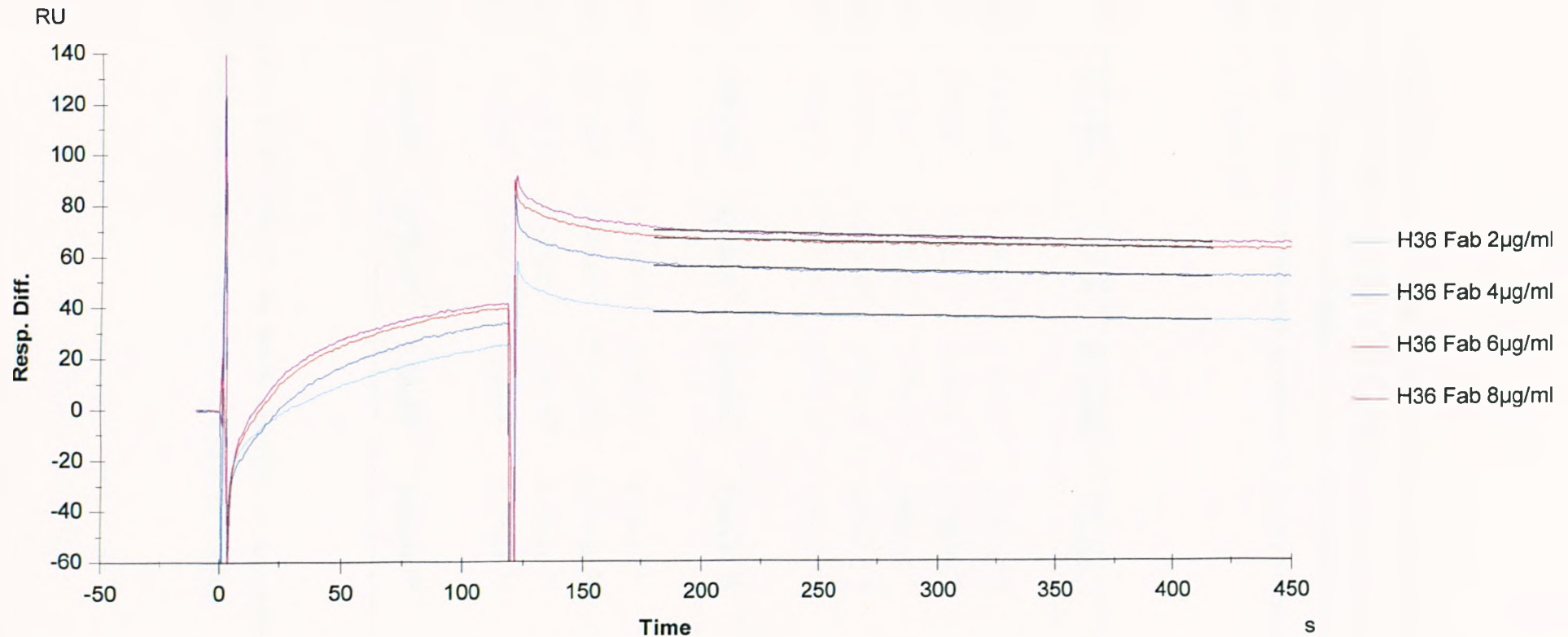


Table 6.5 Local fits of association and dissociation curves for H36 IgG and H36 Fab. Table shows association and dissociation rate constants (k_a and k_d) and equilibrium association and dissociation constants (K_A and K_D) for binding to captured whole virus particles. Chi² value indicates goodness of fit of the Langmuir 1:1 binding model used (<1 = good fit).

Antibody	k_a (1/Ms)	k_d (1/s)	K_A (1/M)	K_D (M)	Chi ²
H36 IgG 1μg/ml	8.40x10 ⁵	4.75x10 ⁻⁴	1.77x10 ⁹	5.65x10 ⁻¹⁰	0.057
H36 IgG 2μg/ml	6.88x10 ⁵	3.62x10 ⁻⁴	1.90x10 ⁹	5.26x10 ⁻¹⁰	
H36 IgG 4μg/ml	5.81x10 ⁵	2.92x10 ⁻⁴	1.99x10 ⁹	5.03x10 ⁻¹⁰	
H36 IgG 6μg/ml	4.71x10 ⁵	2.25x10 ⁻⁴	2.09x10 ⁹	4.78x10 ⁻¹⁰	
H37 IgG 8μg/ml	3.60x10 ⁵	2.65x10 ⁻⁴	1.36x10 ⁹	7.35x10 ⁻¹⁰	
Mean H36 IgG*	5.88x10⁵	3.24x10⁻⁴	1.82x10⁹	5.60x10⁻¹⁰	
H36 Fab 2μg/ml	1.09x10 ⁶	4.43x10 ⁻⁴	2.47x10 ⁹	4.05x10 ⁻¹⁰	0.160
H36 Fab 4μg/ml	8.17x10 ⁵	3.84x10 ⁻⁴	2.13x10 ⁹	4.70x10 ⁻¹⁰	
H36 Fab 6μg/ml	6.13x10 ⁵	3.18x10 ⁻⁴	1.21x10 ⁹	5.19x10 ⁻¹⁰	
H36 Fab 8μg/ml	4.34x10 ⁵	3.59x10 ⁻⁴	1.21x10 ⁹	8.27x10 ⁻¹⁰	
Mean H36 Fab*	7.38x10⁵	3.75x10⁻⁴	1.94x10⁹	5.55x10⁻¹⁰	

* values are the means of each column and hence equations to determine K_A and K_D only apply to raw data in the columns ($K_A = k_d/k_a$ and $K_D = k_d/k_a$)

6.5 H36 F(ab)₂

6.5.1 Analysis of the relationship between attachment and infectivity of A/PR/8 to MDCK cells as a function of H36 F(ab)₂ concentration.

The analysis of the effect of H36 F(ab)₂ on virus attachment is shown in Figure 6.9. Neuraminidase pre-treatment reduced the level of attachment of virus by 85% and this decreased with increasing IgG, showing that the majority of the attachment in these attachment ELISAs is specific to sialic acid-containing receptors and that Fc receptor capture of neutralized virus was not involved.

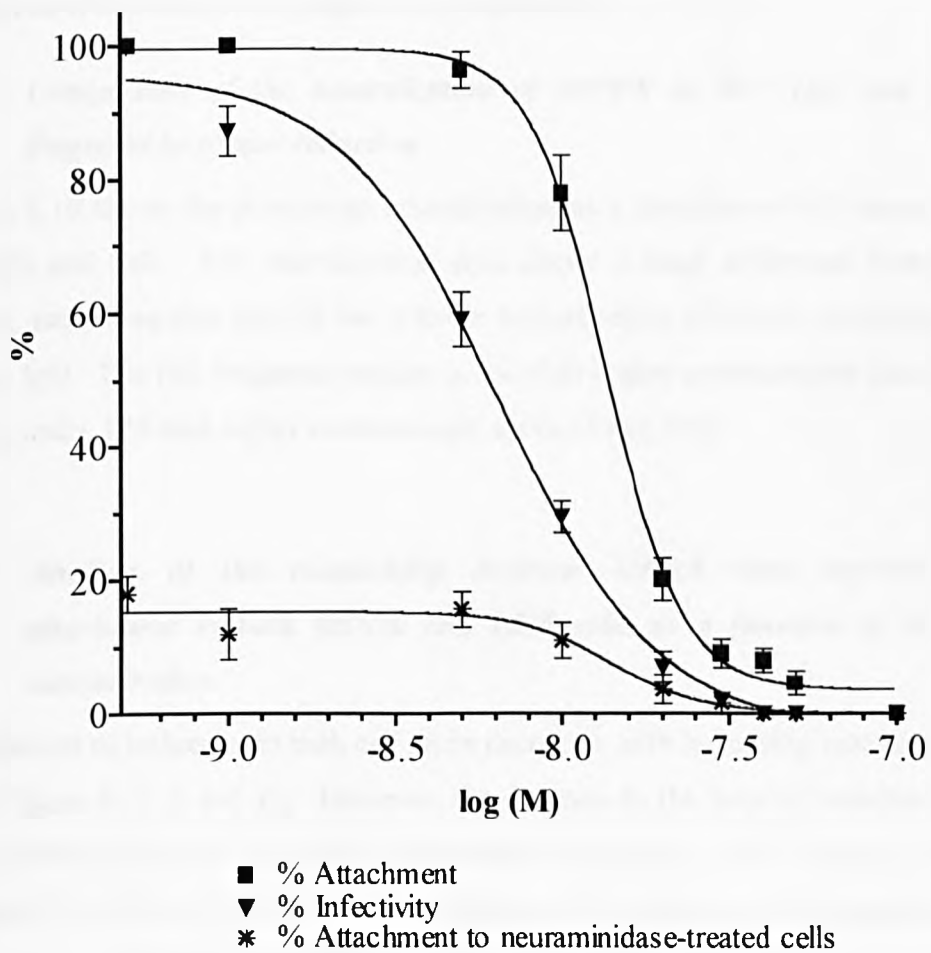
In common with H36 IgG, the F(ab)₂ also shows disparity between the loss of infectivity and the inhibition of attachment (Figure 6.9). This discrepancy between inhibition of attachment and infectivity indicates that inhibition of attachment is not the sole mechanism acting in the neutralization by this antibody fragment. At higher concentrations of F(ab)₂, inhibition of attachment is responsible for a larger component of the neutralization, at N₉₀ inhibition of attachment was 78%, whereas, at N₅₀, inhibition of attachment was only 2%. Thus the mechanism of neutralization of the H36 IgG and the H36 F(ab)₂ are similar, and are in contrast with the H36 Fab. No further analysis of the F(ab)₂ was carried out.

6.6 Summary: Comparison of the characteristics of neutralization of H36 IgG and its antibody fragments.

The order of neutralization efficiency was IgG>F(ab)₂>Fab. However, this difference was not uniform over the entire concentration range, as the N₅₀ of the Fab required 104-fold higher concentration than the IgG, whereas the N₉₀ of the Fab was only 15-fold greater. The Fab and IgG have almost identical affinities (5.5x10⁻¹⁰ M and 5.6x10⁻¹⁰ M respectively) and hence affinity cannot account for the loss of neutralization efficiency.

The IgG neutralized virus by two simultaneous mechanisms, inhibition of attachment of virus to target cells and inhibition of fusion of virus with the target cell membrane. In contrast, the Fab neutralized by inhibition of attachment as its sole mechanism, suggesting that loss of neutralization efficiency relative to the

Figure 6.9 Analysis of the relationship between A/PR8 infectivity and attachment to MDCK cells as a function of H36 F(ab)₂ concentration. Infectivity and attachment were assayed by ELISA in parallel in the same batch of monolayers in 96 well plates, using the same virus-antibody mixtures. Inhibition of attachment of A/PR8 to neuraminidase-treated cells was used as the negative control. Data are the mean of three experiments. Curves were generated as in Figure 6.1 ($R = >0.99$ for all attachment and infectivity data).



IgG may be related to differences in the mechanism of neutralization (discussed in more detail later). The relationship between attachment and infectivity of virus neutralized by the F(ab)₂ and IgG was very similar.

6.7 MAb H37-45-5R3

The H37 MAb is an IgG3 and is specific for antigenic site Ca2 on the viral HA. Hence, analysis of the mechanism of neutralization of virus with this MAb will determine if it is isotype or antigenic site-dependent.

6.7.1 Comparison of the neutralization of A/PR/8 by H37 IgG and its Fab fragment by plaque reduction.

Figure 6.10 shows the percentage neutralization as a function of H37 concentration for IgG and Fab. The neutralization data shows a large difference between the curves, indicating that the Fab has a lower neutralization efficiency compared to the parent IgG. The Fab fragment requires a 360-fold higher concentration than the IgG at N₅₀, and a 178-fold higher concentration at N₉₀ (Table 6.6).

6.7.2 Analysis of the relationship between A/PR/8 virus infectivity and attachment to both MDCK and BHK cells as a function of H37 IgG concentration.

Attachment of influenza to both cell types decreases with increasing concentration of IgG (Figure 6.11 A and B). However, the decrease in the level of attachment does not correlate well with decrease in the level of infectivity. For example, at N₅₀ in Figure 6.11 (A) there is only a 20% inhibition of attachment and the same point in Figure 6.11 (B) there is a 15% reduction in attachment. Comparisons of the attachment and infectivity curves by an unpaired T-test show them to be significantly different (Figure 6.11(A) P value = 0.027 and (B) P value = 0.047, where p = <0.05 is significant). At higher concentrations, inhibition of attachment becomes a larger proportion of the neutralization, for example at N₉₀ in Figure 6.11 (A) there is a 65% inhibition of attachment and the same point in Figure 6.11 (B) there is a 50% inhibition of attachment.

Figure 6.10 Neutralization of A/PR8 by H37 IgG and Fab in MDCK cells. Data are the mean of three experiments, measured by plaque reduction. The bar represents SEM. Curves were generated by non-linear regression using the Graphpad Prism package ($R = >0.98$).

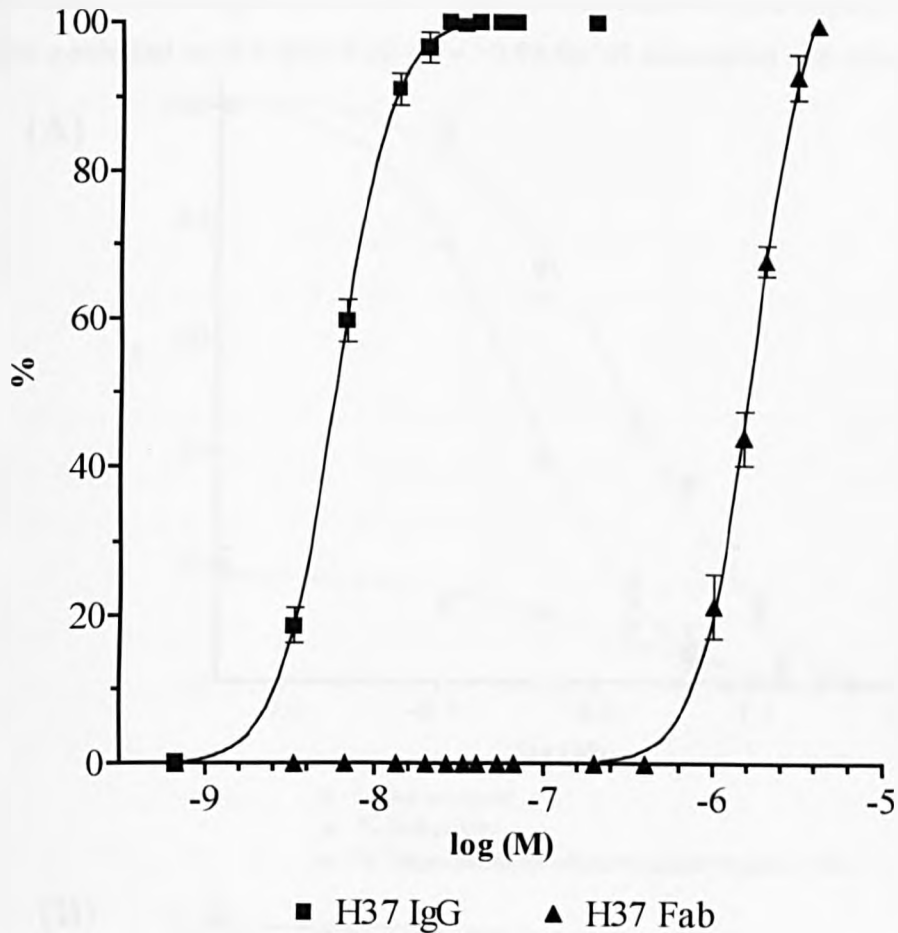
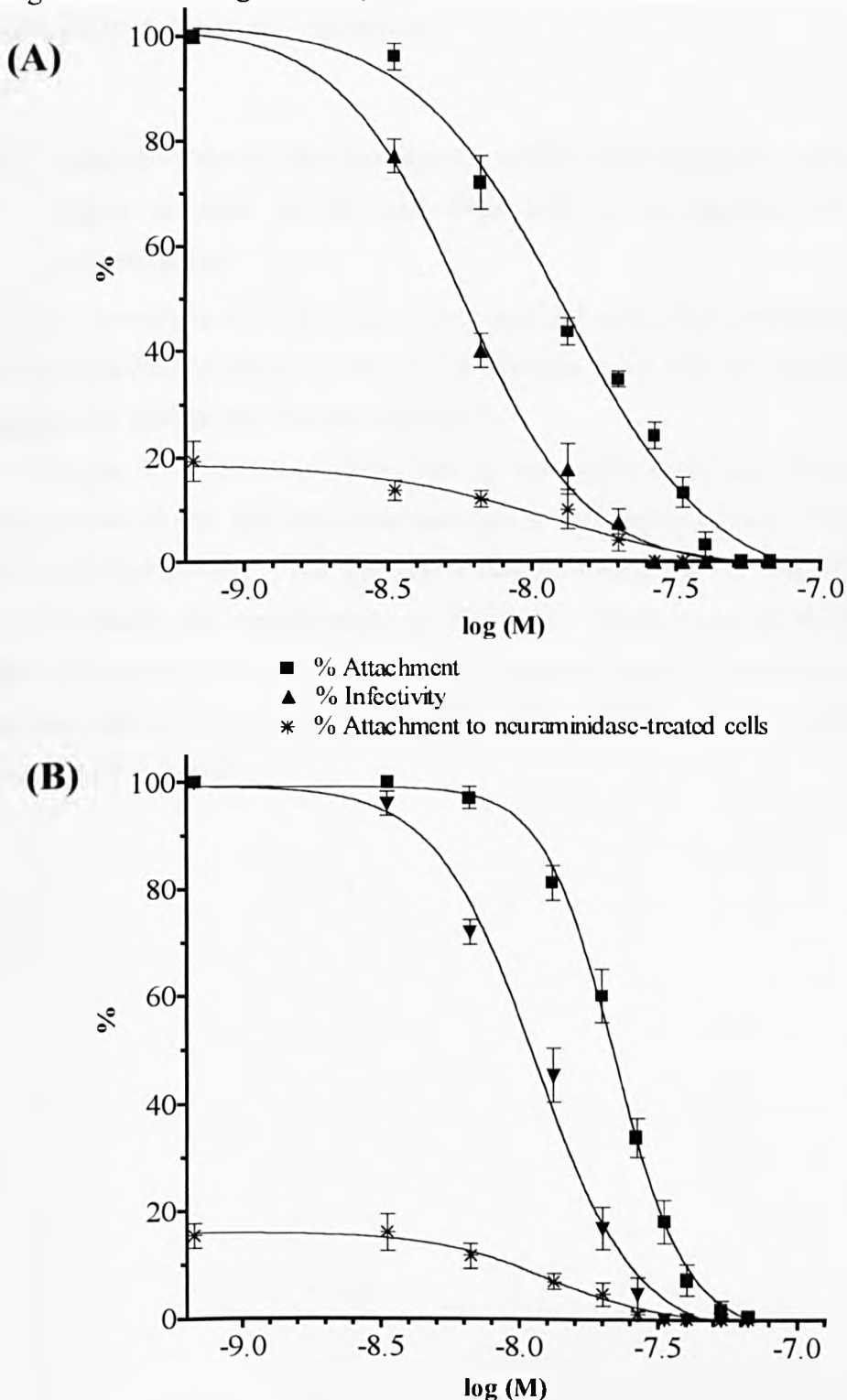


Table 6.6 Comparison of the neutralizing activities of H37 IgG and its Fab fragments. Data from Figure 8.10.

<i>Antibody</i>	<i>Concentration (nM) required to give neutralization of</i>		<i>Fab : IgG ratio at neutralization of</i>	
	<i>50%</i>	<i>90%</i>	<i>50%</i>	<i>90%</i>
IgG	5.0	14.0	-	-
Fab	1800.0	2500.0	360 : 1	178 : 1

Figure 6.11 Analysis of the relationship between A/PR8 infectivity and attachment as a function of H37 concentration. Data with MDCK cells (A) and BHK cells (B) are shown. Infectivity and attachment were assayed by ELISA in parallel in the same batch of monolayers in 96 well plates, using the same virus-antibody mixtures. Inhibition of attachment of A/PR8 to neuraminidase-treated cells was used as the negative control. Data are the mean of five experiments. Curves were generated as in Figure 6.10 ($R = >0.98$ for all attachment and infectivity data).



6.7.3 Analysis of the relationship between A/PR/8 virus infectivity and the internalisation in MDCK cells as a function of H37 IgG concentration.

Figure 6.12 shows that as infectivity decreases with increasing H37 IgG concentration the percentage internalisation (corrected for inhibition of attachment) stays at approximately 100%. These results are again qualitatively consistent with those seen with H36 IgG (section 6.2.3) and suggest that H37 IgG also does not affect receptor-mediated internalisation of influenza virus. Similar results were found with BHK cells (data not shown)

6.7.4 Analysis of the relationship between A/PR/8 virus infectivity and endosomal fusion in both MDCK and BHK cells as a function of H37 IgG concentration.

Negative controls used in this assay were consistent with those used for analysis of H36 IgG and data in tables 6.8 and 6.9 demonstrate again that the fluorescent signal obtained was specific for virus-driven fusion.

Figures 6.13 and 6.14 show that as infectivity decreases with increasing concentration of H36 IgG the percentage fusion also decreases in both MDCK and BHK cells respectively. This indicates a causal relationship between inhibition of virus-cell fusion and neutralization by H37 IgG. Comparisons of the fusion and infectivity curves using an unpaired T-test revealed that in both MDCK and BHK cells that they were not significantly different (for Figure 6.13, $P = 0.443$ and for Figure 6.14 $P = 0.563$).

Figure 6.12 Analysis of the relationship between A/PR8 infectivity and the internalisation in MDCK cells as a function of H37 IgG concentration. Both infectivity and internalisation were assayed in parallel in the same batch of monolayers in 96 well plates, using the same virus-antibody mixtures. Data are corrected for inhibition of attachment to cells measured in the same experimental system. All data are the mean of three experiments. The curve was generated as in Figure 6.10 ($R = >0.99$)

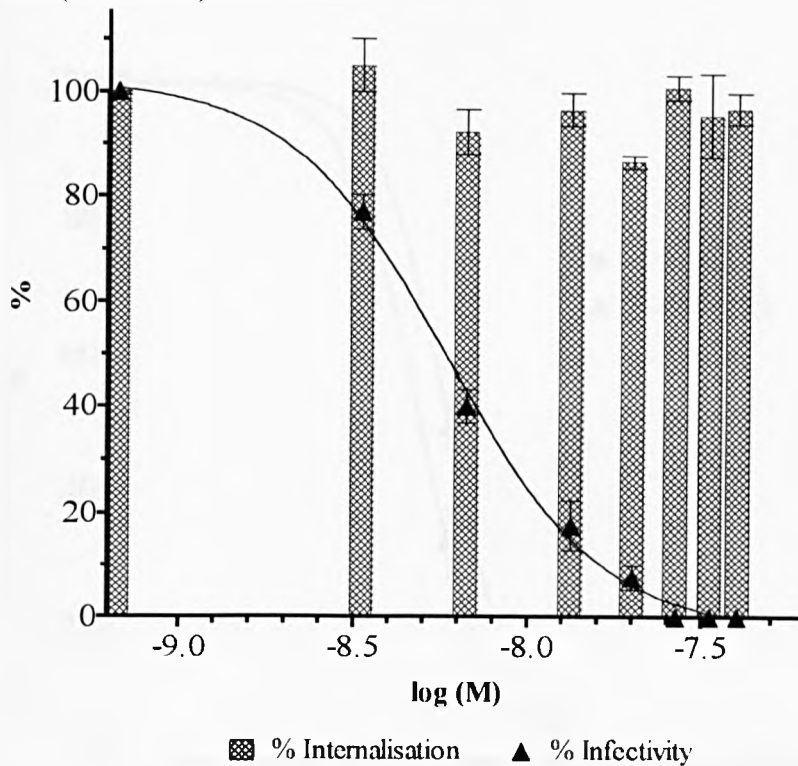


Table 6.7 Analysis of the internalisation of non-neutralized (N_0) and N_{50} virus under the negative control conditions. Data is presented as percentage inhibition of internalisation relative to non-neutralized virus at 37°C (standard conditions). Data for neutralized virus is corrected for inhibition of attachment. Data are the mean of three experiments.

<i>Control conditions</i>	<i>% inhibition of internalisation</i>
Cold (4°C) – N_0	94 (+/- 2)
Cold (4°C) – N_{50}	91 (+/- 9)
Hypertonic treated - N_0	79 (+/- 5)
Hypertonic treated – N_{50}	86 (+/- 9)

Figure 6.13 Analysis of the relationship between A/PR8 infectivity and fusion of virus to MDCK cells as a function of H37 concentration. Both sets of data were obtained using 3 cm monolayers. Infectivity was determined by plaque reduction and fusion was measured by fluorescence dequenching of R18-labelled virus. Data are the mean of three experiments and have been corrected for inhibition of virus attachment to cells. Curves were generated as in Figure 6.10 ($R = >0.99$ for all fusion and infectivity data).

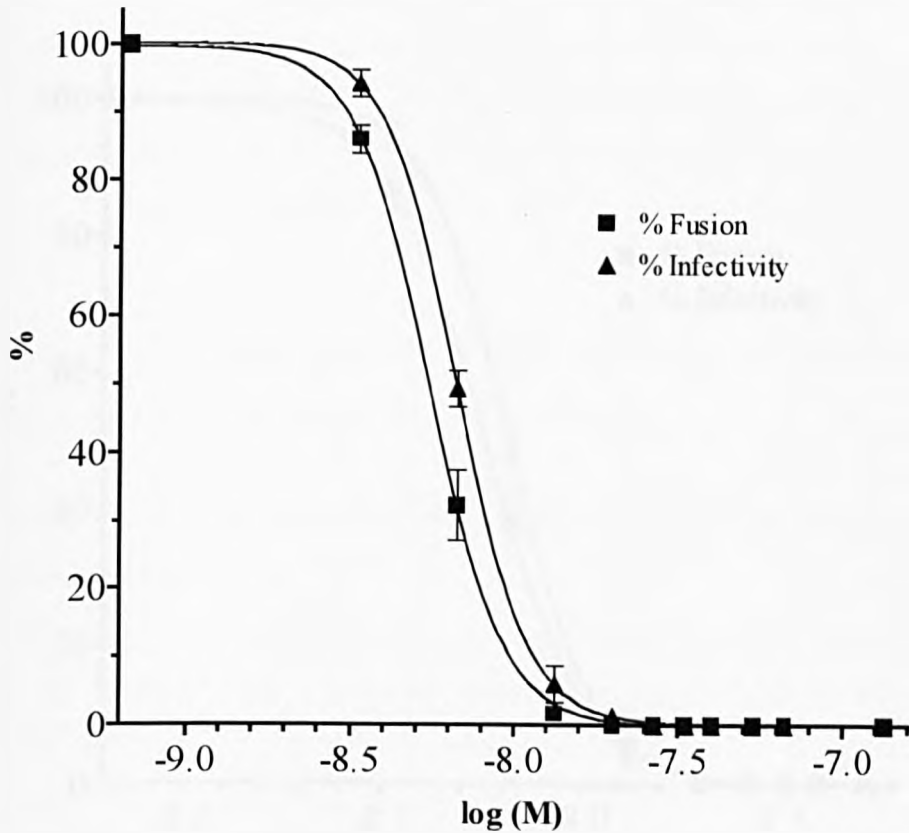


Table 6.8 Analysis of the fusion of non-neutralized virus under the negative control conditions. Data is presented as percentage inhibition of fusion relative to non-neutralized virus at 37°C. Data are the mean of three experiments

<i>Control conditions</i>	<i>% inhibition of internalisation</i>
Cold (4°C) – N ₀	89 (+/- 2)
Bafilomycin treated - N ₀	88 (+/- 4)

Figure 6.14 Analysis of the relationship between A/PR8 infectivity and fusion of virus to BHK cells as a function of H37 concentration. Both sets of data were obtained using 3 cm monolayers. Infectivity was determined by plaque reduction and fusion was measured by fluorescence dequenching of R18-labelled virus. Data are the mean of three experiments and have been corrected for inhibition of virus attachment to cells. Curves were generated as in Figure 8.10 ($R = >0.99$ for all fusion and infectivity data).

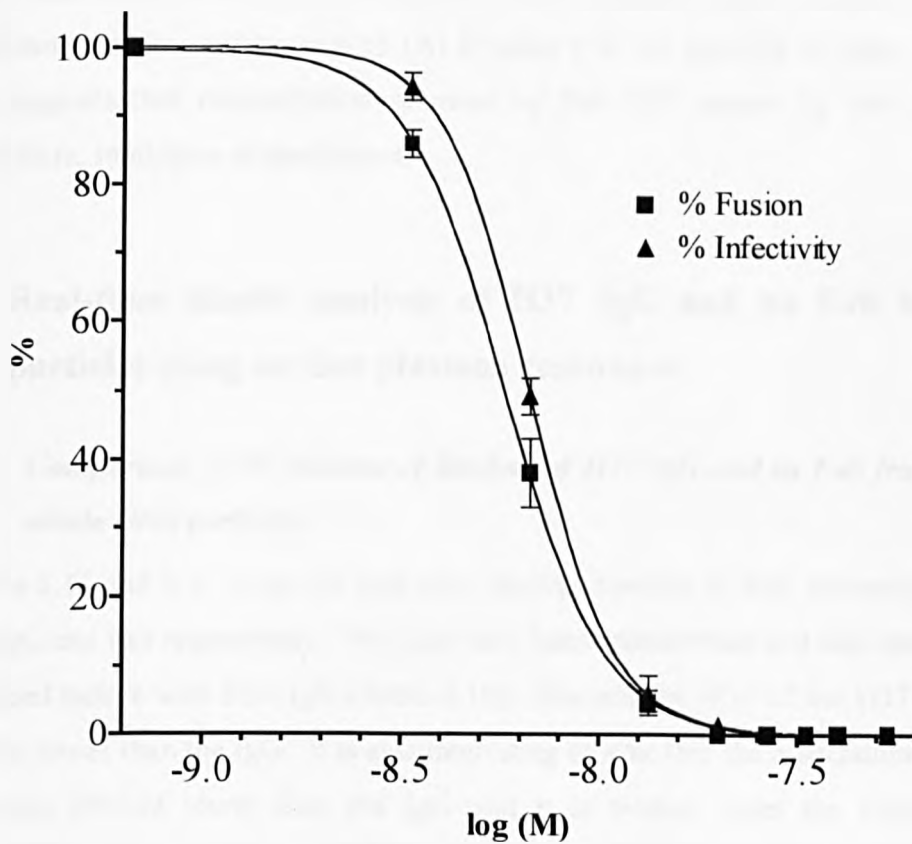


Table 6.9 Analysis of the fusion of non-neutralized virus under the negative control conditions. Data is presented as percentage inhibition of fusion relative to non-neutralized virus at 37°C. Data are the mean of three experiments.

<i>Control conditions</i>	<i>% inhibition of internalisation</i>
Cold (4°C) – N_0	87 (+/- 4)
Bafilomycin treated - N_0	79 (+/- 9)

6.8 Fab H37

6.8.1 *Analysis of the relationship between attachment and infectivity of A/PR/8 virus to both MDCK and BHK cells as a function Fab H37*

Figure 6.15 (A) and (B) indicates that attachment of virus to both types of cell decreases with increasing concentrations of Fab. The decrease in attachment, in contrast to the situation with the IgG, correlates very closely with loss of infectivity, suggesting a causal relationship. Comparison of attachment and infectivity curves for MDCK and BHK cells using an unpaired T-test revealed that the curves were not significantly different (Figure 6.15 (A) P value = 0.765 and (B) P value = 0.716). This suggests that neutralization of virus by Fab H37 occurs by one dominant mechanism, inhibition of attachment.

6.9 Real-time kinetic analysis of H37 IgG and its Fab to virus particles using surface plasmon resonance.

6.9.1 *Comparison of the kinetics of binding of H37 IgG and its Fab fragment to whole virus particles.*

Figures 6.16 and 6.17 show the real-time binding kinetics of four concentrations of H37 IgG and Fab respectively. The data have been transformed and then analysed as described before with H36 IgG (Table 6.10). The affinity (K_D) of the H37 Fab was 4.2-fold lower than the IgG. It is also interesting to note that the association constant (K_A) was 24-fold lower than the IgG and it is evident from the slope of the dissociation phase in Figure 6.17 that the Fab had a faster dissociation (14-fold) and this may be relevant in an equilibrium based neutralization assay. However, neither value can explain the 360-fold difference in neutralization efficiency at N_{50} or the 178-fold difference at N_{90} .

Figure 6.15 Analysis of the relationship between A/PR8 infectivity and attachment as a function of Fab H37 concentration. Data with MDCK cells (A) and BHK cells (B) are shown. Infectivity and attachment were assayed by ELISA in parallel in the same batch of monolayers in 96 well plates, using the same virus-antibody mixtures. Inhibition of attachment of A/PR8 to neuraminidase-treated cells was used as the negative control. Data are the mean of five experiments. Curves were generated as for Figure 6.10 ($R = >0.99$ for all attachment and infectivity data).

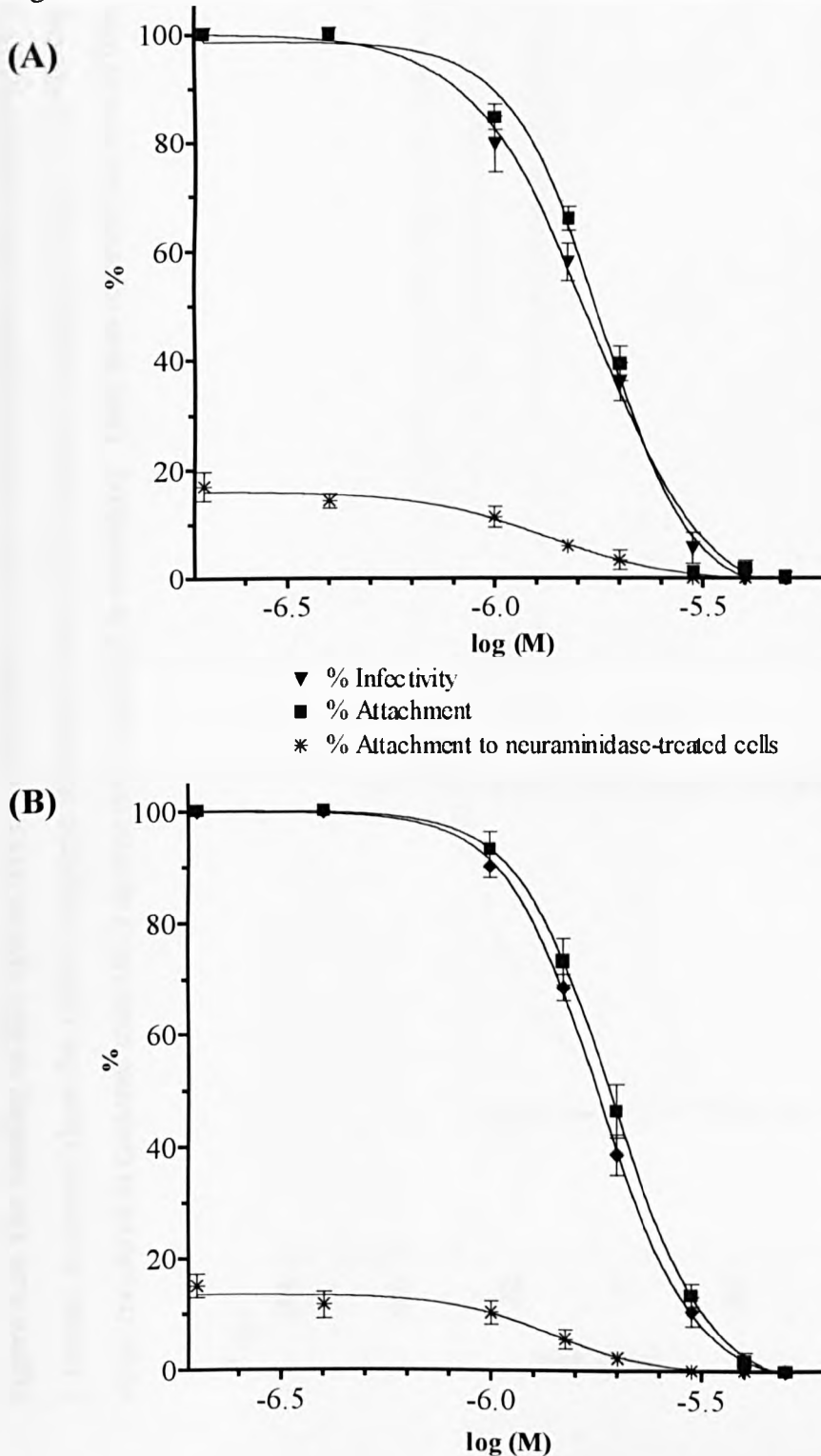


Figure 6.16 The binding of H37 IgG at five concentrations to captured whole influenza virus particles. Analysis was conducted in the 2-1 format, so curves show the relative response difference (Resp Diff) between background control channel and channel containing captured virus, measured in response units (RU) against time measured in seconds(s). Dark lines represent the area of dissociation used in the local fits.

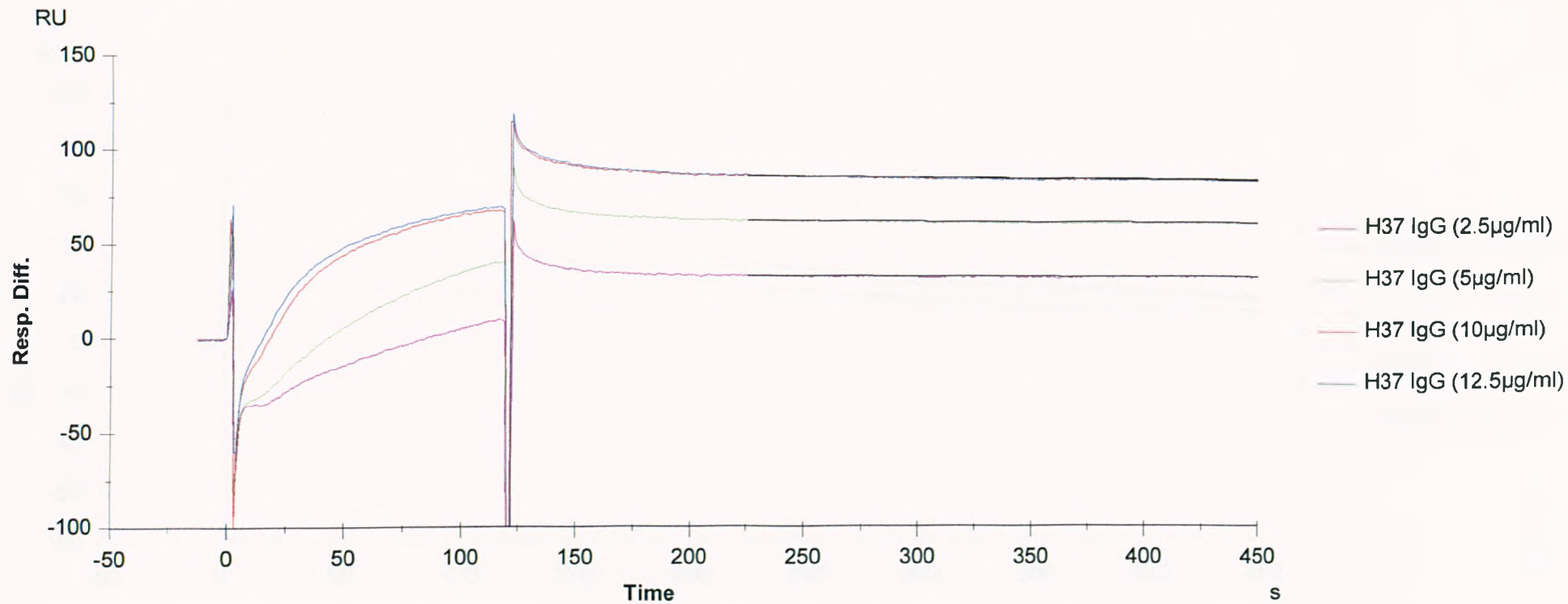


Figure 6.17 The binding of H37 Fab at four concentrations to captured whole influenza virus particles. Analysis was conducted in the 2-1 format, so curves show the relative response difference (Rresp Diff) between background control channel and channel containing captured virus, measured in response units (RU) against time measured in seconds(s). Dark lines represent the area of dissociation used in the local fits.

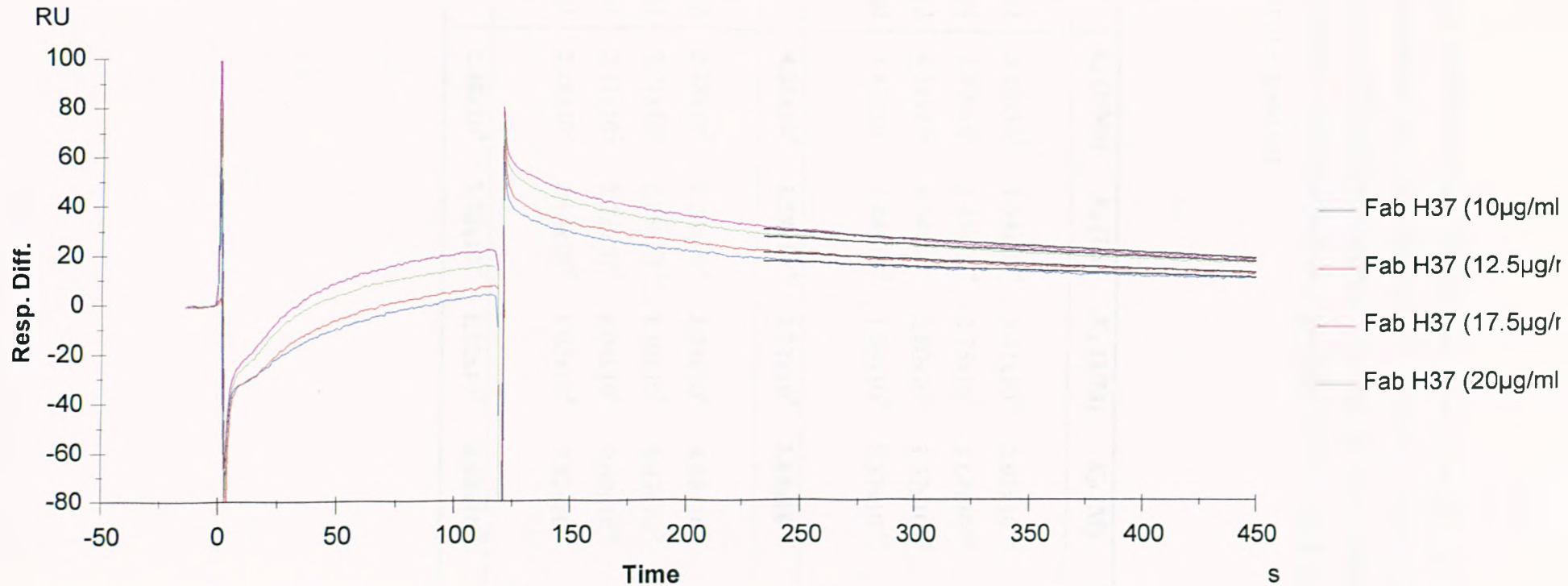


Table 6.10 Local fits of association and dissociation curves for H37 IgG and Fab. Table shows association and dissociation rate constants (k_a and k_d) and equilibrium association and dissociation constants (K_A and K_D) for binding to captured whole virus particles. Chi^2 value indicates goodness of fit of the Langmuir 1:1 binding model used (<1 = good fit).

Antibody	k_a (1/Ms)	k_d (1/s)	K_A (1/M)	K_D (M)	Chi^2
H37 IgG 2.5 $\mu\text{g/ml}$	5.26×10^5	1.54×10^{-4}	3.41×10^9	2.93×10^{-10}	
H37 IgG 5.0 $\mu\text{g/ml}$	3.99×10^5	1.45×10^{-4}	2.75×10^9	3.64×10^{-10}	
H37 IgG 10.0 $\mu\text{g/ml}$	4.31×10^5	1.54×10^{-4}	2.80×10^9	3.57×10^{-10}	
H37 IgG 12.5 $\mu\text{g/ml}$	3.43×10^5	1.84×10^{-4}	1.86×10^9	5.37×10^{-10}	
					0.292
H37 IgG Mean	4.25×10^5	1.59×10^{-4}	2.71×10^9	3.88×10^{-10}	
H37 Fab 10.0 $\mu\text{g/ml}$	2.78×10^5	2.25×10^{-3}	1.24×10^8	8.08×10^{-9}	
H37 Fab 12.5 $\mu\text{g/ml}$	2.71×10^5	2.28×10^{-3}	1.19×10^8	8.43×10^{-9}	
H37 Fab 17.5 $\mu\text{g/ml}$	2.31×10^5	2.22×10^{-3}	1.04×10^8	9.60×10^{-9}	
H37 Fab 20.0 $\mu\text{g/ml}$	2.18×10^5	2.14×10^{-3}	1.02×10^8	9.82×10^{-9}	
					0.223
H37 Fab Mean	2.48×10^5	2.22×10^{-3}	1.12×10^8	8.98×10^{-9}	

6.10 Summary: Comparison of the mechanism of neutralization of influenza by H37 IgG and Fab H37.

The Fab possessed a lower neutralization activity compared to the IgG. However, this difference was not uniform across the neutralization range with the Fab at N_{50} requiring a 360-fold higher concentration compared to the IgG, whilst it only required a 170-fold higher concentration at the N_{90} point. This suggests that the efficiency of neutralization of the Fab increased with increasing concentration. The affinity of the Fab was 4.3-fold lower relative to the IgG, with higher k_d being responsible for the difference. However, this difference could not explain the 170- to 360-fold difference in neutralization activity.

Investigation of the mechanism of neutralization revealed striking similarities with the H36 IgG, being able to simultaneously inhibit attachment of virus to target cells and fusion of virus with target membranes. The Fab also showed similarities to the H36 Fab neutralizing solely by inhibition of attachment of virus to target cells.

6.11 MAb H9-D3-4R2

The H9 MAb differs from the H36 and H37 MAbs in its antigenic site specificity, binding to site Cb.

6.11.1 Comparison of the neutralization by plaque reduction by H9 IgG and Fab.

Figure 6.18 indicates that neutralization efficiency of the Fab fragment is reduced compared to the IgG. The H9 Fab had poor neutralizing activity and it was not possible due to the large quantities required to achieve 100% neutralization of virus. Table 6.11 reveals that there is a difference between the efficiency of neutralization at 50% and at 90% with the Fab compared to the IgG. At N_{50} the Fab requires a 375-fold higher concentration than the IgG, in contrast to the 208-fold higher concentration required at N_{90} .

Figure 6.18 Neutralization of A/PR8 by H9 IgG and Fab. Data are the mean of three experiments of neutralization on MDCK cells, measured by plaque reduction. The bar represents SEM. The curves were generated by non-linear regression using the Graphpad Prism software package ($R = >0.97$).

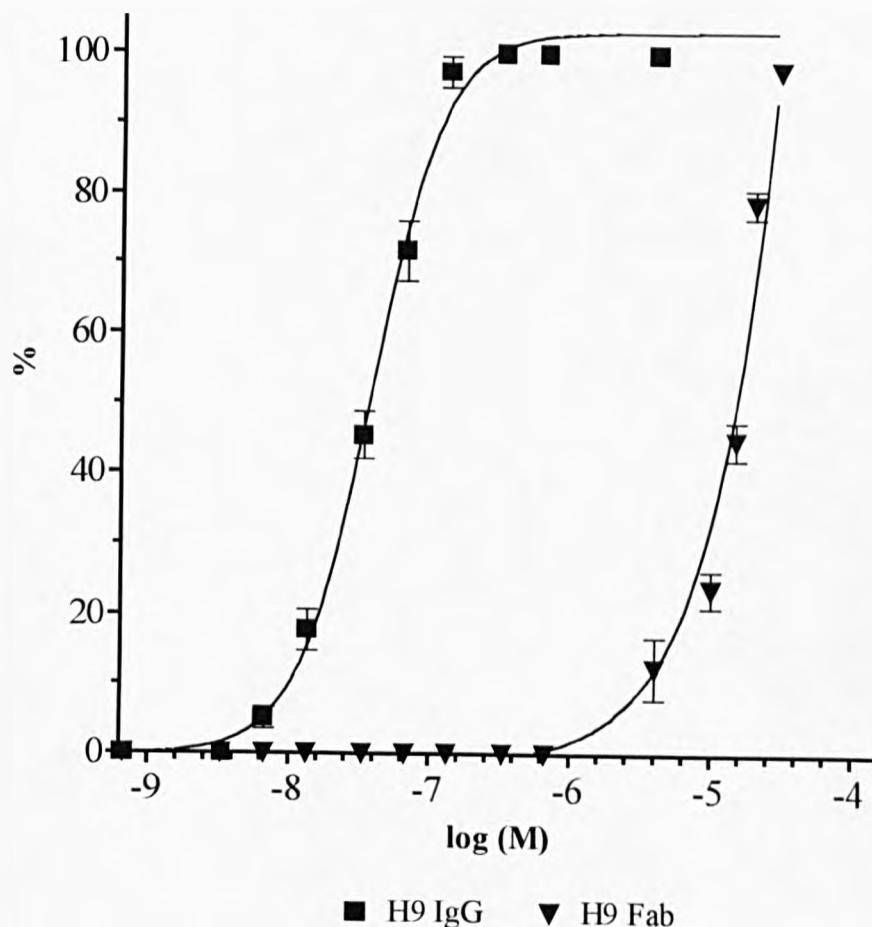


Table 6.11 Comparison of the neutralizing activities of H9 IgG and its Fab fragments. Data from Figure 8. 18.

<i>Antibody</i>	<i>Concentration (nM) required to give neutralization of</i>		<i>Fab : IgG ratio at neutralization of</i>	
	<i>50%</i>	<i>90%</i>	<i>50%</i>	<i>90%</i>
IgG	40.0	120.0	-	-
Fab	15000.0	25000.0	375 : 1	208 : 1

6.11.2 Analysis of the relationship between A/PR8 virus infectivity and attachment to both MDCK and BHK cells as a function of H9 IgG concentration.

Attachment of influenza to both cell types decreased with increasing concentration of IgG (Figure 6.19 A and B). The decrease in the level of attachment, as also seen with the H36 and H37 IgGs, does not correlate well with the decrease in the level of infectivity. For example, at N_{50} in Figure 6.19 (A), there is only a 20% inhibition of attachment and the same point in Figure 6.19 (B) there is a 15% reduction in attachment. An unpaired T-test showed the attachment and infectivity curves to be significantly different (Figure 6.19(A) P value = 0.034 and (B) P value = 0.002, where $p = <0.05$ is significant). At higher concentrations, inhibition of attachment became the dominant mechanism of neutralization.

6.11.3 Analysis of the relationship between A/PR/8 virus infectivity and internalisation as a function of H9 IgG concentration.

This assay was carried out simultaneously with the attachment assay and the level of internalisation was corrected for inhibition of attachment (as described previously for H36 IgG).

Figure 6.20 shows that as infectivity decreased with increasing H9 IgG concentration the percentage internalisation is unaffected. These results are again consistent with those seen with the H36 and H37 IgGs (section 6.2.3) and suggest that H9 IgG also did not affect receptor-mediated internalisation of influenza virus.

Figure 6.19 Analysis of the relationship between A/PR8 infectivity and attachment as a function of H9 IgG concentration. Data with MDCK cells (A) and BHK cells (B) are shown. Both infectivity and attachment were assayed by ELISA in parallel in the same batch of monolayers in 96 well plates, using the same virus-antibody mixtures. Analysis of attachment of A/PR8 to neuraminidase treated cells was used as the negative control. Data are the mean of five experiments. Curves were generated as in Figure 6.18 ($R = >0.98$ for all attachment and infectivity data).

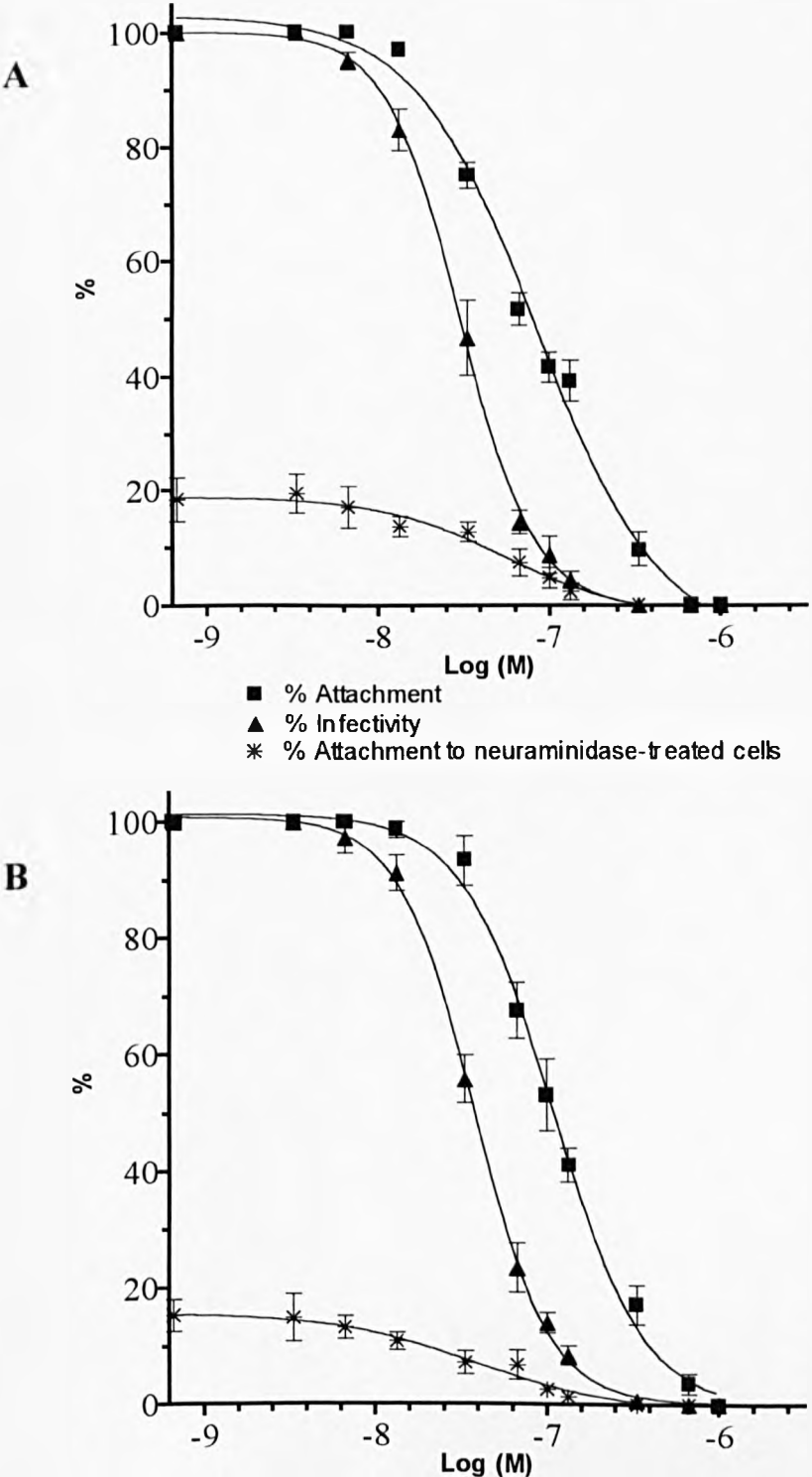


Figure 6.20 Analysis of the relationship between A/PR8 infectivity and the internalisation in MDCK cells as a function of H9 IgG concentration. Both infectivity and internalisation were assayed in parallel in the same batch of monolayers in 96 well plates, using the same virus-antibody mixtures. Data are corrected for inhibition of attachment to cells measured in the same experimental system. All data are the mean of three experiments. Curve was generated as in Figure 6.18 ($R = >0.98$)

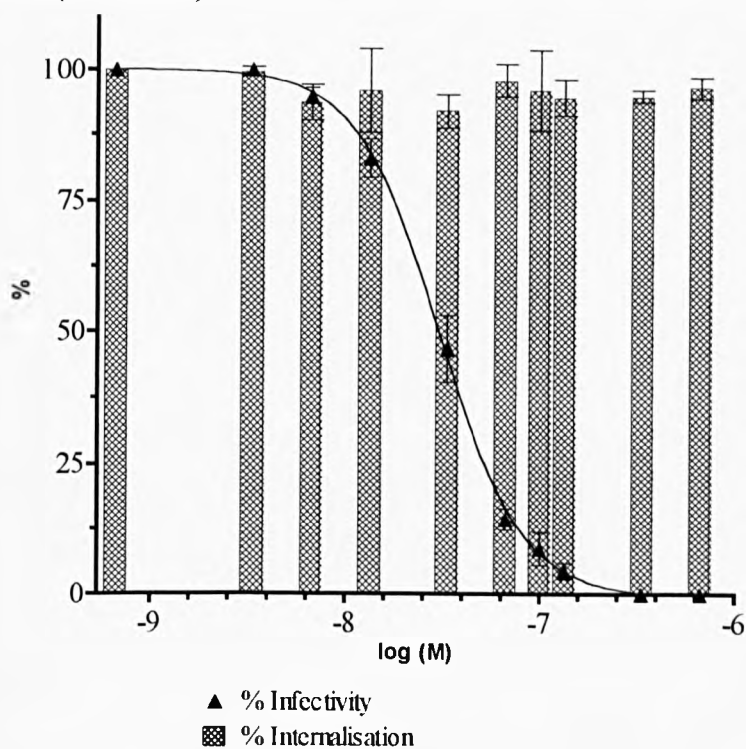


Table 6.12 Analysis of the internalisation of non-neutralized (N_0) and N_{50} virus under the negative control conditions. Data is presented as percentage inhibition of internalisation relative to non-neutralized virus at 37°C (standard conditions). Data for neutralized virus is corrected for inhibition of attachment. Data are the mean of three experiments.

<i>Control conditions</i>	<i>% inhibition of internalisation</i>
Cold (4°C) – N_0	95 (+/- 7)
Cold (4°C) – N_{50}	90 (+/- 11)
Hypertonic treated - N_0	81 (+/- 6)
Hypertonic treated – N_{50}	86 (+/- 5)

6.11.4 Analysis of the effect of H37 IgG on endosomal fusion of A/PR/8 virus in cells

The negative controls used in this assay were consistent with those used for analysis of H36 IgG and data in Tables 6.13 and 6.14 demonstrate again that the fluorescent signal obtained was specific for virus-driven fusion.

Figures 6.21 and 6.22 show that as infectivity decreased with increasing concentration of H9 IgG the percentage fusion also decreases in both MDCK and BHK cells respectively. This indicates a causal relationship between inhibition of virus-cell fusion and neutralization by H9 IgG. Comparisons of the fusion and infectivity curves using an unpaired T-test revealed that in both MDCK and BHK cells that they were not significantly different (for Figure 6.21, P value = 0.164 and for Figure 6.22 P value = 0.267).

6.12 Fab H9-D3-4R2

6.12.1 Analysis of the relationship between A/PR/8 virus infectivity and attachment to both MDCK and BHK cells as a function of Fab H9 concentration.

Attachment of virus to both types of cell was unaffected by increasing concentrations of Fab (Figure 6.23 A and B). This is in direct contrast to the situation seen with the IgG, in which attachment is affected. As a result the H9 Fab must be neutralizing the virus by interfering with a stage(s) further along the virus infectious cycle. This situation is also in direct contrast to the H36 and H37 Fabs which only inhibited attachment in this system and again shows that Fab mechanism of neutralization can be very different to that seen with the IgG.

Figure 6.21 Analysis of the relationship between A/PR8 infectivity and fusion of virus to MDCK cells as a function of H9 concentration. Both sets of data were obtained using 3 cm monolayers. Infectivity was determined by plaque reduction and fusion was measured by fluorescence dequenching of R18-labelled virus. Data are the mean of three experiments and have been corrected for inhibition of virus attachment to cells. Curves were generated as in Figure 6.18 ($R = >0.98$ for all fusion and infectivity data).

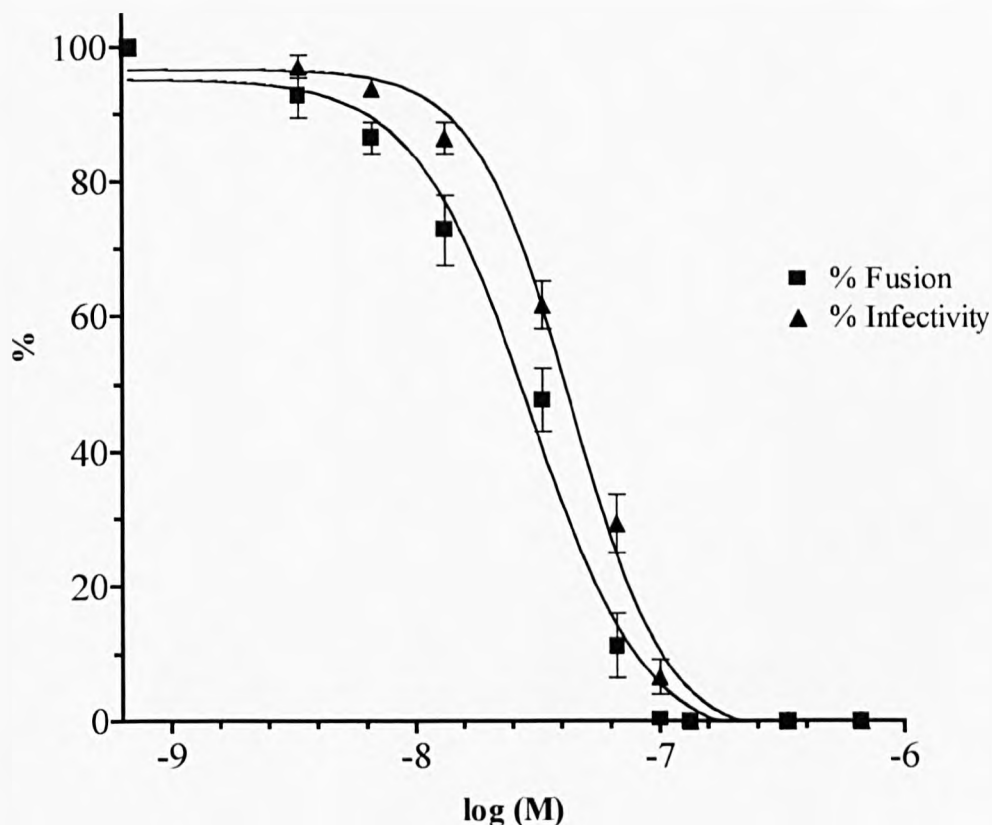


Table 6.13 Analysis of the fusion of non-neutralized virus under the negative control conditions. Data is presented as percentage inhibition of fusion relative to non-neutralized virus at 37°C. Data are the mean of three experiments

<i>Control conditions</i>	<i>% inhibition of internalisation</i>
Cold (4°C) – N ₀	91 (+/- 9)
Bafilomycin treated - N ₀	81 (+/- 12)

Figure 6.22 Analysis of the relationship between A/PR8 infectivity and fusion of virus to MDCK cells as a function of H9 concentration. Both sets of data were obtained using 3 cm monolayers. Infectivity was determined by plaque reduction and fusion was measured by fluorescence dequenching of R18-labelled virus. Data are the mean of three experiments and have been corrected for inhibition of virus attachment to cells. Curves were generated as in Figure 6.18 ($R = >0.98$ for all fusion and infectivity data).

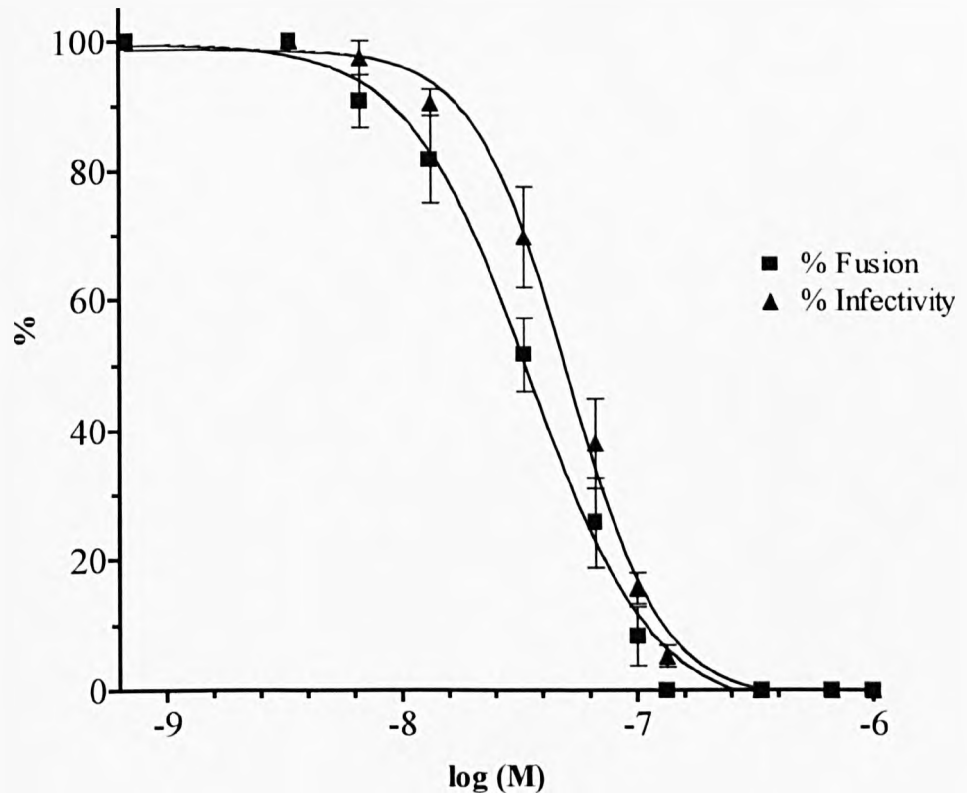
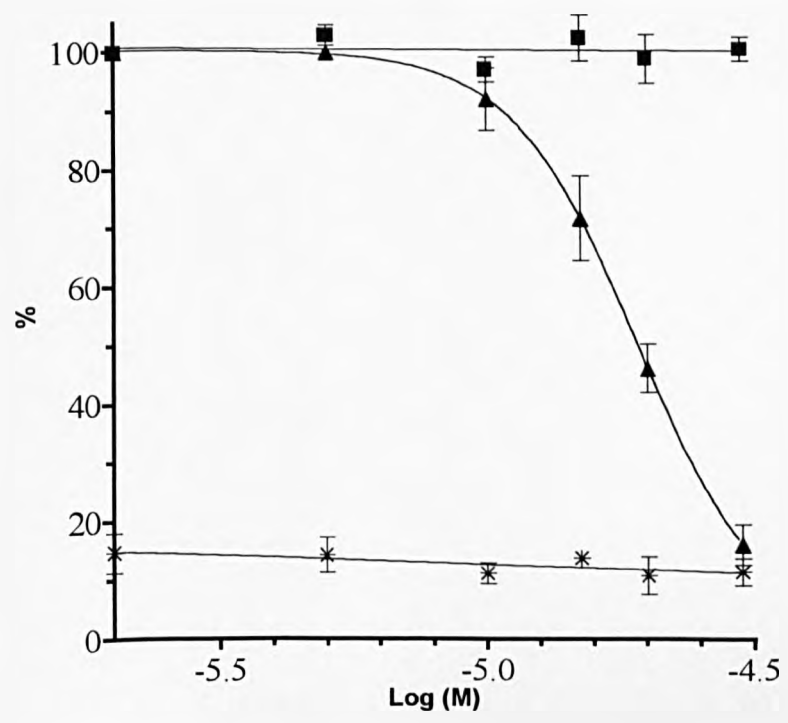
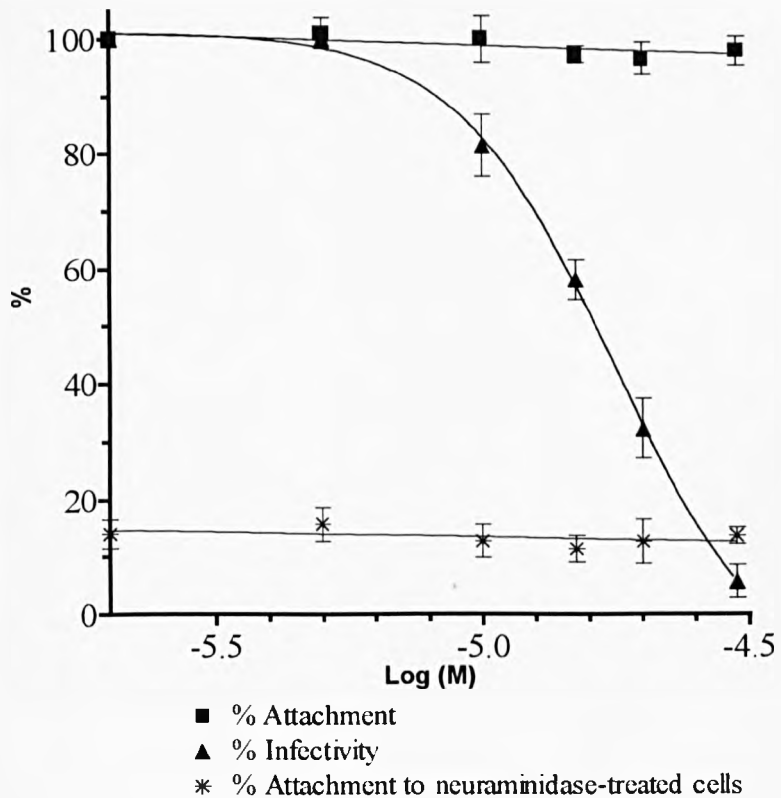


Table 6.14 Analysis of the fusion of non-neutralized virus under the negative control conditions. Data is presented as percentage inhibition of fusion relative to non-neutralized virus at 37°C. Data are the mean of three experiments

<i>Control conditions</i>	<i>% inhibition of internalisation</i>
Cold (4°C) – N ₀	89 (+/- 6)
Bafilomycin treated - N ₀	79 (+/- 15)

Figure 6.23 Analysis of the relationship between A/PR8 infectivity and attachment as a function of Fab H37 concentration. Data with MDCK cells (A) and BHK cells (B) are shown. Infectivity and attachment were assayed by ELISA in parallel in the same batch of monolayers in 96 well plates, using the same virus-antibody mixtures. Inhibition of attachment of A/PR8 to neuraminidase-treated cells was used as the negative control. Data are the mean of five experiments. Curves were generated as in Figure 6.18 ($R = >0.99$ for all infectivity data).



6.12.2 Analysis of the relationship between A/PR/8 virus infectivity and internalisation as a function of H9 Fab concentration.

This assay was carried out simultaneously with the attachment assay and the level of internalisation was corrected for inhibition of attachment (as described previously for H36 IgG).

Figure 6.24 shows that as infectivity decreased with increasing H9 Fab concentration the percentage internalisation stayed at approximately 100%. These results are again consistent with those seen with the other antibodies described previously and suggest that H9 Fab also did not affect receptor-mediated internalisation of influenza virus.

Figure 6.24 Analysis of the relationship between A/PR8 infectivity and the internalisation in MDCK cells as a function of H9 Fab concentration. Both infectivity and internalisation were assayed in parallel in the same batch of monolayers in 96 well plates, using the same virus-antibody mixtures. Data are corrected for inhibition of attachment to cells measured in the same experimental system. All data are the mean of three experiments. Curve was generated as in Figure 6.18 ($R = > 0.99$)

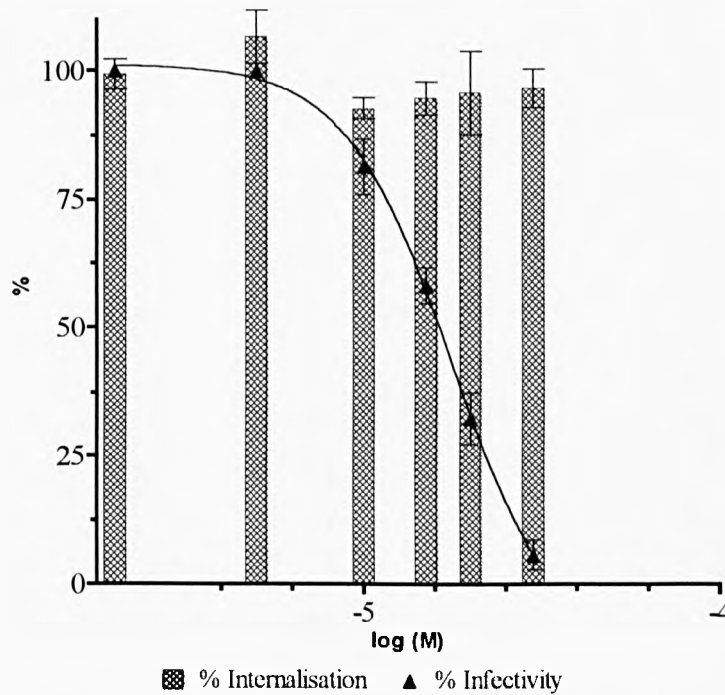


Table 6.15 Analysis of the internalisation of non-neutralized (N_0) and N_{50} virus under the negative control conditions. Data is presented as percentage inhibition of internalisation relative to non-neutralized virus at 37°C (standard conditions). Data for neutralized virus is corrected for inhibition of attachment. Data are the mean of three experiments.

<i>Control conditions</i>	<i>% inhibition of internalisation</i>
Cold (4°C) – N_0	94 (+/- 8)
Cold (4°C) – N_{50}	90 (+/- 7)
Hypertonic treated - N_0	78 (+/- 8)
Hypertonic treated – N_{50}	85 (+/- 11)

6.12.3 Analysis of the relationship between A/PR/8 virus infectivity and endosomal fusion in both MDCK and BHK cells as a function of H9 Fab concentration.

The negative controls used in this assay were consistent with those used for analysis of H36 IgG and data in Tables 6.16 and 6.17 demonstrate again that the fluorescent signal obtained was specific for virus-driven fusion.

Figures 6.25 and 6.26 show that as infectivity decreased with increasing concentration of H9 Fab the percentage fusion also decreased in both MDCK and BHK cells respectively. This indicates a causal relationship between inhibition of virus-cell fusion and neutralization by H9 Fab. Comparisons of the fusion and infectivity curves using an unpaired T-test revealed that in both MDCK and BHK cells that they were not significantly different (for Figure 6.25, P value = 0.302 and for Figure 6.26 P value = 0.908). Therefore, it is possible to conclude that the H9 Fab neutralizes by inhibition of fusion and hence demonstrates that bivalency is not vital for fusion inhibition. It is interesting to note that in both cell types that fusion inhibition is not complete and at higher concentration of Fab cannot account for the entire loss of infectivity. However, without further experimentation it is unknown whether these differences are significant or are just a factor of the very poor neutralizing ability of the Fab.

6.13 Real-time kinetic analysis of H9 IgG and its Fab to virus particles using surface plasmon resonance.

6.13.1 Comparison of the kinetics of binding of H9 IgG and its Fab fragment to whole virus particles.

Figures 6.27 and 6.28 show the real-time binding kinetics of four concentrations of H9 IgG and Fab respectively. The data have been transformed and then analysed in an equivalent manner to H36 IgG (Table 6.18). Comparison of the means of the equilibrium dissociation constant (K_D), shows that the H9 IgG and Fab are almost identical with values of 5.29×10^{-10} M and 5.49×10^{-10} M respectively. This suggests that the Fab has not lost any affinity relative to the IgG and hence reduction of affinity cannot explain the reduced neutralization efficiency of the Fab.

Figure 6.25 Analysis of the relationship between A/PR8 infectivity and fusion of virus to MDCK cells as a function of H9 Fab concentration. Both sets of data were obtained using 3 cm monolayers. Infectivity was determined by plaque reduction and fusion was measured by fluorescence dequenching of R18-labelled virus. Data are the mean of three experiments and have been corrected for inhibition of virus attachment to cells. Curves were generated as in Figure 6.18 ($R = >0.97$ for all fusion and infectivity data).

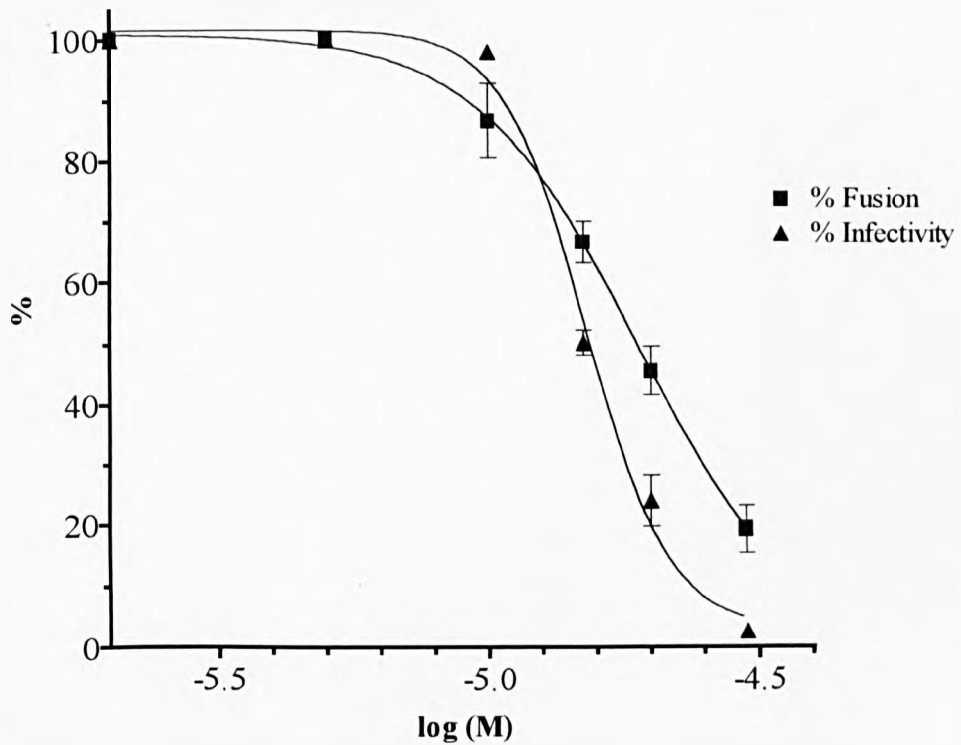


Table 6.16 Analysis of the fusion of non-neutralized virus under the negative control conditions. Data is presented as percentage inhibition of fusion relative to non-neutralized virus at 37°C. Data are the mean of three experiments

<i>Control conditions</i>	<i>% inhibition of internalisation</i>
Cold (4°C) – N ₀	91 (+/- 6)
Bafilomycin treated - N ₀	80 (+/- 9)

Figure 6.26 Analysis of the relationship between A/PR8 infectivity and fusion of virus to MDCK cells as a function of H9 Fab concentration. Both sets of data were obtained using 3 cm monolayers. Infectivity was determined by plaque reduction and fusion was measured by fluorescence dequenching of R18-labelled virus. Data are the mean of three experiments and have been corrected for inhibition of virus attachment to cells. Curves were generated as in Figure 6.18 ($R = >0.97$ for all fusion and infectivity data).

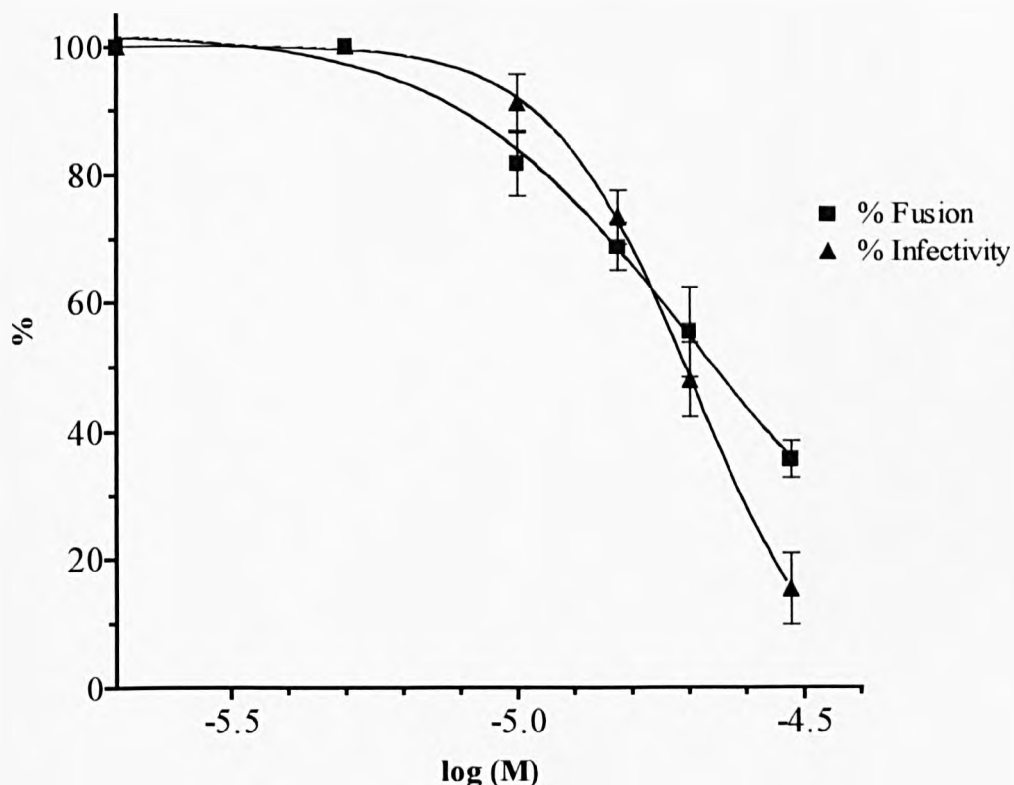


Table 6.17 Analysis of the fusion of non-neutralized virus under the negative control conditions. Data is presented as percentage inhibition of fusion relative to non-neutralized virus at 37°C. Data are the mean of three experiments

<i>Control conditions</i>	<i>% inhibition of internalisation</i>
Cold (4°C) – N ₀	89 (+/- 5)
Bafilomycin treated - N ₀	86 (+/- 15)

6.14 Summary: Comparison of the mechanism of neutralization of influenza A virus by H9 IgG and Fab.

The efficiency of neutralization of H9 Fab increased with increasing concentration, but its neutralization activity was lower than the IgG. The lower neutralization activity of the Fab compared to the IgG could not be explained by differences in affinity.

Investigation of the mechanism of neutralization of the H9 IgG revealed striking similarities with the H36 and H37 IgGs, being able to simultaneously inhibit both attachment of virus to target cells and fusion of virus to target membranes. However, the Fab displayed a unique mechanism of neutralization, inhibiting fusion of virus to target membranes. This demonstrated that bivalency was not required for inhibition of fusion.

Figure 6.27 The binding of H9 IgG at five concentrations to captured whole influenza virus particles. Analysis was conducted in the 2-1 format, so curves show the relative response difference (Resp Diff) between background control channel and channel containing captured virus, measured in response units (RU) against time measured in seconds(s). Dark lines represent the area of dissociation used in the local fits.

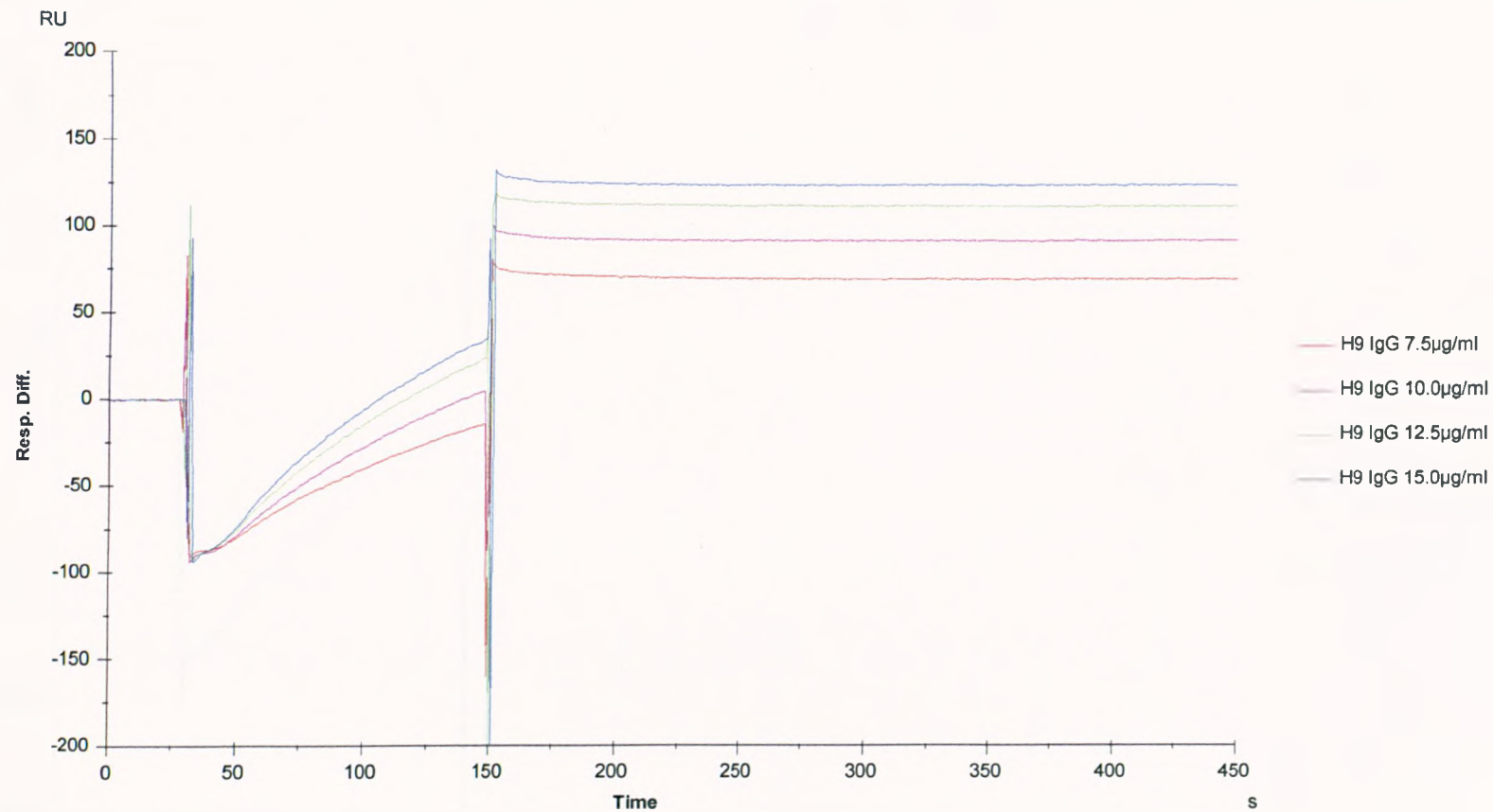


Figure 6.28 The binding of H9 Fab at four concentrations to captured whole influenza virus particles. Analysis was conducted in the 2-1 format, so curves show the relative response difference (Resp Diff) between background control channel and channel containing captured virus, measured in response units (RU) against time measured in seconds(s). Dark lines represent the area of dissociation used in the local fits.

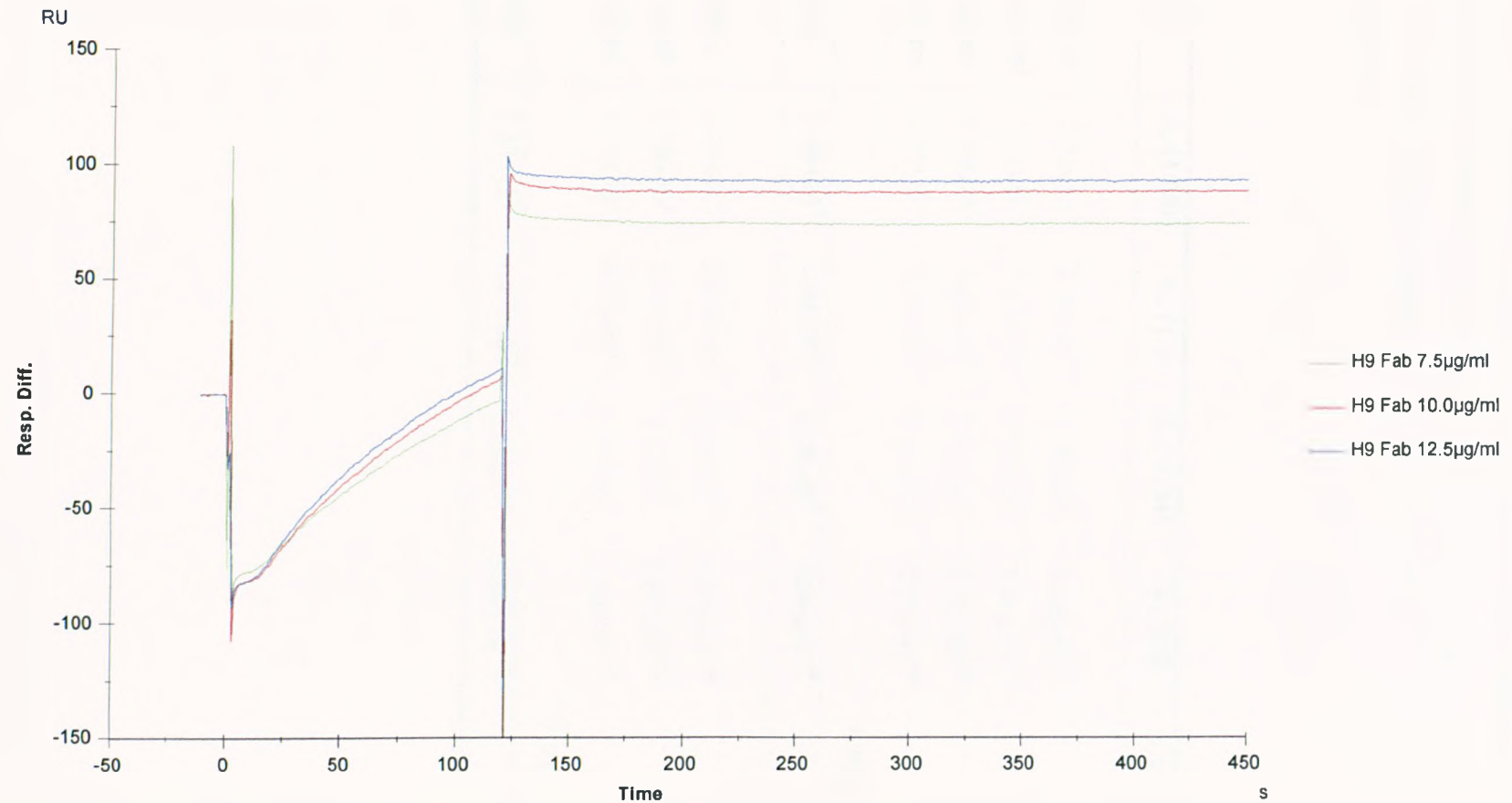


Table 6.18 Local fits of association and dissociation curves for H9 IgG and Fab. Table shows association and dissociation rate constants (k_a and k_d) and equilibrium association and dissociation constants (K_A and K_D) for binding to captured whole virus particles. Chi² value indicates goodness of fit of the Langmuir 1:1 binding model used (<1 = good fit).

Antibody	k_a (1/Ms)	k_d (1/s)	K_A (1/M)	K_D (M)	Chi ²
H9 IgG 7.5µg/ml	1.35x10 ⁵	4.98x10 ⁻⁵	2.76x10 ⁹	3.62x10 ⁻¹⁰	0.034
H9 IgG 10.0µg/ml	1.11x10 ⁵	3.81x10 ⁻⁵	2.92x10 ⁹	3.42x10 ⁻¹⁰	
H9 IgG 12.5µg/ml	9.66x10 ⁴	3.65x10 ⁻⁵	2.65x10 ⁹	3.78x10 ⁻¹⁰	
H9 IgG 15.0µg/ml	8.95x10 ⁴	2.10x10 ⁻⁵	4.26x10 ⁹	2.35x10 ⁻¹⁰	
H9 IgG Mean	1.08x10⁵	3.64x10⁻⁵	3.15x10⁹	3.29x10⁻¹⁰	
H9 Fab 7.5µg/ml	1.45x10 ⁵	6.80x10 ⁻⁵	2.13x10 ⁹	4.69x10 ⁻¹⁰	0.036
H9 Fab 10.0µg/ml	1.18x10 ⁵	2.15x10 ⁻⁵	5.5x10 ⁹	1.82x10 ⁻¹⁰	
H9 Fab 12.5µg/ml	1.13x10 ⁵	4.47x10 ⁻⁵	2.52x10 ⁹	3.96x10 ⁻¹⁰	
H9 Fab Mean	1.25x10⁵	4.47x10⁻⁵	3.38x10⁹	3.49x10⁻¹⁰	

6.15 Discussion :

6.15.1 Comparison of the characteristics of neutralization of A/PR/8 virus by the IgGs and their Fabs.

This study demonstrates that the Fabs are neutralizing, indicating that bivalency is not required for neutralization. However, each Fab had a lower neutralization efficiency than its respective IgG. A trend seen in the Fabs was that they are all more efficient at neutralizing at N_{90} than N_{50} relative to their IgGs (Table 6.19). This suggested that Fab neutralizing activity increased with increasing concentration.

A possible explanation for the loss of neutralization activity by the Fabs is a reduction in affinity compared to the IgGs. However, the IgGs and the Fabs have similar affinities; the 4.3-fold lower affinity of the H37 Fab compared to its IgG being the largest. Therefore, loss of affinity cannot explain the large reduction (104- to 370-fold at N_{50}) in neutralization efficiency. Hence, there appears to be no correlation between neutralization and affinity. The similarity in the affinities of the IgGs and their Fabs could be explained by the affinities of the IgGs being above the $>10^{-9}$ threshold suggested to be sufficiently high that it dominates the loss of bivalency and results in only a small difference in affinity with the Fabs (Parham, 1983). An alternative explanation of the similar affinities is that the IgGs also bind monovalently (Schofield and Dimmock, 1996).

The Fabs can be entered into a classification scheme which has five categories depending on neutralization activity and affinity (Schofield *et al.*, 1997b). H36 and H9 Fab are members of group I, which represents Fabs that have a similar affinity to their IgG, but lower neutralization activity. The H37 Fab is a member of group III, which represents Fab whose loss of neutralization activity exceeds the reduced affinity by at least 10-fold. All the IgGs and Fabs had very high affinities, with all the IgG affinities being higher than those described for anti-Fowl plaque virus (FPV) IgGs (Schofield and Dimmock, 1996).

Table 6.19 Summary of the mechanism of neutralization by H36, H37 and H9 IgGs and their antibody fragments in MDCK cells.

<i>MAb</i>	<i>Antigenic site</i>	<i>Concentration (nM) required to give</i>		<i>Percentage inhibition of attachment at</i>		<i>Inhibition of internalisation</i>	<i>Inhibition of fusion</i>
		<i>N₅₀</i>	<i>N₉₀</i>	<i>N₅₀</i>	<i>N₉₀</i>		
H36 : IgG	Sb	0.5	6.0	10	73	No	Yes
H36 : Fab	Sb	52.0	90.0	42	88	No	-
H36 : F(ab) ₂	Sb	4.0	15.0	3	74	ND	ND
H37 : IgG	Ca2	5.0	14.0	20	65	No	Yes
H37 : Fab	Ca2	1800.0	2500.0	42	87	No	-
H9 : IgG	Cb	40.0	120.0	20	55	No	Yes
H9 : Fab	Cb	15000.0	25000.0	1	1	No	Yes

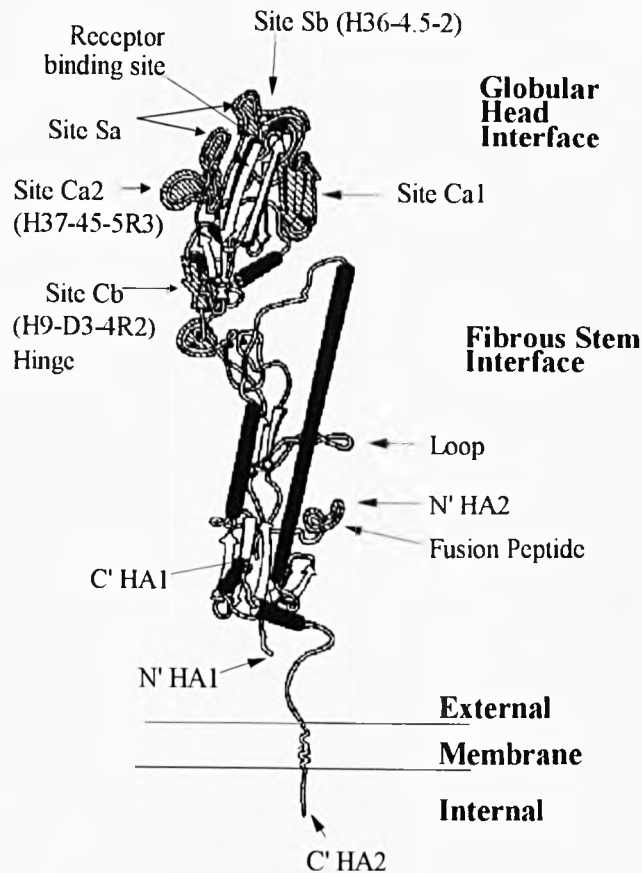
ND = Not done

6.15.2 Comparison of the neutralization activity of H36, H37 and H9 IgGs and Fabs.

The ranking order of the antibodies based on neutralization activity is H36 > H37 > H9 and this order is mirrored when comparing the neutralizing activity of their Fabs. From this arises the interesting question of what are the factors that affect the efficiency of neutralization of virus by each of the antibodies?

Each of the antibodies binds to a different antigenic sites on the HA molecule and it is possible that intrinsic properties of the specific antigenic site or its relationship to the receptor binding site may affect its neutralization activity (Figure 6.29). Previously Brown *et al.* (1990) postulated that MAbs A2, specific for site C (H3 HA numbering system, near to site Cb in the H1 HA) was the least efficient at neutralization and HI because its antigenic site was furthest from the receptor binding site and thus MAbs binding to this site were the least able, relative to the other antigenic sites, to sterically hinder the receptor-HA interaction. This concept has been recently supported by a study which compared the X-ray crystallographic structure of the BHA-Fab complexes of one Fab binding to a site which comprises part of the receptor-binding site and another Fab which binds to a site at a distance from the receptor binding site (Fleury *et al.*, 1999). This showed that the HC19 Fab was an order of magnitude more efficient at neutralization than the HC45 Fab, even though they were had similar affinities. The authors suggested that even the antibodies that bind at a distance from the receptor-binding site can sterically interfere with attachment, with the antibodies binding close to the receptor binding site being more efficient at steric hindrance. The data presented in this thesis is also supportive, as the HI ranking order of H36 > H37 > H9 (data not shown) mirrors the neutralization order, suggesting steric hindrance was lowest in H9 which binds to site Cb the furthest from the receptor binding site. The H9 Fab data is also supportive of this hypothesis, as it has the lowest neutralization activity relative to its IgG, compared with H36 and H37 Fabs. Also the Fab H9 does not inhibit virus attachment to either MDCK and BHK cells and does not give HI. These data suggest that reducing the molecular length of the H9 IgG 2-fold when making its Fab fragment has had the largest impact on the ability to sterically hinder receptor interactions, as one would expect if distance from the receptor-binding site

Figure 6.29 Diagrammatic representation of a monomer of the H1 haemagglutinin, based on the H3 crystal structure. MAb binding sites and cell-receptor binding site are annotated.



was important.

Another study using an H7 virus showed that MAb 8/4 which binds to site III (equivalent of Cb) also has a low neutralization titre and a very poor HI titre (Yoden *et al.*, 1985). Thus three studies have shown that antibodies to the site furthest from the receptor binding site (Cb in H1, III in H7 and C in H3) are the least efficient at neutralizing compared to MAbs to other sites and hence suggests that this could be a general property of these antigenic regions. The primary immune response in BALB/c mice is predominantly restricted to site Cb (Kavaler *et al.*, 1990), suggesting that this may represent an immune evasion strategy during primary influenza

infection in which antibodies are biased to low efficiency neutralizing epitopes. However, many more MAbs need to be analysed to further this hypothesis.

The H37 IgG:Fab neutralization ratio was very low (360:1 at N₅₀) compared to the H36 (104:1) and almost to the H9 Fab levels (375:1). The H37 IgG binds to site Ca2 and it seems unlikely that distance from the receptor binding site can fully explain the large loss of neutralization efficiency. In fact, the study by Brown *et al.*, (1990) concluded that apart from site C there was no absolute correlation between antigenic site recognised by the MAbs and its neutralization and HI activity. Therefore, the orientation of binding of the IgGs may also play a role in the ability to neutralize and give HI (Schofield *et al.*, 1997b); Pountourios *et al.*, 1990). It is possible that relative to the H36 IgG, the H37 IgG has a binding angle that is not efficient at interfering with the receptor-binding site. The reduction of length (or molecular mass) when an IgG is made into a Fab add to this non-optimal binding angle effect, resulting in a low efficiency of steric hindrance of the HA-cell receptor interaction. We therefore postulate that the neutralization efficiency of the IgGs (H36>H37>H9) is affected by both the distance of the epitope from the receptor-binding site and the binding angle of the IgG relative to the receptor site. However, a large panel of MAbs to different antigenic sites needs to be studied to support this.

6.15.3 Comparison of the mechanism of neutralization of A/PR/8 virus by the IgGs and their antibody fragments.

This study is the first to determine the mechanism of neutralization of influenza virus by a Fab. Not only did the Fabs differ in their mechanism of neutralization from the IgGs, but that they also differed from each other. Analysis of the relationship between attachment to target cells and infectivity of virus neutralized by the IgGs indicated that inhibition of attachment was a major mechanism of neutralization, particularly when neutralization was > 90%, but could not account for the entire loss of infectivity. Internalisation of neutralized, but attached virus was unaffected. However, decreases in virus-cell fusion correlated with neutralization suggested a causal relationship. The mechanism of neutralization of the three IgGs was strikingly similar and indicated that antigenic site or isotype had no effect on the mechanism of neutralization. The IgGs seemingly exhibited a complex neutralization process, with comparison of N₅₀ and N₉₀ points revealing a shifting

dominance of mechanisms. At the N_{90} point inhibition of attachment accounts for the majority of loss of virus infectivity, whereas at N_{50} inhibition of attachment accounts for the minority of the loss of infectivity and the majority can be attributed, by inference, to inhibition of fusion. Thus there is a spectrum of neutralization activity which starts with fusion inhibition and ends with attachment inhibition. In between both mechanisms operate simultaneously, with dominance of each mechanism depending on the IgG concentration. An interesting consequence of this conclusion is that inhibition of fusion must operate at a lower density of IgG molecules per virion than inhibition of attachment, indicating it to be the primary neutralization mechanism. The above conclusion could also be relevant to a number of other neutralization studies, including neutralization of influenza A, HIV-1 and transmissible gastroenteritis coronavirus (TGEV) (Outlaw *et al.*, 1990; Ugolini *et al.*, 1997; Suñé *et al.*, 1990). In these studies the level of inhibition of attachment did also not account for the amount of neutralization observed, suggesting that other mechanisms were acting.

In contrast, Fabs H36 and H37 inhibited attachment as their sole mechanism of neutralization, whereas H9 Fab did not inhibit attachment, but decreases in virus-cell fusion with infectivity suggested a causal relationship.

Comparison of the IgG and Fab neutralization at N_{90} -

The mechanism of neutralization at N_{90} for the H36, H37 and H9 IgGs and H36 and H37 Fabs is predominantly inhibition of attachment. It is generally accepted that inhibition of attachment is caused by steric hindrance of the HA-cell receptor interaction and therefore, it is likely that the most important factor in the difference in neutralization at N_{90} is molecular mass of the antibody.

Fab is approximately half the length of an IgG and hence Schofield *et al.*, (1997b) suggested that on a theoretical basis one might expect a reduction of only 2-fold in the efficiency of steric hindrance (inhibition of attachment). Steric hindrance, however, is a complex phenomenon, which is affected not only the length and the molecular mass of the antibody, but also the valency and orientation of antibody binding in relation to the receptor-binding site and the flexibility and rotational freedom displayed by the antibody (Burton, 1990; Nisonoff *et al.*, 1975; Padlan, 1994). It has also been suggested that steric hindrance may be affected by the

valency of the virus-IgG interaction (Schofield, 1996). For example, an IgG that binds monovalently may have a greater degree of rotational freedom increasing the probability of interference with receptor interactions. The valency of the virus-IgG interaction in this study is unknown, but the similar affinity values for IgGs and Fabs suggest that the IgGs may bind monovalently. Also the molecular volume of the antibody is also a useful parameter to consider. In fact combining these properties, which could act synergistically, gives us the concept of the volume occupied by the antibody, i.e., the space in which the antibody can have a physical effect, which would be larger than the molecular volume per se (Outlaw, 1989). A Fab would have a much lower effective volume and this could account for the observed loss of neutralization activity compared to the IgG. The relatively poor ability to sterically hinder the HA-receptor interaction could also explain why Fab has a higher neutralization efficiency at the higher concentrations required to give N_{90} compared to the lower concentrations at N_{50} .

At N_{90} the H9 Fab cannot inhibit attachment of virus to cells but inhibits fusion. This could be due to the relationship between the antigenic site, Cb, and the receptor-binding site, as discussed previously. The H9 Fab has the lowest neutralization activity and this may be due to its inability to inhibit the attachment process.

Comparison of the IgG and Fab neutralization at N_{50} :

The mechanism of neutralization at N_{50} of the H9 Fab was inhibition of fusion, whilst both the H36 and H37 Fabs inhibited attachment. The IgGs all neutralize predominantly, though not exclusively by inhibition of fusion. If we first examine the H36 and H37 Fabs compared to their IgGs. First impressions suggest a simple model, with the difference between the IgGs and the Fabs at N_{50} being inhibition of fusion. However, this situation is more complicated as data presented in chapter 7 shows that these Fabs can inhibit fusion of virus pre-attached to cells. Thus bivalency is not absolutely required for fusion inhibition, which is further supported by the H9 Fab, where inhibition of fusion seems to be sole mechanism of neutralization.

Why do we not see inhibition of fusion by H36 and H37 Fab at N_{50} ?

It is possible that the processes of inhibition of attachment and fusion are both due to steric hindrance, and that this is directly linked to molecular volume. Therefore, the inhibition of attachment and fusion could occur at similar efficiencies, such that they give the impression of a single mechanism. The H9 Fab did not inhibit attachment of virus to cells suggesting that the processes of fusion inhibition and attachment inhibition can be segregated and that binding to different regions of the HA may allow the antibody to interfere with different parts of the fusion process.

The situation with the IgG is complicated and could depend on whether the IgGs bind (I) monovalently or (II) bivalently –

(I) If the IgGs can only bind monovalently then the difference between the IgGs and Fabs must be due to the greater molecular volume. Therefore, the argument would follow that its greater molecular volume allows the IgGs inhibit the fusion process. This occurs even at low IgG:virus ratios, but as the ratio increases the higher density of IgG molecules starts to inhibit attachment. In contrast, the lower molecular volume of the Fab means that they require a high density of molecules per virion to initiate neutralization, so at lower Fab : virion ratios they sterically hinder the fusion process only as efficiently as they inhibit attachment. The concept that fusion inhibition is related to molecular volume is supported by the H9 Fab which inhibits fusion but has the lowest neutralization activity. The $F(ab)_2$ data is also supportive as at N_{50} it requires an 8-fold higher concentration relative to the IgG, but its mechanism of neutralization is very similar. Hence, if bivalency was of sole importance in fusion inhibition then you would expect the $F(ab)_2$ to neutralize with the same efficiency as the IgG. Therefore, the 8-fold loss of neutralization efficiency indicates that molecular volume is important at the N_{50} point.

(II) If the IgGs can bind bivalently too neighbouring HA spikes, then the difference with the Fabs could be due to the IgGs possessing two mechanisms of fusion inhibition. (A) a monovalent inhibition of fusion which may sterically hinder some part of the fusion process and is linked to molecular mass (process possibly used by H9 Fab) and (B) a bivalent inhibition of fusion, where at lower concentrations of IgG where bivalent

binding has a higher probability (due to availability of epitopes), the IgGs crosslink HA spikes and possibly prevent correct orientation into a fusion active pore. Therefore the argument follows that at N_{50} bivalent inhibition of fusion becomes increasingly dominant and hence you see inhibition of fusion at lower IgG concentrations. As the IgG:virus ratio increases, epitope availability decreases, and hence monovalent binding dominates, which has a higher probability of inhibiting attachment.

An important component of future study in this area should be to elucidate the valency of the binding of the IgGs. This could be done in two ways (I) by using cryo-electron microscopy to directly visualise the binding of the antibodies to the virus, and (II) by construction of a monovalent antibody, with one Fab arm specific for A/PR/8 virus and the other arm to a non-viral epitope. This hybrid IgG would only bind monovalently to the virus but would have the equivalent molecular mass as standard IgG. Hence it would allow discrimination between the effects of bivalency and molecular mass in the analysis of the mechanism of neutralization. An attempt was made by fusion of hybridomas to construct a monovalent antibody with H36 IgG and anti-rat CD4 IgG components, but unfortunately time did not allow completion.

In summary, comparison of the mechanisms of neutralization of the IgGs and their Fabs revealed the following features in common:

- (I) Fabs are less efficient at neutralizing than their IgGs.
- (II) Fabs are less efficient at neutralizing at N_{50} than N_{90} relative to their IgGs.
- (III) IgGs have a complex mechanism of neutralization and simultaneously neutralize by inhibition of attachment and fusion.
- (IV) At low concentrations ($<N_{50}$) IgGs neutralize mainly by inhibition of fusion.
- (V) At high concentrations ($>N_{90}$) IgGs neutralize by mainly inhibiting attachment.
- (VI) Fabs have a simpler mechanism of neutralization, compared to their IgGs and neutralize by a single mechanism across the range of concentrations tested.

From the data presented it is my opinion that both molecular volume and bivalency play a role in neutralization by these IgGs and these may vary in importance depending on the concentration analysed. An example of how the importance of bivalency and molecular volume may vary with the MAb being

analysed is exemplified by studies by Schofield *et al.*, (1997b) and Yoden *et al.*, (1985) who both discovered Fabs which showed almost no neutralization activity. These suggested that the mechanism of neutralization of the parental IgG was heavily dependent on bivalency.

6.15.4 Neutralization of influenza and other animal viruses by Fab fragments.

Currently this study represents the only data available on the mechanism of neutralization of influenza by Fabs, with very little known about the mechanism of Fab fragments in general.

Three previous studies have looked at the characteristics of Fab neutralization of influenza. All agreed with the findings of this thesis that a higher concentration Fab than of IgG is required to cause neutralization. An early study examined the neutralization by Fab fragment prepared from polyclonal anti-sera raised in rabbits (Lafferty, 1963). These Fabs were neutralizing, but infectivity was recoverable after dilution of virus-Fab mixtures. This reversibility was attributed to Fab dissociating from antigen due to its lower affinity and hence it was suggested bivalent interaction with virus was important for IgG neutralization. However, there were no affinity data to back-up this assertion.

A second study of Fab neutralization of influenza A virus focussed on four MAbs to different antigenic regions (I-IV) on the HA of influenza A/seal/Massachusetts/1/80 (H7N7) (Yoden *et al.*, 1985). Two MAbs from groups I and II were able to neutralize virus and give HI, however, two MAbs from groups III and IV were able to neutralize but had very poor HI activity. Fabs to group I and II displayed a 32- to 64-fold drop in neutralization titres respectively compared to parent IgG, whilst Fabs to groups III and IV had a greater than 100-fold loss of neutralization and no HI titre. However, analysis by ELISA of Fab binding, indicated that they bound equally well to the virus as their IgGs. Addition of the anti-Fab improved Fab neutralization to the same order of magnitude as parent IgG, but did not recover HI titre. All of the MAbs inhibited haemolysis of RBCs, which is considered to be analogous to inhibition of fusion, whereas only Fabs to groups I and II showed this ability. The authors concluded that bivalent binding was important in HI and was crucial for neutralization by MAbs to group III and IV. This proposal was supported by a follow-up study which showed that MAb 81/6 to group IV bound

bivalently to HA rosettes and inhibited virus fusion in MDCK cells (Imai *et al.*, 1998). However, generally conclusions made in the study were poor, they did not show conclusively that anti-Fab antibodies cross-linked Fabs to restore bivalency, they paid no attention to the fact that Fabs have reduced molecular mass, and they gave no thought to orientation of the antibody and its effect on HI.

More recently a study of neutralization and HI ability of five anti-HA influenza A/fowl plague/Rostock/34 (H7N1) (FPV) virus IgG MAbs, their Fabs and F(ab)₂s (Schofield *et al.*, 1997b) was carried out. This study showed that Fabs required 54- to 542-fold higher concentration to achieve 90% neutralization than IgG, and 14- to 66-fold more for HI. The F(ab)₂s required only 1.4- to 4-fold higher concentration to achieve 90% neutralization than their IgGs. The functional affinities determined by SPR, of IgGs and Fabs only differed by 3- to 4-fold and is similar to the results I obtained, which was not considered to be sufficient to explain losses of neutralization. The small differences in dissociation constant between the IgG and the Fab suggested that the Fab bound monovalently and hence reduction in neutralization activity may have resulted from a decrease in molecular mass. However, it should be stressed that this study did not determine the valency of the virus-IgG interaction and it is possible the reduction of affinity of Fabs isolated from very high affinity IgGs will be small, not affected greatly by loss of bivalent interaction (Parham, 1983). Therefore, this study did not rule out bivalency as a cause of the loss of neutralization activity. Collectively, the studies by Yoden *et al.*, (1985) and Schofield *et al.*, (1997) have implicated both molecular mass and valency in the efficiency of neutralization of Fab fragments. This thesis has examined this question from a mechanistic angle and again has indicated that both molecular mass and valency are probably involved in loss of neutralization efficiency.

Very little is known of the mechanism of neutralization of other viruses by Fabs, with only a few studies available in the literature. A study of the mechanism of neutralization of HIV-1 virus by the human b12 IgG and Fab fragment indicated that the Fab differed from its IgG, similar to that shown with the anti-A/PR/8 virus Fabs in this study (McInerney *et al.*, 1997). Neither of the antibodies affected attachment to a C8166 T-cell line as judged by FACs analysis. The b12 IgG inhibited virus-cell fusion by a variety of assays including cell to cell fusion, R18 fluorescence fusion assay and resistance to trypsin removal. In contrast, these assays suggested that the Fab did not have any effect on virus-cell fusion and immunofluorescence data

showed the same pattern of p24 staining of Fab neutralized virus as non-neutralized virus. The authors concluded by inference that the Fab inhibiting a post-fusion event. Another study showed that the Fab could inhibit attachment of virus to cells. However, a direct causal relationship was not established as attachment inhibition was much lower than neutralization. For example, at >99% neutralization inhibition of attachment was at only 55% (Ugolini *et al.*, 1997). This suggests that the remaining level of neutralization must be due to effects on other stages of the HIV-1 virus infectious cycle, similar to that proposed in this study.

Only two other studies of the mechanism of neutralization of Fab fragments are available and these studies concluded that the Fabs have the same mechanisms as their parent IgGs. In a study of Western equine encephalitis virus, a Fab to epitope E2^c inhibited attachment of virus to Vero cells, but was 10-fold less efficient than its parent IgG (Roehrig *et al.*, 1988). Interestingly, addition of anti-Fab F(ab)₂ to the Fab did not increase its ability to inhibit attachment of virus to cells. This is, however, a poor study in that only one Fab fragment out of a panel of MAbs was analysed, attachment data was not correlated with infectivity and also only one neutralizing concentration was used.

A study of human rhinovirus type-14 used MAbs to the four distinct neutralization sites at conditions giving 95% neutralization (Colonno *et al.*, 1989). A HeLa cell membrane-binding assay was used to investigate the effect of non-aggregating MAbs on attachment, and all MAbs were found to affect attachment to varying extents. For example, the concentration of MAbs NimIA-34 and NimIB-29 required to inhibit attachment by 95% was equal to the concentration required to give 95% neutralization, while for MAbs NimII-28 and NimIII-33 the ratio of the inhibition of attachment to cells : neutralization was 1:6. Analysis of Fab fragments showed that they required a 13- to 61-fold higher concentration to achieve 95% neutralization than their IgGs. Membrane-binding analysis revealed that they all exhibited a dose response inhibition of attachment to membrane preparations. However, this again is a poor study, with only one point (95% neutralization) being given for neutralization, rather than a full concentration versus neutralization analysis and hence comparison of neutralization and inhibition of attachment are not possible over a range of concentrations as I have done in this thesis. The deficiencies in the past two studies makes comparisons with my study difficult. However, it is interesting that their Fabs inhibit attachment, similar to that seen with H36 and H37

Fabs. Currently, no Fabs have been reported that neutralize by inhibition of fusion indicating that H9 Fab has a novel mode of action.

Other studies of Fab neutralization in the literature have not examined the mechanism of neutralization. However, four recent studies have examined functional affinity in relation to the neutralizing ability of Fabs. The HIV-1 specific F105 IgG and Fab had similar affinities of 6.9×10^{-8} M and 5.7×10^{-8} M respectively (Cavacini *et al.*, 1994). The Fab required between 4- and 10-fold higher concentration than its IgG to neutralize HIV-1 IIIB, whilst the neutralizing activity of the F(ab)₂ was similar to the IgG. As in my study the authors found that the functional affinity did not predict neutralizing activity. The authors argued that valency affected the neutralizing activity of the F105 IgG, with the influence of bivalency not being a function of affinity or steric effects (molecular mass). They concluded that differences were due to the bivalent binding inducing conformational changes in the oligomeric gp120.

In contrast, a recent investigation of panel of HIV-1 specific IgGs and Fabs determined that the gp120 oligomer-binding : neutralization ratios fell within a relatively narrow range for antibodies to different neutralization epitopes (Parren *et al.*, 1998). The authors suggested that the affinity of binding was the major factor in neutralization efficiency. They expanded this by suggesting that occupancy of the neutralization epitopes by antibodies rather than epitope specificity was the most important factor, as the large size of the antibody relative to the gp120 should allow steric hindrance of the CD4-binding region from any of the neutralization epitopes (Klasse and Moore, 1996; Parren *et al.*, 1998). This report differs from results described by Schofield and Dimmock, (1996) and Schofield *et al.*, (1997) and in this thesis, which indicated that intrinsic properties of the epitope are important. It is possible that differences between HIV-1 and influenza A viruses are responsible.

A study comparing the neutralizing activities of murine hepatitis virus (MHV) by a MAb 7-10A IgG, its F(ab)₂ and its Fab showed that the Fabs were less efficient at neutralizing than the IgG (Lamarre and Talbot, 1995). The Fab required a 197-fold higher concentration than its IgG to give 50% neutralization, whereas the F(ab)₂ only required 3-fold more. Examination of functional affinity revealed that the Fab had a dissociation constant (K_D) of 2.0×10^{-9} M, which was 14-fold higher than the IgG. However, the affinities were calculated to an anti-idiotypic MAb mimicking the epitope recognised by the MAb 7-10A and this has to be less ideal than using whole

virus particles. Lamarre and Talbot, (1995) concluded that bivalency was not essential for neutralization by MAb 7-10A, but did enhance its neutralization ability *in vitro*.

A comparison of the neutralizing activity of Rabies virus by a recombinant Fab (rFab57) of MAb 57 described a Fab:IgG neutralization ratio of 13:1 (Dietzschold *et al.*, 1990). The dissociation constants measured by ELISA against whole Rabies virus showed that the Fab was 12-fold higher than the MAb. This indicated that the affinity and neutralization were reduced by the same proportion. This is in direct contrast to the anti-influenza Fabs in this thesis that either have the same or slightly lower affinity than their IgGs, but with much lower neutralization levels (104- to 375-fold lower at N_{50}).

6.15.5 Critique of the techniques used in this chapter.

It has been previously established and reinforced in this thesis that neutralization is a complex and multi-factorial process. Therefore, numerous methods must be used to try to correlate loss of viral infectivity with loss of a particular viral function essential in the initial stages of infection. Causal relationships can be established with care, but these depend on the compatibility of the assays. Therefore, it is important to illustrate the limitations and strengths of the techniques used.

6.15.5.1 Preparation of Fabs -

The Fabs were prepared by enzymatic digestion and are different isotypes. Hence it is possible that the loss of efficiency of the H37 and H9 Fabs compared to H36 Fab could be due to a lower stability of the IgG3 isotype under the reducing and enzymatic conditions used in their preparation. However, this was probably not so as the Fabs had similar affinities to their IgGs. Protease damage of Fabs could be avoided by expressing recombinant Fabs.

6.15.5.2 Attachment and infectivity ELISA assays -

The ELISA used to detect virus attached to cells involved permeabilisation of virions and detection of internal viral-NP antigen. In this way anti-HA neutralizing MAb

does not interfere with the detection system. However, it is susceptible to interference by contaminating free NP antigen, either from cell debris or broken virus particles. In order to reduce these levels to a minimum the virus preparations were double purified by both velocity and density centrifugation, and freeze-thawing of the virus was kept to a minimum to prevent viral envelope fracture. NP detection of paraformaldehyde-fixed virus bound to MDCK cell monolayers was only 5% of the methanol treated virus indicating that free NP contributed little to the signal.

Every effort was made in this study to keep the assay of attachment and assay of infectivity (both ELISAs) comparable. This included using cell monolayers seeded from the same batch of cells, equal volumes of virus from the same neutralization mixture were inoculated on to the monolayers and the same detection substrate was used with ELISAs being developed simultaneously. Also the level of attachment and infectivity was calculated as a percentage of the non-neutralized virus control and hence allowed results to be directly compared.

6.15.5.3 *Virus internalisation ELISA –*

This assay was designed to be directly comparable to the attachment and infectivity ELISAs, using the same cell and neutralization mixtures. However, because the amount of virus used in the mechanism studies was above the percentage law (the range of antibody dilutions which can neutralize a fixed amount of virus to the same extent) (Andrewes and Elford, 1933; Brioen and Boeyé, 1985), a fixed amount of virus was used in the attachment and internalisation assays. Hence, the assay suffered from a low signal compared to the attachment and infectivity ELISAs. This was possibly due to the fact that only a fraction of attached virus actually internalises and/or also the permeabilisation methods used were very harsh. Therefore, it is possible that this ELISA was less sensitive, but differences were again kept to a minimum by calculating the percentage of internalisation.

6.15.5.4 *Virus-cell fusion assay –*

This assay uses R18 labelled virus, which has the disadvantage of causing some loss of infectivity (Wunderli-Allenspach *et al.*, 1993). Therefore preparing the virus stock involved a balance between fluorescent label and infectivity. The stock of

labelled virus used in this study had approximately a 2.5-fold loss of infectivity compared to unlabelled stocks. As a result it is possible that the behaviour of the remaining infectious population did not accurately reflect the behaviour of the fully infectious stocks (unlabelled). Possibly the most accurate fusion assays are those in which the target membranes are labelled so that the R18 does not affect infectivity. However, this is only possible with model membrane systems, such as erythrocyte ghosts and liposomes and was not possible with the cells used in this study.

This assay examined only one time point, whereas a more complete analysis would have been to monitor the virus-cell fusion over a range of time points. This data would have allowed us to investigate the effect of the antibodies on the kinetics of virus-cell fusion.

Finally the R18 fluorescence assay detects virus envelope to cell membrane lipid mixing, known as hemi-fusion and does not detect full fusion pore formation and the passage of aqueous material in full fusion. Therefore, extrapolating the R18 fluorescence data to fusion must be done with care. A complete fusion analysis should also use techniques that allow detection of full fusion, such as calcein label. However, it must be highlighted that the perfect fusion assay is not yet available, and in this study we have only used the fluorescence data to indicate a causal relationship between loss of infectivity and inhibition of fusion.

7 Results: Investigation of the post-attachment neutralization (PAN) of influenza A/PR/8/34 virus by monoclonal IgGs and their Fabs.

7.1 Introduction

Post-attachment neutralization (PAN) is defined as a reduction in viral infectivity achieved by antibody reacting with virus that has already attached to the target cell, but has not yet fused with the target membrane or been internalised (Armstrong and Dimmock, 1996). If a MAb or Fab can give PAN, it can evidently inhibit an event(s) beyond viral attachment (Jackson, 1998). This chapter investigates the ability of the anti-A/PR/8 virus IgGs and Fabs to PAN. Results presented in chapter 6 indicated that IgGs were able to simultaneously neutralize by both inhibition of attachment and inhibition of fusion. Analysis of the relationship between attachment and infectivity showed them to be significantly different; however, inhibition of attachment made a major contribution to the neutralization process. PAN was investigated here to –

- (1) Provide compelling evidence of the ability of the antibodies to neutralize by mechanisms other than inhibition of attachment.
- (2) Examine the relevance of molecular mass and valency to PAN, by the use of Fabs.

The ability of antibodies to give PAN of influenza A virus is confined to a single study in which polyclonal rabbit antiserum gave complete PAN of A/PR/8 virus at 3°C, whereas at 37°C the virus became progressively more resistant to PAN (Ishida and Ackermann, 1956). As this paper only examined polyclonal sera and hence this area requires revisiting with MAbs.

PAN is self-evidently not concerned with inhibition of attachment; hence examination of the mechanism of PAN is of interest. The mechanism of PAN of influenza virus has not yet been addressed, although there are a limited number of studies of other viral systems. A study of the PAN of rabies virus, suggested that the neutralizing MAbs caused a 3-fold increase in the release of cell bound virus (Dietzschold *et al.*, 1987). The virus that remained attached was endocytosed, which lead the authors to propose that the virus was neutralized by inhibition of an event beyond internalisation. Antiserum to West Nile Fever virus (WNFV) was capable of PAN (Gollins and Porterfield, 1986). The virus was not eluted from the cell surface and loss of infectivity paralleled inhibition of uncoating of viral RNA. This indicated that the antibodies caused PAN by inhibition of endosomal virus-cell fusion. Endosomal virus-cell fusion of vesicular stomatitis virus (VSV) with Vero

cells was also inhibited by neutralizing antiserum (Blumenthal *et al.*, 1987). A study of poliovirus showed that out of 19 neutralizing MAbs, 6 showed PAN (Vrijssen *et al.*, 1993). PAN was shown to involve the inhibition of the cell-mediated shift from the 135S native virus to an 80S particle. Evidence from one of the PAN positive MAbs suggested it bound bivalently, whilst a PAN negative MAb probably bound monovalently. Therefore, the authors suggested that the ability to give PAN was dependent on valency.

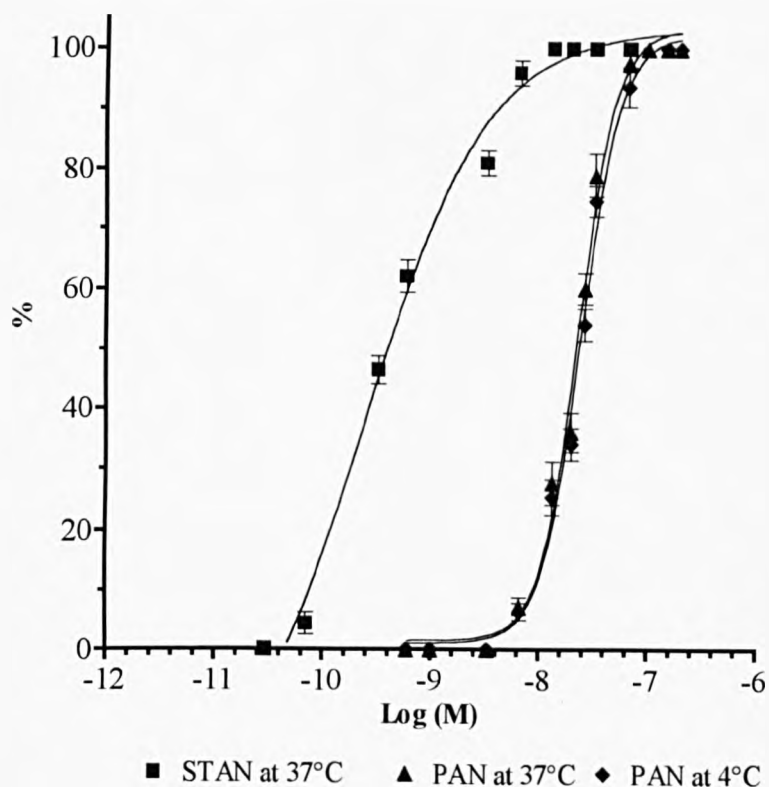
In this section I have examined the dose-response relationship of PAN and its temperature dependence using three IgGs and their Fabs. All of the antibodies were capable of PAN with varying degrees of efficiency relative to their standard neutralization activity (neutralization of virus before its attachment to cells). The mechanism of PAN was investigated and of endosomal virus-cell fusion proportional to loss of infectivity indicated a causal relationship. The process of the antibody-mediated fusion inhibition was investigated, and results indicated that the low pH-dependent conformational change of the viral HA was unaffected and that there was a requirement for the antibodies to be present prior to initiation of the cold-fusion intermediate (low pH at 4°C). Collectively, these data suggested that all the antibodies were inhibiting an early stage of virus-cell fusion.

7.2 Comparison of the standard neutralization (STAN) and PAN at 4°C and 37°C of the IgGs and their Fabs.

7.2.1 STAN and PAN at 4°C and 37°C by H36 IgG.

Figure 7.1 indicates that the H36 IgG had a PAN activity. The H36 IgG had a similar efficiency of PAN at both 4°C and 37°C. However, PAN at both 4°C and 37°C was less efficient than STAN. At the 50% neutralization point (N_{50}) it was 50-fold less efficient, whereas it was only 10.3-fold less efficient at the 90% neutralization point (N_{90}). This indicated that the efficiency of PAN activity increases with increasing concentration.

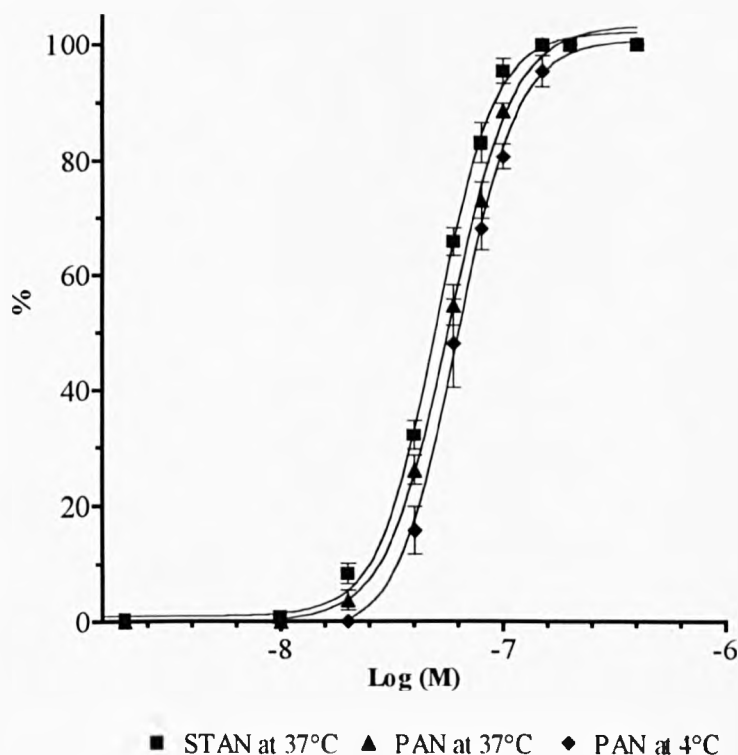
Figure 7.1 Comparison of the standard neutralization (STAN) and post-attachment neutralization (PAN) of A/PR/8 virus by H36 IgG in MDCK cells. Data are the mean of three experiments measured by plaque assay. The bars represent the standard error of the means (SEM). Curves were generated by non-linear regression using the Graphpad Prism package ($R = > 0.98$ for all curves).



7.2.2 STAN and PAN at 4°C and 37°C of A/PR/8 by H36 Fab.

Figure 7.2 shows that H36 Fab also had PAN activity. The Fab also showed similar efficiencies of PAN at 4°C and 37°C, indicating its activity to be independent of temperature. However, unlike the H36 IgG whose PAN efficiency was significantly lower than its STAN, the efficiency of Fab PAN and STAN were very similar. A comparison of the STAN and PAN at 37°C at N_{50} by unpaired T-test showed that they were not significantly different ($P = 0.617$, where significance is < 0.05).

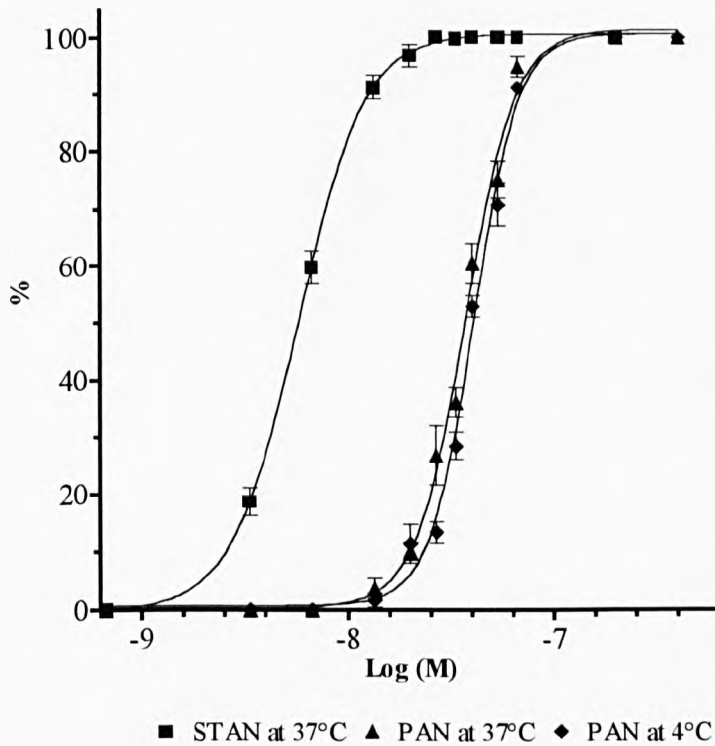
Figure 7.2 Comparison of the STAN and PAN of A/PR/8 virus by H36 Fab in MDCK cells. Data are the mean of three experiments measured by plaque assay. The bars represent the SEM. Curves were generated as in Figure 7.1 ($R = >0.99$).



7.2.3 STAN and PAN at 4°C and 37°C of A/PR/8 virus by H37 IgG.

H37 IgG also showed PAN activity (Figure 7.3). Levels of PAN activity were similar at 4°C and 37°C, suggesting that PAN was temperature independent. However, PAN activity was significantly ($P = <0.0001$ at N_{50}) less efficient than STAN. The lower efficiency of PAN is not uniform being 7-fold lower than STAN at N_{50} , whilst only 1.8-fold lower at N_{90} . H37 and H36 IgGs are thus similar with respect to PAN.

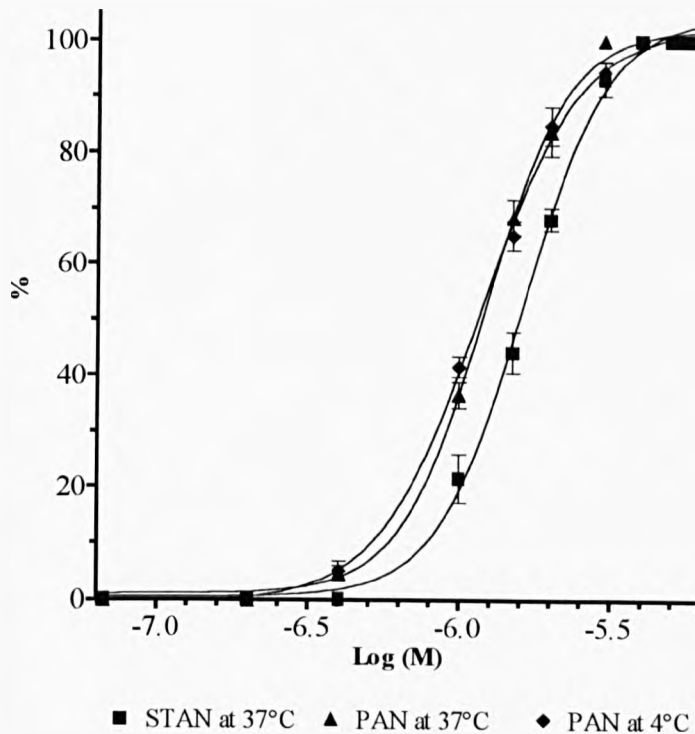
Figure 7.3 Comparison of the STAN and PAN of A/PR/8 virus by H37 IgG in MDCK cells. Data are the mean of three experiments measured by plaque assay. The bars represent the SEM. Curves were generated as in Figure 7.1 ($R = >0.98$).



7.2.4 STAN and PAN at 4°C and 37°C of A/PR/8 virus by H37 Fab.

H37 Fab also had PAN activity (Figure 7.4). The PAN activity at 4°C and 37°C was similar. However, in contrast to the H36 Fab PAN activity, the H37 Fab PAN was slightly more efficient than STAN. This was a consistent and interesting result, but the difference between the curves at N_{50} was found not to be significant by an unpaired T-test ($P = 0.175$). Therefore, it must be concluded that the PAN activity of the H37 Fab is similar to its STAN.

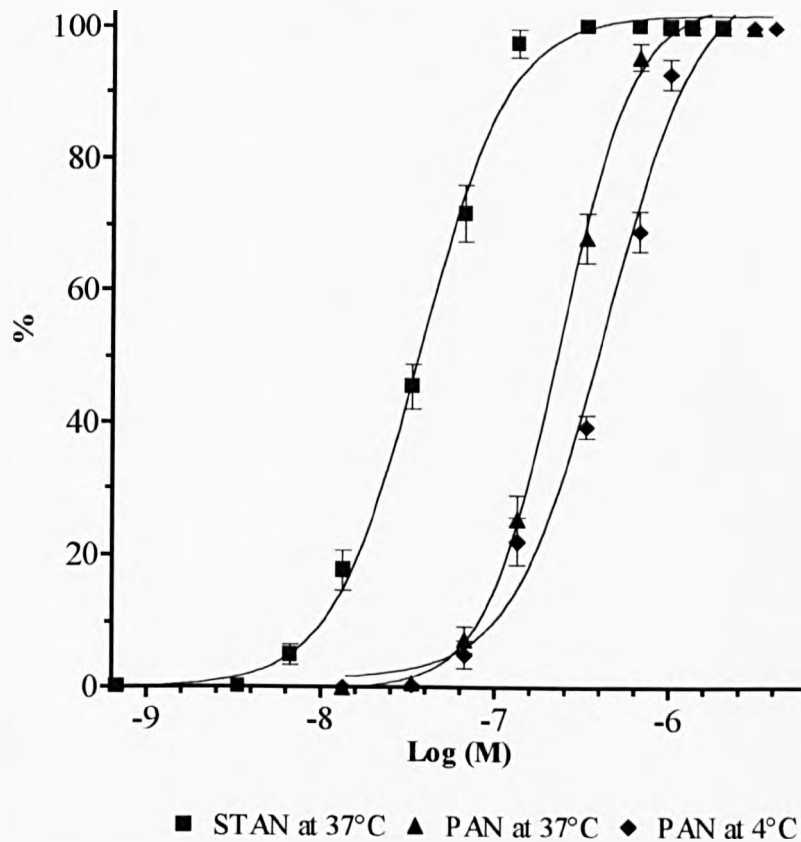
Figure 7.4 Comparison of the STAN and PAN of A/PR/8 virus by H37 Fab in MDCK cells. Data are the mean of three experiments measured by plaque assay. The bars represent the SEM. Curves were generated as in Figure 7.1 ($R = >0.99$).



7.2.5 STAN and PAN at 4°C and 37°C of A/PR/8 virus by H9 IgG.

Figure 7.5 shows that the H9 IgG also had PAN activity. The PAN activity of the H9 IgG was very similar to the H36 and H37 IgGs, being of similar efficiency at the two temperatures tested and having a lower efficiency at N_{50} than N_{90} . The PAN was also of significantly lower efficiency ($P = 0.01$) than the STAN.

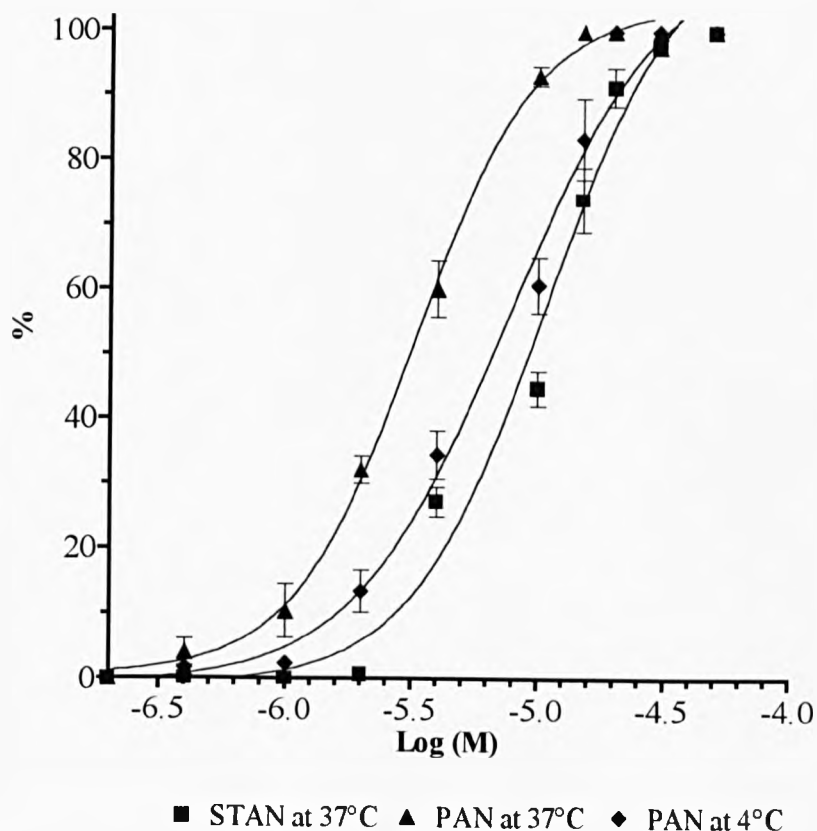
Figure 7.5 Comparison of the STAN and PAN of A/PR/8 virus by H9 IgG in MDCK cells. Data are the mean of three experiments measured by plaque assay. The bars represent the SEM. Curves were generated as in Figure 7.1 ($R = >0.98$).



7.2.6 STAN and PAN at 4°C and 37°C of A/PR/8 virus by H9 Fab.

Figure 7.6 shows that H9 Fab also had PAN activity. The PAN activity of the H9 Fab unlike the other antibodies had a greater efficiency at 37°C than at 4°C. It also had a greater efficiency of PAN than STAN. Comparison of the STAN and PAN at N_{50} by unpaired T-test indicated that they were significantly different ($P = <0.0001$). This suggested that the H9 Fab neutralized pre-attached virus at a greater efficiency than it could neutralize unattached virus.

Figure 7.6 Comparison of the STAN and PAN of A/PR/8 virus by H9 Fab in MDCK cells. Data are the mean of three experiments measured by plaque assay. The bars represent the SEM. Curves were generated as in Figure 7.1 ($R = >0.97$).



7.3 Kinetics of PAN of A/PR/8 virus by H36 IgG and Fab.

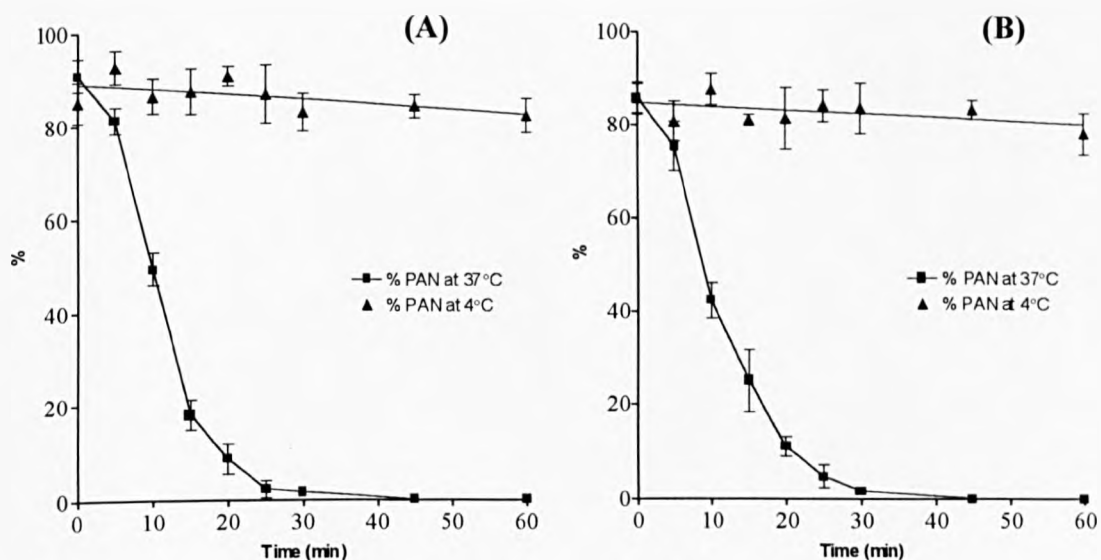
7.3.1 Comparison of the kinetics of PAN of A/PR/8 virus by H36 IgG and Fab at 4°C and 37°C in MDCK cells.

If it is to cause PAN, an antibody has to interact with the attached virus before it is internalised into the cell. This relationship was investigated by initially allowing virus to attach to MDCK cells at 4°C and then shifting the temperature to 37°C. Antibody was added at 5-minute intervals for 60 minutes. The assay was controlled by leaving the attached virus at 4°C for the entire 60 minutes, to inhibit internalisation of virus.

Figure 7.7 (A) shows the kinetics of PAN by H36 IgG at 4°C and 37°C. Kinetics of PAN at 37°C shows that the virus becomes refractory to PAN with increasing time, being approximately 50% refractory in 10 minutes and 90%

refractory at 20 minutes. However, there was only a loss of approximately 10% PAN in the first 5 minutes, which is slower than a previous study in chicken chorioallantoic cells which showed almost a complete loss of PAN activity in a 5 minute incubation (Ishida and Ackermann, 1956). This difference could represent the cells warming to 37°C after the previous 15 minute incubation of the cells at 4°C prior to infection designed to inhibition internalisation. The kinetics at 4°C showed that over a 60 minute period there was almost no loss of PAN activity indicating that virus was not being internalised. Figure 7.7(B) shows that the kinetics of PAN by H36 Fab at 37°C and 4°C were very similar to those obtained with the IgG, indicating that both interacted with the virus for the same period of time.

Figure 7.7 Analysis of the kinetics of PAN by H36 IgG and Fab at 4°C and 37°C in MDCK cells. (A) PAN with H36 IgG at 55 nM and (B) PAN with H36 Fab at 100 nM. PAN was measured by plaque assay. Data are the mean of two experiments. The bars represent the SEM.



7.4 Mechanism of PAN by IgGs and their Fabs

7.4.1 Analysis of the relationship between A/PR/8 virus internalisation in MDCK cells and PAN as a function of H36 IgG concentration.

This assay was controlled as described in the previous chapter, section 6.2.3. Briefly, this involved (a) incubating the cells at 4°C which inhibits endocytosis and (b) pre-treatment of cells with hypertonic media which disperses the clathrin lattice.

Figure 7.8 Analysis of the relationship between A/PR/8 virus internalisation in MDCK cells and PAN as a function of H36 IgG. PAN and infectivity were assayed in parallel in the same batch of monolayers in 96 well plates, using the same virus and antibody stocks. All data are the mean of three experiments. The curve has been generated as in Figure 7.1 ($R = 0.97$).

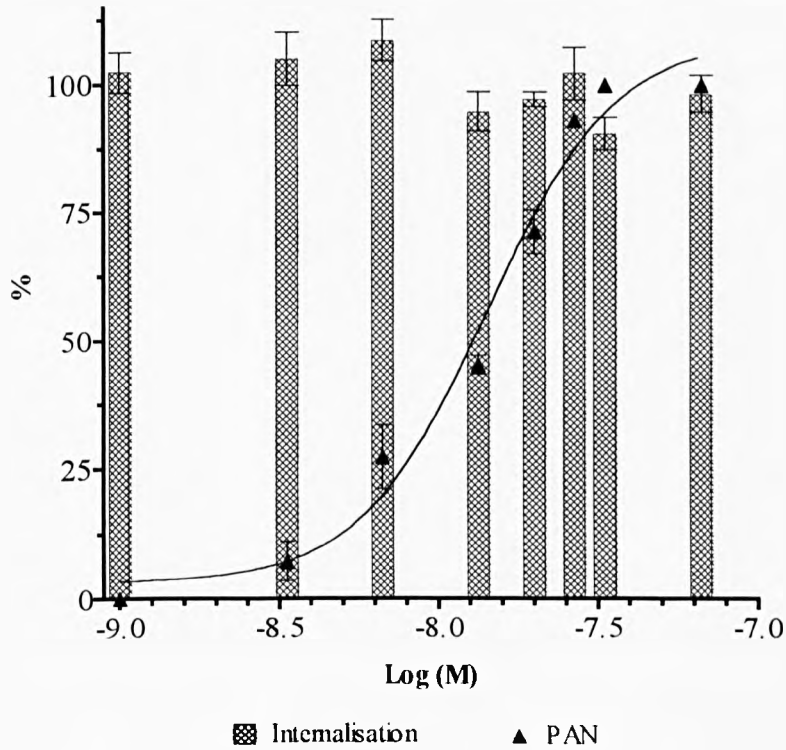


Table 7.1 Analysis of the internalisation of non-neutralized (N_0) virus under the negative control conditions. Data are presented as percentage inhibition of internalisation relative to non-neutralized virus at 37°C.

<i>Control conditions</i>	<i>% inhibition of internalisation</i>
Cold (4°C) – N_0	94 (+/- 8)
Hypertonic treated - N_0	82 (+/- 7)

Table 7.1 shows that at 4°C internalisation of non-neutralized virus was inhibited by 94% compared to internalisation at 37°C. Pre-treatment of cells with hypertonic media inhibited non-neutralized virus internalisation by 82%. Collectively these data indicate that virus is internalised into the cell by clathrin lattice-mediated endocytosis and not by an alternative pathway.

Figure 7.8 shows that PAN increased with increasing H36 IgG concentration as expected, but the percentage of virus internalised stayed at approximately 100%. This also shows that the H36 IgG does not cause release of the virus from the cell surface, as total level of input virus remains relatively constant across the IgG concentration range. This indicates that neutralized virus is internalised and that the mechanism of PAN does not involve inhibition of internalisation in MDCK cells.

7.4.2 Analysis of the relationship between A/PR/8 virus internalisation in MDCK cells and PAN as a function of H36 Fab.

The controls in this assay were as described in section 6.3.1, and again showed good inhibition of internalisation indicating that virus was being internalised by receptor-mediated endocytosis (Table 7.2). Figure 7.9 shows that as PAN increases with increasing concentration of H36 Fab, the percentage internalisation remains at approximately 100% relative to the non-neutralized control. These data again showed that the H36 Fab did not cause release of virus from the cell surface, with input virus remaining relatively constant. This indicates that PAN by the H36 Fab did not involve inhibition of internalisation.

The relationship between virus internalisation and PAN was also investigated with the H37 and H9 IgGs and their Fabs. The results were again very similar to the H36 antibody, with PAN not affecting internalisation. These data can be seen in Appendix I and a summary of the data is given in Table 7.6.

Figure 7.9 Analysis of the relationship between A/PR/8 virus internalisation in MDCK cells and PAN as a function of H36 Fab. PAN and internalisation were assayed in parallel in the same batch of monolayers in 96 well plates, using the same virus and antibody stocks. All data are the mean of three experiments. The curve has been generated as in Figure 7.1 ($R = 0.98$).

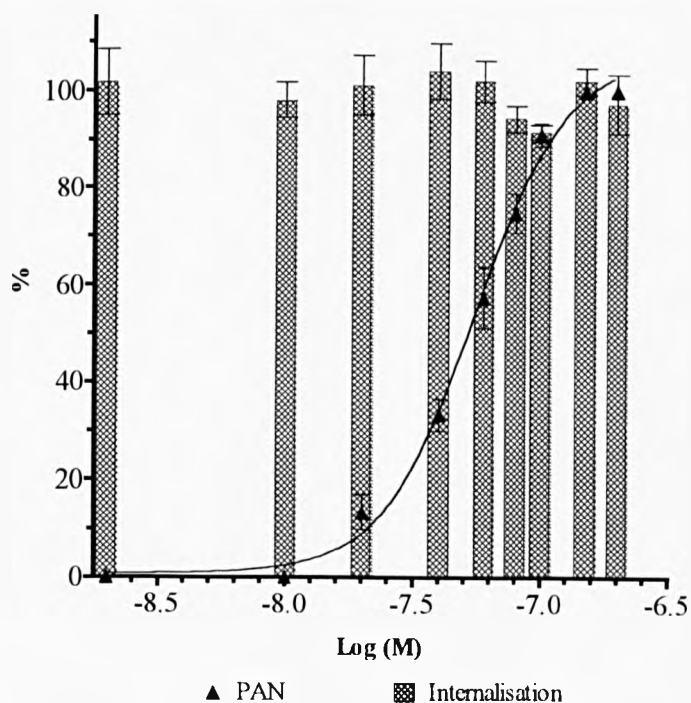


Table 7.2 Analysis of the internalisation of non-neutralized (N_0) virus under the negative control conditions. Data are presented as percentage inhibition of internalisation relative to non-neutralized virus at 37°C.

<i>Control conditions</i>	<i>% inhibition of internalisation</i>
Cold (4°C) – N_0	90 (+/- 3)
Hypertonic treated - N_0	79 (+/- 10)

7.4.3 Analysis of the relationship between A/PR/8 virus PAN and the virus-cell fusion in MDCK cells as a function of H36 IgG concentration.

As PAN was not mediated by inhibition of internalisation, it was possible that it acted by inhibiting virus-cell fusion. Fusion was measured by a fluorescence assay using R18-labelled virus, as described in section 6.2.4. The controls included (a) fusion carried out at 4°C and (b) pre-treatment of cells with bafilomycin (section 6.2.4). Table 7.3 shows that at 4°C virus-cell fusion of non-neutralized virus was inhibited by 93% and with bafilomycin treated cells by 85%, demonstrating that the majority (>85%) of the fluorescent signal was due to virus-cell fusion.

Figure 7.10 shows that as PAN increased with increasing concentration of the H36 IgG, the percentage of fusion-inhibition also increased. Comparison of the curves with an unpaired T-test showed them not to be significantly different ($P = 0.27$), indicating a causal relationship between PAN and inhibition of virus-cell fusion.

7.4.4 Analysis of the relationship between A/PR/8 virus PAN and the virus-cell fusion in MDCK cells as a function of H36 Fab concentration.

Negative controls indicated that the majority of the fluorescent signal was specific for virus-cell fusion (Table 7.4).

Figure 7.11 shows that as PAN increased with increasing H36 Fab concentration, the inhibition of fusion also increased. An unpaired t-test showed that the curves were not significantly different ($P = 0.08$), indicating a causal relationship between inhibition of virus-cell fusion and PAN by H36 Fab, and that bivalency is not required for inhibition of fusion.

The relationship between PAN and virus-cell fusion was also investigated with the H37 IgG and Fab and H9 IgG. The results can be seen in Appendix I and a summary of the data is presented in Table 7.6. These antibodies all exhibited distinct similarities with the H36 IgG and its Fab with increases of PAN correlating with increases in inhibition of virus-cell fusion.

Figure 7.10 Analysis of the relationship between A/PR/8 virus PAN and virus-cell-fusion as a function of H36 IgG concentration. PAN and fusion were assayed in parallel in the same batch of monolayers in 3-cm plates, using the same virus and antibody stocks. All data are the mean of three experiments. The curve has been generated as in Figure 9.1 ($R = >0.97$ for both curves).

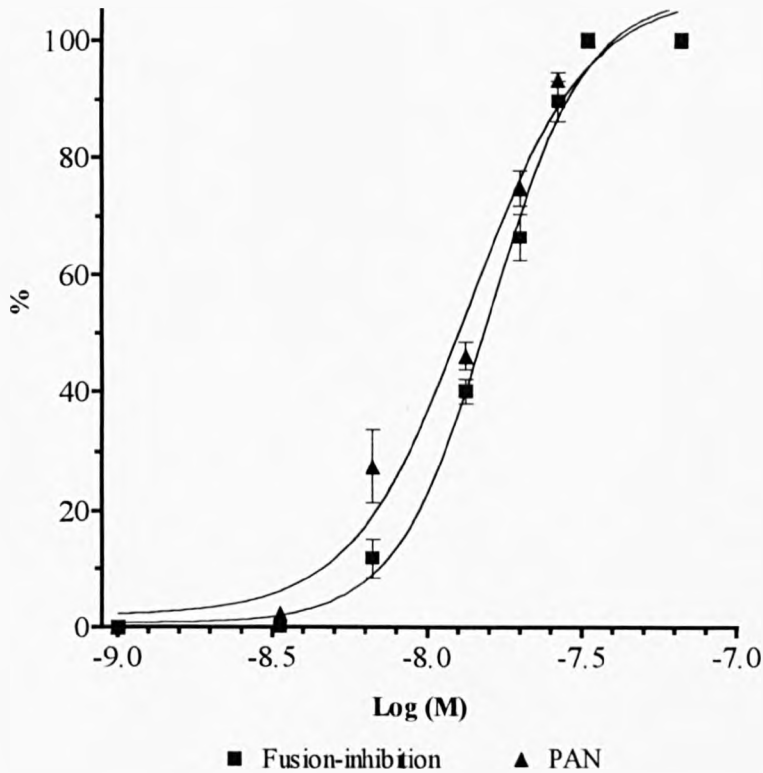


Table 7.3 Analysis of the fusion of non-neutralized virus under the negative control conditions. Data are presented as percentage inhibition of fusion relative to non-neutralized virus at 37°C. Data are the mean of three experiments

<i>Control conditions</i>	<i>% inhibition of internalisation</i>
Cold (4°C) – N ₀	93 (+/- 6)
Bafilomycin treated - N ₀	85 (+/- 6)

Figure 7.11 Analysis of the relationship between A/PR/8 virus PAN and virus-cell-fusion as a function of H36 Fab concentration. PAN and fusion were assayed in parallel in the same batch of monolayers in 3-cm plates, using the same virus and antibody stocks. All data are the mean of three experiments. The curve has been generated as in Figure 7.1 ($R = >0.98$ for both curves).

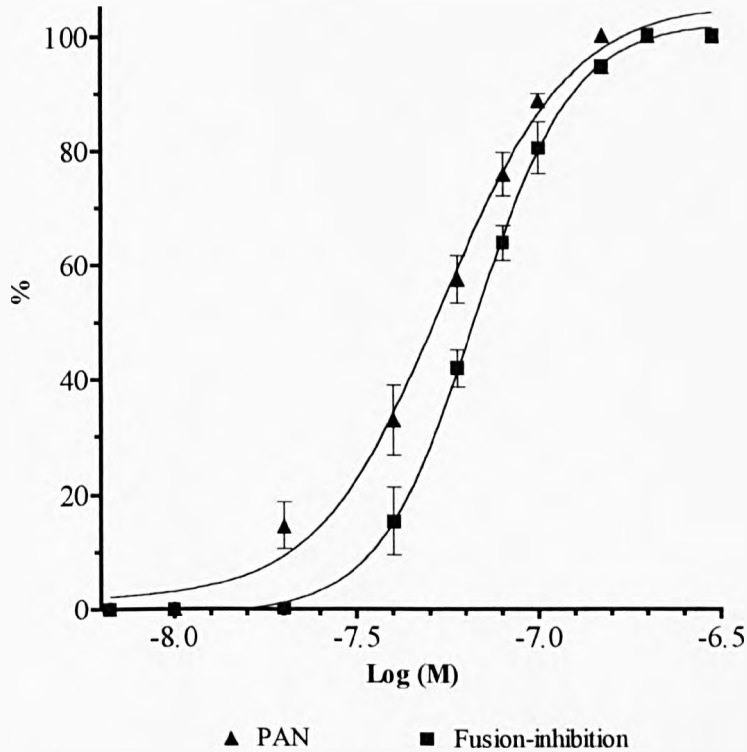


Table 7.4 Analysis of the fusion of non-neutralized virus under the negative control conditions. Data are presented as percentage inhibition of fusion relative to non-neutralized virus at 37°C. Data are the mean of three experiments

<i>Control conditions</i>	<i>% inhibition of internalisation</i>
Cold (4°C) – N ₀	87 (+/- 4)
Bafilomycin treated - N ₀	79 (+/-12)

7.4.5 Analysis of the relationship between A/PR/8 virus PAN and virus-cell fusion as a function of H9 Fab concentration.

Results for the controls shown in Table 7.5 again show that the majority of the fluorescent signal obtained was specific for virus-cell fusion.

Figure 7.12 shows that as PAN increases with increasing H9 Fab concentration, the percentage inhibition of virus-cell fusion also increases, and indicates a causal relationship between inhibition of virus-cell fusion and PAN by H9 Fab. However, unlike earlier data with H36 and H37 IgGs and Fabs, the inhibition of fusion by H9 Fab did not fully correlate with neutralization at higher levels and curves were found to be significantly different ($P = 0.02$, where significance is <0.05) by unpaired T-test. For example, even though $>99\%$ PAN could be obtained with the H9 Fab, complete inhibition of fusion could not be obtained. This difference does not appear to represent variability in the assay as it is seen with no other antibody and was consistent over the three assays carried out.

7.4.6 Analysis of the effect of H36 IgG on haemolysis of chick red blood cells (CRBCs) by attached A/PR/8 virus.

Haemolysis of RBCs by influenza virus is a convenient model to investigate fusion. The process involved is not strictly the same as virus-cell fusion, but is thought to be analogous (Huang *et al.*, 1981). Therefore, investigation of the effect of antibodies on haemolysis of RBCs by attached A/PR/8 virus (analogous to PAN) was used here to complement the fluorescence based MDCK cell fusion assay.

Figure 7.13 shows that inhibition of haemolysis increased with increasing H36 IgG concentration compared to the non-neutralized virus control. These data support the findings of the fluorescence-based assay in section 7.3.3, and suggest that the mechanism of PAN by H36 IgG is inhibition of virus-driven fusion.

Figure 7.12 Analysis of the relationship between A/PR/8 virus PAN and virus-cell-fusion as a function of H9 Fab concentration. PAN and fusion were assayed in parallel in the same batch of monolayers in 3-cm plates, using the same virus and antibody stocks. All data are the mean of three experiments. The curve has been generated as in Figure 7.1 ($R = >0.98$ for both curves).

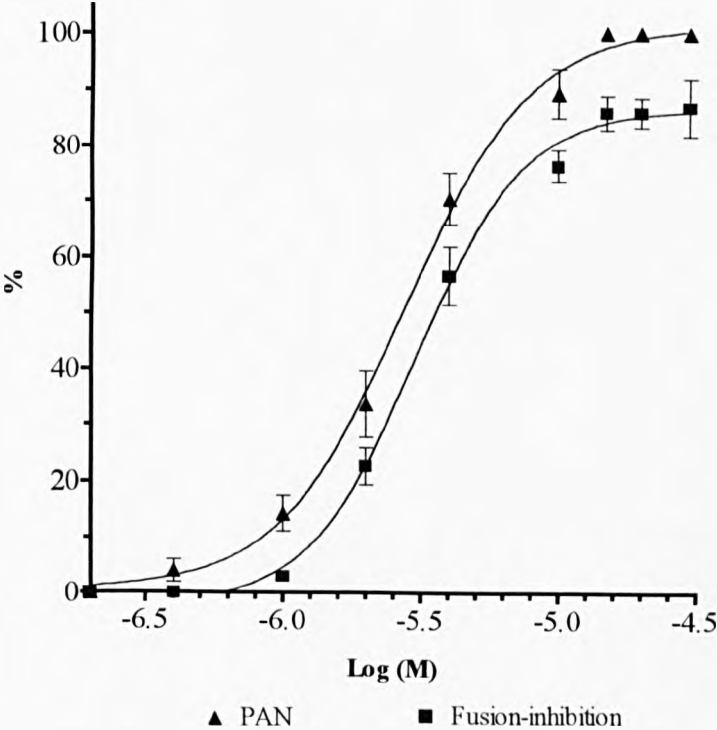
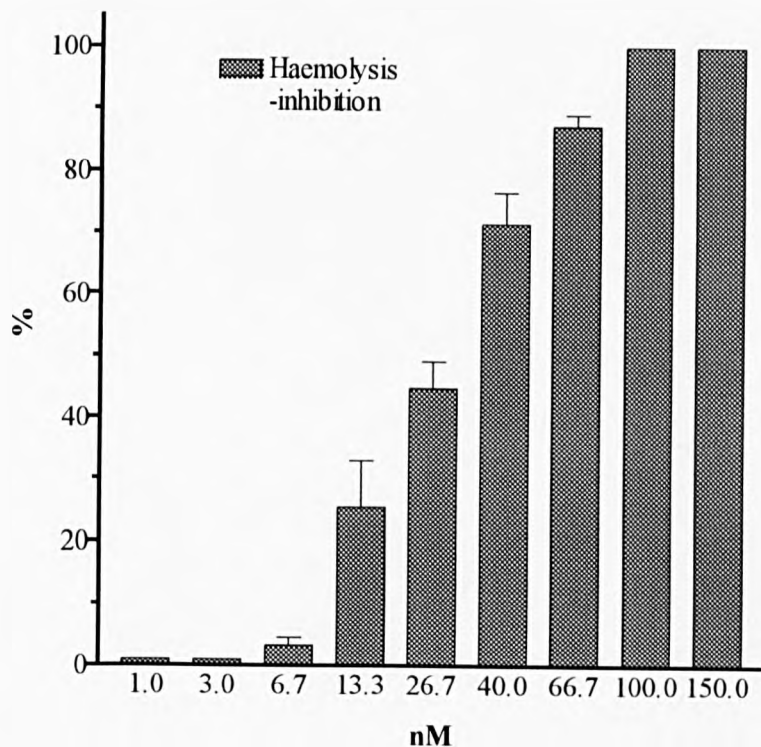


Table 7.5 Analysis of the fusion of non-neutralized virus under the negative control conditions. Data are presented as percentage inhibition of fusion relative to non-neutralized virus at 37°C. Data are the mean of three experiments

<i>Control conditions</i>	<i>% inhibition of internalisation</i>
Cold (4°C) – N ₀	91 (+/- 7)
Bafilomycin treated - N ₀	79 (+/-10)

Figure 7.13 Analysis of the effect of H36 IgG concentration on the haemolysis of CRBCs by pre-attached A/PR/8 virus. Data are the mean of four experiments. Bars represent the SEM.

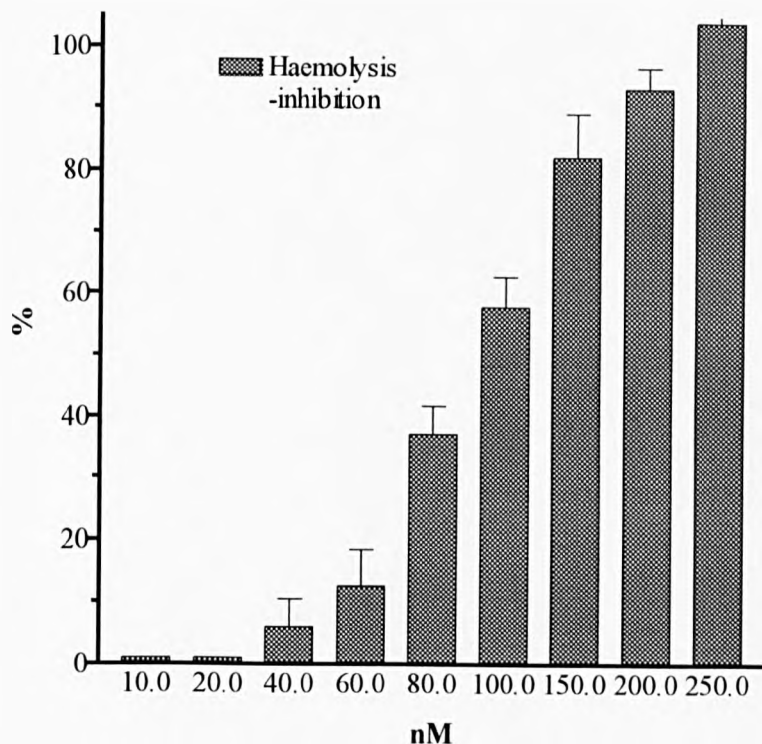


7.4.7 Analysis of the effect of H36 Fab on haemolysis of CRBCs by pre-attached A/PR/8 virus.

Figure 7.14 shows that inhibition of haemolysis increased with increasing H36 Fab concentration, compared to a non-neutralized virus control. These data are supportive of the findings of the fluorescence-based assay (section 7.3.4) and indicates that H36 Fab can inhibit virus-driven fusion.

The effect of H37 IgG and Fab and H9 IgG on the haemolysis of RBCs by pre-attached A/PR/8 virus was also investigated. The results obtained were similar to the H36 IgG and Fab, with all the antibodies being able to inhibit haemolysis (Appendix I). A summary of the data can be seen in Table 7.6.

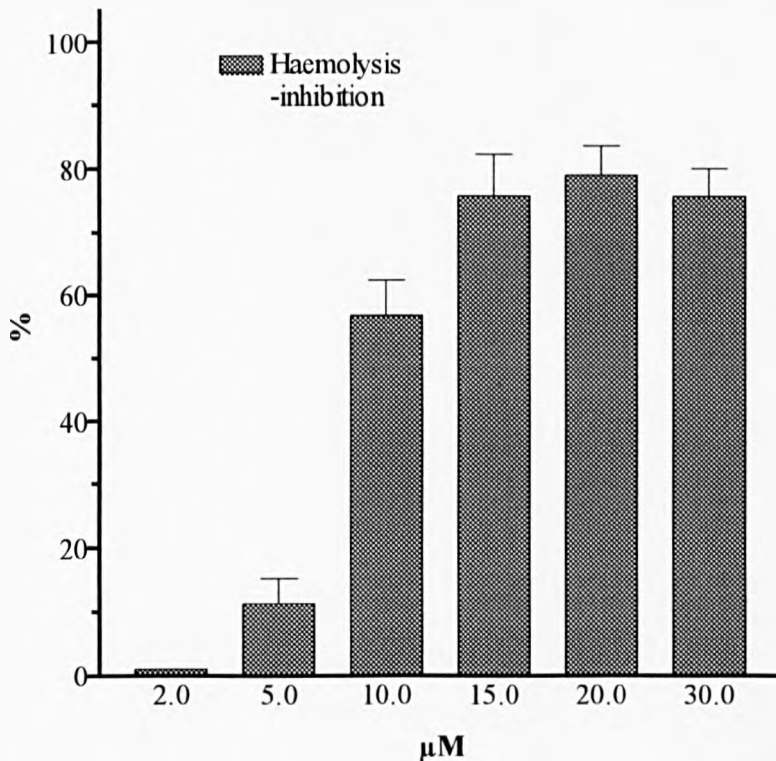
Figure 7.14 Analysis of the effect of H36 Fab concentration on the haemolysis of CRBCs by pre-attached A/PR/8 virus. Data are the mean of four experiments. Bars represent the SEM.



7.4.8 Analysis of the effect of H9 Fab on haemolysis of CRBCs by pre-attached A/PR/8 virus.

Figure 7.15 shows that inhibition of haemolysis increased with increasing H9 Fab concentration, compared to a non-neutralized control. However, in common with the fluorescence-based fusion assay (section 7.3.5), complete inhibition of haemolysis has not been achieved, with the maximum obtainable being approximately 80% inhibition of haemolysis. This result was consistent over the four experiments carried out. These data suggest that the H9 Fab can partially inhibit virus-driven fusion.

Figure 7.15 Analysis of the effect of H9 Fab concentration on the haemolysis of CRBCs by pre-attached A/PR/8 virus. Data are the mean of four experiments. Bars represent the SEM.



7.4.9 Summary of the mechanism of PAN by the antibodies and their Fabs.

A comparison of the mechanism of PAN of the antibodies reveals that neither of the antibodies can inhibit internalisation, whereas they are all able to inhibit virus-cell fusion and haemolysis of CRBCs (Table 7.6). This suggests that the antibodies and their Fabs share a common mechanism of PAN, being inhibition of virus-driven fusion. The results also show that the antibodies differ in their efficiency of PAN with the ranking order being H36>H37>H9, which is mirrored by their Fabs.

Table 7.6 Summary of the mechanism of PAN by the antibodies and their Fabs.

MAb	Antigenic site	50% PAN (nM)		Inhibition of internalisation		Inhibition of fusion		Inhibition of haemolysis	
		IgG	Fab	IgG	Fab	IgG	Fab	IgG	Fab
H36	Sb	9	75	No	No	Yes	Yes	Yes	Yes
H37	Ca2	58	1060	No	No	Yes	Yes	Yes	Yes
H9	Cb	550	1450	No	No	Yes	Yes*	Yes	Yes*

* Inhibition of fusion/haemolysis not complete, maximum obtainable approximately 80%.

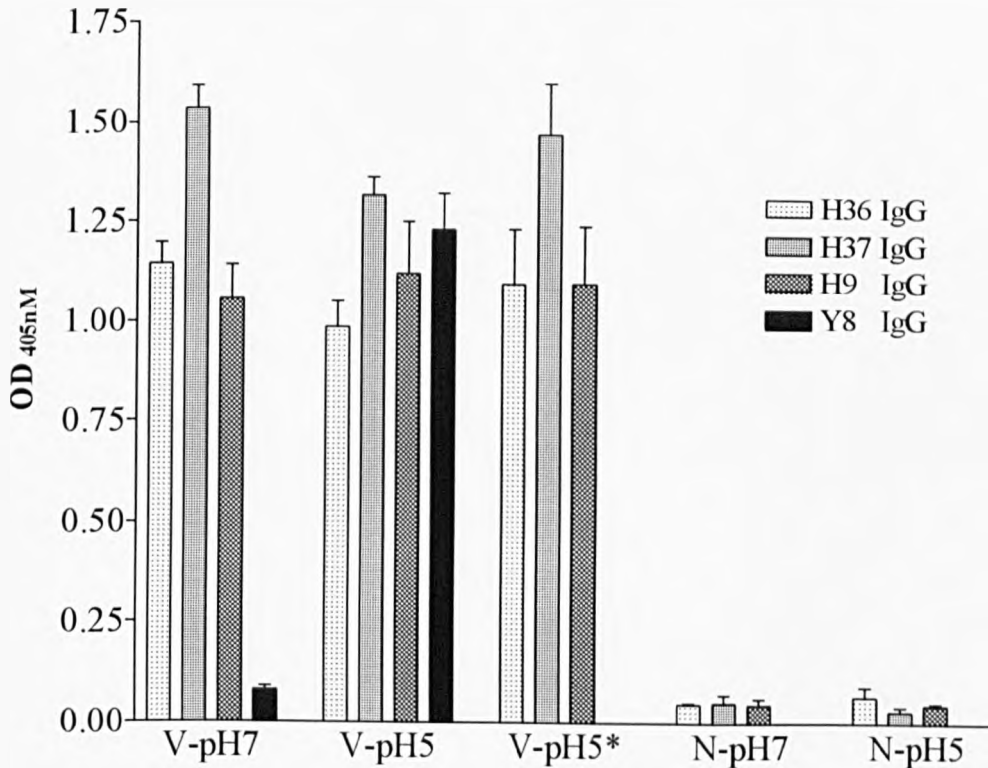
7.5 Investigation of inhibition of fusion during PAN by the antibodies.

Influenza A virus fusion is triggered by a low pH-dependent conformational change(s) of the viral HA (Skehel *et al.*, 1982). Recent evidence has suggested that the conformational changes can be segregated into a number of intermediates (reviewed in the introduction). At 4°C A/PR/8 virus does not fuse at pH 5, but its HA undergoes some conformational changes and release of its fusion peptide (Stegmann *et al.*, 1990; Tsurudome *et al.*, 1992; Pak *et al.*, 1994). This stage is considered to be a pre-fusion intermediate of A/PR/8. As fusion does not occur at 4°C with this virus strain, it was assumed that further changes caused by increased temperature (37°C) are required to make this virus fully fusion competent. Therefore, the pre-fusion intermediate was considered to be a first step in the fusion process and would allow investigation of whether the antibodies can PAN once the fusion process had initiated.

7.5.1 Analysis of the sensitivity of MAb binding to conformational changes of the HA induced by low pH.

In order to determine if MAbs would give PAN once the pre-fusion intermediate of A/PR/8 virus had been established, it was necessary to show that the binding of the antibodies was not sensitive to pH 5. This was carried out by ELISA where virus was captured on a plate by an anti-HA IgA. The captured virus was treated at either pH 7 or pH 5 and the effect on the binding of MAbs was determined (Figure 7.16). Control wells without virus showed that background binding of MAb was low. The binding of MAb Y8, which is specific for the low pH conformation of the HA, increased 18-fold to the pH 5 treated virus compared to the pH 7 treated virus. This demonstrated that captured virus had changed to its low pH conformation. Binding of the H36, H37 and H9 IgGs to virus treated with either pH 7 or pH 5 was similar, indicating that their epitopes were not pH sensitive and therefore, that they should bind to the pre-fusion intermediate.

Figure 7.16 Analysis of the effect of low pH on MAb binding to captured virus. Virus (50 HAU) was captured by anti-HA IgA coated to the plate. The data are the mean of four repeats. Bars represent the SEM. X-axis labels – **V-pH7** = virus treated at pH 7, **V-pH5** = virus treated at pH 5, **V-pH5*** = virus treated at pH 5 at 4°C, **N-pH7** = no virus treated at pH 7 and **N-pH5** = no virus, treated at pH 5).



7.5.2 Analysis of the effect of H36 IgG and Fab on haemolysis of CRBCs by the pre-fusion intermediate of A/PR/8 virus.

The pre-fusion intermediate was investigated using haemolysis of CRBCs. Briefly, virus was attached to CRBCs at 4°C and then treated with pH 7 buffer at 4°C or at pH 5 to trigger formation of the pre-fusion intermediate. Previous studies have shown that prolonged incubation of A/PR/8 at 4°C and pH 5 did not result in fusion and this was confirmed in this system (data not shown) (Tsurudome *et al.*, 1992; Pak *et al.*, 1994). Virus-CRBC complexes were then adjusted to pH 7 and incubated with the antibodies. The effect of antibodies on haemolysis was analysed by shifting pH to 5 at 37°C to trigger haemolysis.

Figure 7.17 shows that virus-CRBC complexes that were pre-treated at pH5 gave a greater degree of haemolysis compared with pH 7 treated complexes. The lack of haemolysis in the inactivated virus control demonstrates that the level of haemolysis seen in the virus controls is virus specific. An interesting observation was that haemolysis by the pre-fusion intermediate (pH 5 treated) could be triggered by increasing temperature to 37°C at neutral pH, and did not require further pH 5 treatment. This is in direct contrast to results of others who failed to get the A/PR/8 virus pre-fusion intermediate to fuse at 37°C, pH 7, until further pH 5 treatment (Pak *et al.*, 1994). The concentration of H36 IgG and Fab used gave >90% inhibition of haemolysis by pH 7 treated virus. However, levels of haemolysis after treatment with H36 IgG and Fab were very similar to those of the pH 5 treated virus control, indicating that the antibodies had to be present prior to initiation of fusion to give PAN.

These investigations were also carried out on the H37 and H9 IgGs and their Fabs and gave similar results, not being able to inhibit haemolysis of CRBCs by virus pre-treated at pH5 (see Appendix I for results).

7.5.3 Analysis of the effect of the Fabs on the low pH induced conformational change of the HA of pre-attached virus (in PAN-like format).

In order to inhibit haemolysis of CRBCs by virus the MAbs are required prior to induction of intermediates (that have undergone some of the conformational changes of the HA) in the fusion process. This suggested that antibodies may act by inhibiting the conformational changes of the HA and thus prevent haemolysis. To investigate this, we used a panel of MAbs specific for epitopes present only in the low pH form of the HA (Table 7.7). These antibodies were used in an ELISA that was designed to be very similar to the standard PAN assay (section 7.2), except that the MDCK monolayers were fixed to prevent internalisation of virus. Virus was attached to monolayers at 4°C and then incubated with 200 nM of H36 Fab. This concentration was sufficient to cause >99% PAN in an assay carried out simultaneously (data not shown).

Figure 7.17 Analysis of the effect of H36 IgG and Fab on haemolysis by the cold-fusion intermediate of A/PR/8 virus. All data have been subtracted from the background haemolysis obtained from CRBC controls without virus. All control samples were treated as the virus containing samples. Data are the mean of three experiments. Bars represent the SEM. X-axis labels – **V-pH7** = pre-attached virus incubated at 4°C and pH 7, **V-pH5** = pre-attached virus at 4°C and pH 5, **V-IA** = virus inactivated at 37°C and pH 5 prior to attachment, **IgG-pH7** = H36 IgG at 66.7 nM, incubated with pH 7 treated virus, **Fab-pH7** = H36 Fab at 200 nM, incubated with pH 7 treated virus, **IgG-pH5** = H36 IgG at 66.7 nM, incubated with pH 5 treated virus, **Fab-pH5** = H36 Fab at 200 nM, incubated with pH 5 treated virus.

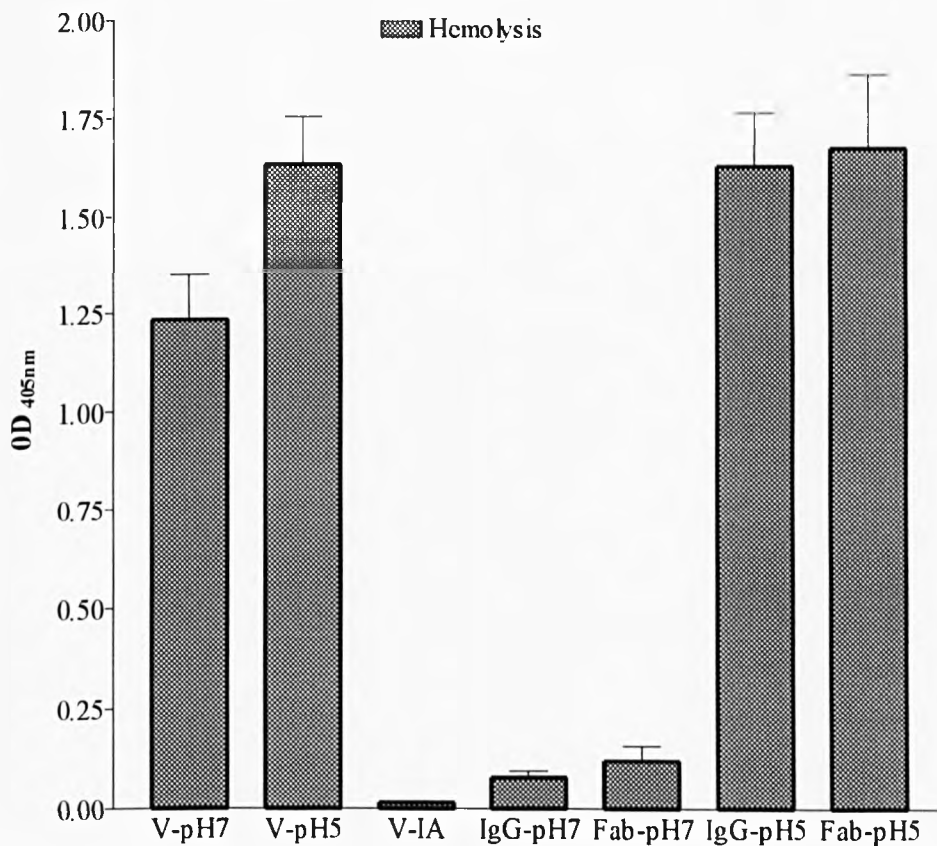


Table 7.7 Characteristics of the conformation-specific MAbs.

<i>MAb</i>	<i>Binding Site</i>	<i>Specificity</i>
Y8 IgG	Sa	Low pH HA
H2 IgG	Cb	Low pH HA
H3 IgG	Ca2	Low pH HA
H18 IgG	Cb	Low pH HA
H17 IgG	Ca2	Native HA

(Yewdell *et al.*, 1983)

Virus-Fab complexes were then incubated at pH 7 or pH 5 and at 37°C or 4°C to induce conformational changes in the viral HA, and then incubated with the conformation-specific MAbs at 4°C. An anti-Fc IgG detection system allowed quantitation of the bound conformation-specific IgGs. As a result only the effect of the neutralizing Fabs on the HA conformation could be tested by this assay, as the Fc region of the H36, H37 and H9 MAbs would interfere with detection of conformation-specific MAbs. Attachment detection ELISAs were carried out to show that virus attachment remained constant under the different pH conditions (data not shown).

Figure 7.18 shows the difference in binding to virus treated with either pH 5 or pH 7 at either 4°C or 37°C of the conformation-specific IgGs. The H17 IgG which binds specifically to native HA, had a 4.3-fold decrease in binding to pH 5 (37°C) treated virus compared to virus treated at pH 7(37°C). This demonstrated that conditions used in the assay caused the viral HA to adopt its low pH conformation. The fold differences in binding between pH 7(37°C) treated virus and pH 5(37° or 4°C) treated virus of the four low pH specific IgGs is shown in Table 7.8. Collectively, these results show that all the IgGs have increased binding to pH 5(37°C) treated virus, again indicating adoption of the low pH conformation of the HA. The analysis of the pH 5(4°C) (pre-fusion intermediate) treated virus indicated that conformational changes of the HA occurred, but at a lesser extent than with the pH 5(37°C) treated virus. The H17 IgG is specific for site Ca2, which spans the monomer-monomer interface in the HA trimer, and it is specific for the native HA conformation. It is interesting that this IgG binds to

Figure 7.18 Analysis of the effect of H36 Fab on the low pH-induced conformational change of the HA of A/PR/8 virus (in PAN-like format). Virus was attached to fixed cell monolayers at 4°C and then incubated with Fab at 4° or 37°C. Neutralized virus was then incubated with pH 5 or 7 at 4° or 37°C, and then probed with conformation-specific MAbs. Graph shows binding of conformation-specific MAbs to virus. All data have been subtracted from a cell monolayer control without virus. Data are the mean of three experiments. The bars represent the SEM. X-axis labels – **V-pH7 (37°C)** = MDCK cell attached virus incubated at pH 7 and 37°C, **V-pH5 (37°C)** = attached virus incubated at pH 5 and 37°C, **V-pH5(4°C)** = as previous but at 4°C, **Fab-pH7 (37°C)** = H36 Fab at 200nM incubated with attached virus treated at pH 7 and 37°C, **Fab-pH5 (37°C)** = H36 Fab at 200nM incubated with attached virus treated at pH 5 and 37°C, **Fab-pH5 (4°C)** = as previous but at 4°C.

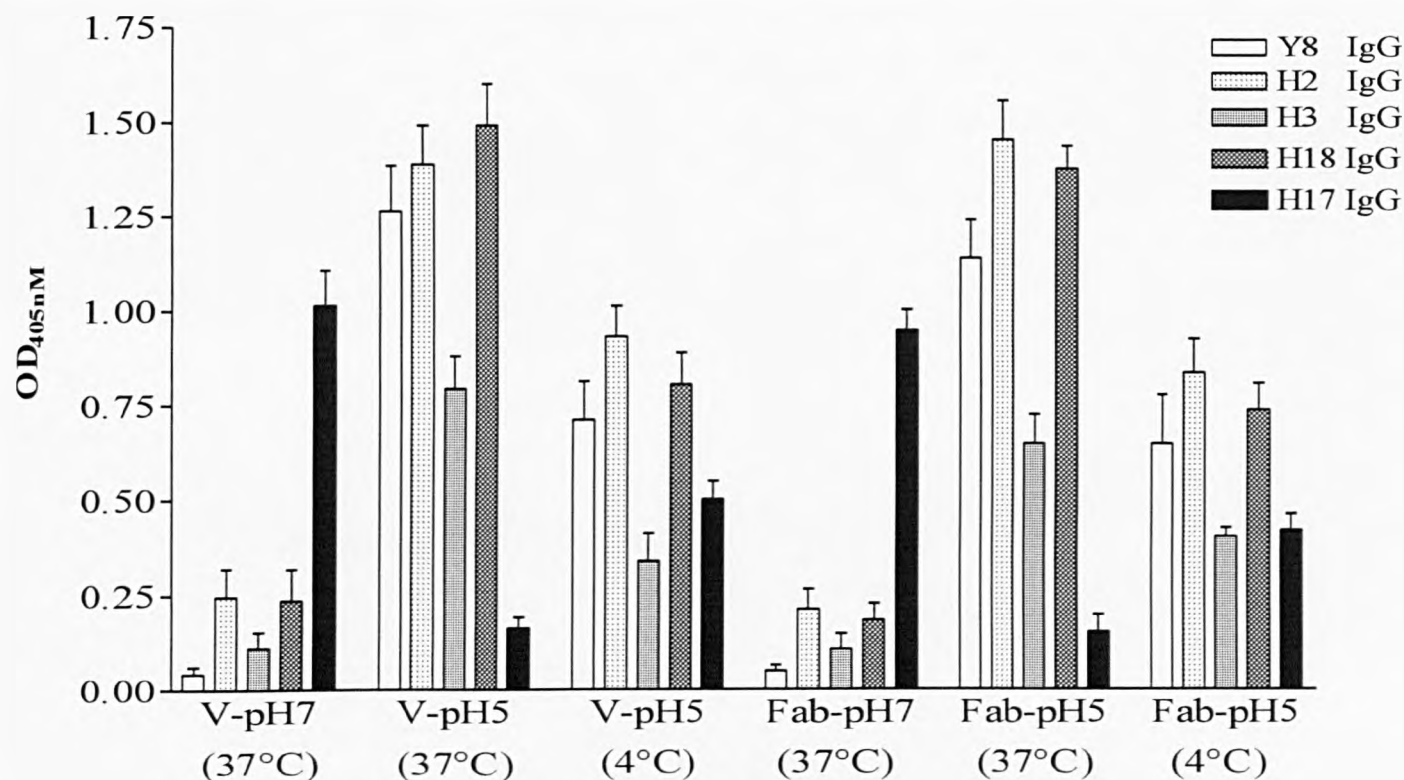


Table 7.8 Comparison of the binding of the low pH conformation specific MAbs to A/PR/8 virus in different stages of fusion.

MAb	Fold difference in binding between pH 7 virus and pH 5 viruses.	
	pH5(4°C)	pH5(37°C)
Y8 IgG	14.0	25.0
H2 IgG	3.4	5.4
H3 IgG	2.0	5.4
H18 IgG	3.2	6.0

a slightly greater extent to the pre-fusion intermediate virus than the pH 5(37°C) treated virus. This together with the lower binding to cold-fusion intermediate virus of the H3 IgG, also specific for site Ca2, suggests that the pre-fusion intermediate retains a higher proportion of its HA1 globular head structure than the pH 5(37°C) treated virus.

Incubation with sufficient H36 Fab to cause >99% PAN revealed no significant differences in the binding of the conformation-specific MAbs between the virus controls representing each treatment condition and the virus incubated with neutralizing Fabs (Figure 7.18). This indicated that the Fab could not inhibit the low pH induced conformational change of the HA. H36 Fab was also tested at 100nM, sufficient to give 90% PAN and at 500nM. The 100nM concentration of Fab gave similar results to those described, however, at 500nM binding to the virus by all of the conformation-specific MAbs was restricted (data not shown). This was interpreted as steric hindrance by the high concentration of Fab.

These investigations were also carried out with the H37 and H9 Fabs and gave similar results to those described above (see Appendix I.7). This indicates that neither of the Fabs can inhibit the low pH induced conformational change of the HA and that the Fabs must inhibit fusion/haemolysis by an alternative process. In support of this conclusion are the results of proteinase-K experiments. These experiments involved proteinase-K treatment of H36 Fab neutralized virus (free virus in solution, not PAN format). The proteinase-K cleaves the HA only in its low pH form and no difference in the cleavage

pattern of the HA of pH 5 treated neutralized virus could be seen compared to the non-neutralized control (see Appendix I.8). This again indicated that Fab could not inhibit the conformational change of the HA.

7.6 Discussion :

7.6.1 Comparison of the STAN and PAN of A/PR/8 virus by the antibodies.

This study is the first to show PAN activity of influenza by monoclonal IgGs. In every case standard neutralization (STAN) by H36, H37 and H9 IgGs was more efficient than their PAN. However, the efficiency of PAN was higher at PAN₉₀ than at PAN₅₀ at 37°C (Table 7.9). This suggests that PAN increased in efficiency as antibody concentration increased. In contrast, the STAN and PAN activity of the H36 and H37 Fabs were very similar, while PAN activity of the H9 Fab was significantly higher (18-fold at 37°C) than its STAN activity.

Table 7.9 The relative difference between PAN and STAN by the IgGs at 50% PAN (PAN₅₀) and 90% PAN (PAN₉₀).

<i>Mab</i>	<i>Fold difference</i>	
	<i>STAN₅₀ : PAN₅₀</i>	<i>STAN₉₀ : PAN₉₀</i>
H36 IgG	50.0	10.3
H37 IgG	7.5	5.4
H9 IgG	8.0	5.0

Why do the Fabs have a better PAN efficiency relative to their STAN than the IgGs?

A possible explanation for the lower efficiency of PAN by the IgGs assumes that the different areas on the viral surface have a greater importance in the PAN process than other areas. For example, a spherical virus particle attaching to a cell will have only one sector in contact with the cell. Hence, the remaining HAs on the virus surface not in close association with the cell surface should be as freely available to bind IgG as they are in unattached virus. If HA availability was the same in both unattached and attached virus then the efficiency of PAN by the IgGs should be similar to their STAN. However, the lower efficiency of PAN relative to STAN, suggests that IgGs must have restricted access to HAs on regions of the virus crucial for the PAN process. It is possible that the area of the virus-cell contact may contain the HAs crucial for the PAN process. It follows that access of IgG to this area would be restricted, due to steric hindrance by both cellular and viral proteins in close apposition at the virus-cell contact zone, resulting in lower efficiency of PAN. In contrast, it is likely that access of the smaller Fabs is less restricted to the crucial virus-cell contact zone. As a result, their PAN activity, relative to their STAN activity, is of higher efficiency compared to their IgGs. However, it should be emphasised that the IgGs have a greater PAN activity in molar terms than their Fabs. Thus suggesting that they are more efficient at PAN when they do gain access to the crucial sites, possibly due to their greater molecular mass. A corollary of this hypothesis is that large areas of HA on the viral surface must be redundant or of a limited importance in the PAN process. However, further experimentation is required to establish this point.

Interestingly, the H9 Fab PAN activity was greater than its STAN (Figure 7.6). This is counter-intuitive as it is difficult to understand how an antibody can neutralize attached virus with limited availability (due to internalisation) better than virus free in solution. One possible explanation is that there is a change in HA conformation upon receptor-binding that allows increased access to the H9 antigenic site (Cb). The increased efficiency of PAN by H9 Fab is seen only at 37°C, whereas at 4°C its efficiency is similar to its STAN. This supports the idea that a temperature-dependent conformational change is involved. However, this hypothesis is tentative as the difference between the PAN and STAN by the H9 Fab even though statistically significant, is actually only 1.8-fold. Therefore, the importance of this difference should

be interpreted with care, especially in the light of the published 3Å resolution structure of BHA complexed with its receptor indicating that there were no major conformation changes (Weis *et al.*, 1988). However, it is possible that the behaviour of BHA does not truly reflect that of complete HA in the virion envelope and that monovalent receptor-HA interactions do not adequately reflect the multivalent receptor-HA interactions which occurs between virus and cell (Glick and Knowles, 1991).

Comparison of PAN at 4°C and PAN at 37°C showed that they occurred at similar efficiencies relative to STAN (except for H9 Fab). This indicated that variation in epitope availability was not a factor affecting the PAN of influenza in this temperature range as has been suggested for HIV (Armstrong and Dimmock, 1996). Obviously, the PAN activity will depend on the rate of internalisation of virus into the cell. Virus attached to cells at 4°C remained susceptible to PAN for a 60 minute period. However, at 37°C PAN activity decreased rapidly with time and after 10 minutes approximately 50% of the virus was refractory to PAN. This suggested that the kinetics of PAN is very fast as at 37°C, as the majority of virus is only accessible on cell surface for approximately 5 minutes and yet the level of PAN is similar to that at 4°C, where virus is accessible for over 60 minutes. A comparison of the kinetics of PAN by the H36 Fab at 4°C and 37°C gave very similar results to those obtained with the IgG. This suggested that epitope availability was not responsible for increased efficiency of PAN, relative to STAN seen in the Fabs, compared to the IgGs, as both IgGs and Fabs had similar reaction times before internalisation of virus.

7.6.2 Mechanism of PAN by the IgGs and their Fabs.

This study is the first to determine the mechanism of PAN of influenza virus by monoclonal IgGs and their Fabs. The data suggest that all three IgGs and their Fabs shared a similar mechanism of PAN. Antibodies could not inhibit receptor-mediated internalisation of virus into MDCK cells, decreases in virus-cell fusion correlated with PAN and indicated a causal relationship. This was supported by all of the IgGs and Fabs being able to inhibit haemolysis of CRBCs in a dose dependent fashion.

In contrast to the H36 and H37 Fabs, inhibition of fusion by Fab H9 did not correlate well with higher levels of PAN. For example, at >95% PAN there was only approximately 80% inhibition of fusion. In addition the H9 Fab inhibited haemolysis of CRBCs by approximately 80%. It is currently unknown why inhibition of fusion by H9 Fab did not show a complete correlation with PAN, as seen with the other antibodies. It is possible that either neutralization of A/PR/8 virus can be brought about by less than a 100% reduction of fusion activity or that inhibition of a post-fusion event contributes to the remaining 20% neutralization. However, the small difference could also be due to variability in the experimental system. A similar observation has been made with a neutralizing 17 amino acid micro-antibody against HIV-1 (Jackson *et al.*, 1999). Analysis by fluorescence fusion (R18 based) assay and cell-cell fusion assay showed that only approximately 50% of the neutralization level could be accounted for by inhibition of fusion by the micro-antibody.

Collectively, these data strongly suggest that all the IgGs and their Fabs caused PAN by inhibition the virus-cell fusion. Thus antigenic site, isotype or valency of the antibody had no affect on the mechanism of PAN. The PAN activity of the IgGs and Fabs increases with increasing antibody concentration being more efficient at PAN₉₀ than PAN₅₀. Therefore, it can be assumed that the process of inhibition of fusion also increases in efficiency with increasing antibody concentration. At higher antibody concentration the epitope availability decreases and hence the proportion of antibodies bound monovalently would increase. Hence, it may be that antibody bound monovalently is more efficient at PAN and thus more efficient at inhibition of fusion. Together, this lends support to a steric hindrance (monovalent binding) model of fusion-inhibition, as discussed in Chapter 6, section 6.14.3.

7.6.3 Investigation of inhibition of fusion during PAN.

7.6.3.1 Characteristics of the pre-fusion intermediate of A/PR/8 virus.

As reviewed in the introduction (section 3.4.1) the X-ray crystal structure at 3Å resolution has been obtained for BHA trimer at pH 7 and at pH 5. The pH 5 structure is characterised by dissociation of the top HA1 globular domains and extensive

rearrangements of HA2 domain, including exposure of the normally hidden hydrophobic fusion peptides. The pH 5 structure was originally proposed as the fusion active conformation (Wilson *et al.*, 1981; Bullough *et al.*, 1994). However, recent evidence has strongly suggested that this pH 5 structure corresponds to an inactive terminal structure marking the end of the fusion process, whilst the fusion active form is mediated by a transient conformational intermediate (pre-fusion intermediate), in most viral strains (White and Wilson, 1987; Stegmann *et al.*, 1990). Based on these observations a 3-state model relating the conformational transitions of the HA to the fusion process has been proposed (Korte *et al.*, 1999). This model describes the pH-driven transition from a tense (T) state, corresponding to the pH 7 crystal structure, to a relaxed (R) state. The R state is followed by a transition to the desensitised (D) state, corresponding to the pH 5 crystal structure. The R state is considered to be the fusion active conformational intermediate (pre-fusion intermediate). Cryo-EM studies have correlated a fuzzy spike (HA) morphology with the D state, whilst a defined HA morphology has been correlated with the T state. The R state retains most of its T spike morphology except they seemed less well defined than the T state (Korte *et al.*, 1999; Shangguan *et al.*, 1998). The pre-fusion intermediate (correlating with R state, but is not fusion active) of A/PR/8 virus is not well defined, but can be obtained at low pH and lower temperature (pH 5, 4°C) (Tsurudome *et al.*, 1992). The A/PR/8 viral HA at pH 5, 4°C has been shown to release its fusion peptides both by the ability to bind target membranes (via a hydrophobic interaction) and by immunoprecipitation by anti-fusion peptide antibody (Tsurudome *et al.*, 1992; Pak *et al.*, 1994). Immunoprecipitation of the pre-fusion intermediate HA by Y8-10C2 MAbs, specific for an epitope in the HA1 exposed in the low pH conformation (D state), also indicated that there were some conformational alterations in the globular head domain. However, the precipitation was only 1.6-fold lower than obtained with virus treated at pH 5, 37°C indicating that these conformational changes are restricted in the pre-fusion intermediate.

The pre-fusion intermediate was studied here through haemolysis of CRBCs. In agreement with previous studies, it was shown that the pre-fusion intermediate (pH 5, 4°C) did not cause haemolysis during a prolonged (4 hour) incubation at 4°C (Stegmann *et al.*, 1990; Tsurudome *et al.*, 1992). In addition the A/PR/8 pre-fusion intermediate could not be committed to fuse by increasing the temperature to 37°C, at pH 7 (Pak *et al.*, 1994). In contrast, results obtained in this thesis showed that haemolysis by the pre-

fusion intermediate could be triggered at neutral pH by increasing the temperature to 37°C. The reason(s) for this difference are unknown, but it is possible that differences between the fusion assays are responsible. For example, Pak *et al* (1994) used erythrocyte ghosts labelled with R18 and hence analysed the virus-RBC lipid mixing (hemi-fusion), whereas in this thesis I have used haemolysis of CRBCs. However, the process of haemolysis has not been well characterised and it is possible that differences exist compared to the actual fusion process. It is also possible that differences in the virus HA sequence or differences in the species of erythrocyte (human RBCs were used by Pak *et al* (1994) could be responsible. Future work in this area should use R18-labelled CRBCs ghosts to try to correlate both fusion and haemolysis results. However, results in this thesis are agreement with a study with the X-31 strain of influenza (H3), which showed that virus-erythrocyte complexes pre-treated at pH 5, 4°C could be committed to fusion at neutral pH (37°C), suggesting subtle differences in the virus could be the important factor (Schoch *et al.*, 1992).

Results in this thesis also showed that haemolysis by the pre-fusion intermediate (pH 5, 4°C), which had been shifted to pH 7, 37°C, was more efficient than virus that had been treated at pH 7, 4°C. This suggests that during the low pH pre-incubation, the virus is undergoing changes that prime the virus for the fusion process. This idea is supported by Schoch *et al* (1992), who showed that efficiency of the fusion by the pre-fusion interval was dependent on the duration of the low pH pre-incubation.

This thesis is the first study to analyse the conformation of the pre-fusion intermediate of A/PR/8 virus attached to MDCK cells with a panel of conformation-specific MAbs (Figure 7.18). Binding of four MAbs specific for low pH HA conformation to the pre-fusion intermediate (pH 5, 4°C) increased relative to neutral HA conformation, but was approximately 2-fold less than binding to virus in the pH 5, 37°C conformation. Hence, this indicated that the conformation of the viral HA of the pre-fusion intermediate had undergone changes in three antigenic sites on the HA globular head domain, but that these were not as extensive as in the pH 5, 37°C structure.

Binding of the H17 MAb, that is specific for native HA, to the pre-fusion intermediate (pH 5, 4°C) was only 2-fold lower than the binding to the native HA. In contrast, the binding to virus treated at pH 5, 37°C decreased by 6.6-fold. Also the binding of H3 MAb, specific for epitopes in the HA1 exposed after treatment at low pH,

had the lowest increase in binding to the pre-fusion intermediate compared to the other MAbs specific for epitopes exposed at low pH. Together, these data suggest that the Ca2 antigenic site spanning the monomer-monomer interface of the HA trimer is relatively conserved in the pre-fusion intermediate. Conservation of the monomer-monomer interface in the pre-fusion intermediate agrees with cryo-EM pictures of HA spikes in which there was no detectable dissociation of the HA1 globular heads in the HA trimer (Korte *et al.*, 1999; Shangguan *et al.*, 1998).

Interestingly, the MAbs specific for site Cb showed the highest binding to both the pre-fusion intermediate (pH 5, 4°C) and pH 5, 37°C treated virus. This result is in agreement with a previous study of pH 5, 37°C treated-A/PR/8, which showed that with one exception (MAb Y8-10C2), that binding of 19 MAbs specific for sites Sa and Sb was decreased, whilst the binding of all 9 MAbs specific for site Cb had an increased binding compared to pH 7, 37°C-treated virus (Yewdell *et al.*, 1983). Collectively, this suggests that in the low pH treated HA conformation access to site Cb is less restricted than in the neutral pH HA conformation. If we extrapolate this idea to possible changes in site Cb that occur on binding to the cell receptor, then this may explain the increased PAN activity of H9 Fab compared to its STAN activity.

In summary, probing the structure of the pre-fusion intermediate HA indicates that the HA1 globular head has undergone conformation changes, but that monomer-monomer interface is relatively conserved. Future work in this area should use the fusion-peptide specific MAbs available to determine whether the fusion-peptide has been released.

7.6.3.2 *Analysis of the process of fusion-inhibition during PAN.*

This study has investigated the affect of the IgGs and Fabs on the low pH-induced haemolysis of CRBCs by a pre-fusion intermediate (pH 5, 4°C) of A/PR/8 virus and on the low pH-dependent conformational change of the viral HA. Initial investigation showed that binding of H36, H37 and H9 MAbs to HA was not sensitive to low pH treatment. As a result, any change in the PAN activity of pre-fusion intermediates should not be due to an inability of the antibodies to bind to virus. It was found that neither of the IgGs nor the Fabs could inhibit the haemolysis of CRBCs by the A/PR/8

virus pre-fusion intermediate. This indicated that the antibodies had to bind to virus prior to the changes induced in the viral HA when it becomes the pre-fusion intermediate. Probing the HA of virus previously incubated with neutralizing Fab with a panel of conformation-specific MAbs, indicated that under all of the pH and temperature conditions studied its conformation was similar to that of virus not treated with neutralizing Fab. This indicated that Fab neutralization could not inhibit the low pH-induced conformation changes in the HA.

These results suggest that the HA of neutralized virus is functional (i.e. can adopt required fusion conformations) and hence that the IgGs and Fabs are inhibiting a very early stage of the fusion process. Therefore, it is possible that the inhibition of fusion seen with PAN is due to steric hindrance of some early part of the fusion process. A recent study of influenza virosome fusion liposomes containing specific anti-HA Fabs as surrogate receptors, suggested that high density of Fabs inhibits fusion (Millar *et al.*, 1999). Therefore, a possible explanation of PAN by the IgGs and Fabs is that their binding to the crucial HA-cell contact zone (discussed earlier) increases the overall protein density at this site. This overcrowding sterically inhibits the fusion process perhaps by preventing correct orientation of the HA for delivery of the fusion peptide. In support of this hypothesis are the following –

- (1) Antibodies did not inhibit haemolysis of CRBCs by pre-fusion intermediates (the possible first stage of the fusion process), hence the antibodies are required prior to initiation of fusion/haemolysis.
- (2) Antibodies did not inhibit conformational changes in the HA, indicating that the neutralized virus HA is fusion functional.
- (3) PAN by the IgG is more efficient in molar terms than the Fab, possibly due to its larger molecular mass. The larger molecular mass would enhance its ability to sterically hinder an event in the early fusion process.
- (4) PAN is more efficient at higher IgG concentrations. At higher concentrations the probability that the IgGs bind monovalently is greatly increased due to the limited availability of epitopes. Monovalent binding increases the IgGs steric hindrance capacity (see chapter 6).

7.6.4 PAN of other animal viruses.

This thesis is the first study to determine the mechanism of PAN of influenza A virus by monoclonal IgGs and their Fabs. However, PAN has been investigated in a number of other viral systems.

The temperature dependence of PAN of HIV-1 virus by a number of monoclonal IgGs has been investigated (Armstrong *et al.*, 1996; Armstrong and Dimmock, 1996). MAbs ICR 39.13g and F58 were able to give PAN at 21°C and 35°C. However, MAb ICR 41.1i could only give PAN below 21°C. As a result, it was suggested that this phenomenon was linked to a temperature-dependent conformational change in the CD4-gp120 complex, which possibly masks the ICR 41.1i epitope. Other MAbs including ICR 39.3b do not give PAN at any temperatures, inferring that its epitope is blocked by the CD4 interaction. These findings are in contrast with results in this thesis with PAN of A/PR/8 being temperature-independent, apart from a difference between PAN at 37°C and 4°C with the H9 Fab. Another study showed that a MAb to the CD4 protein, M-T413 (non-viral epitope) gave PAN of HIV-1 when it was added as late as 120 minutes post-infection (Rieber *et al.*, 1992). It was also shown that the M-T413 Fab could also give effective PAN, indicating that crosslinking was not involved. These findings suggested that the PAN activity of the MAb and Fab M-T413 was due to the inhibition of conformational rearrangements in the CD4-gp120 complex. Therefore, collectively, the studies on PAN of HIV-1 suggest that it is dependent on conformational changes in the receptor complex, which have been previously characterised (Sattentau and Moore, 1991; Sattentau *et al.*, 1993). Conformational changes upon receptor binding of influenza have not been found.

The importance of the virus-host cell receptor interaction in PAN activity was also indicated in a study of enterovirus 71 (Kjellén, 1985). This study showed that components of an anti-enterovirus 71 immune serum could only neutralize virus after attachment to rhabdomyosarcoma cells but not after attachment to green monkey kidney cells. Formation of *de novo* epitopes was also seen in a study of neutralization of Sindbis virus, where glycoprotein E1 and E2 underwent conformational changes as a consequence of the virus-cell interaction (Flynn *et al.*, 1990). This suggested that conformational changes in virus proteins upon receptor interaction revealed *de novo* epitopes that antibodies in the serum could interact with. This is of interest in relation

to the H9 Fab PAN results in this thesis, as this suggests that a possible relaxation of conformation of the HA upon receptor interaction could allow increased PAN.

Two studies of the PAN of CMV virus found MABs that gave PAN and others that did not (Farrell and Shellam, 1990; Ohizumi *et al.*, 1992). The study with HCMV found that MAB C-23 could neutralise virus absorbed to cells and could also block cell-cell infection. Furthermore, the virus remained sensitive to PAN for 120 minutes after shifting temperature from 4°C to 37°C (Ohizumi *et al.*, 1992). The sensitivity of attached virus to PAN after incubation periods seems to be a feature of viruses that fuse with the plasma membrane by a pH-independent mechanism. For example, a study of PAN of respiratory syncytial virus by a convalescent serum showed that virus had susceptibility of PAN after >60 minutes incubation at 37°C (Osiowy and Anderson, 1995). In contrast, a study of the PAN of Newcastle disease virus (NDV), which is internalised by receptor-mediated endocytosis, showed that it became refractory to PAN after only 90 seconds of shifting temperature from 4°C to 37°C (Russell, 1984). However, it was shown in this thesis that A/PR/8 virus only starts to become refractory to PAN after 5 minutes of the temperature shift from 4°C to 37°C. This is accepted as being quite slow for receptor-mediated endocytosis and suggested that the prolonged (approximately 15 minutes) incubation at 4°C prior to infectivity that was responsible for this delay.

The importance in PAN of the specificity of the antibody was indicated by a study of adenovirus neutralization (Wohlfart, 1988). This showed that PAN was seen only with anti-hexon serum and not anti-fiber or anti-penton base serum. The authors suggested that the mechanism of PAN could be inhibition of low pH-induced conformational change of the viral capsid.

Determination of the mechanism of PAN of the IgGs and their Fabs in this thesis indicated that they all neutralise by inhibition of fusion/haemolysis. The mechanism of PAN has been investigated in only a limited number of other viral systems.

A study of the PAN of rabies virus by MABs has described two mechanisms of action (Dietzschold *et al.*, 1987). This study found that MABs added after attachment of virus to cells caused up to 30% of the bound virus to be released from the cell surface. This mechanism has since also been described in PAN of rhesus monkey rotavirus, where MAB to the VP8 antigen caused release of virus from MA104 cells (Ruggeri and Greenberg, 1991). The virus that remained attached to cells in the rabies virus study

was endocytosed, and it was hypothesised that MAbs neutralize virus by inhibition of the virus-cell fusion. Release of attached A/PR8 virus by antibody was not found in this thesis as the amount of neutralized virus internalisation was the same as the non-neutralized control. Two further studies have also implicated inhibition of fusion as being the mechanism of PAN. A study of PAN of West Nile virus indicated PAN correlated with inhibition of uncoating of viral RNA (Gollins and Porterfield, 1986). Alternatively a study of vesicular stomatitis virus (VSV) used a fluorescent fusion (R18-based) assay to analyse fusion and showed that antibody could inhibition fusion by >90% (Blumenthal *et al.*, 1987). Investigation of the PAN of African Swine fever virus, indicated the antibodies in convalescent sera could PAN (Gómez-Puertas *et al.*, 1996). This study showed that the PAN antibodies were specific for protein p30 and that these were implicated in inhibition of internalisation as proteinase-K treatment could detach approximately 90% of neutralised virus after incubation at 37°C compared to detachment of only approximately 5% in the non-neutralised virus control.

Six MAbs had PAN activity for poliovirus (Vrijssen *et al.*, 1993). This was caused by the antibody preventing the cell-mediated conversion of virus to 135S and 80S particles. The valency of binding of the MAbs were implicated in this mechanism, where it was suggested that PAN positive MAbs bound bivalently, whereas PAN negative MAbs bound only monovalently.

Collectively, the studies in the other viral systems often implicate inhibition of the fusion step in enveloped virus or an uncoating step in non-envelope viruses as responsible for PAN. This is in supportive of results presented in this thesis which indicate that all three IgGs and their Fabs also inhibit fusion of the mechanism of PAN.

8 Results: Analysis of the reversibility of the haemagglutination-inhibition and neutralization of influenza A/PR/8 virus by MAbs.

8.1 Introduction

A number of MAbs have been described that irreversibly neutralize influenza A virus. The mechanism of neutralization of A/PR/8 virus by a monoclonal IgA, H37-66, was determined to be inhibition of virus-cell fusion (Armstrong and Dimmock, 1992). However, when neutralized virus was treated with acidified PEG, to artificially bypass the block to fusion, infectivity was not recovered. Immunofluorescence studies of PEG fused virus indicated that distribution of internal viral antigens mimicked that of infectious virus. A similar situation was also encountered with a monoclonal IgG, HC2, to A/fowl plague/Rostock/34 (FPV/R) virus, where viral RNA was found to reach the nucleus, but did not undergo transcription or replication (Possee *et al.*, 1982; Rigg *et al.*, 1989). As a result, it is apparent that internal components of the neutralized virus remain dysfunctional independent of the antibody. This requires that MAbs binding to the HA on the exterior of the virus transduce a signal through the envelope to the core components which results in a permanent (irreversible) loss of infectivity. However, evidence for this signal transduction by antibodies and permanent loss of infectivity has not been found.

This area was investigated in a study of the reversibility of haemagglutination-inhibition (HI) and neutralization of virus by a panel of anti-FPV/R IgGs and the monoclonal IgA, H37-66 (Schofield, 1996). In this study ammonium hydroxide (AmOH) at pH 11.5 was used as a mild denaturant to remove MAbs from the virus post-neutralization, as crucially this treatment did not affect virus infectivity. It was found that with half of the MAbs tested (HC3W, HC10 and IgA) the HI and neutralization could be reversed. The reversibility correlated well with antibody affinities as HC3W and HC10 had lower affinities than the MAbs that could not be reversed (the affinity of IgA is unknown). The attachment of virus to cell receptors was analysed to determine if the cell receptor acts synergistically with the MAb to trigger irreversible neutralization. This study proved inconclusive, as only approximately 10% of the total HA and infectivity could be recovered. A very interesting possible explanation of this low recovery was that the binding of the IgA to virus attached to a cell receptor caused a global conformational change in the viral HA, which resulted in an increase in affinity of IgA, and that it became refractory to removal by AmOH. However, further investigation of the low recovery phenomenon was not carried out and

the point at which neutralization becomes irreversible was not found. Hence, continuation of this area is warranted and of interest.

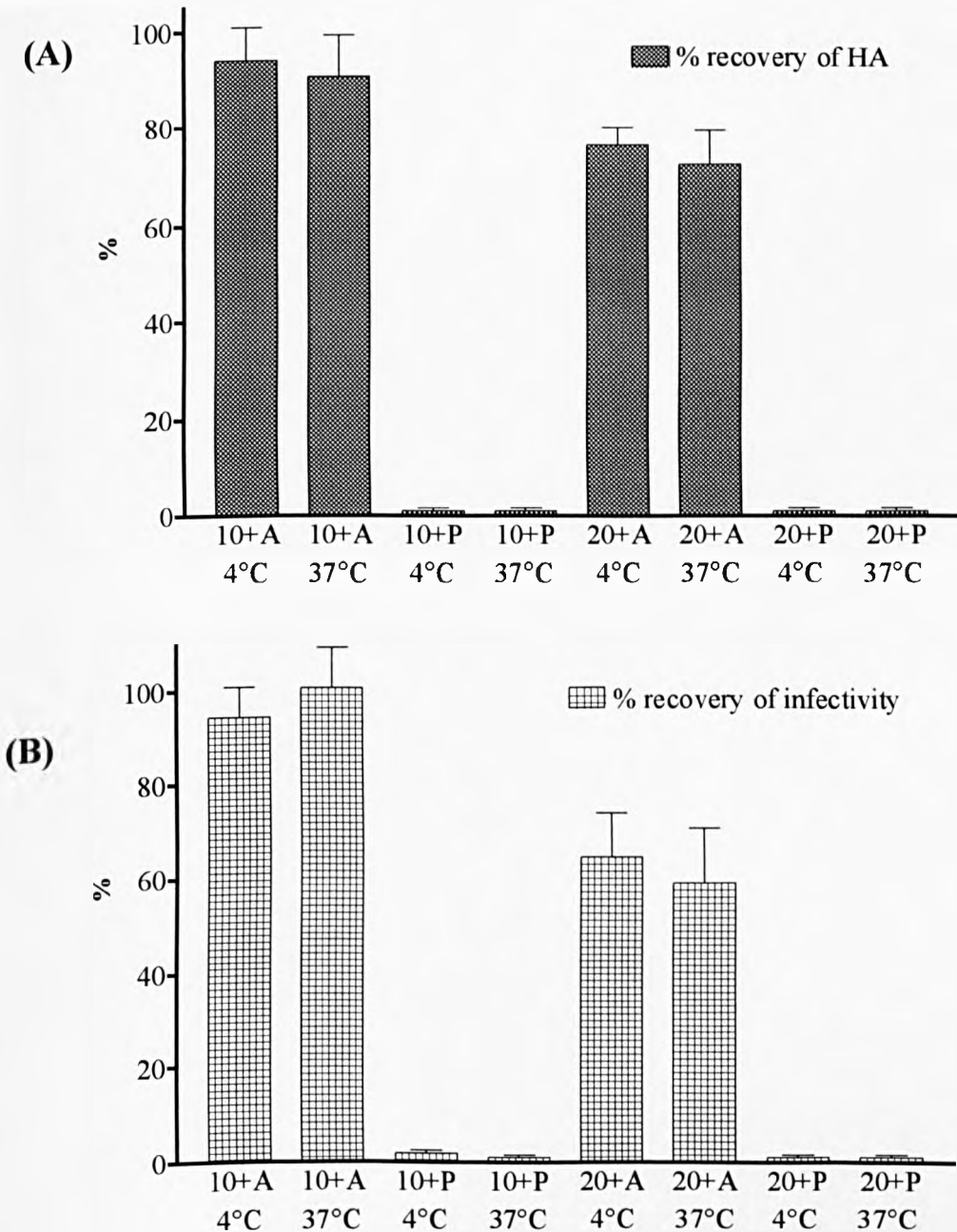
In this section the reversibility of the HI and neutralization, both of virus in solution and virus attached to cells, by the anti-A/PR/8 virus IgGs, H36, H37 and H9 was examined. Neutralization of virus in solution at 4°C and 37°C by the H36, H37 and H9 IgGs was reversible. Investigation of reversibility of neutralization by the three IgGs of virus attached to cells gave results similar to those seen previously with the IgA, in that recovery of HA and infectivity as a result of treatment with bacterial neuraminidase was very low. Examination of the low recovery of virus induced by the IgA indicated that it was due to the bacterial neuraminidase not removing the virus-MAb complexes from the cell surface, possibly due to steric hindrance by the fringe of neutralizing antibody. The low recovery phenomenon only occurred at temperatures >20°C, suggesting that conformational changes of the viral HA upon receptor binding may play a role. Analysis of the reversibility of the HI of attached virus treated at pH 5 and 4°C, showed a good HA recovery, indicating virus was removed from the cell surface.

8.2 Analysis of the reversibility of haemagglutination-inhibition (HI) and neutralization of virus in solution by MAbs.

8.2.1 Investigation of the reversibility of HI and neutralization of virus in solution by the monoclonal IgA (H37-66) at 4°C and 37°C.

This assay compared the reversibility of HI and neutralization of A/PR/8 virus by 10 and 20 µg/ml of IgA MAb at 4 and 37°C. 10 µg/ml of IgA MAb represented the minimum concentration sufficient to cause complete HI and >99% neutralization. Hence removal of antibody by AmOH could be assayed by the recovery of HA and infectivity. HI and neutralization of the A/PR/8 virus by IgA MAb was reversed by incubation with AmOH and passage through a Sephacryl S-1000 column to separate MAb from virus (Figure 8.1). Reversal of HI was not found if virus was not passed

Figure 8.1 Analysis of the reversibility of HI and neutralization of virus free in solution: IgA MAb (H37-66). (A) This shows the percentage recovery of HA compared to a non-neutralized virus control. Data are the sum of the ten fractions collected from the S-1000 column. (B) This shows the percentage recovery of infectivity compared to a non-neutralized virus control. Data are the sum of the infectivity of the three peak HA fractions. Data are the mean of three experiments. The lines represent the standard error of the mean (SEM). **10+A** = virus neutralized with 10 μ g/ml of IgA, followed by treatment with AmOH; **10+P** = virus neutralized with 10 μ g/ml of IgA, followed by treatment with PBS; **20+A** and **20+P** = same as above, but with 20 μ g/ml IgA. **4°C** and **37°C** below labels refer to temperature at which the virus was neutralized.



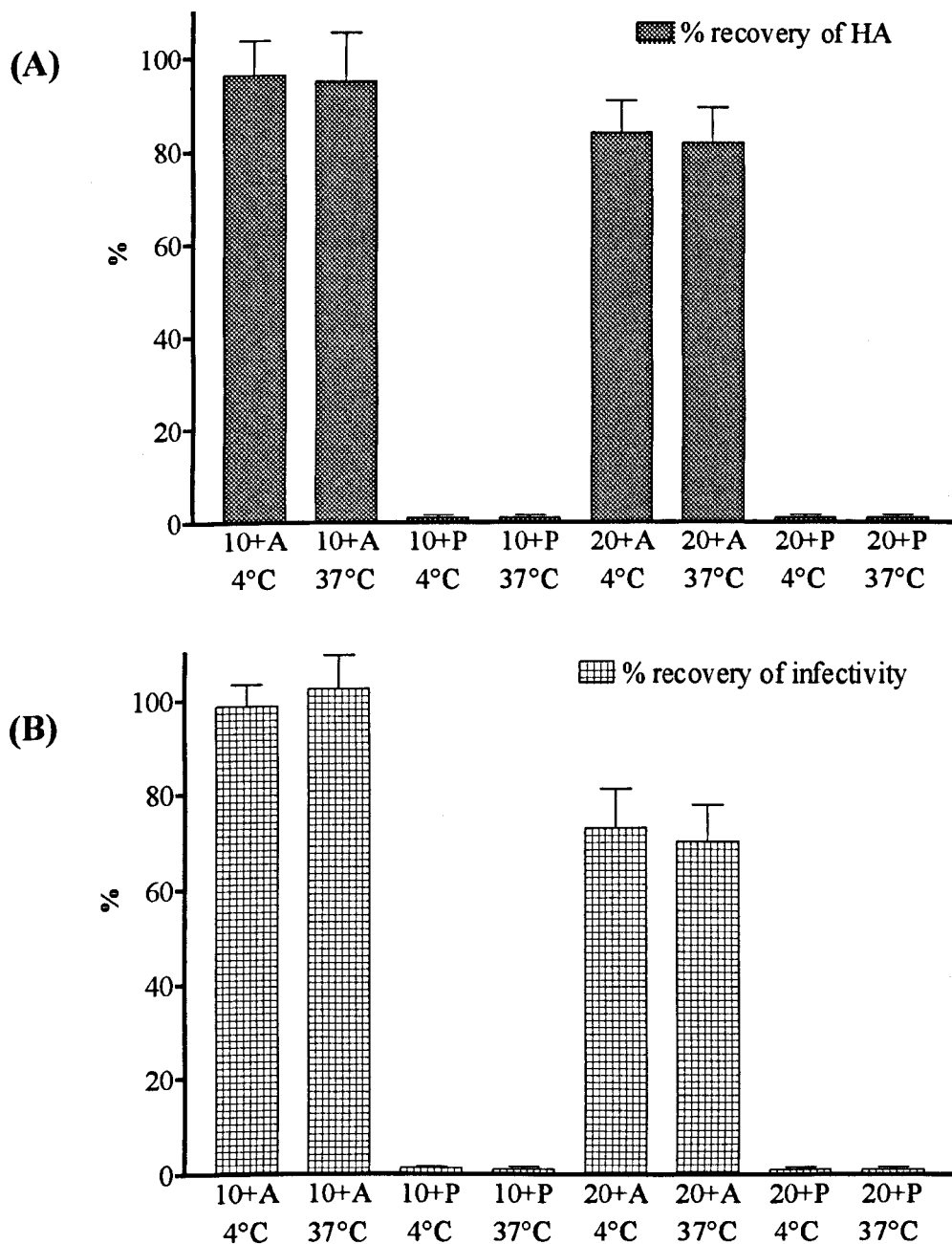
through an S-1000 column, indicating that the IgA rebound to virus upon neutralization of pH. This suggested that AmOH did not permanently denature the paratope or epitope but rather increased the dissociation rate. The total HA was given by the sum of the HA titres of the ten fractions eluted from the S-1000 column (an example of the recovery of HA from the S1000 column is shown in Appendix I, Figure I.9). The total infectivity was given by the sum of the infectivity of the three peak HA fractions. The total recovery of HA and infectivity was calculated as a percentage of the recovery of a non-neutralized virus control.

No reversibility of HI or neutralization could be detected when IgA neutralized virus was incubated in PBS rather than AmOH, showing that IgA did not dissociate upon dilution. The reversibility of HI and neutralization was not temperature-dependent, giving a similar percentage recovery at 4°C and 37°C. However, the percentage recovery of HA was affected by the concentration of IgA (Figure 8.1 (A)). The recovery when virus was neutralized by 20 µg/ml IgA was approximately 15% lower than the recovery of HA obtained with virus neutralized by 10 µg/ml of IgA. This suggested that AmOH did not remove all of the antibody at higher concentrations of IgA. The percentage recovery of infectivity was also IgA concentration-dependent (Figure 8.1(B)). Virus neutralized by 20 µg/ml of IgA gave approximately 35% lower percentage recovery of infectivity than virus neutralized by 10 µg/ml of IgA. This again indicated that a proportion of IgA remained on the virus after treatment with the AmOH and that the remaining IgA gave a higher degree of neutralization than HI.

8.2.2 Investigation of the reversibility of HI and neutralization of virus in solution by the monoclonal H36 IgG at 4°C and 37°C.

Figure 8.2 (A and B) indicates that the HI and neutralization of A/PR/8 virus by 10 µg/ml H36 IgG could be reversed by treatment with AmOH. 10 µg/ml of H36 IgG was the minimum concentration sufficient to cause complete HI and >99% neutralization. The H36 IgG did not reverse when diluted in PBS, rather than AmOH.

Figure 8.2 Analysis of the reversibility of HI and neutralization of virus free in solution: H36 IgG. (A) This shows the percentage recovery of HA compared to a non-neutralized virus control. Data are the sum of the ten fractions collected from the S-1000 column. **(B)** This shows the percentage recovery of infectivity compared to a non-neutralized virus control. Data are the sum of the infectivity of the three peak HA fractions. Data are the mean of three experiments. The lines represent the standard error of the mean (SEM). 10+A = virus neutralized with 10 $\mu\text{g/ml}$ of H36 IgG, followed by treatment with AmOH; 10+P = virus neutralized with 10 $\mu\text{g/ml}$ of H36 IgG, followed by treatment with PBS; 20+A and 20+P = same as above, but with 20 $\mu\text{g/ml}$ H36 IgG. 4°C and 37°C below labels refer to the temperature at which the virus was neutralized.

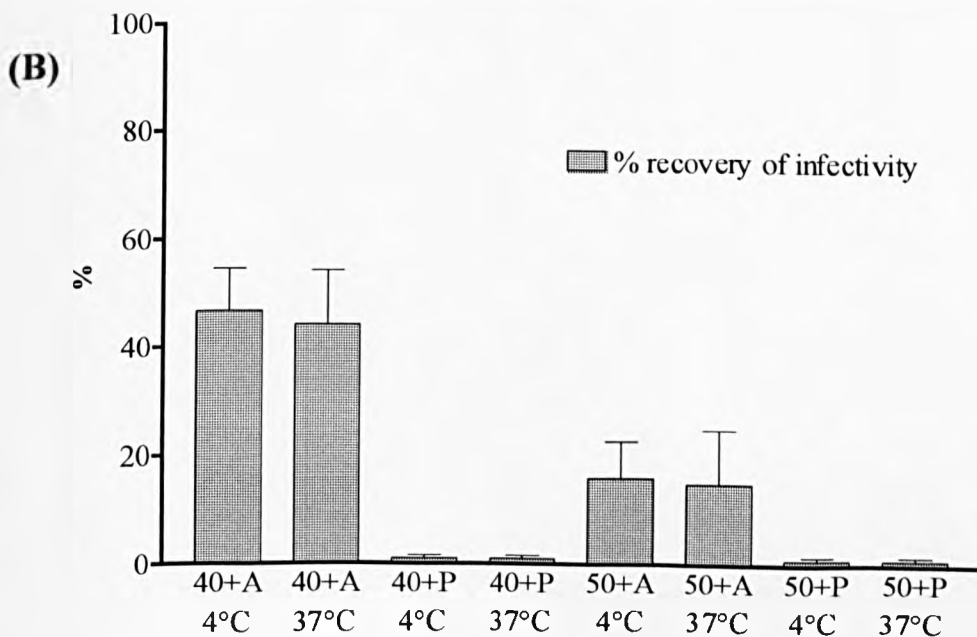
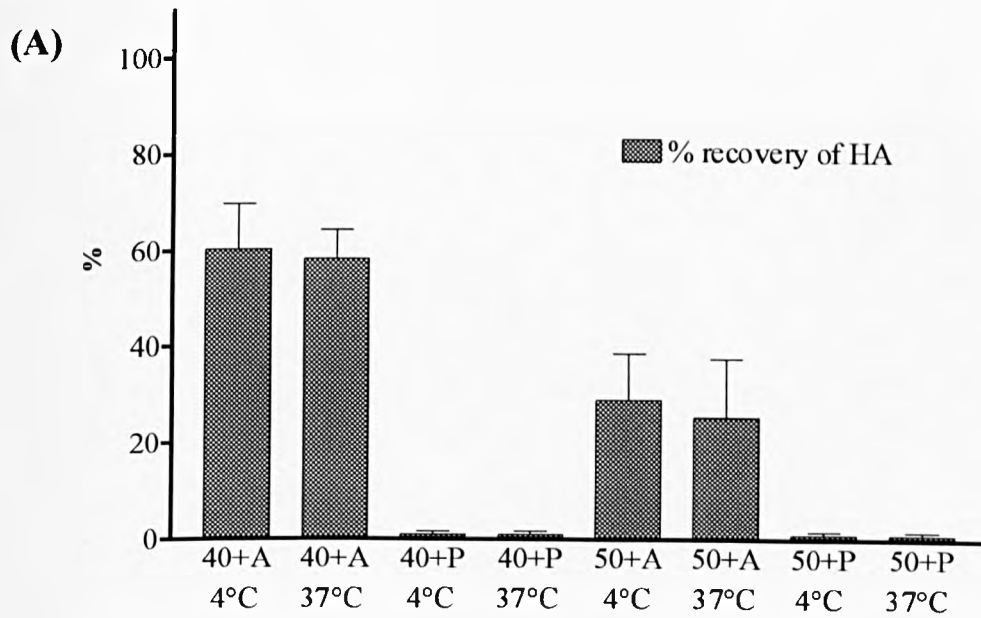


Like the IgA MAb, reversibility of HI and neutralization could be obtained with the H36 IgG at both 4°C and 37°C, indicating that it also was not temperature-dependent. However, the reversibility of both HI and neutralization was concentration-dependent, with virus neutralized by 20 µg/ml of H36 IgG giving lower recoveries of both HA and infectivity than virus neutralized by 10 µg/ml of H36 IgG.

8.2.3 Investigation of the reversibility of HI and neutralization of virus in solution by the monoclonal H37 IgG at 4°C and 37°C.

Figure 8.3 (A and B) shows that HI and neutralization of A/PR/8 virus by 40 µg/ml of H37 IgG could be partially reversed by treatment with AmOH. 40 µg/ml of H37 IgG was the minimum sufficient to cause complete HI and >99% neutralization. The percentage recovery of HA for 40 µg/ml was approximately 60%, whereas the percentage recovery of infectivity was approximately 50%. The recovery, as with previous antibodies, was not temperature-dependent. However, the percentage recovery of both HA and infectivity was approximately 2-fold less with virus neutralization by 50 µg/ml than virus neutralization by 40 µg/ml. This indicated that recovery was dependent on the concentration of the antibody.

Figure 8.3 Analysis of the reversibility of HI and neutralization of virus free in solution: H37 IgG. (A) This shows the percentage recovery of HA compared to a non-neutralized virus control. Data are the sum of the ten fractions collected from the S-1000 column. **(B)** This shows the percentage recovery of infectivity compared to a non-neutralized virus control. Data are the sum of the infectivity of the three peak HA fractions. Data are the mean of three experiments. The lines represent the standard error of the mean (SEM). **40+A** = virus neutralized with 40 $\mu\text{g/ml}$ of H37 IgG, followed by treatment with AmOH; **40+P** = virus neutralized with 40 $\mu\text{g/ml}$ of H37 IgG, followed by treatment with PBS; **50+A** and **50+P** = same as above, but with 50 $\mu\text{g/ml}$ H37 IgG. 4°C and 37°C below labels refer to the temperature at which the virus was neutralized.



8.2.4 Investigation of the reversibility of HI and neutralization of virus in solution by the monoclonal H9 IgG at 4°C and 37°C.

Figure 8.4 (A and B) shows that HI and neutralization of A/PR/8 virus by 50µg/ml of H9 IgG is reversible after treatment with AmOH. Reversibility with the H9 IgG is similar to the antibodies described previously, being temperature-independent, but IgG concentration-dependent.

8.3 Determination of whether antibody bound to virus is completely removed by treatment with AmOH.

8.3.1 Investigation of whether some antibody remains bound to virus after AmOH treatment by reactivity with anti-Fab antiserum.

Previous data indicated that lower recoveries of HI and neutralization were obtained from virus that had been neutralized with high concentrations of MAb. This suggested that AmOH was not removing all of the antibody. Incubation of virus neutralized by either the H36, H37 or H9 IgGs with anti-Fab antiserum causes an increase in the HI titre of each of the antibodies (data not shown). Therefore, to test whether the virus that had been treated with AmOH to remove MAb still had MAb bound, it was incubated with anti-Fab antiserum. Decreases of haemagglutination ability of the AmOH-treated virus after addition of the anti-Fab antiserum would indicate presence of MAb bound to virus after AmOH treatment.

Table 8.1 shows that recovery of HA by virus whose neutralization by the MAbs had been reversed by treatment with AmOH was similar to that described previously. However, addition of anti-Fab antiserum to this AmOH treated virus resulted in a lower recovery of HA. The decrease of HA due to the addition of anti-Fab antiserum was dependent on the concentration of the neutralizing MAb prior to AmOH treatment. For example, addition of anti-Fab antiserum to virus previously neutralized by 10µg/ml of H36 IgG resulted in a 1.8-fold loss of HA, whilst there was a 3.2-fold loss of HA for virus previously neutralized with 20µg/ml H36 IgG. This suggested that at higher concentrations of MAb the AmOH was less efficient at removal of antibody. The fold

Figure 8.4 Analysis of the reversibility of HI and neutralization of virus free in solution: H9 IgG. (A) This shows the percentage recovery of HA compared to a non-neutralized virus control. Data are the sum of the ten fractions collected from the S-1000 column. (B) This shows the percentage recovery of infectivity compared to a non-neutralized virus control. Data are the sum of the infectivity of the three peak HA fractions. Data are the mean of three experiments. The lines represent the standard error of the mean (SEM). 50+A = virus neutralized with 50 $\mu\text{g/ml}$ of H9 IgG, followed by treatment with AmOH; 50+P = virus neutralized with 50 $\mu\text{g/ml}$ of H9 IgG, followed by treatment with PBS; 75+A and 75+P = same as above, but with 75 $\mu\text{g/ml}$ H9 IgG. 4°C and 37°C below refer to temperature at which the virus was neutralized.

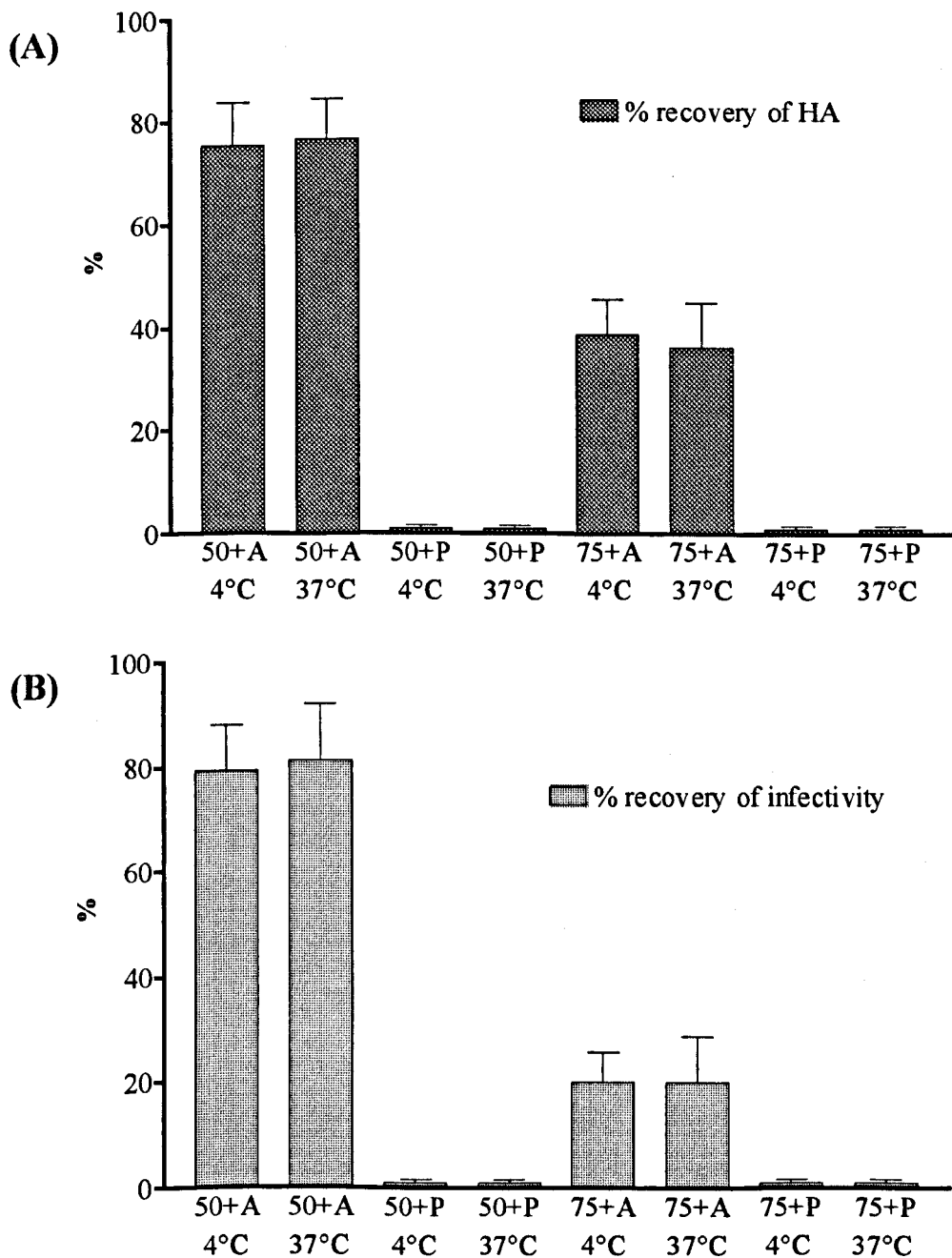


Table 8.1 The affect of the addition of anti-Fab antiserum to virus neutralized by the MAbs at 37°C following treatment by AmOH. Virus neutralized by either of the MAbs was treated with AmOH, recovered from the S1000 column and incubated with a 1 in 500 dilution of the anti-Fab antiserum. The recovery of HA was calculated as a percentage of a non-neutralized control.

<i>MAb</i>		<i>% recovery of HA</i>		<i>Fold decrease in HA after addition of anti-Fab</i>
		<i>no anti-Fab</i>	<i>+ anti-Fab</i>	
IgA	10µg/ml	91	65	1.4
	20µg/ml	76	31	2.5
H36	10µg/ml	98	54	1.8
	20µg/ml	83	26	3.2
H37	40µg/ml	63	18	3.5
	50µg/ml	31	4	7.8
H9	50µg/ml	78	25	3.1
	75µg/ml	44	7	6.3

decrease in HA after addition of anti-Fab was highest with virus neutralized by the H37 MAb. This MAb gave the poorest reversibility of HI, suggesting that the recovery of HA was poor as the AmOH treatment did not efficiently remove the H37 MAb.

8.4 Analysis of the reversibility of HI and neutralization of virus attached to chicken red blood cells (CRBCs).

8.4.1 Investigation of the reversibility at 4°C and 37°C of HI and neutralization of virus pre-attached to CRBCs: IgA (H37-66).

As HI and neutralization of virus in solution by four IgGs could be reversed in a temperature-dependent fashion, it was investigated whether the antibodies act synergistically with the target cell receptor to cause an irreversible neutralization. Virus was attached to CRBCs at 4°C and then neutralized by addition of MAb. Following

neutralization, the virus-MAb complexes were removed from the CRBCs by treatment with a bacterial neuraminidase. This enzyme cleaves the sialic acid, which constitutes the virus receptor, hence allowing removal of virus from the cell surface. The resulting virus-MAb complexes were then treated with AmOH and virus and MAbs were separated through a Sephacryl S-1000 column.

The percentage recovery of HA and infectivity was <10% with virus neutralized by IgA at 37°C, consistent with results described by Schofield (1998) (Figure 8.5 (A) and (B)). Also virus diluted with PBS rather than AmOH, showed no recovery of HA or infectivity. However, the reversibility of HI and neutralization of virus pre-attached to CRBCs was temperature-dependent. In contrast, >90% recovery of HA and infectivity was achieved at 4°C, similar to the recoveries seen with virus in solution. The reversibility of HI and neutralization was also dependent on antibody concentration, with percentage recoveries of HA and infectivity being lower with virus neutralized by 20 µg/ml IgA, than virus neutralized by 10 µg/ml IgA.

8.4.2 Investigation of the reversibility at 4°C and 37°C of HI and neutralization of virus pre-attached to CRBCs: IgGs.

Consistent with earlier findings the monoclonal IgA (H37-66) showed a low recovery of HA and infectivity after neutralization of pre-attached virus at 37°C. Therefore, investigation of whether monoclonal IgGs would also give a similar low recovery was carried out.

Less than 10% of HA and infectivity was recovered from virus pre-attached to CRBCs and neutralized at 37°C by 10 and 20 µg/ml of H36 IgG (Figure 8.6 A and B). However, as seen with the IgA MAb, the percentage recovery of HA and infectivity at 4°C was >85%, indicating that the reversibility was temperature-dependent. The percentage recovery of HA and infectivity was again lower at higher concentrations of H36 IgG indicating that reversibility was antibody concentration-dependent.

Figure 8.5 Analysis of the reversibility of HI and neutralization of virus pre-attached to CRBCs: IgA MAb (H37-66). (A) This shows the percentage recovery of HA compared to a non-neutralized virus control. Data are the sum of the ten fractions collected from the S-1000 column. (B) This shows the percentage recovery of infectivity compared to a non-neutralized virus control. Data are the sum of the infectivity of the three peak HA fractions. Data are the mean of three experiments. The lines represent the standard error of the mean (SEM). **10+A** = pre-attached virus neutralized with 10 $\mu\text{g/ml}$ of IgA, treated with 1 U/ml bacterial neuraminidase and then incubated with AmOH; **10+P** = pre-attached virus neutralized with 10 $\mu\text{g/ml}$ of IgA, treated with 1 U/ml bacterial neuraminidase and then incubated with PBS; **20+A** and **20+P** = same as above, but with 20 $\mu\text{g/ml}$ IgA. **4°C** and **37°C** below labels refer to the temperature that the virus was neutralized.

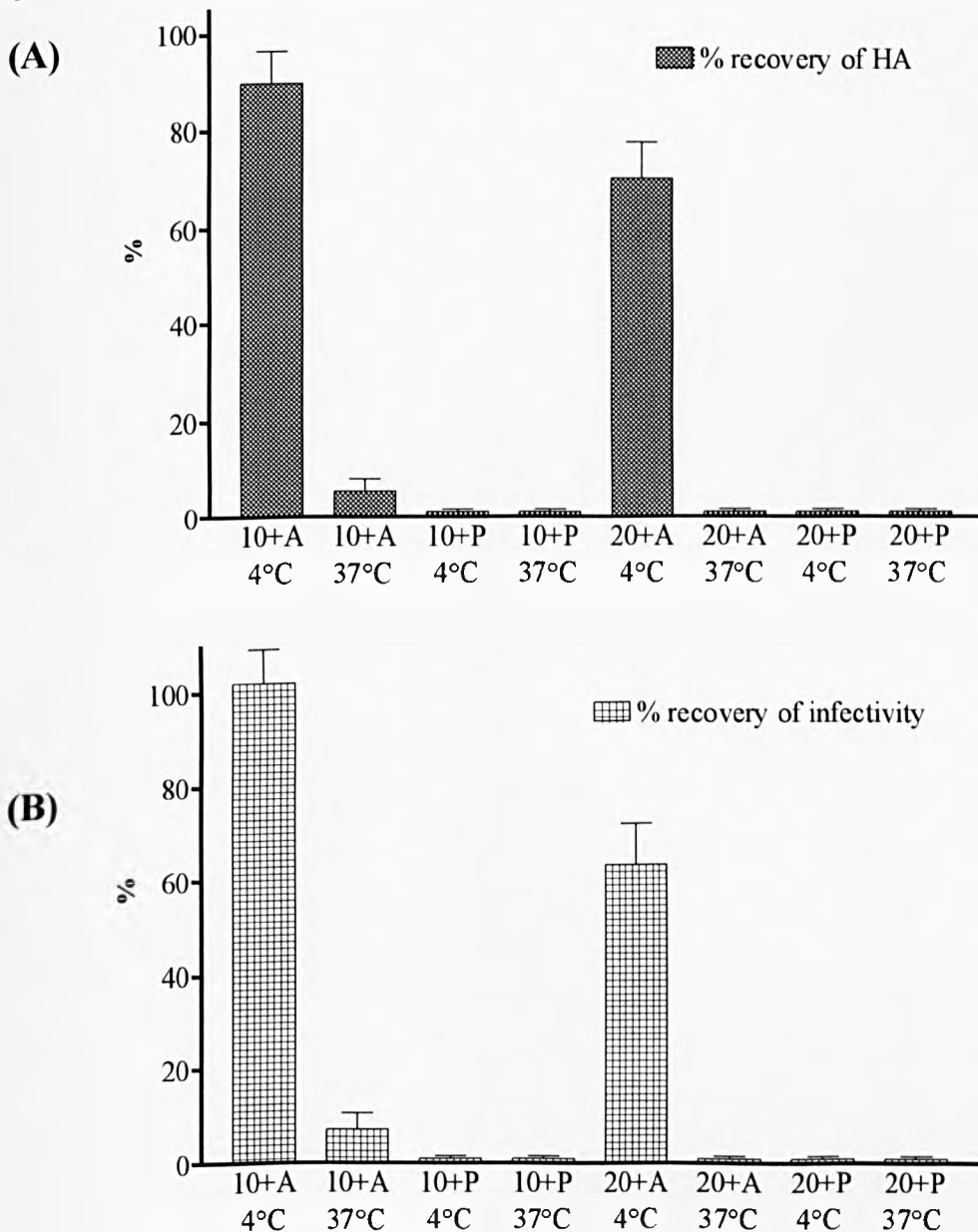
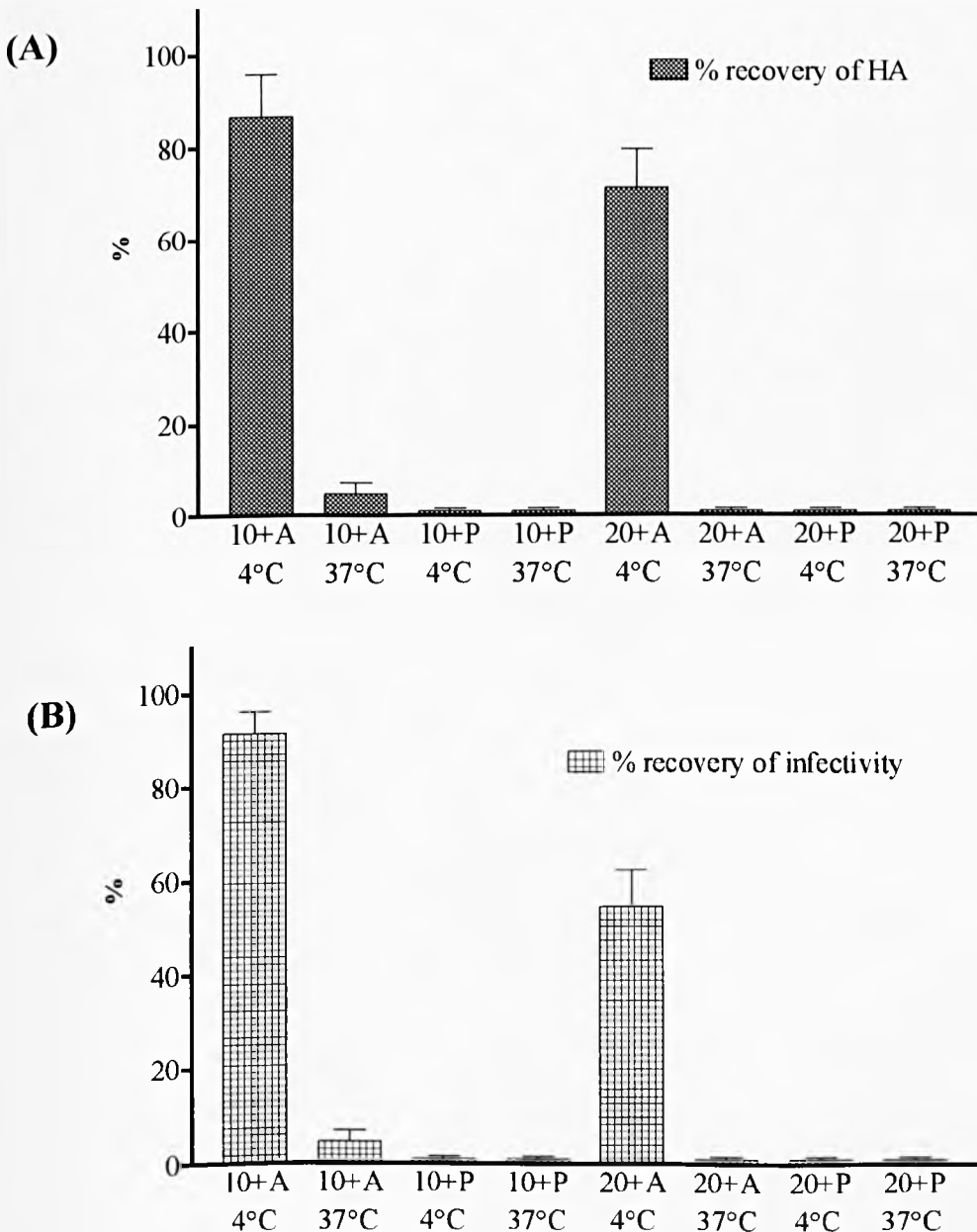


Figure 8.6 Analysis of the reversibility of HI and neutralization of virus pre-attached to CRBCs: H36 IgG. (A) This shows the percentage recovery of HA compared to a non-neutralized virus control. Data are the sum of the ten fractions collected from the S-1000 column. **(B)** This shows the percentage recovery of infectivity compared to a non-neutralized virus control. Data are the sum of the infectivity of the three peak HA fractions. Data are the mean of three experiments. The lines represent the standard error of the mean (SEM). **10+A** = pre-attached virus neutralized with 10 $\mu\text{g/ml}$ of H36 IgG, treated with 1 U/ml bacterial neuraminidase and then incubated with AmOH; **10+P** = pre-attached virus neutralized with 10 $\mu\text{g/ml}$ of H36 IgG, treated with 1 U/ml bacterial neuraminidase and then incubated with PBS; **20+A** and **20+P** = same as above, but with 20 $\mu\text{g/ml}$ H36 IgG. **4°C** and **37°C** below labels refer to the temperature that the virus was neutralized.



The reversibility of HI and neutralization of virus pre-attached to CRBCs by the H37 and H9 IgGs was also investigated (see Appendix I.10). The reversibility of HI and neutralization by both H37 and H9 IgGs was also temperature and antibody concentration-dependent, giving low recovery at 37°C, but relatively high at 4°C.

8.5 Analysis of the poor reversibility at 37°C of HI and neutralization of virus attached to cells: IgA MAb.

8.5.1 Investigation of the effect of temperature on the reversibility of HI and neutralization of virus attached to CRBCs: IgA MAb.

Analysis of the effect of temperature on the recovery of HA and infectivity was investigated by neutralizing virus attached to CRBCs with 10 µg/ml of IgA MAb in different temperature waterbaths. The recovery of HA and infectivity remained >80% up to 15°C, but then decreased with temperature $\geq 20^\circ\text{C}$ (Figure 8.7 A and B).

8.5.2 Analysis of the kinetics of the recovery of HA and infectivity of virus that was attached to CRBCs and then neutralized by 10 µg/ml IgA MAb.

Virus attached to CRBCs at 4°C was neutralized with 10 µg/ml of IgA MAb for 60 minutes at 4°C. The virus-CRBC complexes were pelleted to remove excess IgA, resuspended in warm PBS and incubated at 37°C. 1U/ml bacterial neuraminidase was added to different samples sequentially every 2 minutes to remove virus from CRBCs. The virus was then separated from the IgA by treatment with AmOH and passage through a Sephacryl S-1000 column.

The recovery of HA and infectivity of virus neutralized by IgA and kept at 4°C for 30 minutes remained at approximately 90% (Figure 8.8 A and B). However, the recovery of HA of virus neutralized by IgA at 4°C and then shifted to 37°C decreased very rapidly with time, with decreases of approximately 90% seen after only 4 minutes (Figure 8.8 A). This rapid decrease in recovery with time at 37°C was also mirrored by the recovery of infectivity (Figure 9.8 B).

Figure 8.7 Investigation of the effect of temperature on the reversibility of HI and neutralization of virus attached to CRBCs: 10 $\mu\text{g/ml}$ of IgA MAb. Virus was attached to CRBCs and then neutralized by IgA at different temperatures. The virus-MAb complexes were removed by treatment with bacterial neuraminidase and then incubated with AmOH. **(A)** This shows the percentage recovery of HA compared to a non-neutralized virus control. Data are the sum of the ten fractions collected from the S-1000 column. **(B)** This shows the percentage recovery of infectivity compared to a non-neutralized virus control. Data are the sum of the infectivity of the three peak HA fractions. Data are the mean of two experiments. The lines represent the standard error of the mean (SEM). Temp($^{\circ}\text{C}$) = temperature in which virus was neutralized by the IgA.

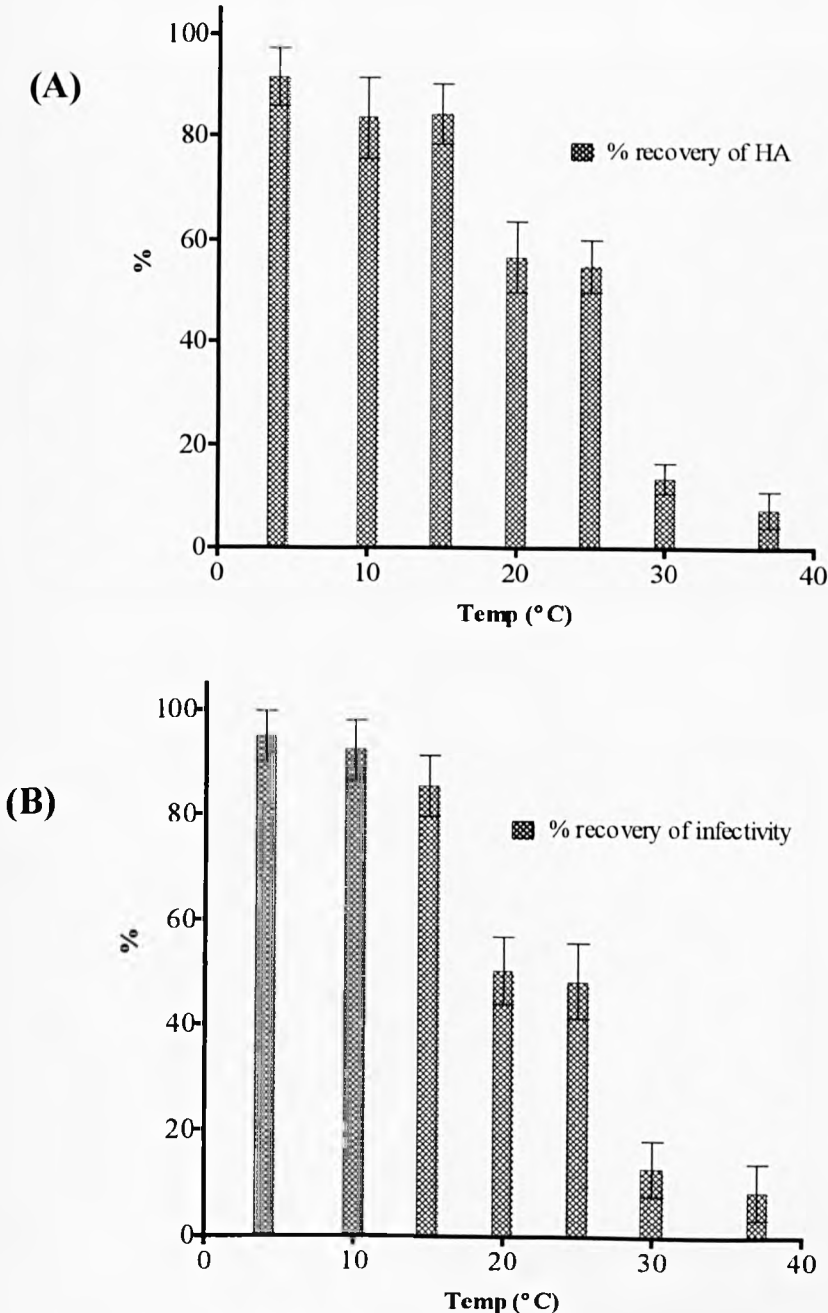
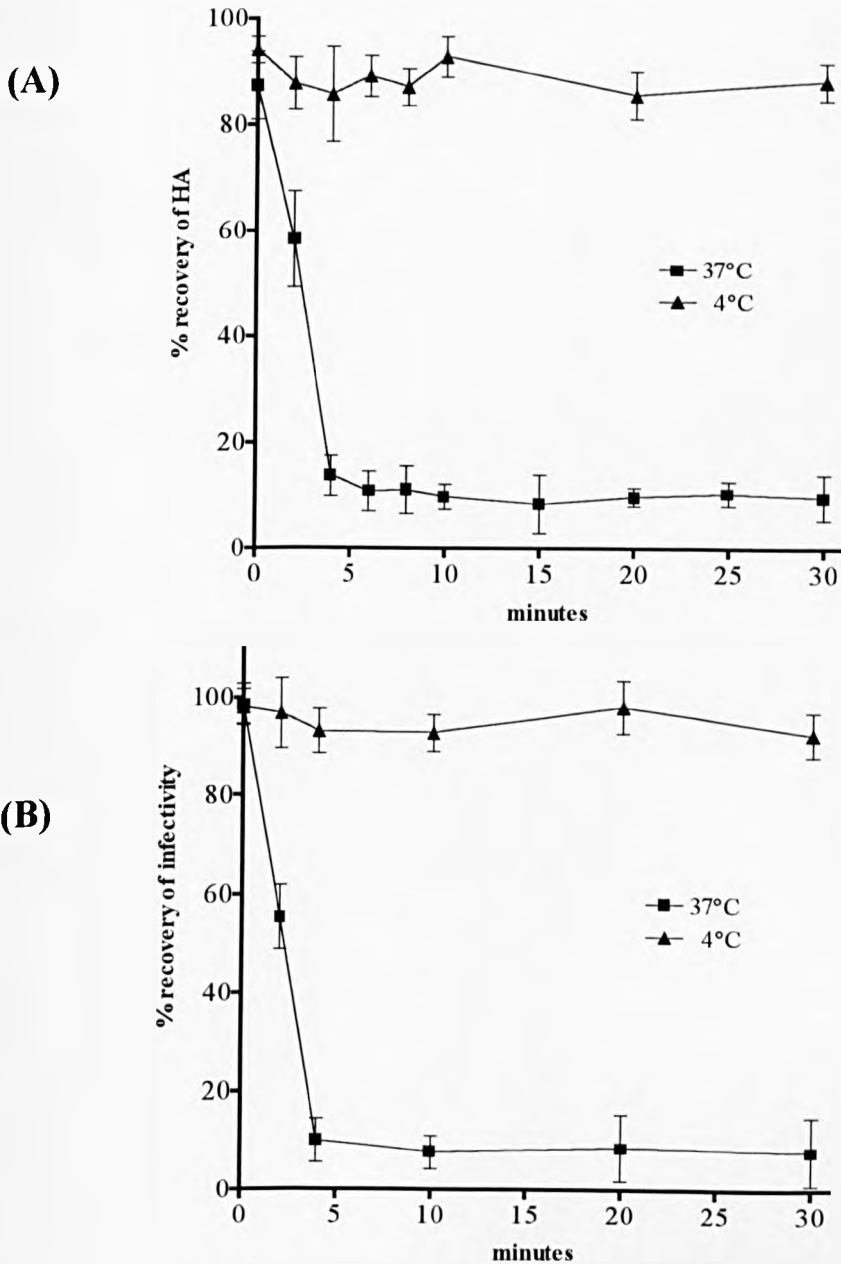


Figure 8.8 Kinetics of the reversibility of HI and neutralization of virus attached to CRBCs: 10 $\mu\text{g/ml}$ IgA. Attached virus that had been neutralized by IgA at 4°C was warmed to 37°C or kept at 4°C and then treated with bacterial neuraminidase at 2 minute intervals to remove the virus-MAb complexes. This was followed by treatment with AmOH. **(A)** This shows the percentage recovery of HA compared to a non-neutralized virus control. Data are the sum of the ten fractions collected from the S-1000 column. **(B)** This shows the percentage recovery of infectivity compared to a non-neutralized virus control. Data are the sum of the infectivity of the three peak HA fractions. Data are the mean of two experiments. The lines represent the standard error of the mean (SEM). Time in minutes indicates the time at which neuraminidase was added to remove virus from the CRBCs, after shifting the temperature from 4°C to 37°C.



8.5.3 Analysis of the reversibility of HI and neutralization of virus attached to cells, other than CRBCs: IgA MAb

8.5.3.1 Investigation of the reversibility of HI and neutralization of virus attached to fixed MDCK cell: 10 µg/ml of IgA MAb.

The aim here was to determine if the low recovery of HA and infectivity seen previously with virus attached to CRBCs by 10 µg/ml IgA could be repeated in other cell types. 5×10^6 MDCK cells were used and fixed with either 2% paraformaldehyde or 1% formaldehyde for 15 minutes to prevent receptor-mediated endocytosis of the attached virus-IgA complexes at 37°C. Virus was not internalised into fixed MDCK cells after a 60 minute incubation at 37°C, as verified by attachment detection ELISA (data not shown).

Recovery of HA and infectivity of virus attached to fixed MDCK cells and neutralized by IgA at 4°C was >75% (Figure 8.9 A and B). However, recovery of HA and infectivity of virus attached to MDCK cells and neutralized by IgA at 37°C was <15%. This indicated that the low recovery phenomenon at 37°C was not restricted to CRBCs.

8.5.3.2 Investigation of the reversibility of HI and neutralization of virus attached to fixed H9 T-cells 10 µg/ml of IgA MAb.

4×10^6 T-cells were fixed as described previously to prevent endocytosis of attached virus-IgA complexes. Attachment of virus to T-cells over a 60 minute period at 37°C was determined by neuraminidase assay (data not shown). Reversibility of HI and neutralization of virus attached to fixed T-cells by IgA at 37°C was also low (Figure 8.10 A and B). The low recovery phenomenon at 37°C was consistent in three different cell types, indicating that it was not cell type specific.

Figure 8.9 The reversibility of HI and neutralization of virus attached to fixed MDCK cells: 10 $\mu\text{g/ml}$ of IgA. Virus was attached to 5×10^6 MDCK cells fixed with either 2% paraformaldehyde or 1% formaldehyde for 15 minutes. Attached virus was neutralized with IgA, treated with bacterial neuraminidase and then the incubated with AmOH. (A) This shows the percentage recovery of HA compared to a non-neutralized virus control. Data are the sum of the ten fractions collected from the S-1000 column. (B) This shows the percentage recovery of infectivity compared to a non-neutralized virus control. Data are the sum of the infectivity of the three peak HA fractions. Data are the mean of three experiments. The lines represent the standard error of the mean (SEM). 10+A = pre-attached virus neutralized with 10 $\mu\text{g/ml}$ of IgA, followed by treatment with AmOH at 4°C; 10+P = pre-attached virus neutralized with 10 $\mu\text{g/ml}$ of IgA, followed by treatment with PBS. 4°C and 37°C below labels refer to the temperature at which the virus was neutralized.

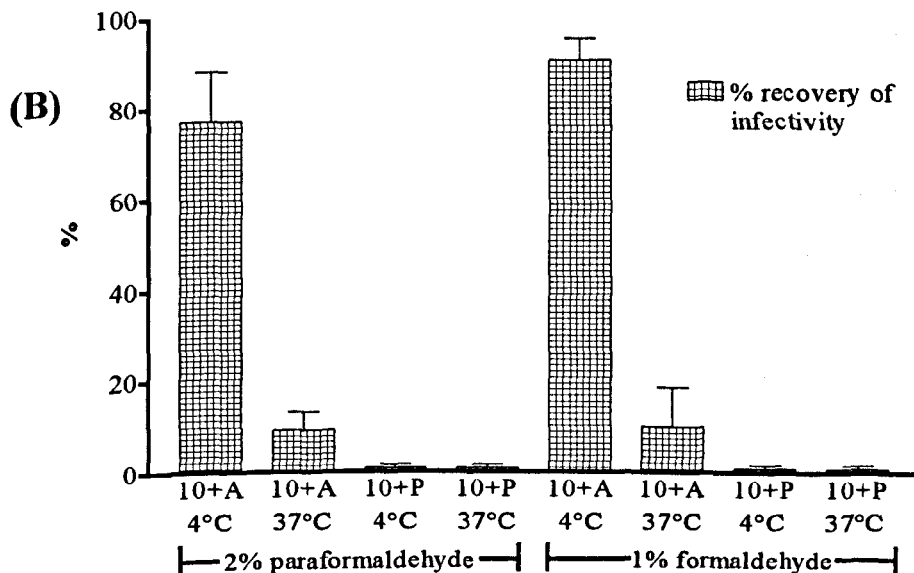
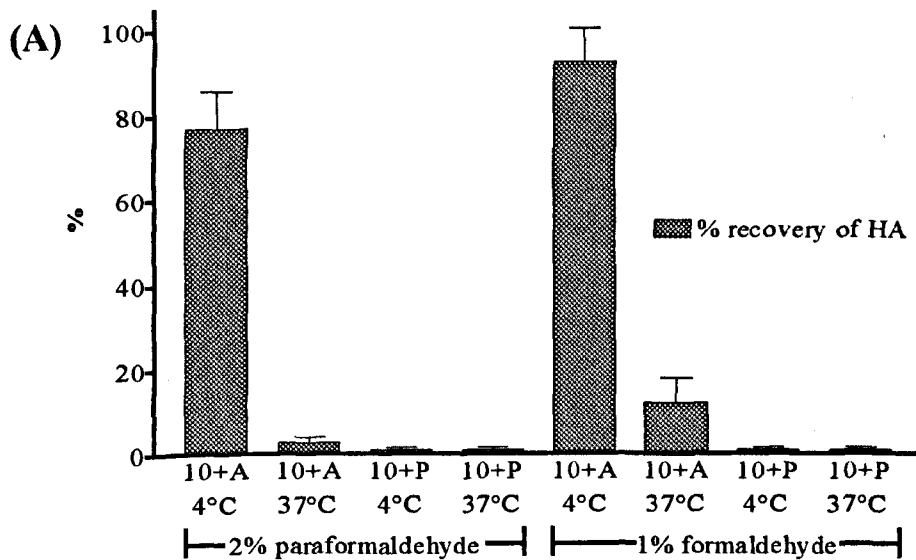
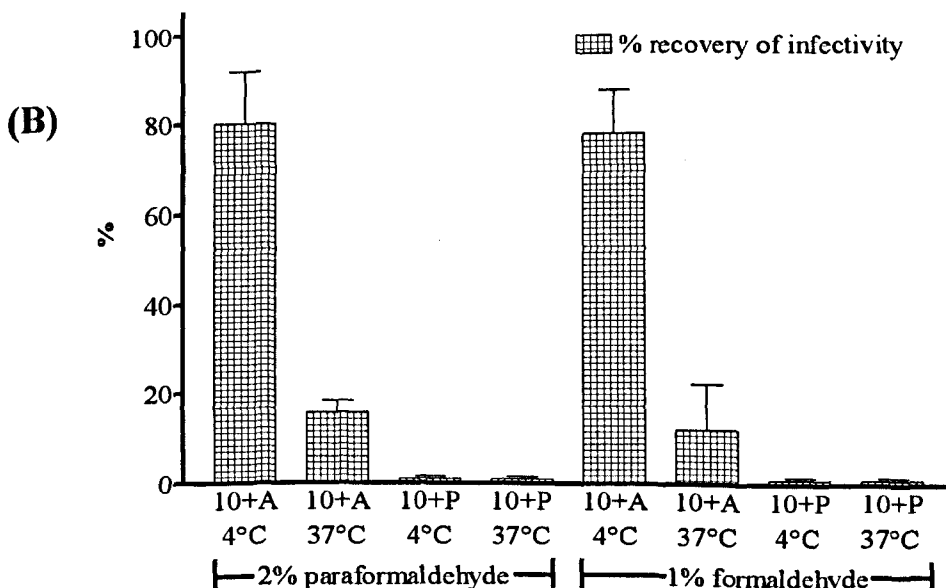
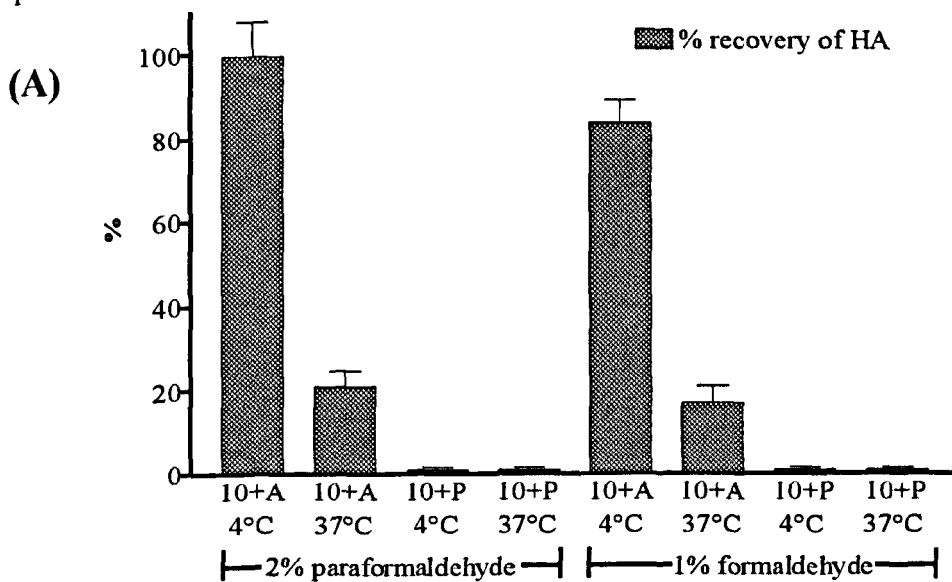


Figure 8.10 The reversibility of HI and neutralization of virus attached to fixed H9 T-cells: 10 $\mu\text{g/ml}$ of IgA. Virus was attached to 5×10^6 MDCK cells fixed with either 2% paraformaldehyde or 1% formaldehyde for 15 minutes. Attached virus was neutralized with IgA, treated with bacterial neuraminidase and then incubated with AmOH. **(A)** This shows the percentage recovery of HA compared to a non-neutralized virus control. Data are the sum of the ten fractions collected from the S-1000 column. **(B)** This shows the percentage recovery of infectivity compared to a non-neutralized virus control. Data are the sum of the infectivity of the three peak HA fractions. Data are the mean of three experiments. The lines represent the standard error of the mean (SEM). 10+A = pre-attached virus neutralized with 10 $\mu\text{g/ml}$ of IgA, followed by treatment with AmOH at 4°C; 10+P = pre-attached virus neutralized with 10 $\mu\text{g/ml}$ of IgA, followed by treatment with PBS. 4°C and 37°C below labels refer to the temperature at which the virus was neutralized.



8.5.3.3 Investigation of the reversibility of HI and neutralization of virus bound to a soluble receptor, fetuin: 10 µg/ml of IgA MAb.

As the poor reversibility of HI and neutralization of virus by IgA at 37°C was not cell type specific, I determined if the same phenomenon could be induced by the binding of virus to a soluble receptor. The sialoglycoprotein, fetuin, was used at 4 mg/ml which was sufficient to give approximately 85% HI of virus, indicating that most of the receptor binding sites on the virus were approaching saturation (data not shown). Virus bound to fetuin was treated as if attached to a cell and treated with bacterial neuraminidase followed by AmOH.

Figure 8.11 (A and B) shows that the recovery of HA and infectivity of virus bound to fetuin and neutralized by 10 or 20 µg/ml of IgA at 4°C or 37°C was >85%. This demonstrates that virus binding to a soluble receptor, fetuin behaves differently from when it binds to receptors on the surface of a cell.

8.5.4 Quantitation of the removal of virus from the CRBC by bacterial neuraminidase after neutralization by MAbs.

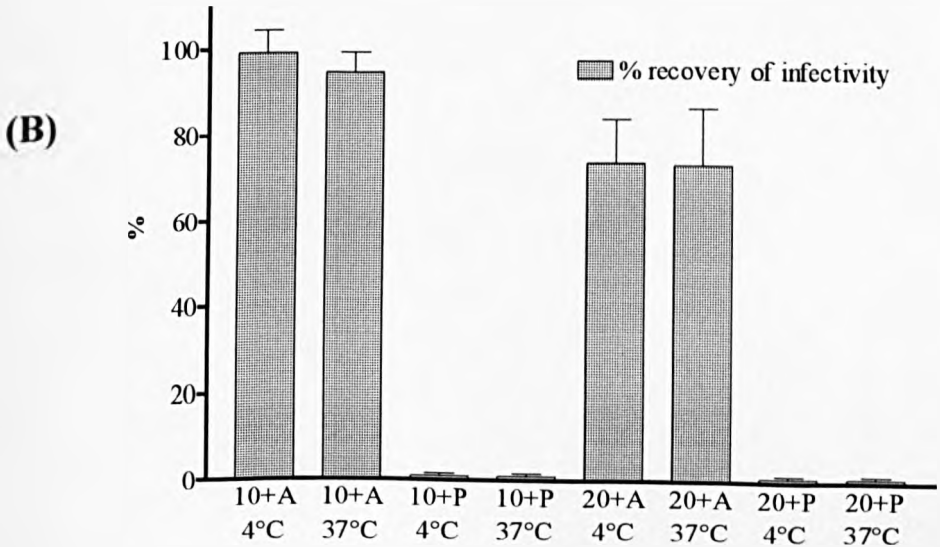
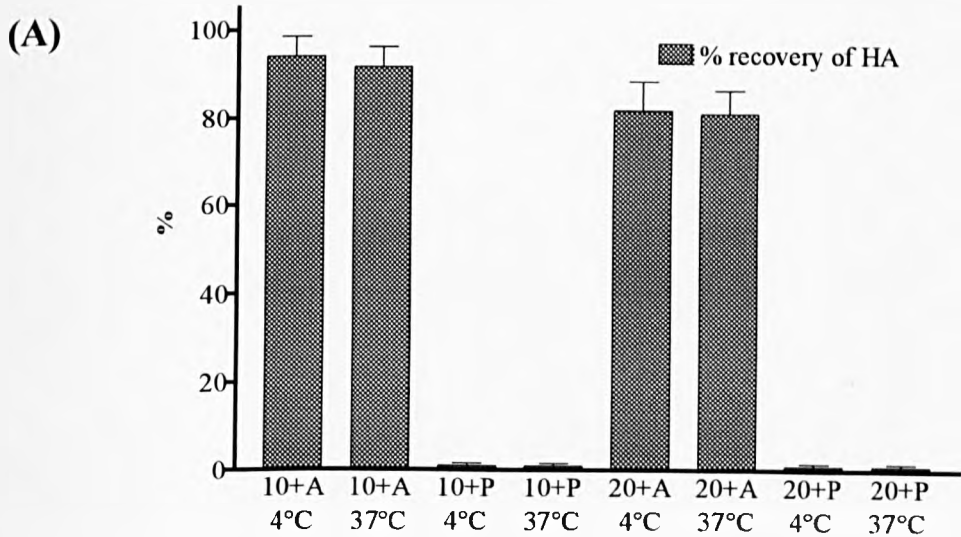
8.5.4.1 Analysis of the effect of temperature on the recovery of virus from the CRBC after neutralization by MAbs.

Two possible explanations for the poor reversibility of HI and neutralization of virus attached to cells by IgA at 37°C were –

- (1) the bacterial neuraminidase was not removing the virus-IgA complexes from the cell surface,
- (2) the virus-IgA complexes were being removed by bacterial neuraminidase, but the IgA had become refractory to removal by AmOH.

To differentiate between these explanations the concentration of virus in the supernatant after neuraminidase treatment was determined using a biotinylated virus stock and a virus-biotin detection ELISA. A/PR/8 virus had biotin attached by sulfo-NHS links as

Figure 8.11 Reversibility of HI and neutralization of virus bound to a soluble receptor, fetuin: the IgA MAb. Virus was incubated with 4mg/ml of fetuin for 60 minutes at 37°C before addition of IgA MAb. Neutralized virus was then treated with bacterial neuraminidase and then the incubated with AmOH. **(A)** This shows the percentage recovery of HA compared to a non-neutralized virus control. Data are the sum of the ten fractions collected from the S-1000 column. **(B)** This shows the percentage recovery of infectivity compared to a non-neutralized virus control. Data are the sum of the infectivity of the three peak HA fractions. Data are the mean of three experiments. The lines represent the standard error of the mean (SEM). **10+A** = virus neutralized with 10 µg/ml of IgA, followed by treatment with AmOH; **10+P** = virus neutralized with 10 µg/ml of IgA, followed by treatment with PBS; **20+A** and **20+P** = same as above, but with 20 µg/ml IgA. **4°C** and **37°C** below labels refer to the temperature at which the virus was neutralized.



this could be used in aqueous conditions, hence reducing problems with loss of infectivity that occur if solvents are used. Using the biotinylated virus stock a quantitative biotin detection ELISA was optimised. Briefly, virus removed by neuraminidase treatment of CRBCs was captured on an ELISA plate by an anti-HA IgG MAb (H16, site Sa) and then assayed for its biotin content using a streptavidin-conjugate. The optical density (OD) obtained for neuraminidase released virus was then compared to a biotinylated virus standard curve of HAU versus OD to determine the quantity of virus present (Figure 8.12). The percentage recovery of biotinylated virus from the CRBC surface was then calculated by comparing the quantity of neutralized virus to a non-neutralized control.

Recovery of virus at 4°C from CRBCs that had been neutralized by either the IgA, H36, H37 or H9 MAbs was >90% (Figure 8.13). Recovery of virus from the cell surface was higher than the recovery of HA described previously for most of the MAbs. For example, virus neutralized by H37 IgG at 4°C gave a recovery of HA of approximately 60%, but approximately 91% of virus was recovered from CRBCs. This suggested that there was efficient removal of H37 neutralized virus from the cell surface, but the AmOH did not efficiently remove the antibody. Recovery of virus from CRBCs after neutralization by either of the four MAbs at 37°C was similar (10%) to the recovery of HA. This indicated that the virus was removed from the surface of the CRBC after neutralization at 4°C, but not after neutralization at 37°C.

8.5.4.2 Analysis of the effect of MAb concentration on the recovery of neutralized virus from the CRBC.

Recovery of virus from CRBCs after neutralization by IgA was concentration-dependent (Figure 8.14). The higher the concentration of IgA, the lower the recovery of virus from the CRBC. For example, recovery of virus neutralized by 4 µg/ml of IgA from the CRBCs was >80%, but recovery of virus neutralized by 20 µg/ml of IgA was <10%.

Recovery of virus from CRBCs after neutralization by the IgGs was also antibody concentration-dependent (data not shown).

Figure 8.12 Standard curve of the optical density (OD) at 405nm against HAU of biotinylated virus. The HA titre of the biotinylated virus stock was first determined and then fixed concentrations in 100 μ l volumes were used on the ELISA plate. (R=0.982)

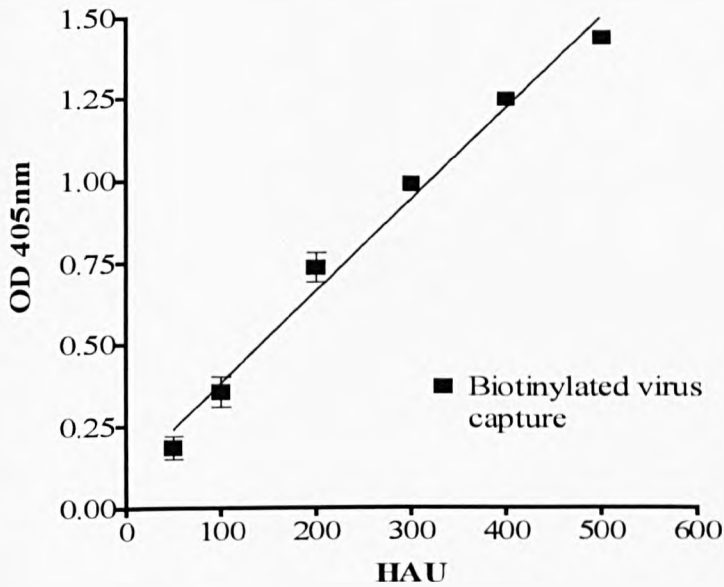


Figure 8.13 The effect of temperature on the recovery of neutralized virus bound to CRBCs. The MAbs were used in the following concentrations – IgA at 10 μ g/ml, H36 at 10 μ g/ml, H37 at 40 μ g/ml and H9 at 50 μ g/ml. Virus attached to CRBCs was neutralized at either 4°C or 37°C and then treated with 1 U/ml bacterial neuraminidase. The released virus samples, after treatment of CRBCs, were diluted in serial 2-fold steps across the ELISA plate to order to achieve an OD that was in the range of the standard curve. The recovery was determined as a percentage of a non-neutralized virus control.

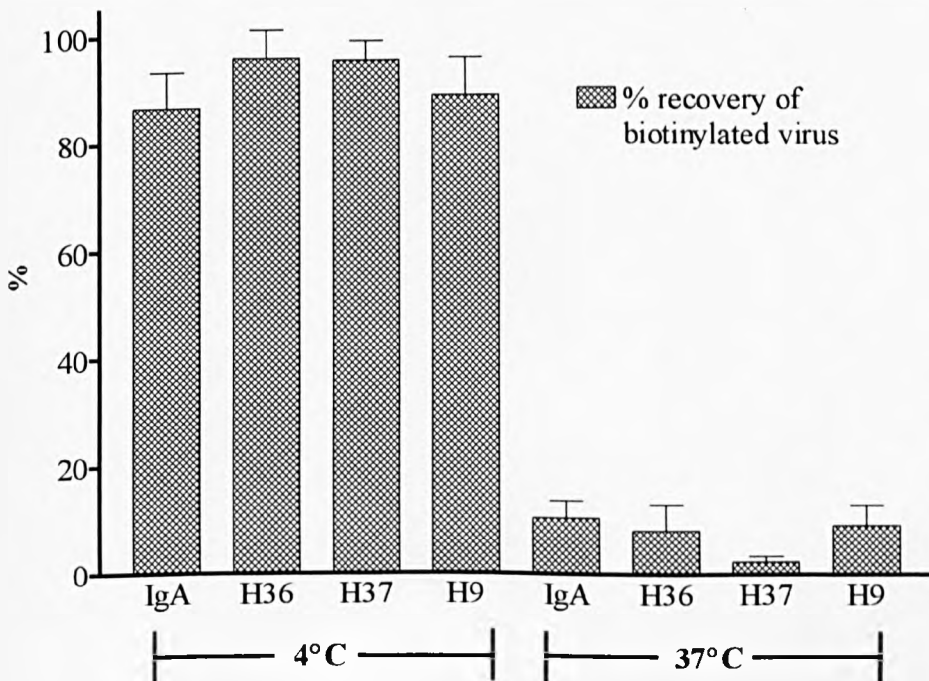
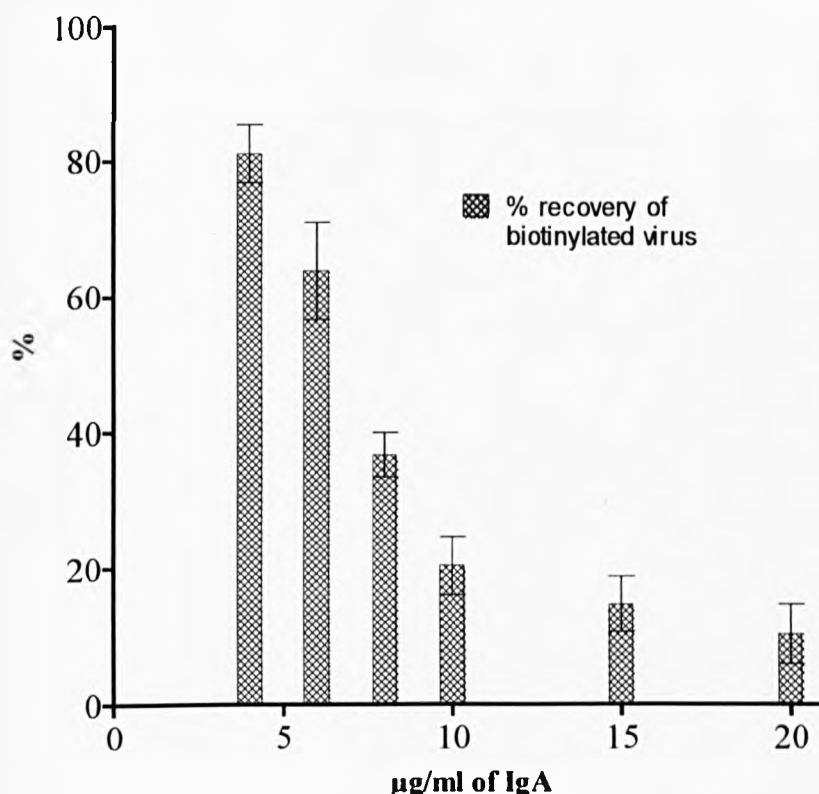


Figure 8.14 The effect of concentration of neutralizing MAb on the recovery of virus from the surface of CRBCs. Virus attached to CRBCs was neutralized at 37°C, followed by bacterial neuraminidase at an activity of 1 U/ml. The released virus samples were diluted in serial 2-fold steps across the ELISA plate to order to achieve an OD that was in the range of the standard curve. The recovery was determined as a percentage of a non-neutralized virus control.



8.5.5 Investigation of whether IgA MAb could sterically inhibit the viral neuraminidase activity.

A possible explanation for the reduced ability of bacterial neuraminidase to remove virus from the CRBC surface at higher MAb concentrations, was that the antibody fringe could sterically hinder access of the enzyme to the virus cell receptor contact sites. To assess this possibility an assay of viral neuraminidase activity was carried out with the CRBC-virus-IgA complexes to determine if the fringe of antibody could restrict the access of fetuin (neuraminidase substrate) to the viral neuraminidase glycoprotein. 10 mg of fetuin was added to the CRBC-virus-IgA complexes for 120 minutes, the cells were then pelleted and the supernatant was used in a standard

neuraminidase assay to determine the extent of cleavage of the terminal N-acetyl neuraminic acid residues from the sugar chains on the fetuin substrate.

Table 8.2 shows that the activity of the viral neuraminidase was reduced at higher IgA concentration. As the IgA is specific for the HA protein, it is unlikely that this had a direct inhibition of viral neuraminidase activity. Hence, this suggests that the higher concentrations of IgA can sterically hinder access of the fetuin substrate to the enzyme active sites on the neuraminidase glycoprotein. This provides an example of antibody steric hindrance to the virus surface and supports the hypothesis that the fringe of IgA molecules bound to virus inhibit removal of the virus from the cell surface by steric hindrance of the bacterial neuraminidase enzyme.

Table 8.2 Inhibition of viral neuraminidase activity by IgA MAbs. Data are the mean of two experiments. 4000 HAU A/PR/8 virus was neutralized IgA at 37°C, followed by 10mg/ml of fetuin.

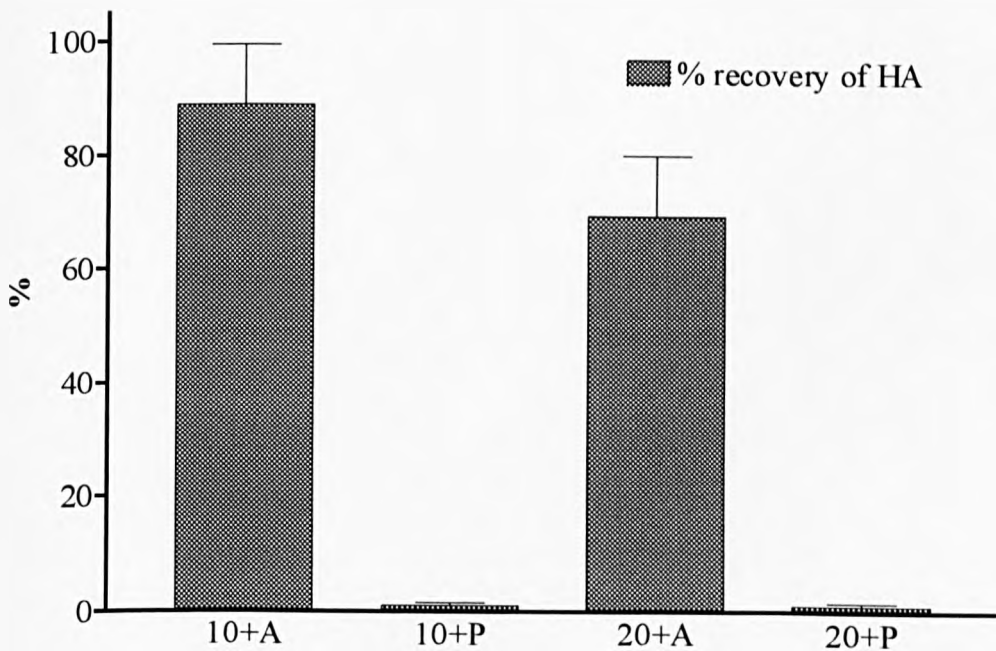
<i>IgA</i> ($\mu\text{g/ml}$)	<i>OD (549nm)</i>	<i>% inhibition of</i> <i>neuraminidase</i> <i>activity</i>
0	1.76 (+/- 0.37)	-
5	1.49 (+/- 0.28)	15.3
10	0.83 (+/- 0.32)	52.9
20	0.51 (+/- 0.43)	71.1

8.6 Analysis of the reversibility of HI and neutralization of virus attached to the CRBC treated at pH 5, 4°C: IgA MAb.

As the neutralization of virus attached to CRBCs by MAbs at 4°C could be reversed, the point of a permanent (irreversible) loss of infectivity had not been found. Therefore, investigation of virus neutralized and incubated at low pH was carried out to determine if mimicking events in the endosome would trigger a permanent loss of infectivity. Treatment of virus with low pH at 4°C does not cause inactivation, hence standard assays for viral infectivity could be used (data not shown). Virus was attached to CRBCs and then neutralized by IgA at 4°C. The pH was then lowered to pH 5, at 4°C for 30 minutes and then virus was removed from the cell surface with bacterial neuraminidase enzyme.

HI of virus that was attached to CRBCs, neutralized with IgA and treated at pH 5, 4°C could be reversed (Figure 8.15). However, unfortunately only 10% of infectivity of non-neutralized virus treated at pH 5, 4°C and with AmOH could be recovered (data not shown). This loss of infectivity was due to exposure to AmOH, as infectivity of virus prior to AmOH treatment was normal. This suggested that conformational changes of the virus HA that occur at pH 5, 4°C (see chapter 7) destabilise the HA so that it was less tolerant to the high pH (11.5) of AmOH. The same amount (10%) of infectivity was also recovered from neutralized virus, suggesting that the conditions used, virus attached to cells, neutralized, treated with pH5, 4°C, were not sufficient to cause a permanent loss of infectivity. However, this remains a tentative conclusion as the majority of the infectivity was lost and the remaining 10% may not be representative.

Figure 8.15 The reversibility of HI of virus attached to CRBCs treated at pH 5, 4°C: IgA MAbs. Virus attached to CRBCs were neutralized and treated with citrate buffer, pH 5 for 30 minutes at 4°C. Virus-IgA complexes were then removed from the cell by 1U/ml bacterial neuraminidase. The graph shows the percentage recovery of HA compared to a non-neutralized virus control. Data are the sum of the ten fractions collected from the S-1000 column. Data are the mean of three experiments. The standard error of the mean (SEM) is shown. **10+A** = pre-attached virus neutralized with 10 µg/ml of IgA, incubated at pH 5, 4°C, followed by treatment with AmOH at 4°C; **10+P** = pre-attached virus neutralized with 10 µg/ml of IgA, incubated at pH 5, 4°C, followed by treatment with PBS; **20+A** and **20+P** = same as above, but with 20 µg/ml IgA.



8.7 Discussion :

8.7.1 *Reversibility of HI and neutralization of virus in solution by MAbs.*

HI and neutralization of virus in solution by IgA MAb (H37-66) was reversible, in agreement with the results obtained previously by Schofield (1996). Reversibility of HI and neutralization was also seen with three high affinity monoclonal IgGs, H36, H37 and H9. The reversibility was not temperature-dependent, giving similar recoveries of HA and infectivity at both 4°C and 37°C. In agreement with the study by Schofield (1996) of reversibility of neutralization of A/FPV/R virus, results in this thesis indicate that neutralization of A/PR/8 virus in solution was also not sufficient to trigger a permanent (irreversible) loss of infectivity.

The reversibility of HI and neutralization of virus in solution by all the MAbs was dependent on the concentration of the antibody used, with higher concentrations giving lower recoveries of both HA and infectivity. Schofield (1996) indicated that dissociation of virus-MAb complexes by AmOH correlated and was dependent on affinity. However, in this thesis the dissociation (reversibility) of the antibodies does not correspond with affinity determined by SPR (see chapter 6). The dissociation of MAbs by AmOH was ranked IgA, H36>H9>H37, whereas affinity ranking order was H36>H37>H9 (IgA not known). The finding that recovery of HA was antibody concentration-dependent indicates that reversibility was not solely dependent on affinity. The concentration of the MAbs used was standardised as the minimum concentration that would give complete HI, as suggested by Schofield (1996). As a result, the concentration of MAb used depended on their ability to HI. The HI ranking order of the MAbs was IgA>H36>H37>H9. Therefore, the H9 and H37 MAbs were used at the highest concentrations in the reversibility experiments. However, as the dissociation by AmOH ranking order does not completely mirror the HI ranking order, other factors are involved, and it seems that the reversibility of HI and neutralization is dependent on both the concentration of the MAb and its affinity. For example, although the AmOH reversibility with 40 µg/ml of H37 MAb was 60% and with 50 µg/ml of H9 MAb was 75%, the affinity of the H37 MAb was higher than H9 MAb. It is interesting that Schofield (1996) used two IgG MAbs to A/FPV/R virus, HC2 and HC58 that had the lowest HI activity and thus had to be used at the highest concentration. These were not dissociated by AmOH, but he did not address the matter of antibody concentration.

However, it should be noted that the H36, H37 and H9 MAbs used in this thesis have similar high affinities, so concentration may be of greater importance than if the MAbs had greater differences between their affinities.

The antibody concentration-dependence of the reversibility of all the MAbs indicated that AmOH did not permanently denature the paratope or epitope, but rather increased the dissociation rate. This suggested that AmOH treatment did not remove all of the bound antibody. This was verified experimentally by the addition of anti-Fab antiserum which reduced the recovery of HA. This effect was greatest with virus that had been neutralized with higher concentrations of MAb prior to AmOH treatment. Interestingly, with higher MAb concentrations recovery of infectivity was generally lower than recovery of HA, indicating that virus was neutralized by lower concentrations of MAb than required for HI.

8.7.2 Reversibility of HI and neutralization of virus attached to CRBCs by MAbs

AmOH treatment almost completely reversed HI and neutralization of virus attached to CRBCs when the experiment was done at 4°C. However, at 37°C reversibility of HI and neutralization with three monoclonal IgGs, H36 (site Sb), H37 (site Ca2) and H9 (site Cb) and a monoclonal IgA (site Sb), at 37°C was <10% indicating that reversibility was not immunoglobulin-type or antigenic site specific. Thus reversibility of HI and neutralization of virus attached to CRBCs was temperature-dependent.

8.7.2.1 Analysis of the low reversibility of HI and neutralization of attached virus: at 37°C

As the low reversibility of HI and neutralization of attached virus at 37°C occurred with all the MAbs, investigation of this phenomenon with the IgA MAb was considered to be representative. The temperature-dependence of the low recovery of HA and infectivity (low recovery phenomenon) was analysed and found to occur between 15-20°C, with further losses of recovery seen over 30°C. Interestingly, this is the same temperature threshold as the incorporation of fusion peptide into a membrane and of the fusion/haemolysis activity of intact A/PR/8 viruses (Brunner *et al.*, 1991). However,

this is unlikely to be the same phenomena as (i) no haemolysis of the CRBCs was seen, and (ii) the low recovery phenomenon was antibody-dependent, as the majority of non-neutralized virus could be recovered from the cell at all the temperatures tested.

The low recovery phenomenon was also found to be similar when fixed MDCK cells or H9 T-cells were used. Fixed cells were employed to prevent receptor-mediated endocytosis of the virus-MAb complexes. This was verified in two ways; (1) using the attachment detection ELISA to monitor attached virus on the cell surface over a 60 minute period at 37°C, which indicated that virus was not internalised and (2) that approximately 70% of input non-neutralization virus was recovered after bacterial neuraminidase treatment. Therefore, this indicated that uptake of virus into the cell was not responsible for the low recovery seen with the virus-MAb complexes at 37°C. The low recovery of virus from fixed cells also suggested that changes in virus rather than cell proteins were involved. It should be noted that the formaldehyde fixative acts by crosslinking, forming methylene bridges at a distance of 2Å and hence for proteins to be fixed they must be or parts of them must be within this distance (Dimmock *et al.*, 1989). However, the methylene bridges are formed with many different groups within proteins, therefore increasing the likelihood that proteins would be fixed.

Experiments replacing cells with a soluble receptor analogue, fetuin, found that the low recovery phenomenon could not be induced after neutralization of virus by IgA at 37°C. This indicated that the low recovery of HA and infectivity was not sialic acid receptor specific, but required the presence of the whole cell. However, it could also be due to a lower stability of interaction with the fetuin compared to a cell.

Use of biotinylated virus showed that the virus-MAb complexes attached to CRBCs had become resistant to removal by bacterial neuraminidase. This neuraminidase-resistance was temperature-dependent and took place at 37°C but not at 4°C. This was consistent with the results for the recovery of HA and infectivity at 4°C. The similarities of the temperature profiles for the low recovery phenomenon and for conformational changes which result in the release of the fusion peptide and fusion/haemolysis of the virus at low pH suggests that the low recovery phenomenon may also be due to conformational changes of the viral HA. The bacterial neuraminidase resistance was also antibody concentration-dependent, with a lower recovery when higher concentrations of MAbs were used. This suggested that the higher concentration of MAbs may sterically hinder the access of the bacterial

neuraminidase to the virus-cell contact sites. Desialylation of fetuin, a neuraminidase substrate by the virus neuraminidase glycoproteins was also inhibited by the fringe of HA-specific MABs, lending support to the idea that steric hindrance of the bacterial neuraminidase might be taking place.

In summary the low recovery phenomenon was:-

- (1) induced by all the MABs after neutralization of attached virus at 37°C, indicating it not to be immunoglobulin-type or antigenic site specific.
- (2) concentration-dependent, giving lower recoveries at higher concentrations.
- (3) not cell-type specific, being consistent with CRBCs, fixed MDCK cells and fixed H9 T-cells. This suggested that the low recovery of virus was not dependent on changes in cellular proteins.
- (4) not seen when the virus was bound to the soluble receptor, fetuin.
- (5) temperature-dependent, indicating that conformational changes may be involved.
- (6) due to inhibition of the removal of virus-MAB complexes from the cell surface by bacterial neuraminidase.

Why does neutralization of attached virus by MABs at 37°C result in a low recovery of virus from the cell surface?

A hypothesis to explain the low recovery of HA and infectivity of attached virus neutralization by MABs at 37°C is described below and attempts to integrate all of the data described previously -

When attached to cells at 37°C the viral HA undergoes conformational or orientational changes, with respect to the cell receptors, with the result that the virus is drawn closer to the cell surface. Binding of MAB to the virus in high concentrations forms a fringe around the virus preventing access to HA-receptor contact site. The conformational change of the HA, which draws the virus closer to the surface, begins to occur at $\geq 20^{\circ}\text{C}$. At 4°C, similar quantities of MAB bind but do not inhibit virus release by bacterial neuraminidase as the virus is attached at a distance from cell surface. It is possible that soluble receptors also induce this change, but without a cell membrane the low recovery phenomenon due to steric hindrance would not be observed. However, it is also possible that the change in the HA-receptor complex may be caused by the MAB binding, but this is unlikely as MABs to 3 different antigenic sites on the HA caused the

same effect. The main problem with this hypothesis is that no evidence has yet been described to confirm the existence of a conformational change of the HA upon receptor binding at 37°C and neutral pH. In fact a number of studies have been published that were antagonistic to this hypothesis. Firstly, the X-ray crystal structure of BHA complexed with its sialic acid receptor indicated no major conformational changes, but it is possible that BHA is not truly representative of the behaviour of the complete HA. In addition the structural analysis was carried out at 4°C, hence a high temperature-dependent change would not be seen (Weis *et al.*, 1988). Also a study of the proteinase-K stability of HA and HA attached to N-acetyl-neuraminyl lactose receptor analogue indicated that there were very little differences (Stegmann *et al.*, 1995). Again this study analysed changes of the HA upon receptor binding at 4°C and hence would not observe high temperature-dependent changes. However, there are a number of studies in support of a conformational or orientational change upon receptor binding. For example, a study of A/PR/8 virus liposome binding at low pH and 0°C indicated that only a subpopulation of the HA underwent a conformational change and exposed their fusion peptide (Tsurudome *et al.*, 1992). The authors speculated that the change in this subpopulation of HAs was triggered by interactions with ganglioside receptors on the liposomes. Recently, a study analysing virosome fusion to liposomes containing surrogate anti-HA Fab receptors, indicated that fusion is carried out by receptor bound HAs (Millar *et al.*, 1999). These authors suggested that receptors cause the orientational changes that prime (or target) the HA for delivery of fusion peptide. This model is speculative and without further experimentation alternative explanations are possible. For example, it is possible that the virus-MAb complexes could be internalised into the CRBCs by pinocytosis. A study demonstrating the pinocytosis of influenza virus by CRBCs using E.M indicated that only about 9% of attached virus was internalised and pinocytotic vesicles are only detected after 5 minutes (Bossart *et al.*, 1973). This would seem to be an unlikely explanation, as recoveries of virus are expressed as a percentage of the recovery of a non-neutralization virus control. As a result, the virus-MAb complexes would have to be pinocytosed preferentially and at a much faster rate than the virus control, as kinetics of low recovery of virus indicated that 75% could not be recovered after only 2 minutes. Perhaps a more plausible explanation could be that at 37°C 'blebbing' of the CRBC membrane occurs which surrounds the virus particles. This effect, together with the fringe of MAb, sterically hinders access of the bacterial

neuraminidase. Future work should involve investigation by electron microscopy to rule out the uptake of virus-MAb complexes into the cell and secondly to use receptor containing liposomes to try to repeat the low recovery phenomenon.

8.7.3 Reversibility of HI and neutralization of virus attached to CRBCs after incubation at low pH and 4°C: IgA MAb

As HI and neutralization of attached virus at 4°C could be reversed, and as at 37°C, lack of recovery is likely to be due to steric hindrance, the point at which antibody induces an irreversible loss of infectivity had not yet been defined. The final investigation analysed the reversibility of HI and neutralization of attached virus after incubation at low pH, 4°C, which was intended to mimic early events that normally occur in the endosome of the infected cell. This represents the last stage of the influenza infectious cycle at which the antibody bound to the HA could trigger a signal that resulted in a permanent loss of infectivity. Unfortunately this experiment had to be carried out at 4°C to -

- (1) prevent steric hindrance of the bacterial neuraminidase enzyme,
- (2) prevent virus fusing with the CRBCs at low pH, which would prevent recovery virus,
- (3) prevent loss of virus infectivity (pre-incubation of virus without the cell at low pH and at temperatures above 4°C results in loss of infectivity) (Korte *et al.*, 1999).

The recovery of HA under these conditions was >85%. This indicated that the conformational changes in the viral HA that occur at pH5, 4°C (described in chapter 7) do not result in steric hindrance and low recovery. This suggests that the changes in the viral HA that take place at 37°C are of a different nature to those that occur at low pH and at low temperatures. A previous study has indicated that the X:31 strain of influenza A virus (H3N2) treated with low pH, at 4°C, could not be removed from a cell surface by neuraminidase, probably due to incorporation of the fusion peptide into the lipid bilayer (Chernomordik *et al.*, 1998). The >85% recovery of low pH, 4°C treated virus with neuraminidase indicates that the majority of the A/PR/8 strain does not insert

its fusion peptide into the lipid bilayer under these conditions, in agreement with previous studies (Brunner *et al.*, 1991; Tsurudome *et al.*, 1992; Pak *et al.*, 1994). However, Pak *et al.*, (1994) have demonstrated that at pH 5, 4°C the fusion peptide of A/PR/8 has been released. This suggests that the low pH induces changes in the stem region causing release of the fusion peptide, whilst higher temperatures (>15°C) cause different conformational or orientational changes that facilitate the fusion peptide interaction with the target membrane.

Unfortunately, analysis of the recovery of infectivity of virus incubated at low pH and 4°C was inconclusive. Only approximately 10% of the infectivity of non-neutralized and neutralized virus was recovered as the low pH treated virus had become unstable in the AmOH treatment. However, comparison of the 10% recovered showed no differences between non-neutralized and neutralized virus. Therefore, this allows a tentative conclusion to be made that the permanent loss of infectivity had not been found. It is possible that the low amount of infectivity recovered may not have been representative of the 90% unaccounted for and secondly the signal for permanent loss of infectivity may require a high temperature (37°C). However, in my opinion these data argue against the existence of antibody mediated signal transduction and therefore data indicating that neutralization of influenza virus by the IgA MAbs (H37-66) involves interference of a post-fusion event should be re-evaluated.

9 Summary of results / discussion

9.1 Overview

Previous examination of the relevance of antibody molecular mass and valency to neutralization of influenza virus was inconclusive (Yoden *et al.*, 1985; Schofield, 1996; Schofield *et al.*, 1997b). Schofield (1996) suggested that both valency and molecular mass are involved in efficient neutralization. These authors also found that antibody affinity was not the sole determinant of the efficiency of neutralization, and suggested that other factors, such as intrinsic properties of the epitope and differences in the mechanism of neutralization may be important (Schofield *et al.*, 1997a). In this thesis the effect of antibody molecular mass and valency on the mechanism of neutralization was investigated.

It is commonly assumed that most antibodies neutralized by only one mechanism, being a steric inhibition of virus attachment to target cells (Jackson, 1998). PAN provides the strongest evidence in support of mechanisms of neutralization other than inhibition of viral attachment. Therefore, the ability to give PAN and the mechanism of PAN by HA-specific IgGs and their Fabs was investigated.

Earlier studies of the mechanisms of neutralization of influenza by MAbs have shown that some neutralize by inhibiting a post-fusion event (Possee *et al.*, 1982; Rigg *et al.*, 1989; Armstrong and Dimmock, 1992). Implicit for this mechanism is the ability of the antibody to transduce a signal from the envelope proteins to the core of the virus and result in an irreversible loss of infectivity. Schofield (1996) investigated the reversibility of HI and neutralization by MAbs, using mild denaturant AmOH to dissociate the MAbs from virus after neutralization. This initial study did not elucidate the point at which neutralization becomes irreversible and hence further investigation was carried out in this thesis.

9.2 The efficiency of neutralization

Fab neutralization efficiency was lower than its corresponding IgGs. At lower concentrations of Fab required to give 50% neutralization (N_{50}) the neutralization efficiency was 104- to 370-fold lower than the IgGs, whilst at higher concentrations required to give 90% neutralization (N_{90}) the neutralization efficiency was 15- to 208-

fold lower than the IgGs. Affinity was not a major factor in the lower neutralization efficiency of the Fabs. Measurements by SPR indicated that affinities of Fabs were very similar to their IgGs. The H37 Fab had the largest difference in affinity compared to its IgG, being 4.3-fold lower, but this was not able to explain either the 360-fold lower neutralization efficiency at N_{50} or the 170-fold lower efficiency at N_{90} compared to the IgG. These results support those obtained for a panel of HA-specific IgGs and Fabs to A/FPV/R virus (Schofield and Dimmock, 1996). Differences in the functional affinities of the Fabs and IgGs were too small to be solely responsible for the loss of neutralization seen when the IgGs are converted to Fabs. The authors suggested that the similar affinities of the Fabs and IgGs indicated that the IgGs were binding to virus monovalently, and hence the difference in neutralization efficiency could be due to the lower molecular mass of the Fab. However, the valency of the virus-IgG interaction was not established in this thesis or by Schofield and Dimmock, (1996) and hence it is possible that bivalent binding may have contributed to neutralization efficiency.

Schofield *et al* (1997a) suggested that the neutralization efficiency is affected by unknown properties of the epitope. The neutralization efficiency of the IgGs and Fabs in this thesis were ranked H36>H37>H9. These antibodies are specific for different antigenic sites, suggesting that the antigenic site may be important in the neutralization efficiency. It is possible that the relationship between the antigenic site and the receptor-binding site on the HA may be a property of the epitope that affects neutralization efficiency. For example, the H9 MAb which binds to site Cb, the furthest from the receptor-binding site, had a 20-fold lower efficiency of neutralization than the H36 IgG, which binds to site Sb on the tip of the HA, close to the receptor-binding site. This was further supported by results with the H9 Fab which showed that it did not inhibit virus attachment to target cells. In contrast, the H36 and H37 Fabs inhibited virus attachment to target cells, indicating that Fabs could sterically hinder the HA-cell receptor interaction. This suggested that the H9 Fab did not inhibit virus attachment to cells due to the distance of its antigenic site from the receptor-binding site. Therefore, results in this thesis support the view of Schofield *et al* (1997a), that neutralization is affected by epitope specificity. However, a recent study of the neutralization of HIV-1 by a panel of MAbs to different epitope groups suggested that neutralization was epitope-independent (Parren *et al.*, 1998). It was found that the 50% antibody binding values to oligomeric gp120 and the 50% neutralization titres for MAbs specific for different epitope groups correlated. The authors concluded, by inference,

that the occupancy of binding, i.e. the number of neutralization sites occupied, determines neutralization efficiency and not epitope specificity. It is possible that these contradictory views are due to the different viruses used, with epitope specificity being of greater importance in influenza neutralization than in HIV-1 neutralization. It is my opinion that the efficiency of neutralization by MAbs is multi-factorial, being dependent on the affinity, epitope specificity and also affected by molecular mass and valency when converted to Fab fragments.

9.3 The mechanism of neutralization of influenza A virus

The mechanism of neutralization of influenza virus by Fabs was different from their corresponding IgGs. The mechanism of neutralization of influenza virus by the IgGs was dependent on antibody concentration. At higher concentrations inhibition of attachment accounted for the majority of the loss of infectivity, whereas at lower concentrations inhibition of fusion was the dominant mechanism. In between these extremes both mechanisms operate simultaneously. In contrast, the mechanism of neutralization of the influenza virus by the Fabs was independent of antibody concentration. A good correlation between the inhibition of virus attachment to cells and the loss of infectivity was found with a range of concentrations of H36 and H37 Fabs. However the H36 and H37 Fabs could also give PAN by inhibition of virus-cell fusion, indicating that they could neutralize by mechanisms other than inhibition of attachment under different conditions. The H9 Fab, did not inhibit virus attachment to cells, but inhibited virus-cell fusion. Interestingly, inhibition of virus attachment to cells by high concentrations of the H36 F(ab)₂ accounted for the majority of the loss of infectivity, whilst at lower concentrations inhibition of attachment accounted for a minority of the loss of infectivity, in a similar manner to the IgGs. This suggested that bivalency was important for the ability of the IgGs to neutralize by two mechanisms simultaneously. However, it should be noted that molecular mass of the antibody must also play a role in the neutralization process, as F(ab)₂ had an 8-fold and 2.5-fold loss of neutralization efficiency compared to its IgG at N₅₀ and N₉₀ respectively.

9.4 PAN of influenza A virus

PAN by H36, H37 and H9 IgGs was of lower efficiency than the standard neutralization of unattached virus (STAN). However, PAN by the H36 and H37 Fabs was of similar efficiency to the STAN. This suggested that the IgGs may have limited access to the important sites on the virus for the PAN process, whereas the smaller size of the Fabs allowed for a less restricted access. The H9 Fab gave PAN that was of significantly higher efficiency than its STAN, suggesting that changes in the HA may have occurred to allow a greater access to the antigenic site Cb.

All of the IgGs and their Fabs shared a common mechanism of PAN, being inhibition of virus-cell fusion. This demonstrated the IgGs and Fabs can neutralize virus by mechanisms other than inhibition of virus attachment to cells, and supports the concept of simultaneous neutralization mechanisms as described previously for the mechanism of STAN. Collectively, these data suggest that inhibition of virus-cell fusion by the IgGs represents their primary neutralization mechanism, with inhibition of attachment probably a secondary event occurring at higher concentration of applied IgG.

Investigation of the inhibition of fusion by the antibodies, suggested that they inhibited an early stage in the fusion process. The efficiency of PAN is greater at high antibody concentration, hence antibodies may inhibit virus-cell fusion by molecular overcrowding (steric hindrance) at the fusion site (Millar *et al.*, 1999). Therefore, this suggests that molecular mass of the antibody is the important factor in its neutralization process, with valency being of lesser importance.

9.5 Reversibility of HI and neutralization of influenza A virus

Investigation of the reversibility of HI and neutralization of influenza A virus was carried out to find conditions that would trigger a permanent loss of infectivity. Neutralization of virus in solution by three HA-specific IgGs and an IgA MAb could be reversed. Neutralization by the MAbs at 4°C of virus attached to CRBCs, could also be reversed. However, at 37°C the virus could not be recovered from the CRBC surface due to steric hindrance of the bacterial neuraminidase used to release the virus. The

reversibility of neutralization of virus treated at low pH was analysed in order to mimic events encountered by the virus in the endosomal stage of its infectious cycle. When virus was neutralized and then induced to the pre-fusion intermediate, by treatment at pH 5 and 4°C, the virus could be recovered from the CRBC surface, but infectivity was about 10%. The loss of infectivity was due to the AmOH (pH 11.5) treatment, suggesting that changes occur in the HA when induced in the pre-fusion intermediate, that destabilize the HA making it more sensitive to high pH. This result strongly supports results in this thesis indicating that the virus HA of the pre-fusion intermediate had undergone conformational changes in its globular head domain as detected by a panel of conformation-specific MAbs. Approximately 10% of infectivity was recovered from both neutralized and non-neutralized low pH treated virus indicating that neutralization could be reversed. Hence, as this stage was designed to mimic the last point at which the antibody is associated with the core of the virus, it suggested that the antibodies do not cause a permanent loss of infectivity.

There are two schools-of-thought of how antibody binding relates to the mechanism of neutralization of viruses that have several neutralization sites, each containing numerous epitopes. The first proposes that viruses with multiple neutralization sites have critical and non-critical epitopes. Binding of one or a few antibodies to the critical sites could achieve neutralization, perhaps by triggering a signal that causes a permanent loss of infectivity, or by preventing a signal critical for infectivity (Dimmock, 1993; McLain and Dimmock, 1994; Dimmock, 1995). The second hypothesis known as the occupancy model, proposes that neutralization results when the number of unoccupied neutralization sites (epitopes) falls below a threshold required for infectivity (Klasse and Moore, 1996; Parren *et al.*, 1998). The inability to detect a permanent loss of infectivity in the analysis of reversibility argues against the single or critical-hit model of neutralization, and supports the occupancy model. The occupancy model assumes that antibodies neutralize by steric hindrance of early events of the virus infectious process. It has been proposed in this thesis that the MAbs inhibit both the virus attachment to cells and virus-cell fusion by steric hindrance, which also fits the occupancy model. However, the occupancy model implies that epitope specificity is of limited importance, whereas in this thesis the converse has been argued, especially with antibodies binding to antigenic site Cb. It should also be noted that neutralized virus was treated with low pH at 4°C which does not accurately represent

physiological conditions. It is possible that the trigger for the signal that causes a permanent loss of infectivity may require a temperature of 37°C.

9.6 Does the influenza virus HA undergo conformational or orientational changes after binding to the cell receptor?

The generally accepted view, based on the X-ray crystal structure of the BHA-sialic acid complex, is that a conformational change does not occur on binding of the HA to its cell receptor (Weis *et al.*, 1988). However, a number of observations in this thesis suggest that the influenza A/PR/8/34 HA does undergo change(s) on binding to the cell receptor. For example, the H9 Fab had a higher efficiency of PAN than STAN at 37°C. This suggested that after binding to the cell receptor the antigenic site, Cb, was more accessible to the Fab. A previous study of a panel of MAbs to A/PR/8 virus demonstrated that MAbs specific for site Cb had higher binding levels after the virus was treated at low pH (Yewdell *et al.*, 1983). Though this study does not implicate the receptor in any changes, it does suggest that conformational changes in the HA can increase the accessibility of site Cb.

The recovery of virus from the surface of CRBCs after neutralization by MAbs at 37°C was <10%. Investigation of the low recovery indicated that the MAbs were sterically hindering access of the bacterial neuraminidase, hence inhibiting release. However, the MAbs could only inhibit release of the virus by the bacterial neuraminidase after the virus had been neutralized at temperatures >20°C. Therefore, it was proposed that changes in the HA after binding to the cell receptor at 37°C draws the virus closer to the cell surface, hence allowing the fringe of MAb to inhibit access of the bacterial neuraminidase. Therefore, this data also supports the idea of changes in the HA on cell receptor binding. Recently, a tilting of the HA (50 to 70° angle) has been observed after low pH treatment (Tatulian *et al.*, 1995); Tatulian and Tamm, 1996). It is possible that the receptor binding may also induce tilting of the viral HA, hence drawing the virus closer to the cell surface. This may function to increase the number of HA-receptor interactions and hence stabilise the attachment of virus to cells. This idea is supported by a recent study showing a higher affinity binding of influenza virus

at 37°C, compared to 4°C, suggesting a higher number of receptors are involved in the virus attachment at 37°C (Nunes-Correia *et al.*, 1999).

A further possible function of changes in the virus HA on cell receptor-binding is in the fusion process. It is possible that conformational or orientational changes 'prime' the virus HA for fusion. The hypothesis that the receptor-bound HAs are involved in the fusion process remains a controversial area, with a number of studies suggested that receptor-bound HAs are not involved (Ellens *et al.*, 1990; Alford *et al.*, 1994). However, studies have provided evidence that receptor-binding facilitates the fusion process by increasing efficiency and decreasing the lag phase (Stegmann *et al.*, 1995). Also a recent study of virosomes containing two antigenically distinct HAs fusing to liposomes containing anti-HA Fabs as surrogate receptors, indicated that the HA bound to the Fabs was responsible for the fusion activity (Millar *et al.*, 1999). Investigation of fusion of influenza A/PR/8/34 (H1N1) virus bound to liposomes at low pH and 0°C, indicated that only a subpopulation of HA underwent a conformational change that exposed the fusion peptide (Tsurudome *et al.*, 1992). The authors speculated that binding to ganglioside receptors triggered the change in this subpopulation. There was a 30-fold greater insertion of fusion peptides into the target liposomes membrane after the temperature was raised to 37°C. Therefore, it is possible that the HA-cell receptor interaction alters the extent or rate of conformational changes and primes the HA for insertion of its fusion peptide into the target membranes. Investigation in this thesis of the pre-fusion intermediate of A/PR/8 virus, that was induced by treatment at pH 5 and 4°C, indicated that the globular head domain undergoes a conformational relaxation, and also changes in the HA2 stem region allowed release of the fusion peptides (Pak *et al.*, 1994). However, even though fusion peptides are released the pre-fusion intermediate does not display any fusion activity indicating that the fusion peptides are not inserted into the target membrane, or that the extent of fusion peptide insertion was not sufficient to cause fusion. Fusion only occurs when the temperature is increased to 37°C. It is tempting to speculate that perhaps tilting of the HA occurs at 37°C that allows insertion of the exposed fusion peptides to the target membrane.

It is interesting that the pre-fusion intermediate forms a fusion-committed state and causes haemolysis of CRBCs with high efficiency when incubated at neutral pH and 37°C. A study with the X:31 strain of influenza virus has also described a fusion-committed state, which fuses to erythrocytes when incubated at neutral pH and 37°C.

The kinetics and extent of the neutral pH fusion was dependent on the time period of the low pH incubation at 4°C, when attached to the erythrocytes (Schoch *et al.*, 1992). These studies suggest that incubation at low pH and 4°C in association with cell receptors prime the HAs for fusion, so that they only require the further conformational changes associated with increased temperature.

It is evident from the literature and data in this thesis that there is a weight of circumstantial evidence indicating that changes in the HA on receptor-binding could occur and may be important in efficient fusion. However, direct structural evidence is lacking and hence this hypothesis requires further investigation.

I. Appendix :

I.1 Calculation of the percentage internalisation of neutralized virus, incorporating the correction for the inhibition of attachment:

Analysis of the internalisation into MDCK cells of virus neutralized by 0.67 nM H36 IgG –

Mean level of internalisation of non-neutralized virus = **1.27** (OD 405nm)

Mean level of internalisation of virus neutralized by 0.67 nM H36 IgG = **0.88** (OD 405nm)

Percentage internalisation of neutralized virus –

$$(0.88/1.27) \times 100 = \mathbf{69.3\%}$$

Percentage inhibition of attachment, calculated by attachment ELISA = **24%**

Therefore, percentage internalisation of neutralized virus, corrected for inhibition of attachment –

$$69.3 + 24 = \mathbf{93.3\%}$$

I.2 Calculation of the percentage fusion of neutralized virus, incorporating the correction for inhibition of attachment:

Analysis of the fusion in MDCK cells of virus neutralized by 0.33 nM H36 IgG –

Mean level of fluorescence due to fusion of non-neutralized virus = 463

Mean total fluorescence after Triton-X100 of non-neutralized virus = 764

Mean level of fluorescence due to fusion of virus neutralized by 0.33 nM H36 IgG
= 192

Mean total fluorescence after Triton-X100 treatment of neutralized virus = 689

Percentage attachment of virus neutralized by 0.33 nM H36 IgG –
 $(689/764) \times 100 = 90.2\%$

Hence, only 90% of the neutralized virus attaches to cells, so must be compared to equivalent amount of non-neutralized virus.

Level of fluorescence due to fusion of 90% of non-neutralized virus control –
 $463 \times 0.9 = 416.7$

Therefore, the percentage fusion of virus neutralized by 0.33 nM H36 IgG –
 $(192/416.7) \times 100 = 46\%$

I.3 Analysis of the relationship between A/PR/8 virus PAN and internalisation as a function of antibody concentration.

I. **Figure I.1 Analysis of the relationship between A/PR/8 virus internalisation in MDCK cells and PAN as a function of H37 IgG.** PAN and infectivity were assayed in parallel in the same batch of monolayers in 96 well plates, using the same virus and antibody stocks. All data are the mean of three experiments. The curve has been generated by non-linear regression using the Graphpad Prism package ($R = 0.99$).

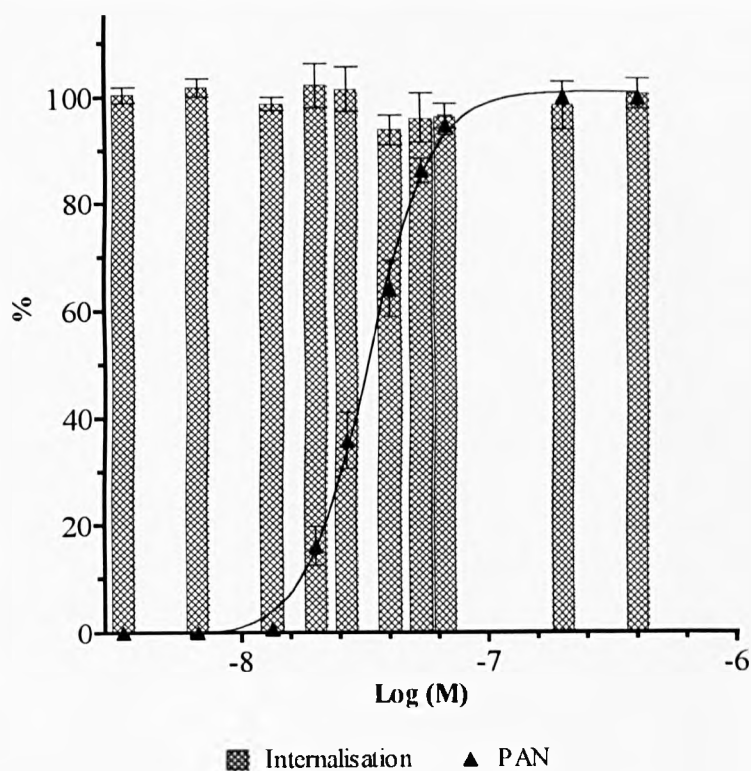


Table I.1 Analysis of the internalisation of non-neutralized (N_0) virus under the negative control conditions. Data are presented as percentage inhibition of internalisation relative to non-neutralized virus at 37°C .

<i>Control conditions</i>	<i>% inhibition of internalisation</i>
Cold (4°C) – N_0	90 (+/- 3)
Hypertonic treated - N_0	87 (+/- 11)

Figure I.2 Analysis of the relationship between A/PR/8 virus internalisation in MDCK cells and PAN as a function of H37 Fab. PAN and infectivity were assayed in parallel in the same batch of monolayers in 96 well plates, using the same virus and antibody stocks. All data are the mean of three experiments. The curve has been generated as in Figure I.1 ($R = 0.98$).

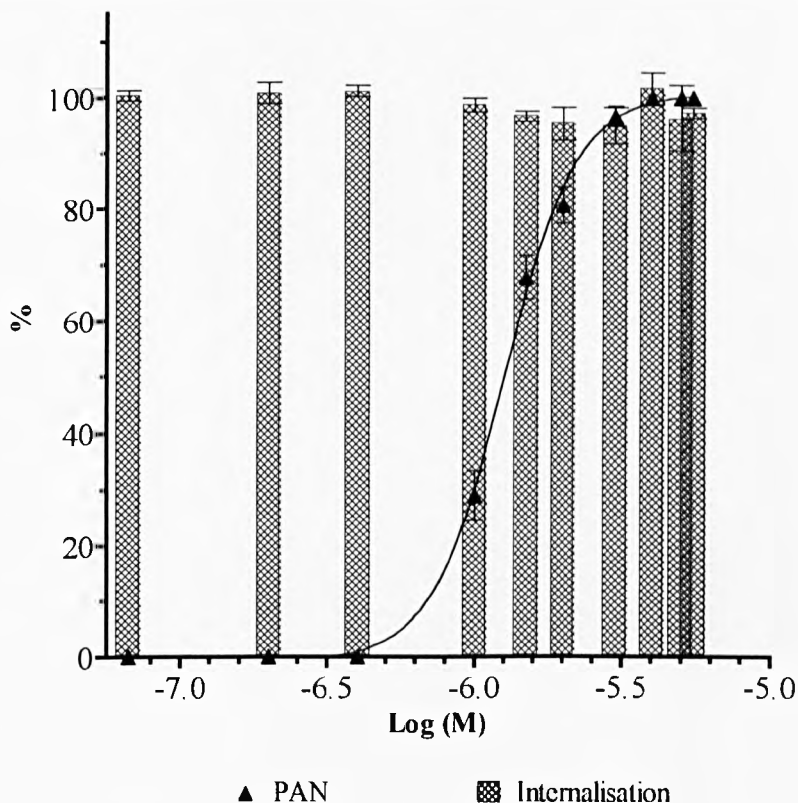


Table I.2 Analysis of the internalisation of non-neutralized (N_0) virus under the negative control conditions. Data are presented as percentage inhibition of internalisation relative to non-neutralized virus at 37°C.

<i>Control conditions</i>	<i>% inhibition of internalisation</i>
Cold (4°C) – N_0	84 (+/- 3)
Hypertonic treated - N_0	79 (+/- 6)

Figure I.3 Analysis of the relationship between A/PR/8 virus internalisation in MDCK cells and PAN as a function of H9 IgG. PAN and infectivity were assayed in parallel in the same batch of monolayers in 96 well plates, using the same virus and antibody stocks. All data are the mean of three experiments. The curve has been generated as in Figure I.1 ($R = 0.98$).

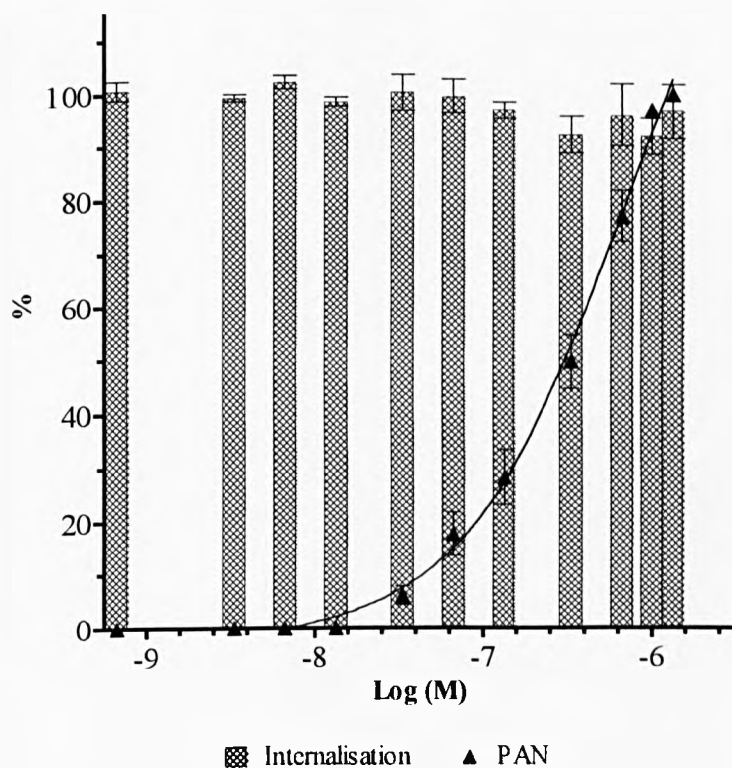


Table I.3 Analysis of the internalisation of non-neutralized (N_0) virus under the negative control conditions. Data are presented as percentage inhibition of internalisation relative to non-neutralized virus at 37°C.

<i>Control conditions</i>	<i>% inhibition of internalisation</i>
Cold (4°C) – N_0	95 (+/- 8)
Hypertonic treated - N_0	84 (+/- 11)

Figure I.4 Analysis of the relationship between A/PR/8 virus internalisation in MDCK cells and PAN as a function of H9 Fab. PAN and infectivity were assayed in parallel in the same batch of monolayers in 96 well plates, using the same virus and antibody stocks. All data are the mean of three experiments. The curve has been generated as in Figure I.1 ($R = 0.97$).

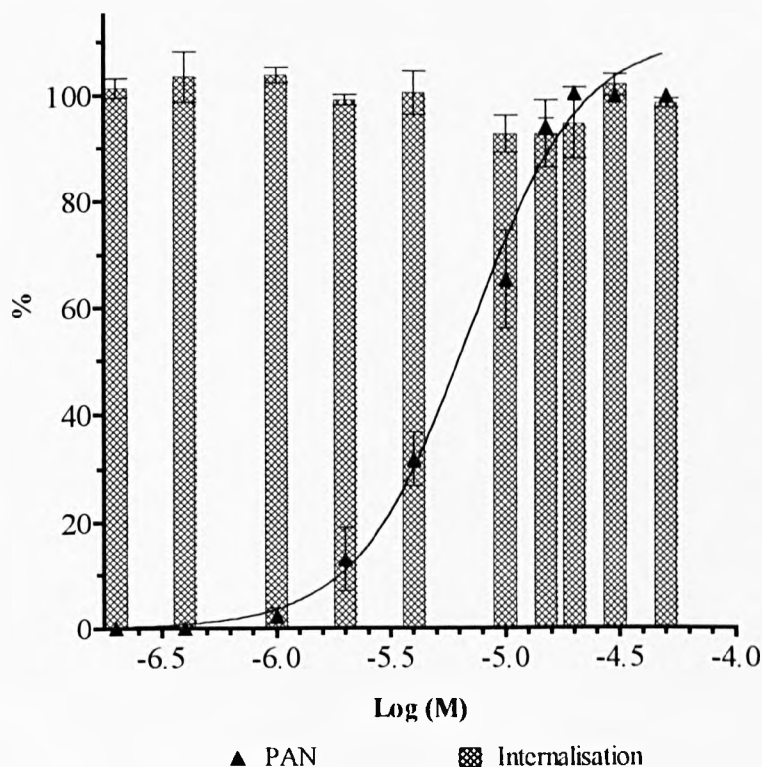


Table I.4 Analysis of the internalisation of non-neutralized (N_0) virus under the negative control conditions. Data are presented as percentage inhibition of internalisation relative to non-neutralized virus at 37°C.

<i>Control conditions</i>	<i>% inhibition of internalisation</i>
Cold (4°C) – N_0	91 (+/- 8)
Hypertonic treated - N_0	80 (+/- 9)

I.4 Analysis of the relationship between A/PR/8 virus PAN and virus-cell fusion as a function of antibody concentration.

Figure I.5 Analysis of the relationship between A/PR/8 virus PAN and virus-cell-fusion as a function of H37 IgG concentration. PAN and fusion were assayed in parallel in the same batch of monolayers in 3cm plates, using the same virus and antibody stocks. All data are the mean of three experiments. The curve has been generated as in Figure I.1 ($R = >0.98$ for both curves).

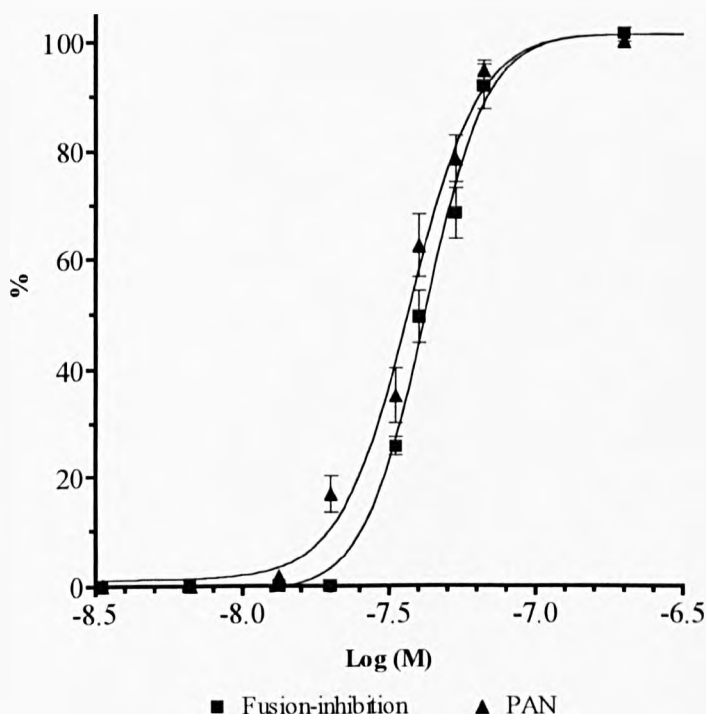


Table I.5 Analysis of the fusion of non-neutralized virus under the negative control conditions. Data are presented as percentage inhibition of fusion relative to non-neutralized virus at 37°C. Data are the mean of three experiments

<i>Control conditions</i>	<i>% inhibition of internalisation</i>
Cold (4°C) – N ₀	93 (+/- 4)
Bafilomycin treated - N ₀	85 (+/- 10)

Figure I.6 Analysis of the relationship between A/PR/8 virus PAN and virus-cell-fusion as a function of H37 Fab concentration. PAN and fusion were assayed in parallel in the same batch of monolayers in 3cm plates, using the same virus and antibody stocks. All data are the mean of three experiments. The curve has been generated as in Figure I.1 ($R = >0.98$ for both curves).

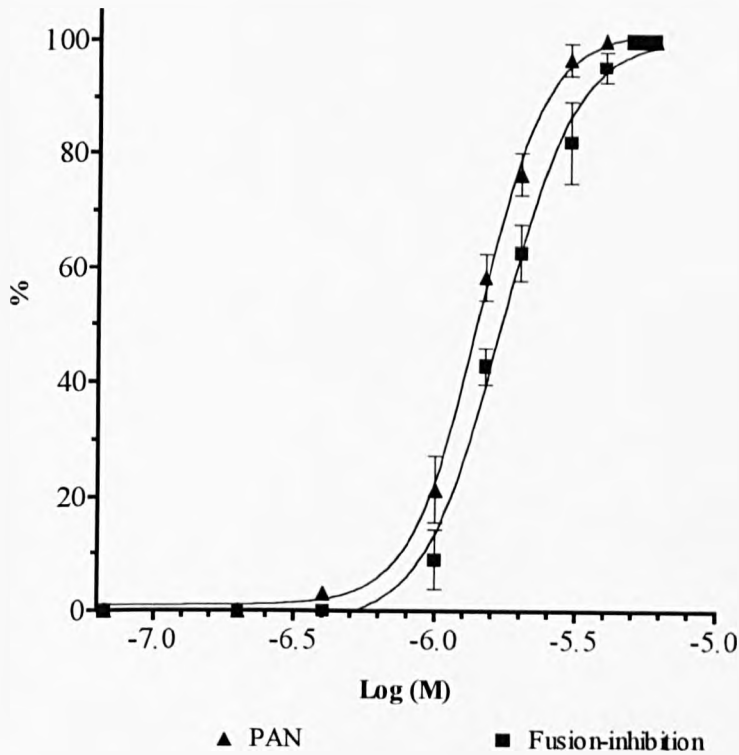


Table I.6 Analysis of the fusion of non-neutralized virus under the negative control conditions. Data are presented as percentage inhibition of fusion relative to non-neutralized virus at 37°C. Data are the mean of three experiments

<i>Control conditions</i>	<i>% inhibition of internalisation</i>
Cold (4°C) – N ₀	87 (+/- 7)
Bafilomycin treated - N ₀	78 (+/- 9)

Figure I.7 Analysis of the relationship between A/PR/8 virus PAN and virus-cell-fusion as a function of H9 IgG concentration. PAN and fusion were assayed in parallel in the same batch of monolayers in 3cm plates, using the same virus and antibody stocks. All data are the mean of three experiments. The curve has been generated as in Figure I.1 ($R = >0.97$ for both curves).

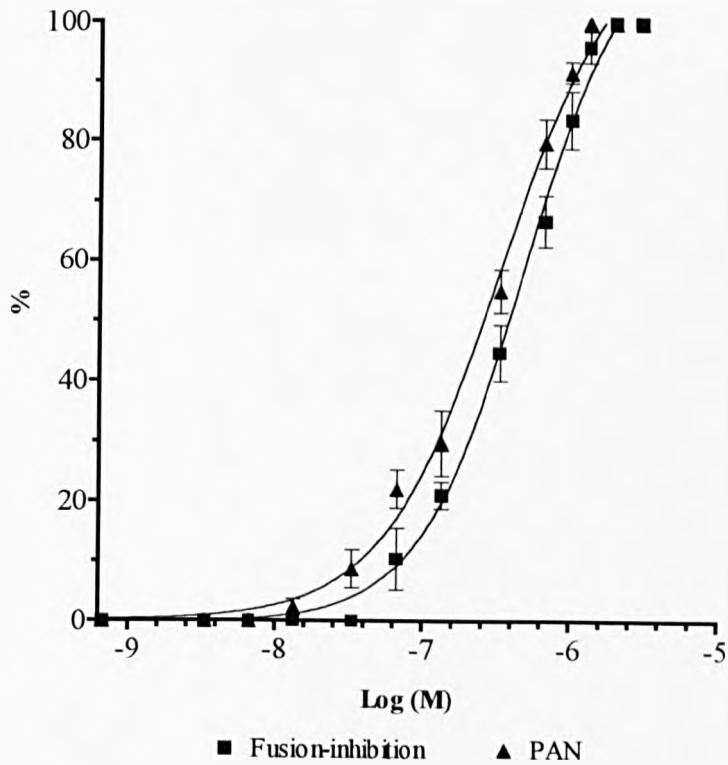


Table I.7 Analysis of the fusion of non-neutralized virus under the negative control conditions. Data are presented as percentage inhibition of fusion relative to non-neutralized virus at 37°C. Data are the mean of three experiments

<i>Control conditions</i>	<i>% inhibition of internalisation</i>
Cold (4°C) – N_0	85 (+/- 7)
Bafilomycin treated - N_0	85 (+/- 11)

I.5 Analysis of the effect of the antibodies on the haemolysis of CRBCs by pre-attached A/PR/8 virus.

Figure I.8 Analysis of the effect of H37 IgG concentration on the haemolysis of CRBCs by pre-attached A/PR/8 virus. Data are the mean of four experiments. Bars represent the SEM.

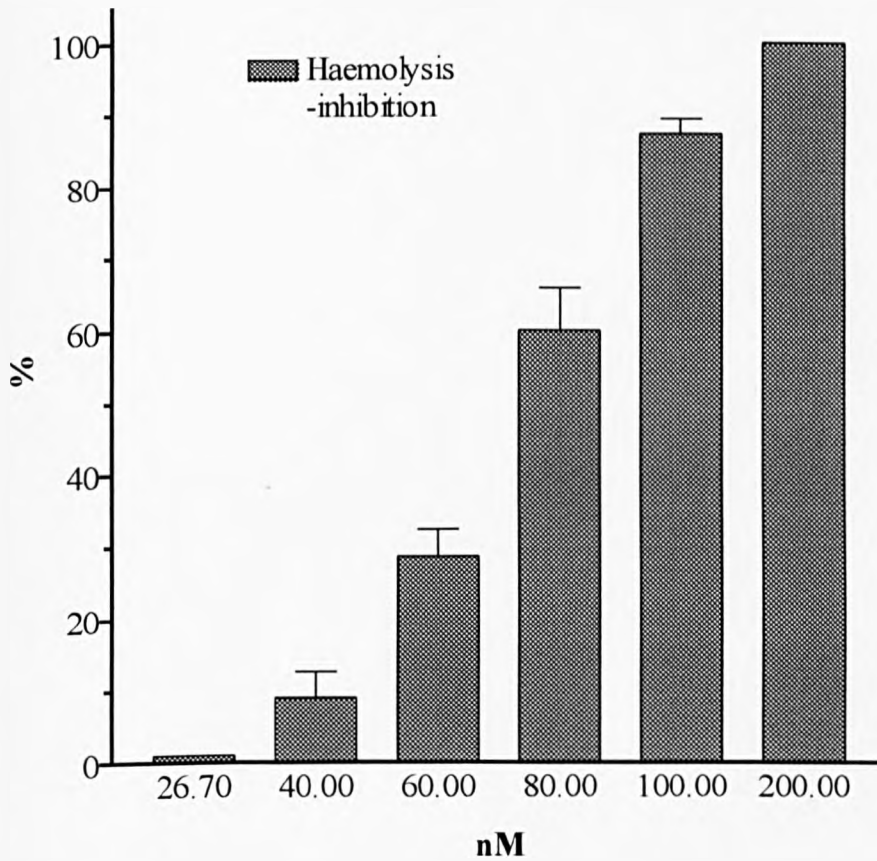


Figure I.9 Analysis of the effect of H37 Fab concentration on the haemolysis of CRBCs by pre-attached A/PR/8 virus. Data are the mean of four experiments. Bars represent the SEM.

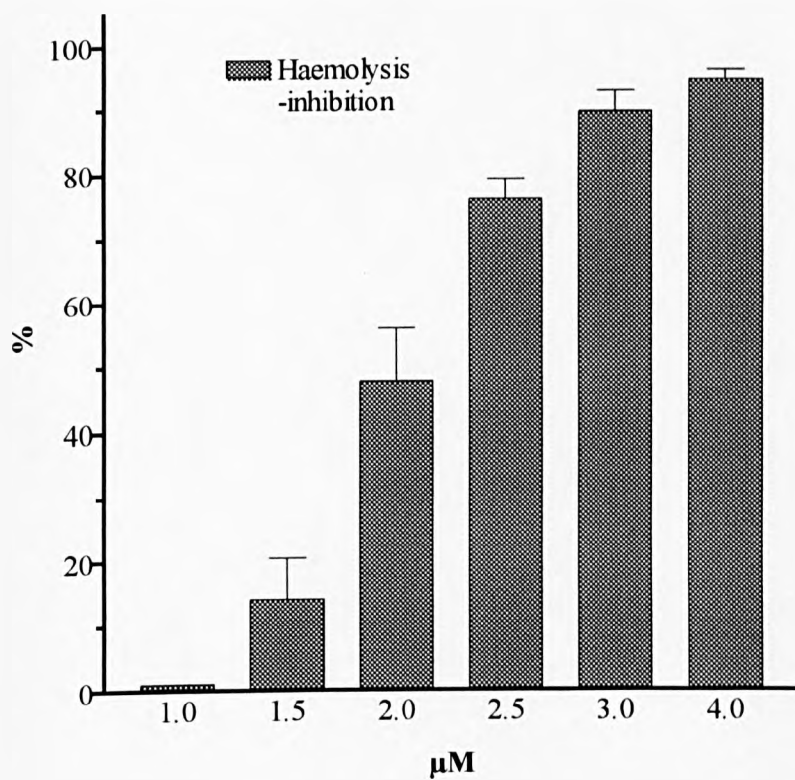
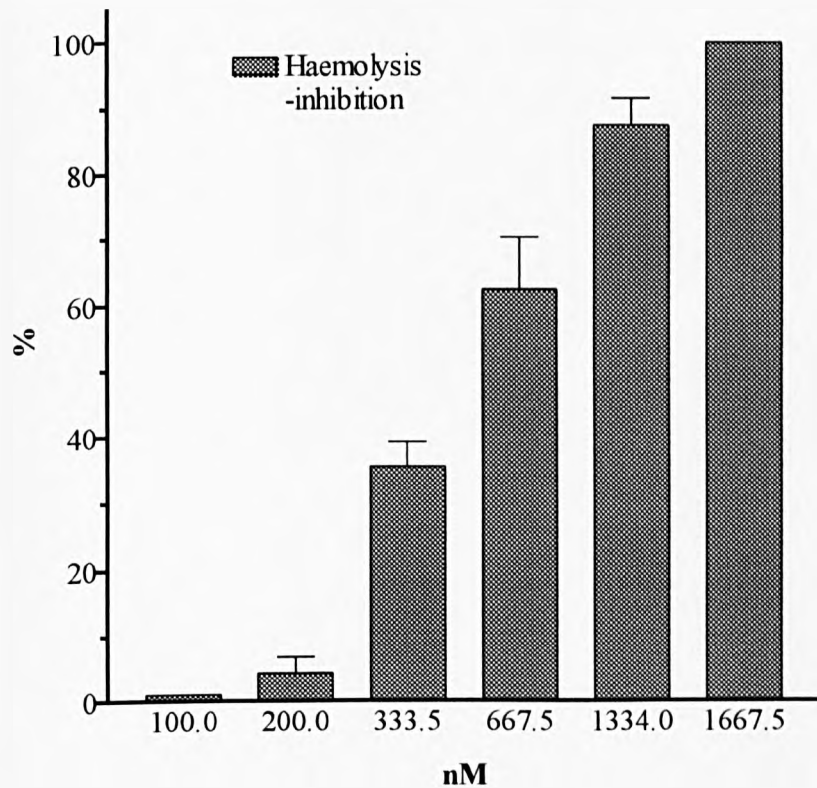


Figure I.10 Analysis of the effect of H9 IgG concentration on the haemolysis of CRBCs by pre-attached A/PR/8 virus. Data are the mean of four experiments. Bars represent the SEM.



I.6 Investigation of the effect of the antibodies on haemolysis of CRBCs by the cold-fusion intermediate of A/PR/8 virus.

Figure I.11 Analysis of the effect of H37 IgG and Fab on haemolysis of CRBCs by the cold-fusion intermediate of A/PR/8 virus. All data have been subtracted from the background haemolysis obtained from CRBC controls without virus. All control samples were treated as the virus containing samples. Data are the means of experiments. Bars represent the SEM. X-axis labels – **V-pH7** = pre-attached virus incubated at 4°C and pH7, **V-pH5** = pre-attached virus at 4°C and pH5, **V-IA** = virus inactivated at 37°C and pH5 prior to attachment, **IgG-pH7** = H37 IgG at 120nM, incubated with pH7 treated virus, **Fab-pH7** = H37 Fab at 3µM, incubated with pH7 treated virus, **IgG-pH5** = H37 IgG at 100nM, incubated with pH5 treated virus, **Fab-pH5** = H37 Fab at 3µM, incubated with pH5 treated virus.

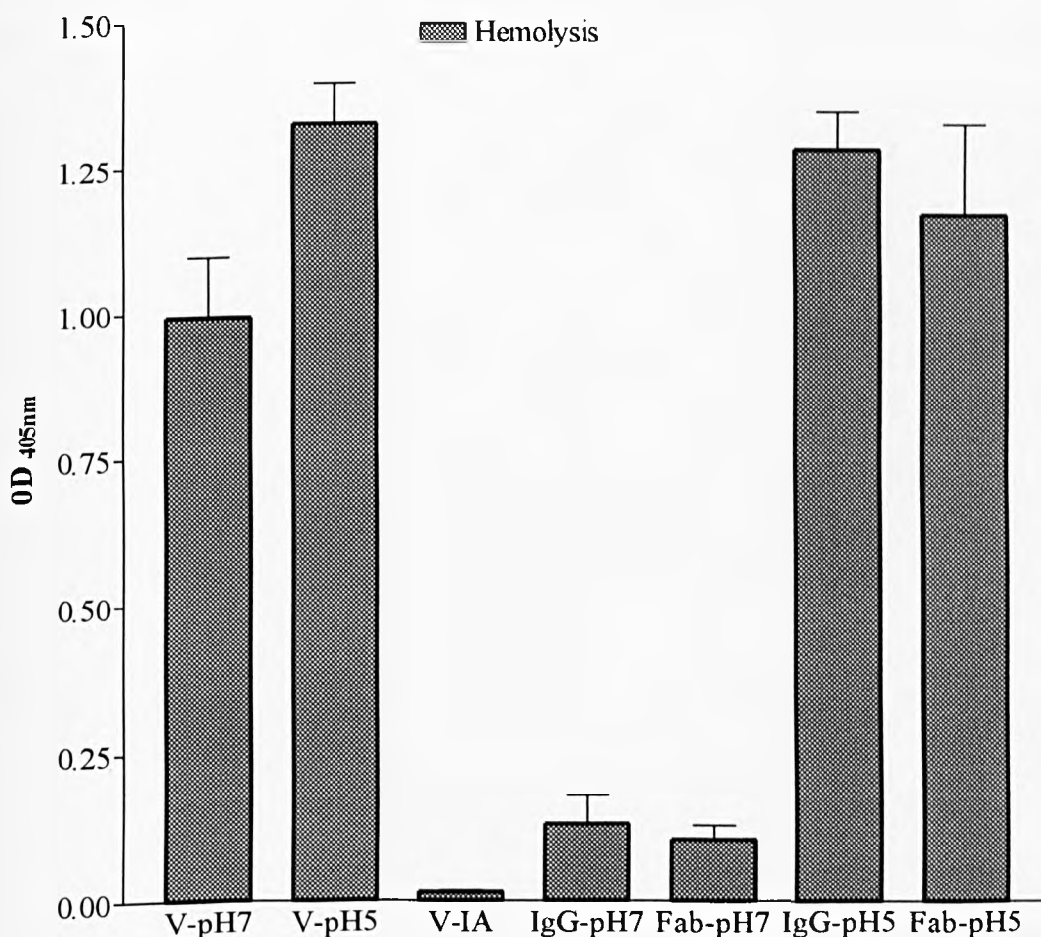
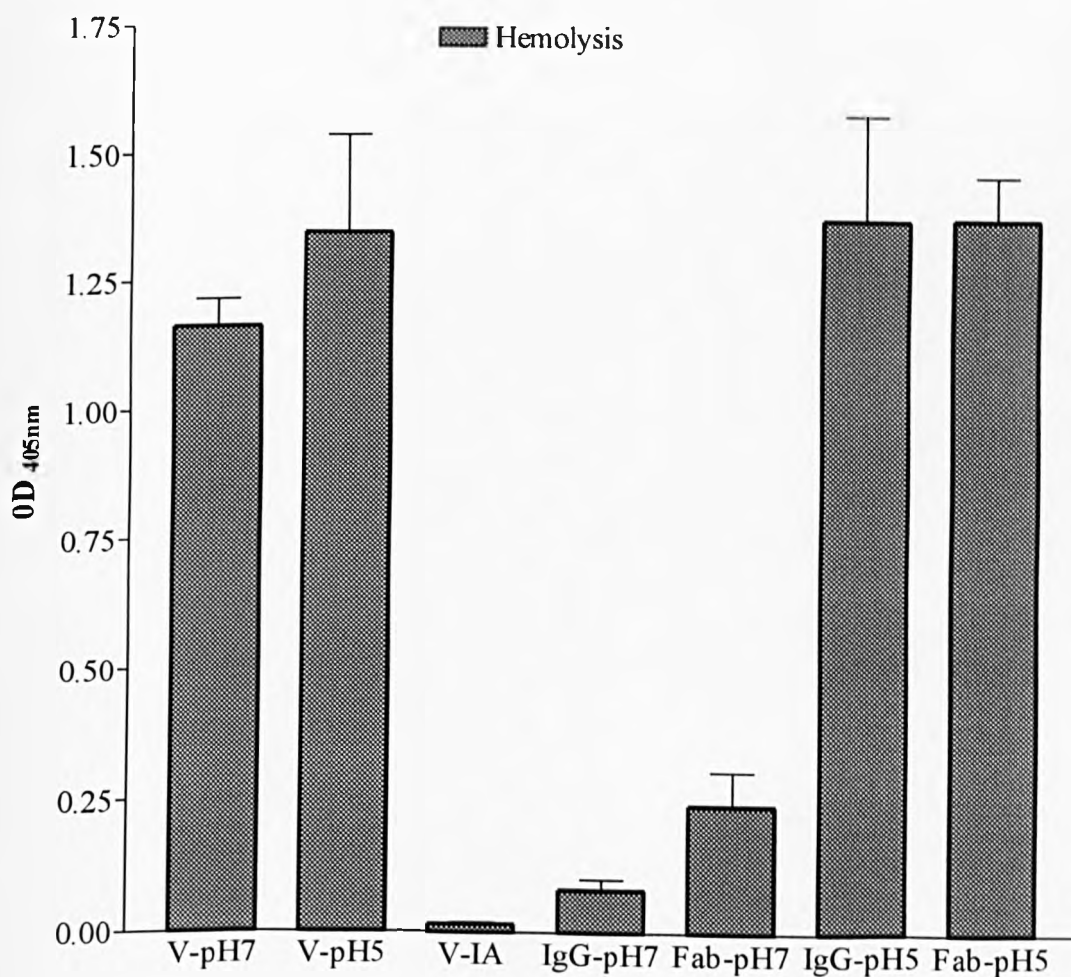


Figure I.12 Analysis of the effect of H9 IgG and Fab on haemolysis of CRBCs by the cold-fusion intermediate of A/PR/8 virus. All data have been subtracted from the background haemolysis obtained from CRBC controls without virus. All control samples were treated as the virus containing samples. Data are the means of experiments. Bars represent the SEM. X-axis labels – **V-pH7** = pre-attached virus incubated at 4°C and pH7, **V-pH5** = pre-attached virus at 4°C and pH5, **V-IA** = virus inactivated at 37°C and pH5 prior to attachment, **IgG-pH7** = H9 IgG at 1334nM, incubated with pH7 treated virus, **Fab-pH7** = H9 Fab at 20µM, incubated with pH7 treated virus, **IgG-pH5** = H9 IgG at 1334nM, incubated with pH5 treated virus, **Fab-pH5** = H9 Fab at 20µM, incubated with pH5 treated virus.



I.7 The affect of PAN by the Fabs on the low pH induced conformational change of the HA.

Figure I.13 Analysis of the affect of H37 Fab on the low pH-induced conformational change of the HA of A/PR/8 virus (in PAN-like format). Virus was attached to fixed monolayers at 4°C and then incubated with Fab at 4 or 37°C. Neutralized virus was then incubated with pH 5 or 7 at 4 or 37°C, and then probed with conformation-specific MAbs. Graph shows binding of conformation-specific MAbs to virus. All data have been subtracted from a cell monolayer control without virus. Data are the mean of three experiments. The bars represent the SEM. X-axis labels – **V-pH7(37°C)** = attached virus incubated at pH7 and 37°C, **V-pH5(37°C)** = attached virus incubated at pH5 and 37°C, **V-pH5(4°C)** = as previous but at 4°C, **Fab-pH7(37°C)** = H37 Fab at 3µM incubated with attached virus treated at pH7 and 37°C, **Fab-pH5(37°C)** = H37 Fab at 3µM incubated with attached virus treated at pH5 and 37°C, **Fab-pH5(4°C)** = as previous but at 4°C.

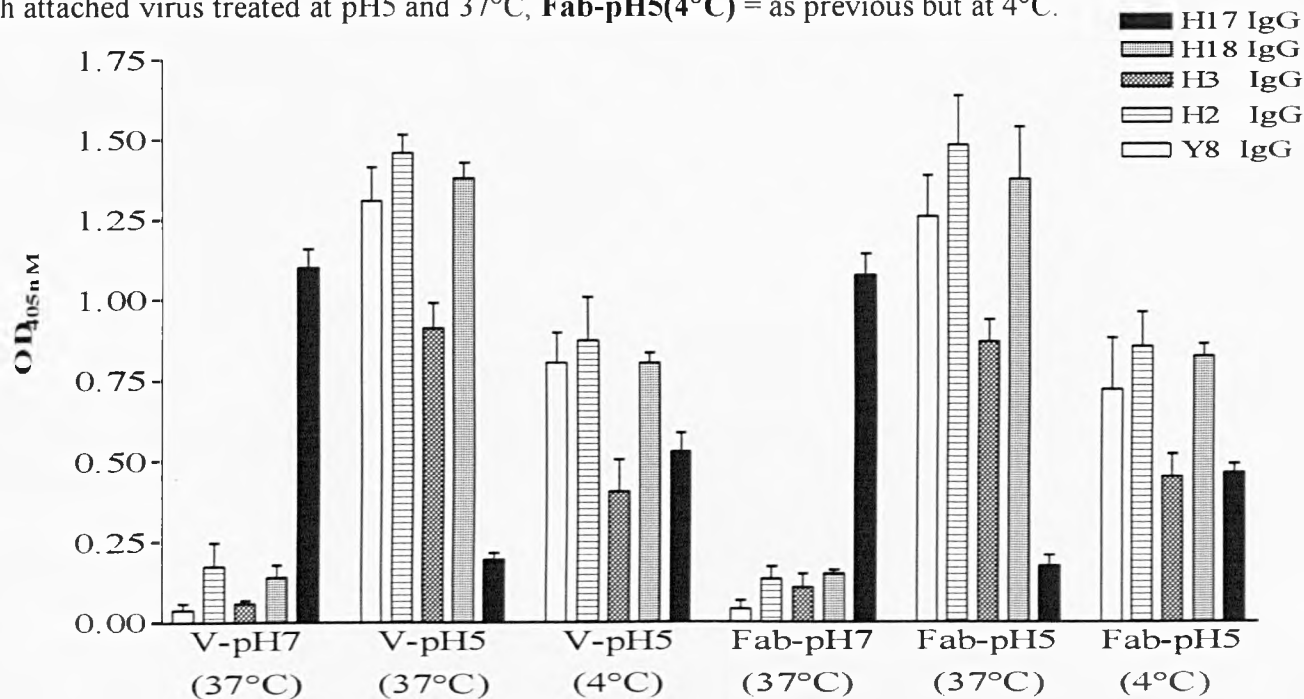
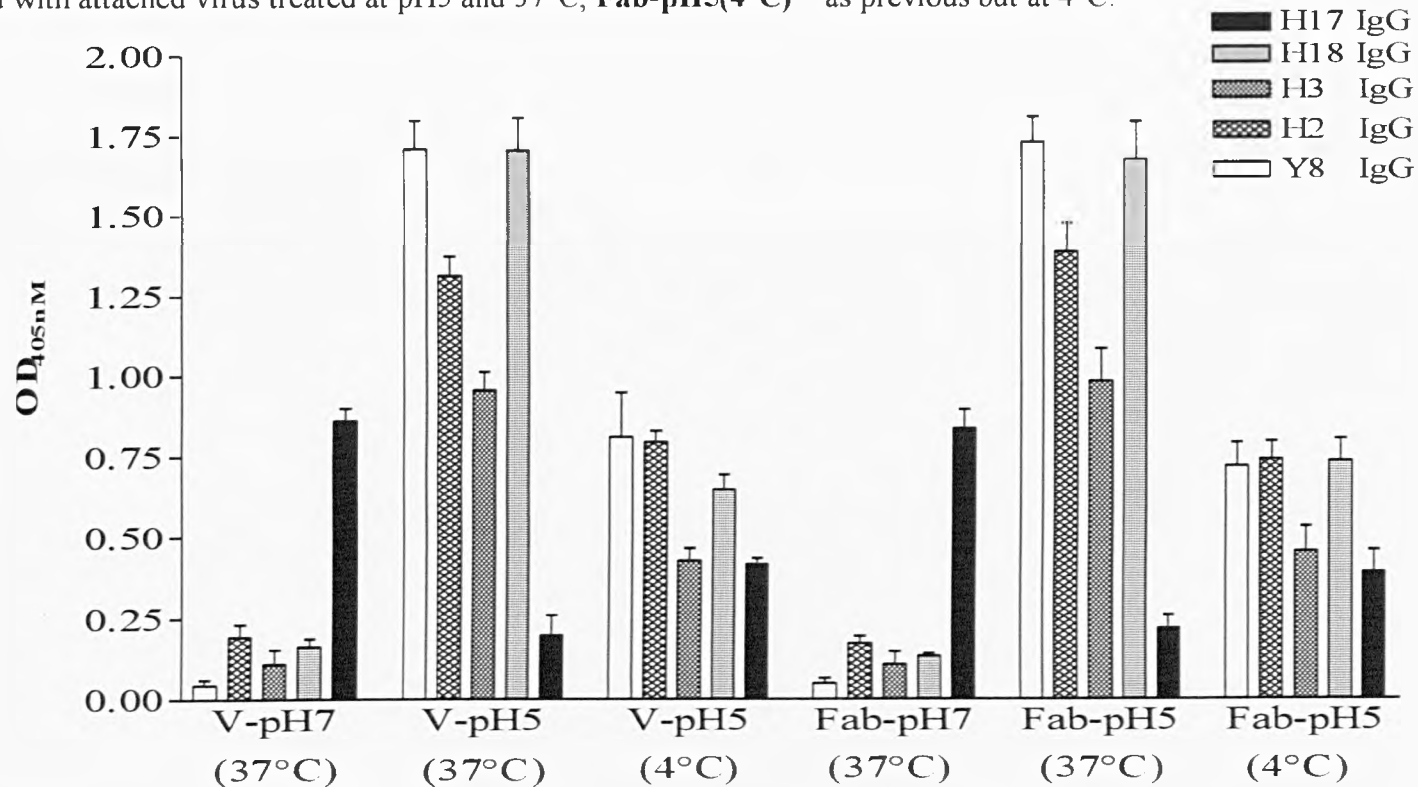
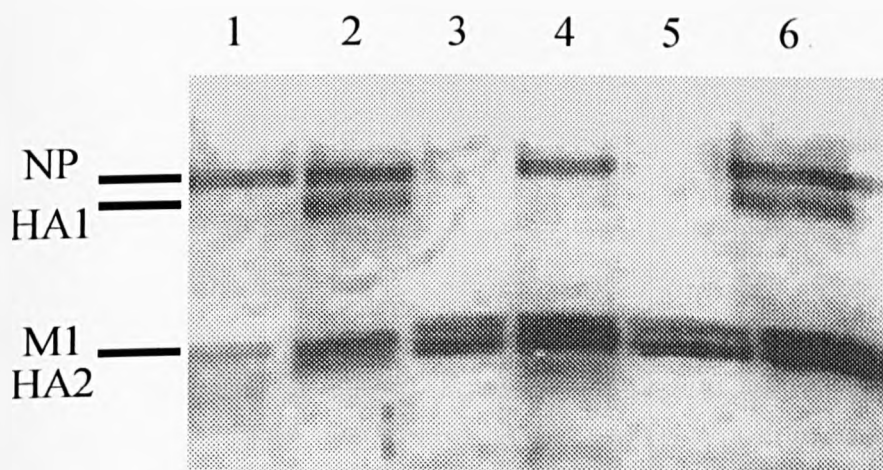


Figure 1.14 Analysis of the affect of H9 Fab on the low pH-induced conformational change of the HA of A/PR/8 virus (in PAN-like format). Virus was attached to fixed monolayers at 4°C and then incubated with Fab at 4 or 37°C. Neutralized virus was then incubated with pH 5 or 7 at 4 or 37°C, and then probed with conformation-specific MAbs. Graph shows binding of conformation-specific MAbs to virus. All data have been subtracted from a cell monolayer control without virus. Data are the mean of three experiments. The bars represent the SEM. X-axis labels – **V-pH7(37°C)** = attached virus incubated at pH7 and 37°C, **V-pH5(37°C)** = attached virus incubated at pH5 and 37°C, **V-pH5(4°C)** = as previous but at 4°C, **Fab-pH7(37°C)** = H9 Fab at 20µM incubated with attached virus treated at pH7 and 37°C, **Fab-pH5(37°C)** = H9 Fab at 20µM incubated with attached virus treated at pH5 and 37°C, **Fab-pH5(4°C)** = as previous but at 4°C.



I.8 Investigation of the effect of H36 Fab on the low pH induced conformational change of the viral HA by proteinase-K digestion.

Figure I.15 Susceptibility to proteinase-K digestion following low pH treatment of neutralized or non-neutralized virus. Virus was incubated with H36 Fab or PBS, followed by exposure to pH 5 or pH 7.5 for 30 minutes, returned to pH 7.5 and then digested with 1 µg/ml of proteinase-K for 30 minutes at 37°C.

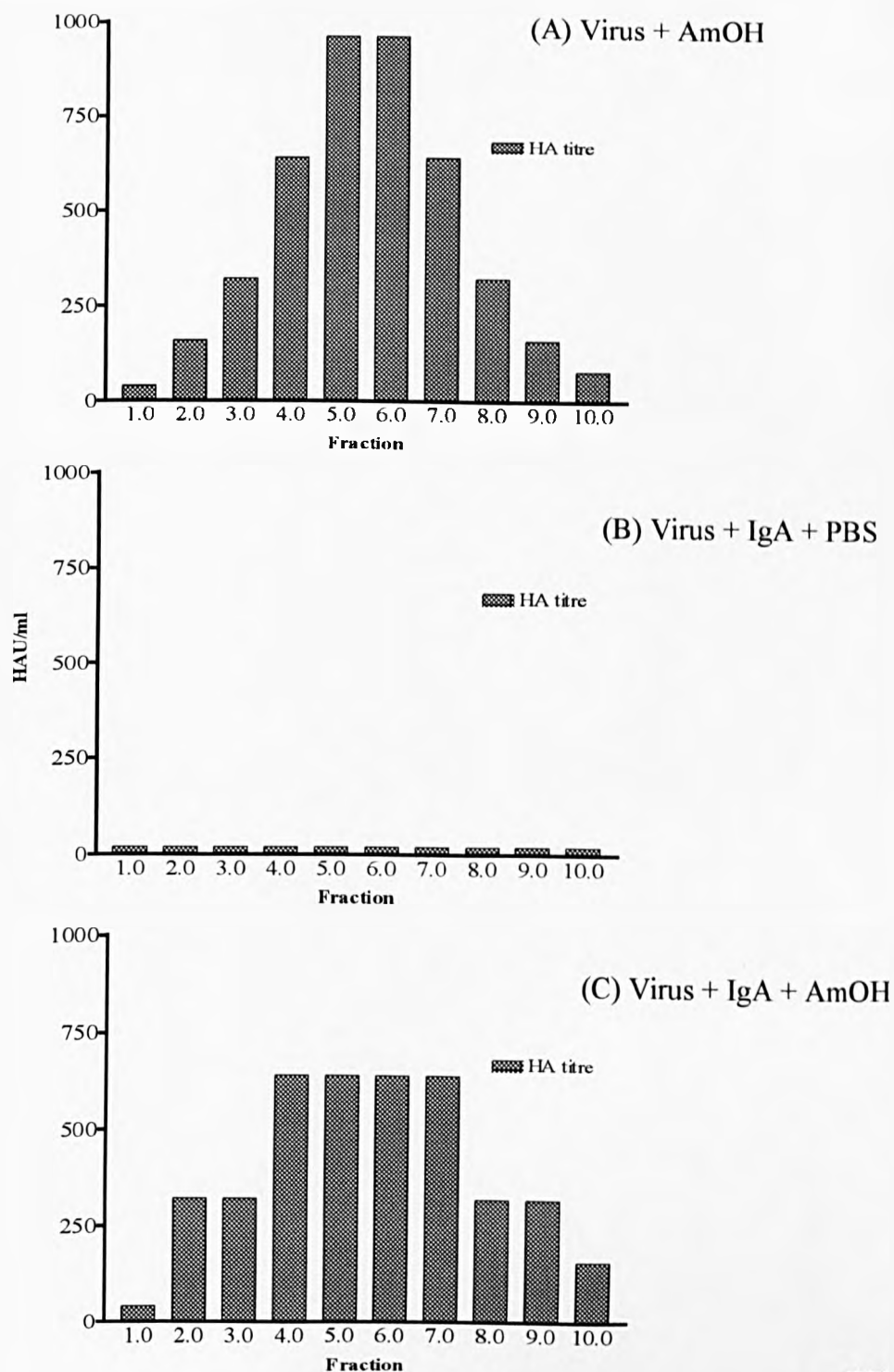


- Lane 1 = non-neutralized virus, incubated at pH 5
2 = non-neutralized virus, incubated at pH 7.5
3 = H36 Fab incubated at pH 7.5
4 = neutralized virus, incubated at pH 5
5 = H36 Fab incubated at pH 5
6 = neutralized virus, incubated at pH 7.5.

NP, nucleoprotein; M1, matrix protein; HA1 and 2, haemagglutinin protein

I.9 Reversibility of HI by ammonium hydroxide.

Figure I.16 Reversibility of HI by ammonium hydroxide: IgA. Enough IgA was used to completely inhibit the HA titre. This mixture was incubated with 0.1M AmOH (pH 11.5) for 30 minutes at 4°C and then virus was separated from antibody by size exclusion on a Sephacryl S1000 column. 100 µl fractions were collected, returned to neutral pH and assayed for HA activity. Graphs show example of the recovery of HA in each fraction.



I.10 Reversibility of HI and neutralization of virus pre-attached to CRBCs

Figure I.17 Analysis of the reversibility of HI and neutralization of virus pre-attached to CRBCs: H37 IgG. (A) This shows the percentage recovery of HA compared to a non-neutralized virus control. Data are the sum of the ten fractions collected from the S-1000 column. **(B)** This shows the percentage recovery of infectivity compared to a non-neutralized virus control. Data are the sum of the infectivity of the three peak HA fractions. Data are the mean of three experiments. The lines represent the standard error of the mean (SEM). 40+A = pre-attached virus neutralized with 40 $\mu\text{g/ml}$ of H37 IgG, treated with 1 U/ml bacterial neuraminidase and then incubated with AmOH; 40+P = pre-attached virus neutralized with 40 $\mu\text{g/ml}$ of H37 IgG, treated with 1 U/ml bacterial neuraminidase and then incubated with PBS; 50+A and 50+P = same as above, but with 50 $\mu\text{g/ml}$ H37 IgG. 4°C and 37°C below labels refer to the temperature that the virus was neutralized.

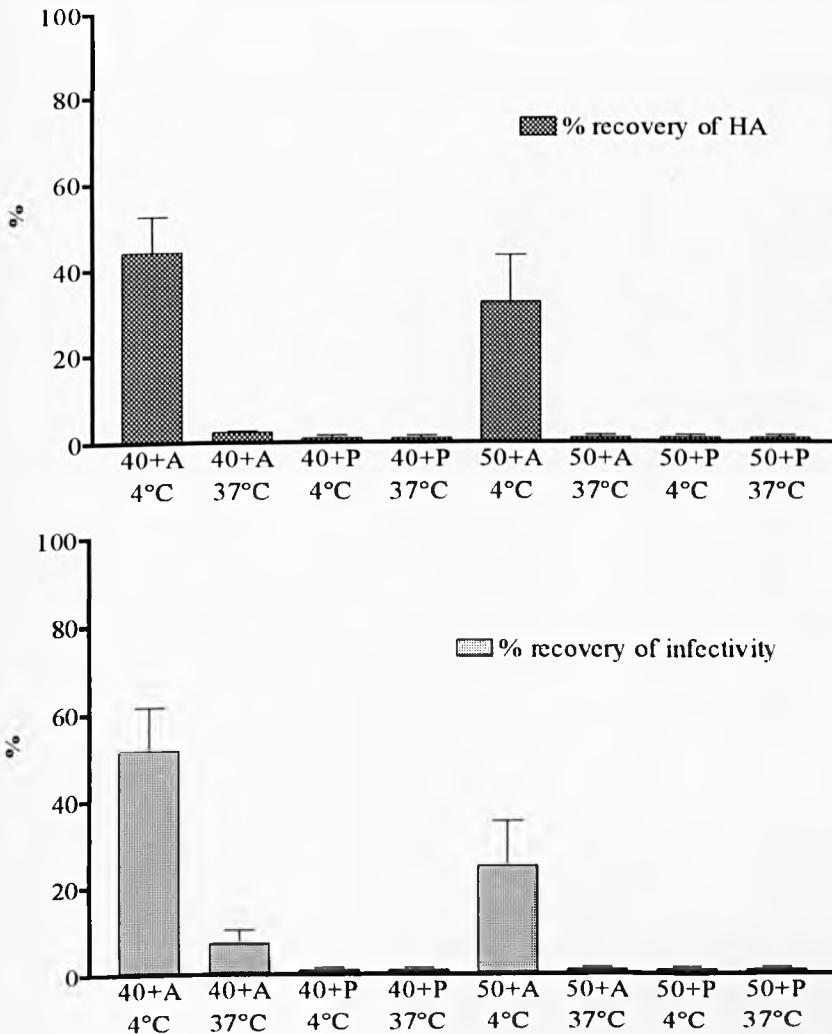
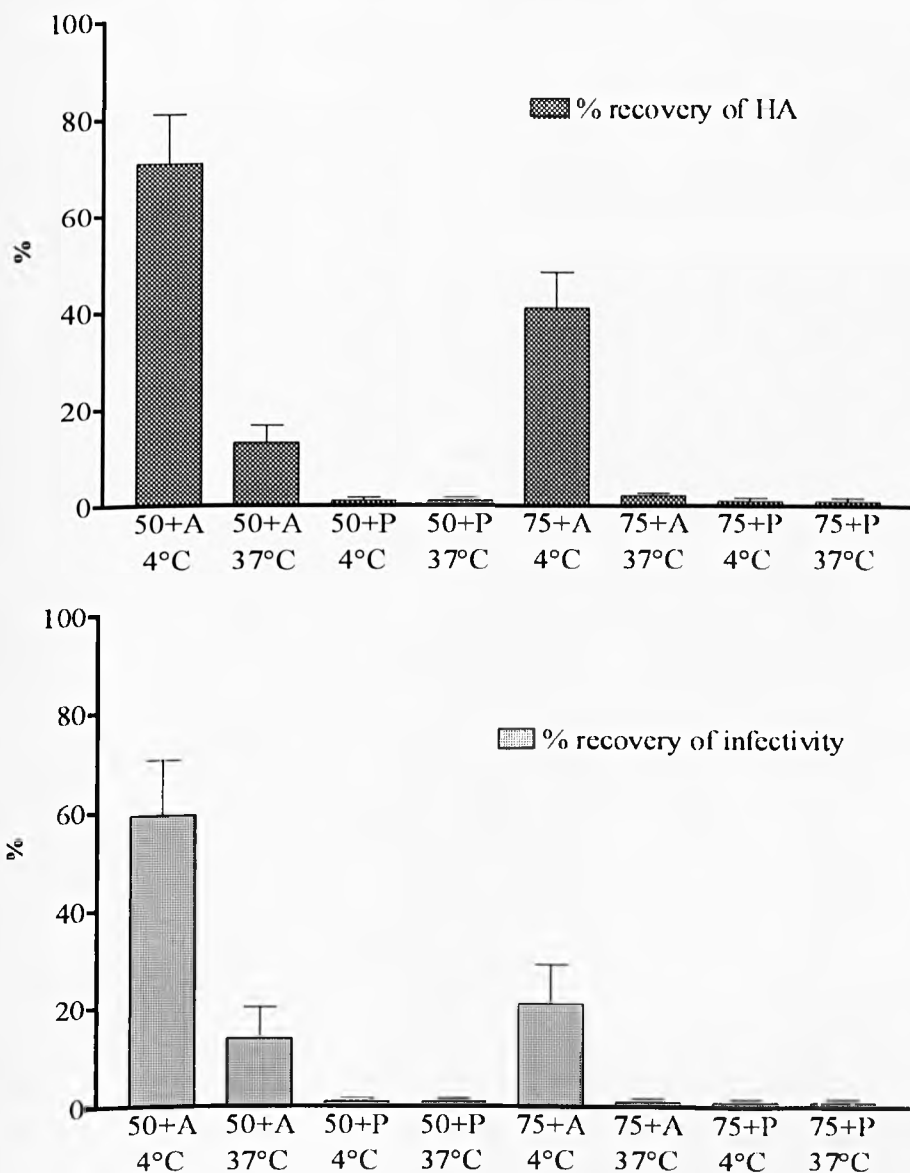


Figure I.18 Analysis of the reversibility of HI and neutralization of virus pre-attached to CRBCs: H9 IgG. (A) This shows the percentage recovery of HA compared to a non-neutralized virus control. Data are the sum of the ten fractions collected from the S-1000 column. **(B)** This shows the percentage recovery of infectivity compared to a non-neutralized virus control. Data are the sum of the infectivity of the three peak HA fractions. Data are the mean of three experiments. The lines represent the standard error of the mean (SEM). 50+A = pre-attached virus neutralized with 50 $\mu\text{g/ml}$ of H9 IgG, treated with 1 U/ml bacterial neuraminidase and then incubated with AmOH; 50+P = pre-attached virus neutralized with 50 $\mu\text{g/ml}$ of H9 IgG, treated with 1 U/ml bacterial neuraminidase and then incubated with PBS; 75+A and 75+P = same as above, but with 75 $\mu\text{g/ml}$ H9 IgG. 4°C and 37°C below labels refer to the temperature that the virus was neutralized



References

- Abbas, A. K., Lichtman, A. H., and Pober, J. S., Eds. (1994) "Cellular and molecular immunology", 2nd ed. W.B. Saunders, Philadelphia, USA.
- Ada, G. L., and Jones, P. D. (1986). The immune response to influenza infection. *Curr. Topics Microbiol. Immunol.* **128**, 1-54.
- Air, G. M., and Laver, W. G. (1989). The neuraminidase of influenza virus. *Proteins Struct. Funct. Genetic.* **6**, 341-356.
- Albo, C, Valencia, A., and Portela, A. (1995). Identification of an RNA binding region within the N-terminal third of the influenza A virus nucleoprotein. *J. Virol.* **69**, 3799-3806.
- Alford, D., Ellens, H., and Bentz, J. (1994). Fusion of influenza virus with sialic acid-bearing targets membranes. *Biochem* **33**, 1977-1978.
- Andrewes, C. H., and Elford, W. J. (1933). Observations on antiphage sera. *Brit. J. Exp. Path.* **14**, 367-375.
- Arese, M., and Portela, A. (1996). Serine 3 is critical for phosphorylation at the N-terminal end of the nucleoprotein of influenza virus A/Victoria/3/75. *J. Virol.* **70**, 3385-3391.
- Armstrong, S. J., Outlaw, M. C., and Dimmock, N. J. (1990). Morphological studies of the neutralization of influenza virus by IgM. *J. Gen. Virol.* **71**, 2313-2319.
- Armstrong, S. J., and Dimmock, N. J. (1992). Neutralization of influenza virus by low concentrations of HA-specific polymeric IgA inhibits viral fusion activity but activation of the ribonucleoprotein is also inhibited. *J. Virol.* **66**, 3823-3832.
- Armstrong, S. J., and Dimmock, N. J. (1996). Varying temperature-dependence of post-attachment neutralization of human immunodeficiency virus type 1 by monoclonal antibodies to gp120: identification of a very early fusion-independent event as a neutralization target. *J. Gen. Virol.* **77**, 1397-1402.
- Armstrong, S. J., McInerney, T. L., McLain, L., Wahren, B., Hinkula, J., Levi, M., and Dimmock, N. J. (1996). Two neutralizing anti-V3 monoclonal antibodies act by affecting different functions of human immunodeficiency virus type 1. *J. Gen. Virol.* **77**, 2931-2941.
- Assad, F. A., Bres, P., Chi-Ming, C., and Dowdle, W.R. (1980). A revision of the system of nomenclature for influenza viruses: a WHO memorandum. *Bull. Wld. Hlth. Org.* **58**, 585-591.
- Avery, R. J., and Dimmock, N. J. (1975). Temporal control of transcription of influenza viral RNA. *Virol.* **64**, 409-414.

- Baez, M., Palese, P., and Kilbourne, E. D. (1980). Gene composition of high-yielding influenza vaccine strains obtained by recombination. *J. Infect. Dis.* **141**, 362-365.
- Banks, J., Speidel, E., and Alexander, D. J. (1998). Characterisation of an avian influenza A virus isolated from a human - is an intermediate host necessary for the emergence of pandemic influenza viruses? *Arch. Virol.* **143**, 781-787.
- Barrett, T., and Inglis, S. C. (1985) Growth, purification and titration of influenza viruses. In "Virology - a practical approach" (B. M. J. Mahy, Ed.), pp. 119-150. Oxford University Press: Oxford, UK.
- Basak, S., Tomana, M., and Compans, R. W. (1985). Sialic acid is incorporated into influenza hemagglutinin glycoproteins in the absence of viral neuraminidase. *Virus Res.* **2**, 61-68.
- Baudin, F., Bach, C., Cusack, S., and Ruigrok, R. W. H. (1994). Structure of influenza virus RNP. I Influenza virus nucleoprotein melts secondary structure in panhandle RNA and exposes the bases to the solvent. *EMBO J.* **13**, 3158-3165.
- Bean, W. J., Schell, M., Katz, J., Kawaoka, Y., Naeve, C., Gorman, O., and Webster, R. G. (1992). Evolution of the H3 virus hemagglutinin from human and nonhuman hosts. *J. Virol.* **66**, 1129-1138.
- Beare, A. S., and Webster, R. G. (1991). Replication of avian influenza viruses in humans. *Arch. Virol.* **119**, 37-42.
- Beaton, A. R., and Krug, R. M. (1984). Synthesis of the templates for influenza virion RNA replication *in vitro*. *Proc. Natl. Acad. Sci. USA* **81**, 4682-4686.
- Beaton, A. R., and Krug, R. M. (1986). Transcription antitermination during influenza viral template RNA synthesis requires the nucleocapsid protein and the absence of a 5' capped end. *Proc. Natl. Acad. Sci. USA* **83**, 6282-6286.
- Beloso, A., Martínez, C., Valcárcel, J., Fernández-Santaren, J., and Ortín, J. (1992). Degradation of cellular mRNA during influenza virus infection: its possible role in protein synthesis shutoff. *J. Gen. Virol.* **73**, 575-581.
- Bender, C., Hall, H., Huang, J., Klimov, A., Cox, N., Hay, A., Gregory, V., Cameron, K., Lim, W., and Subbarao, K. (1999). Characterisation of the surface proteins of influenza A (H5N1) viruses isolated from humans in 1997-1998. *Virol.* **254**, 115-123.
- Benne, C. A., Harmsen, M., De Jong, J. C., and Kraaijeveld, C. A. (1994). Neutralization enzyme immunoassay for influenza virus. *J. Clin. Microbiol.* **32**, 987-990.
- Bentz, J., Ellens, H., and Alford, D. (1990). An architecture for the fusion site of influenza hemagglutinin. *FEBS Letts.* **276**, 1-5.

- Bentz, J., Ellens, H., and Alford, D. (1993) Architecture of the influenza hemagglutinin fusion site. In "Viral fusion mechanisms" (J. Bentz, Ed.), pp. 163-199. CRC Press, Inc: Boca Raton, Fla.
- Bilsel, P., Castrucci, M. R., and Kawaoka, Y. (1993). Mutations in the cytoplasmic tail of influenza A virus neuraminidase affect incorporation into virions. *J. Virol.* **67**, 6762-6767.
- Bishop, D. H. L., Obijeski, J. F., and Simpson, R. W. (1971a). Transcription of the influenza virus ribonucleic acid genome by a virion polymerase. I Optimal conditions for in vitro activity of the ribonucleic acid-dependent ribonucleic acid polymerase. *J. Virol.* **8**, 66-73.
- Bishop, D. H. L., Obijeski, J. F., and Simpson, R. W. (1971b). Transcription of the influenza virus ribonucleic acid genome by a virion polymerase. II Nature of the in vitro polymerase product. *J. Virol.* **8**, 74-80.
- Bishop, D. H. L., Roy, P., Bean, W. J., and Simpson, R. W. (1972). Transcription of the influenza virus ribonucleic acid genome by a virion polymerase. III Completeness of the transcription process. *J. Virol.* **10**, 689-697.
- Bishop, N. E. (1997). An update on non-clathrin-coated endocytosis. *Rev. Med. Virol.* **7**, 199-209.
- Bisno, A. L., Griffin, K. A., Van Epps, K. A., Niell, H. B., and Rytel, M. W. (1971). Pneumonia and Hong Kong influenza : a prospective study of the 1968-1969 epidemic. *Am. J. Med. Sci.* **261**, 251-263.
- Biswas, S. K., Boutz, P. L., and Nayak, B. P. (1998). Influenza virus nucleoprotein interacts with influenza virus polymerase proteins. *J. Virol.* **72**, 5493-5501.
- Blaas, D., Patzelt, E., and Kuechler, E. (1982). Cap-recognising protein of influenza virus. *Virology* **116**, 339-348.
- Blick, T. J., Tiong, T., Sahasrabudhe, A., Varghese, J. N., Colman, P. M., Hart, G. J., Bethell, R. C., and McKimm-Breschkin, J. L. (1995). Generation and characterisation of an influenza virus neuraminidase variant with decreased sensitivity to the neuraminidase specific inhibitor 4-guanidino-Neu5Ac2en. *Virology* **214**, 475-484.
- Blumenthal, R., Bali-Puri, A., Walter, A., Covell, D., and Eidelman, O. (1987). pH-dependent fusion of vesicular stomatitis virus with Vero cells. *J. Biol. Chem.* **262**, 13614-13619.
- Bossart, W., Meyer, J., and Bienz, K. (1973). Electron microscopic study on influenza virus haemagglutination : Pinocytosis of virions by red cells. *Virology* **55**, 295-298.
- Both, G. W., Sleight, M. J., Cox, N. J., and Kendal, A. P. (1983). Antigenic drift in influenza virus H3 haemagglutinin from 1968 to 1980 : multiple evolutionary pathways and sequential amino acid changes at key antigenic sites. *J. Virol.* **48**, 52-60.

- Braam, J., Ulmanen, I., and Krug, R. M. (1983). Molecular model of a eucaryotic transcription complex: functions and movements of influenza P proteins during capped RNA-primed transcription. *Cell* **34**, 609-618.
- Brandtzaeg, P. (1981). Transport models for secretory IgA and secretory IgM. *Clin. Exp. Immunol.* **44**, 221-232.
- Brioen, P., and Boeyé, A. (1985). Poliovirus neutralization and the percentage law. *Arch. Virol.* **83**, 105-111.
- Bron, R., Kendal, A. P., Klenk, H.-D., and Wilschut, J. (1993). Role of the M2 protein in influenza virus membrane fusion: effects of amantadine and monensin on fusion kinetics. *Viol.* **195**, 808-811.
- Brown, L. E., Murray, J. M., White, D. O., and Jackson, D. C. (1990). An analysis of the properties of monoclonal antibodies directed to epitopes on influenza virus hemagglutinin. *Arch. Virol.* **114**, 1-26.
- Brunner, J., Zugliani, C., and Mischler, R. (1991). Fusion activity of influenza virus PR8/34 correlates with a temperature-induced conformational change within the haemagglutinin ectodomain detected by photochemical labeling. *Biochem* **30**, 2432-2438.
- Bucher, D. J., Kharitonov, I. G., Zakomirdin, J. A., Gregoriev, V. B., Klimenko, S. M., and Davis, J. F. (1980). Incorporation of influenza M-protein into liposomes. *J. Virol.* **36**, 586-590.
- Bui, M., Whittaker, G., and Helenius, A. (1996). Effect of M1 protein and low pH on nuclear transport of influenza virus ribonucleoproteins. *J. Virol.* **70**, 8391-8401.
- Bukrinskaya, A. G., Vorkunova, N. K., Kornilayeva, R., Narmanbetova, R. A., and Vorkunova, G. K. (1982). Influenza virus uncoating in infected cells and effect of rimantadine. *J. Gen. Virol.* **60**, 49-59.
- Bullough, P. A., Hughson, F. M., Skehel, J. J., and Wiley, D. C. (1994). Structure of influenza haemagglutinin at the pH of membrane fusion. *Nature (Lond.)* **371**, 37-43.
- Burton, D. R. (1990). Antibody: the flexible adaptor molecule. *TIBS* **15**, 64-69.
- Castrucci, M. R., and Kawaoka, Y. (1993). Biologic importance of neuraminidase stalk length in influenza A virus. *J. Virol.* **67**, 759-764.
- Caton, A. J., Brownlee, G. G., Yewdell, J. W., and Gerhard, W. (1982). The antigenic structure of the influenza virus A/PR/8/34 hemagglutinin (H1 subtype). *Cell* **31**, 417-427.
- Cavacini, L. A., Emes, C. L., Power, J., Duval, M., and Posner, M. R. (1994). Effect of antibody valency on interaction with cell-surface expressed HIV-1 and viral neutralization. *J. Immunol.* **152**, 2538-2545.

- Chanturiya, A., Chernomordik, L. V., and Zimmerberg, J. (1997). Flickering fusion pores comparable with initial exocytotic pores occur in protein-free phospholipid bilayers. *Proc. Natl. Acad. Sci. USA* **94**, 14423-14428.
- Chen, J., Lee, K. H., Steinhauer, D. A., Stevens, S. J., Skehel, J. J., and Wiley, D. C. (1998). Structure of the hemagglutinin precursor cleavage site, a determinant of influenza pathogenicity and the origin of the labile conformation. *Cell* **95**, 409-417.
- Chen, Z., Li, Y., and Krug, R. M. (1999). Influenza A virus NS1 protein targets poly(A)-binding protein II of the cellular 3'-end processing machinery. *EMBO J.* **18**, 2273-2283.
- Chernomordik, L. V., Frolov, V. A., Leikina, E., Bronk, P., and Zimmerberg, J. (1998). The pathway of membrane fusion catalyzed by influenza hemagglutinin: restriction of lipids, hemifusion, and lipidic fusion pore formation. *J. Cell Biol.* **140**, 1369-1382.
- Ciampor, F. ac, Bayley, P. M., Nermut, M. V., Hirst, E. M., Sugrue, R. J., and Hay, A. J. (1992). Evidence that the amantadine-induced, M2-mediated conversion of influenza A virus hemagglutinin to the low pH form occurs in an acidic trans-Golgi compartment. *Virology* **188**, 14-24.
- Cianci, C., Tiley, L., and Krystal, M. (1995). Differential activation of the influenza virus polymerase via template RNA binding. *J. Virology* **69**, 3995-3999.
- Claas, E. C. J., Kawaoka, Y., de Jong, J. C., Masurel, N., and Webster, R. G. (1994). Infection of children with avian-human reassortant influenza virus from pigs in Europe. *Virology* **204**, 453-457.
- Claas, E. C. J., and Osterhaus, A. D. M. E. (1998). New clues to the emergence of flu pandemics. *Nature Medicine* **4**, 1122-1123.
- Claas, E. C., Osterhaus, A. D. M. E., van Beek, R., de Jong, J. C., Rimmelzwaan, G. F., Senne, D. A., Krauss, S., Shortridge, K. F., and Webster, R. G. (1998). Human influenza A (H5N1) virus related to a highly pathogenic avian influenza virus. *Lancet* **351**, 472-477.
- Clague, M. J., Schoch, C., and Blumenthal, R. (1991). Delay time for influenza virus hemagglutinin-induced membrane fusion depends on hemagglutinin surface density. *J. Virology* **65**, 2402-2407.
- Clements, M.L., Betts, R.F., Tierney, E.L., and Murphy, B.R. (1986). Serum and nasal wash antibody associated with resistance to experimental challenge with influenza A wild type virus. *J. Clin. Microbiol.* **24**, 157-160.
- Cleveland, S. M., Taylor, H. P., and Dimmock, N. J. (1997). Selection of neutralizing antibody escape mutants with type A influenza virus HA-specific polyclonal antisera: possible significance for antigenic drift. *Epidemiol. Infect.* **118**, 149-154.

- Colman, P. M., and Ward, C. W. (1985). Structure and diversity of influenza virus neuraminidase. *Curr. Topics Microbiol. Immunol.* **114**, 177-255.
- Colman, P. M., Varghese, J. N., and Laver, W. G. (1983). Structure of the catalytic and antigenic sites in influenza virus neuraminidase. *Nature (Lond.)* **303**, 41-44.
- Colonno, R. J., Callahan, P. L., Leippe, D. M., Rueckert, R. R., and Tomassini, J. E. (1989). Inhibition of rhinovirus attachment by neutralizing monoclonal antibodies and their Fab fragments. *J. Virol.* **63**, 36-42.
- Compans, R. W., and Caligiuri, L. (1973). Isolation and properties of an RNA polymerase from influenza virus-infected cells. *J. Virol.* **10**, 441-448.
- Compans, R. W., and Choppin, P. W. (1975) "Reproduction of myxoviruses": "Comprehensive Virology", Vol. IV. Plenum, New York.
- Connor, R. J., Kawaoka, Y., Webster, R. G., and Paulson, J. C. (1994). Receptor specificity in human, avian and equine H2 and H3 virus isolates. *Virol.* **205**, 17-23.
- Copeland, C., Doms, R. W., Bolzau, R. W., Webster, R. G., and Helenius, A. (1986). Assembly of influenza haemagglutinin and its role in intracellular transport. *J. Cell Biol.* **103**, 1179-1191.
- Couch, R. B., and Kasel, J. A. (1983). Immunity to influenza in man. *Ann. Rev. Microbiol.* **37**, 529-549.
- Cox, N. J., and Bender, C. A. (1995). The molecular epidemiology of influenza viruses. *Sem. Virol.* **6**, 359-370.
- Danieli, T., Pelletier, S. L., Henis, Y. I., and White, J. M. (1996). Membrane fusion mediated by the influenza hemagglutinin requires the concerted action of at least three hemagglutinin trimers. *J. Cell Biol.* **133**, 559-569.
- Daniels, R. S., Downie, J. C., Hay, A. J., Knossow, M., Skehel, J. J., Wang, M. L., and Wiley, D. C. (1985). Fusion mutants of the influenza virus hemagglutinin glycoprotein. *Cell* **40**, 431-439.
- Daniels, R. S., Jeffries, S., Yates, P., Schild, G. C., Rogers, G. N., Paulson, J. C., Wharton, S. A., Douglas, A. R., Skehel, J. J., and Wiley, D. C. (1987). The receptor-binding and membrane-fusion properties of influenza virus variants selected using anti-haemagglutinin monoclonal antibodies. *EMBO J.* **6**, 1459-1465.
- Davey, J., Dimmock, N. J., and Colman, A. (1985). Identification of the signal responsible for nuclear accumulation of the influenza virus nucleoprotein in *Xenopus* oocytes. *Cell* **40**, 667-675.
- Davis, A. C., and Schulman, M. J. (1989). IgM: molecular requirements for its assembly and function. *Immunol. Today* **10**, 118-22; 127-128.

- De, B. K., and Nayak, D. P. (1980). Defective-interfering influenza viruses: establishment and maintenance of persistent influenza virus infection in MDBK and HeLa cells. *J. Virol.* **36**, 847-859.
- de la Luna, S., Fortes, P., Beloso, A., and Ortin, J. (1995). Influenza virus NS1 protein enhances the rate of translation of viral mRNAs. *J. Virol.* **69**, 2417-2433.
- Desselberger, U., Racaniello, V. R., Zazra, J. J., and Palese, P. (1980). The 3' and 5' terminal sequences of influenza A, B and C virus RNA segments are highly conserved and show partial inverted complementarity. *Gene* **8**, 315-328.
- Dhar, R., and Ogra, P. L. (1985). Local immune responses. *Brit. Med. Bull.* **41**, 28-33.
- Dietzschold, B., Tollis, M., Lafon, M., Wunner, W. H., and Koprowski, H. (1987). Mechanisms of rabies virus neutralization by glycoprotein specific monoclonal antibodies. *Virology* **161**, 29-36.
- Dietzschold, B., Gore, M., Casali, P., Ueki, Y., Rupprecht, C. E., Notkins, A. L., and Koprowski, H. (1990). Biological characterization of human monoclonal antibodies to rabies virus. *J. Virol.* **64**, 3087-3090.
- Digard, P., Elton, D., Bishop, K., Medcalf, E., Weeds, A., and Pope, B. (1999). Modulation of nuclear localisation of the influenza virus nucleoprotein through interaction with actin filaments. *J. Virol.* **73**, 2222-2231.
- Dimmock, N. J., Dolbear, H. S., and Guest, A. R. (1989). Chemical crosslinking of proteins of the influenza virion. 1. Interrelationships. *Arch. Virol.* **108**, 183-190.
- Dimmock, N. J. (1993). Neutralization of animal viruses. *Curr. Topics Microbiol. Immunol.* **183**, 1-149.
- Dimmock, N. J. (1995). Update on the neutralisation of animal viruses. *Rev. Med. Virol.* **5**, 165-179.
- Doherty, P. C., Allan, W., Eichelberger, M., and Carding, S. R. (1992). Roles of $\alpha\beta$ and $\tau\delta$ T cell subsets in viral immunity. *Ann. Rev. Immunol.* **10**, 123-151.
- Doms, R. W., and Helenius, A. (1986). Quaternary structure of influenza virus hemagglutinin after acid treatment. *J. Virol.* **60**, 833-839.
- Doms, R. W. (1993). Protein conformational changes in virus-cell fusion. *Methods Enzymol.* **221**, 61-82.
- Duff, K. C., and Ashley, R. H. (1992). The transmembrane domain of influenza A M2 protein forms amantadine-sensitive proton channels in planar lipid bilayers. *Virology* **190**, 485-489.
- Eisenlohr, L. C., Gerhard, W., and Hackett, C. J. (1987). Role of receptor-binding activity of the viral hemagglutinin molecule in the presentation of influenza virus antigens to helper T cells. *J. Virol.* **61**, 1375-1383.

- Ellens, H., Bentz, J., Mason, D., Zhang, F., and White, J. M. (1990). Fusion of influenza haemagglutinin-expressing fibroblasts with glycophorin-bearing liposomes: role of haemagglutinin surface density. *Biochem* **29**, 9697-9707.
- Elton, D., Medcalf, E., Bishop, K., and Digard, P. (1999). Oligomerization of the influenza virus nucleoprotein : identification of positive and negative sequence elements. *Virology* **260**, 190-200.
- Enami, K., Sato, T. A., Nakada, S., and Enami, M. (1994). Influenza virus NS1 protein stimulates translation of the M1 protein. *J. Virology* **68**, 1432-1437.
- Ennis, A. (1982). Some newly recognised aspects of resistance against and recovery from influenza. *Arch. Virology* **73**, 207-217.
- Fang, R., Min Jou, M., Huylebroeck, D., Devos, R., and Fiers, W. (1981). Complete structure of A/duck/Ukraine/63 influenza hemagglutinin gene : animal virus as progenitor of human H3 Hong Kong 1968 influenza haemagglutinin. *Cell* **25**, 315-323.
- Farrell, H. E., and Shellam, G. R. (1990). Characterization of neutralizing monoclonal antibodies to murine cytomegalovirus. *J. Gen. Virology* **71**, 655-664.
- Fitch, W. M., Leiter, J. M. E., Li, X., and Palese, P. (1991). Positive Darwinian evolution in human influenza A viruses. *Proc. Natl. Acad. Sci. USA* **88**, 4270-4274.
- Fleury, D., Barrère, B., Bizebard, T., Daniels, R. S., Skehel, J. J., and Knossow, M. (1999). A complex of influenza hemagglutinin with a neutralizing antibody that binds outside the virus receptor binding site. *Nature Struct. Biol.* **6**, 530-534.
- Flynn, D. C., Meyer, W. J., MacKenzie, J. M., and Johnston, R. E. (1990). A conformational change in Sindbis glycoproteins E1 and E2 is detected at the plasma membrane as a consequence of early virus-cell interaction. *J. Virology* **64**, 3643-3653.
- Fortes, P., Beloso, A., and Ortin, J. (1994). Influenza virus NS1 protein inhibits pre-messenger RNA splicing and blocks messenger RNA nucleocytoplasmic transport. *EMBO J.* **13**, 704-712.
- Frielle, D. W., Huang, D. D., and Youngner, J. S. (1984). Persistent infection with influenza A virus: evolution in virus mutants. *Virology* **138**, 103-107.
- Fujiyoshi, Y., Kume, N. P., Sakata, K., and Sato, S. B. (1994). Fine structure of influenza A virus observed by electron cryomicroscopy. *EMBO J.* **13**, 318-326.
- Gaudin, Y., Ruigrok, R. W. H., and Brunner, J. (1995). Low-pH induced conformational changes in viral fusion proteins: implications for the fusion mechanism. *J. Gen. Virology* **76**, 1541-1556.
- Gerhard, W., Mozdzanowska, K., Furchner, M., Washko, G., and Maiese, K. (1997). Role of the B-cell response in the recovery of mice from primary influenza virus infection. *Immunol. Revs.* **159**, 95-103.

- Gething, M. J., Bye, J., Skehel, J., and Wakefield, M. (1980). Cloning and DNA sequence of double stranded copies of haemagglutinin genes from H2 and H3 strains elucidates antigenic shift and drift in human influenza virus. *Nature (Lond.)* **287**, 301-306.
- Gething, M. J., Doms, R. W., York, D., and White, J. M. (1986a). Studies on the mechanism of membrane fusion: site-specific mutagenesis of the hemagglutinin of influenza virus. *J. Cell Biol.* **102**, 11-23.
- Gething, M.-J., McCammon, K., and Sambrook, J. (1986b). Expression of wild-type and mutant influenza virus hemagglutinin: the role of folding in intracellular transport. *Cell* **46**, 939-950.
- Glass, S. E., McGeoch, D. J., and Barry, R. D. (1975). Characterization of the mRNA of influenza virus. *J. Virol.* **16**, 1435-1443.
- Glick, G. D., and Knowles, J. R. (1991). Molecular recognition of bivalent sialosides by influenza virus. *J. Amer. Chem. Soc.* **113**, 4701-4703.
- Godley, L., Pfeifer, J., Steinhauer, D., Ely, B., Shaw, G., Kaufman, R., Suchanek, E., Pabo, C., Skehel, J. J., Wiley, D. C., and Wharton, S. (1992). Introduction of intersubunit disulfide bonds in the membrane-distal region of the influenza hemagglutinin abolishes membrane fusion activity. *Cell* **68**, 635-645.
- Gojobori, T., Moriyama, E. N., and Kimura, M. (1990). Molecular clock of viral evolution and the neutral theory. *Proc. Natl. Acad. Sci. USA* **87**, 10015-10018.
- Gollins, S., and Porterfield, J. S. (1986). A new mechanism for the neutralization of enveloped viruses by antiviral antibody. *Nature (Lond.)* **321**, 244-246.
- Gómez-Puertas, P. et al. (1996). Neutralizing antibodies to different proteins of African swine fever virus inhibit both virus attachment and internalization. *J. Virol.* **70**, 5689-5694.
- Gonchoroff, N. J., Kendal, A. P., Phillips, D. J., and Reimer, C. B. (1982). Immunoglobulin M and G antibody response to type- and subtype-specific antigens after primary and secondary exposures of mice to influenza A viruses. *Infect. Immun.* **35**, 510-517.
- González, S., and Ortín, J. (1999). Characterization of influenza virus PB1 protein binding to viral RNA : two separate regions of the protein contribute to the interaction domain. *J. Virol.* **73**, 631-637.
- Gorman, O. T., Bean, W. J., et al. (1991). Evolution of influenza virus A virus nucleoprotein genes: implications for the origins of H1N1 human and classical swine viruses. *J. Virol.* **65**, 3704-3714.
- Gottschalk, A. (1957). The specific enzyme of influenza virus and *Vibrio cholerae*. *Bioch. Biophys. Acta* **23**, 645-646.

- Grambas, S., and Hay, A. J. (1992). Maturation of the influenza A virus hemagglutinin - estimates of the pH encountered during transport and its regulation by the M2 protein. *Viol.* **190**, 11-18.
- Greenspan, D., Palese, P., and Krystal, M. (1988). Two nuclear location signals in the influenza virus NS1 non-structural protein. *J. Virol.* **62**, 3020-3026.
- Gregoriades, A., and Frangione, B. (1981). Insertion of influenza M protein into the viral lipid bilayer and localization of site of insertion. *J. Virol.* **40**, 323-328.
- Griffin, J. A., Basak, S., and Compans, R. W. (1983). Effects of hexose starvation and the role of sialic acid in influenza virus release. *Viol.* **125**, 324-334.
- Gubareva, L. V., Bethell, R., Hart, G. J., Murti, K. G., Penn, C. K., and Webster, R. G. (1996). Characterization of mutants of influenza A virus selected with the neuraminidase inhibitor 4-guanidino-neu5Ac2en. *J. Virol.* **70**, 1818-1827.
- Guinea, R., and Carrasco, L. (1995). Requirement for vacuolar proton-ATPase activity during entry of influenza virus into cells. *J. Virol.* **69**, 2306-2312.
- Gutman, O., Danieli, T., White, J. M., and Henis, Y. I. (1993). Effects of exposure to low pH on the lateral mobility of influenza hemagglutinin expressed at the cell surface. *Biochem* **32**, 101-106.
- Hagen, M., Chung, T. D. Y., Butcher, J. A., and Krystal, M. (1994). Recombinant influenza virus polymerase: requirement of both 5' and 3' viral ends for endonuclease activity. *J. Virol.* **68**, 1509-1515.
- Hansen, S. H., Sandvig, K., and Deurs, B. (1993). Clathrin and HA2 adaptors: effects of potassium depletion, hypertonic medium and cytosol acidification. *J. Cell Biol.* **121**, 61-72.
- Harris, L. J., Larson, S. B., Hasel, K. W., Day, J., Greenwood, A., and McPherson, A. (1992). The three-dimensional structure of an intact monoclonal antibody for canine lymphoma. *Nature (Lond.)* **360**, 369-372.
- Harter, C., James, P., Bächli, T., Semenza, G., and Brunner, J. (1989). Hydrophobic binding of the ectodomain of influenza hemagglutinin to membranes occurs through the "fusion peptide". *J. Biol. Chem.* **264**, 6459-6464.
- Hatada, E., Saito, S., and Fukuda, R. (1999). Mutant influenza viruses with a defective NS1 protein cannot block the activation of PKR in infected cells. *J. Virol.* **73**, 2425-2433.
- Hay, A. J. (1982). Characterisation of influenza virus RNA complete transcripts. *Viol.* **116**, 517-522.
- Hay, A. J., Wolstenholme, A. J., Skehel, J. J., and Smith, M. H. (1985). The molecular basis of the specific anti-influenza action of amantadine. *EMBO J.* **4**, 3021-3024.

- Hay, A. J. (1992). The action of adamantanamines against influenza A viruses: inhibition of the M2 ion channel protein. *Sem. Virol.* **3**, 21-30.
- Herget, M., and Scholtissek, C. (1993). A temperature-sensitive mutation in the acidic polymerase gene of an influenza A virus alters the regulation of viral protein synthesis. *J. Gen. Virol.* **74**, 1789-1794.
- Hernandez, L. D., Hoffman, L. R., Wolfsberg, T. G., and White, J. M. (1996). Virus-cell and cell-cell fusion. *Ann. Rev. Cell Dev. Biol.* **12**, 627-661.
- Heuser, J. (1989). Effects of cytoplasmic acidification on clathrin lattice morphology. *J. Cell Biol.* **108**, 401-411.
- Heuser, J. E., and Anderson, R. G. W. (1989). Hypertonic media inhibit receptor-mediated endocytosis by blocking clathrin-coated pit formation. *J. Cell Biol.* **108**, 389-400.
- Holsinger, L. J., Shaughnessy, M. A., Pinto, L. H., and Lamb, R. A. (1994). Analysis of the post-translational modification of the influenza virus M2 ion channel protein. *J. Virol.* **69**, 1219-1225.
- Hope-Simpson, R. E. (1981). The role of season in the epidemiology of influenza. *J. Hyg. (Cambridge)* **86**, 35-47.
- Hope-Simpson, R. E., and Golubev, D. B. (1987). The new concept of the epidemic process of influenza A virus. *Epidemiol. Infect.* **99**, 5-54.
- Hope-Simpson, R. E. (1992) "The transmission of epidemic influenza virus". Plenum Press, New York.
- Horimoto, T., and Kawaoka, Y. (1994). Reverse genetics provides direct evidence for a correlation of hemagglutinin cleavability and virulence of an avian influenza virus. *J. Virol.* **68**, 3120-3128.
- Horisberger, M. A. (1980). The large P proteins of influenza A viruses are composed of one acidic and two basic polypeptides. *Virol.* **107**, 302-305.
- Horne, R. W., Waterson, A. P., Wildy, P., and Farnham, A. E. (1960). The structure and composition of the myxoviruses. I Electron microscope studies of the structure of myxovirus particles by negative staining techniques. *Virol.* **11**, 79-98.
- Hsu, M.-T., Parvin, J. D., Gupta, S., Krystal, M., and Palese, P. (1987). Genomic RNAs of influenza viruses are held in a circular conformation in virions and in infected cells by a terminal panhandle. *Proc. Natl. Acad. Sci. USA* **84**, 8140-8144.
- Huang, R. T. C., Rott, R., Wahn, K., Klenk, H.-D., and Kohama, T. (1980). The function of the neuraminidase in membrane fusion induced by myxoviruses. *Virol.* **107**, 313-319.

- Huang, R. T. C., Rott, R., and Klenk, H. D. (1981). Influenza viruses cause haemolysis and fusion of cells. *Viol.* **110**, 243-247.
- Huang, R. T. C., Dietsch, E., and Rott, R. (1985). Further studies on the role of neuraminidase and the mechanism of low pH dependence in influenza virus-induced membrane fusion. *J. Gen. Virol.* **66**, 295-301.
- Huang, R. T. C., Lichtenberg, B., and Rick, O. (1996). Involvement of annexin V in the entry of influenza viruses and role of phospholipids in infection. *FEBS Letts.* **392**, 59-62.
- Hughey, P. G., Compans, R. W., Zebedee, S. L., and Lamb, R. A. (1992). Expression of the influenza A virus M2 protein is restricted to apical surfaces of polarized cells. *J. Virol.* **66**, 5542-5552.
- Hull, J. D., Gilmore, R., and Lamb, R. A. (1988). Integration of a small integral membrane protein, M2, of influenza virus into the endoplasmic reticulum: analysis of the internal signal-anchor domain of a protein with an ectoplasmic NH₂ terminus. *J. Cell Biol.* **106**, 1489-1498.
- Imai, M., Sugimoto, K., Okazaki, K., and Kida, H. (1998). Fusion of influenza virus with the endosomal membrane is inhibited by monoclonal antibodies to defined epitopes on the hemagglutinin. *Virus Res.* **53**, 129-139.
- Inglis, S. C., and Mahy, B. W. J. (1979). Polypeptides specified by the influenza virus genome. 3 Control of synthesis in infected cells. *Viol.* **95**, 154-164.
- Inglis, S. C. (1982). Inhibition of host protein synthesis and degradation of cellular mRNAs during infection by influenza and herpes simplex virus. *Mol. Cell. Biol.* **2**, 1644-1648.
- Ishida, N., and Ackermann, W. W. (1956). General characteristics of influenza virus: properties of the initial cell-virus complex. *J. Exp. Med.* **104**, 501-515.
- Ito, T., Couceiro, J. N. S. S., Kelm, S., Baum, L. G., Krauss, S., Castrucci, M. R., Donatelli, I., Kida, H., Paulson, J. C., Webster, R. G., and Kawaoka, Y. (1998). Molecular basis for the generation in pigs of influenza A viruses with pandemic potential. *J. Virol.* **72**, 7367-7373.
- Iwasaki, T., and Nozima, T. (1977). Defence mechanisms against primary influenza virus infection in mice. I The roles of interferon and neutralizing antibodies and thymus dependence of interferon and antibody production. *J. Immunol.* **118**, 256-263.
- Jackson, D. C., and Webster, R. G. (1982). A topographic map of the enzyme active center and antigenic sites on the neuraminidase of influenza virus A/Tokyo/3/67 (H2N2). *Viol.* **123**, 69-77.
- Jackson, D. C., Tang, X.-L., Murti, K. G., Webster, R. G., Tregear, G. W., and Bean, W. J. (1991). Electron microscopic evidence for the association of M2 protein with the influenza virion. *Arch. Virol.* **118**, 199-207.

- Jackson, N. A. C. (1998) "Properties and mechanism of action of a 17-amino acid V3-loop specific HIV-1 neutralizing miniantibody," Ph.D. Thesis, Univ of Warwick.
- Jackson, N. A. C., Levi, M., Wahren, B., and Dimmock, N. J. (1999). Properties and mechanism of action of a 17 amino acid, V3 loop-specific microantibody that binds to and neutralizes HIV-1 virions. *J. Gen. Virol.* **80**, 225-236.
- Jones, I. M., Reay, P. A., and Philpott, K. L. (1986). Nuclear location of three influenza polymerase proteins and a nuclear signal in polymerase PB2. *EMBO J.* **5**, 2371-2376.
- Junankar, P. R., and Cherry, R. J. (1986). Temperature and pH dependence of the haemolytic activity of influenza virus and of the rotational mobility of the spike protein. *Bioch. Biophys. Acta* **854**, 198-206.
- Kates, M., Allison, A. C., Tyrrell, D. A. J., and James, A. T. (1961). Lipids of influenza virus and their relation to those of the host cell. *Bioch. Biophys. Acta* **52**, 455-466.
- Katze, M. G., de Corato, D., and Krug, R. M. (1986). Cellular mRNA translation is blocked at both initiation and elongation by influenza virus or adenovirus. *J. Virol.* **60**, 1027-1039.
- Kavaler, J., Caton, A. J., Staudt, L. M., Schwartz, D., and Gerhard, W. (1990). A set of closely related antibodies dominates the primary antibody response to the antigenic site Cb of the A/PR/8/34 influenza virus hemagglutinin. *J. Immunol.* **145**, 2312-2321.
- Kaverin, N. V., Gambaryan, A. S., Bovin, N. V., Rudneva, I. A., Shilov, A. A., Khodova, O. M., Varich, N. L., Sinitsin, B. V., Makarova, N. V., and Kropotkina, E. A. (1998). Post-reassortment changes in influenza A virus hemagglutinin restoring HA-NA functional match. *Virol.* **244**, 315-321.
- Kawakami, K., Mizumoto, K., Ishihama, A., and Shinozaki-Yamaguchi, K. (1985). Activation of influenza virus RNA polymerase by cap structure (m7GpppNm). *J. Biochem.* **97**, 655-661.
- Kawaoka, Y., and Webster, R. G. (1988). Sequence requirements for cleavage activation of influenza virus hemagglutinin expressed in mammalian cells. *Proc. Natl. Acad. Sci. USA* **85**, 324-328.
- Kawaoka, Y., Krauss, S., and Webster, R. G. (1989). Avian to human transmission of the PB1 gene of influenza viruses in the 1957 and 1968 epidemics. *J. Virol.* **63**, 4603-4608.
- Kemble, G. W., Bosian, D. L., Rose, J., Wilson, I. A., and White, J. M. (1992). Intermonomer disulfide bonds impair the fusion activity of influenza virus hemagglutinin. *J. Virol.* **66**, 4940-4950.

- Kemble, G. W., Danieli, T., and White, J. M. (1994). Lipid anchored influenza hemagglutinin promotes hemifusion, not complete fusion. *Cell* **76**, 383-391.
- Kemler, I., Whittaker, G., and Helenius, A. (1994). Nuclear import of microinjected influenza virus ribonucleoproteins. *Viol.* **202**, 1028-1033.
- Kida, H., Webster, R. G., and Yanagawa, R. (1983). Inhibition of virus-induced hemolysis with monoclonal antibodies to different antigenic areas of the hemagglutinin molecule of A/Seal/Massachusetts/1/80 (H7N7) influenza virus. *Arch. Virol.* **76**, 91-99.
- Kida, H., Yoden, S., Kuwabara, M., and Yanagawa, R. (1985). Interference with a conformational change in the HA molecule of influenza virus by antibodies as a possible neutralization mechanism. *Vaccine* **3**, 219-222.
- Kida, H., Kawaoka, Y., Naeve, C. W., and Webster, R. G. (1987). Antigenic and genetic conservation of H3 influenza virus in wild ducks. *Viol.* **159**, 109-119.
- Kido, H., Yokogoshi, Y., Sakai, K., Tashiro, M., Kishino, Y., Fukutomi, A., and Katunuma, N. (1992). Isolation and characterization of a novel trypsin-like protease found in rat bronchiolar epithelial Clara cells. *J. Biol. Chem.* **267**, 13573-13579.
- Kilbourne, E. D., and Murphy, J. S. (1960). Genetic studies of influenza viruses. I. Viral morphology and growth capacity as exchangeable genetic traits. Rapid in ovo adaptation of early passage Asian strain isolates by combination with PR8. *J. Exp. Med.* **111**, 387-406.
- Kilbourne, E. D., Laver, W. G., Schulman, J. L., and Webster, R. G. (1968). Antiviral activity of antiserum specific for an influenza virus neuraminidase. *J. Virol.* **2**, 281-288.
- Kilbourne, E. D. (1987) "Influenza". Plenum Medical Book Co., New York.
- Kingsbury, D. W., and Webster, R. G. (1969). Some properties of influenza virus nucleocapsids. *J. Virol.* **4**, 219-225.
- Kitson, J. D. A., Burke, K. L., Pullen, L. A., Belsham, G. J., and Almond, J. W. (1991). Chimeric polioviruses that include sequences derived from two independent antigenic sites of foot-and-mouth disease virus (FMDV) induce neutralizing antibodies against FMDV in guinea pigs. *J. Virol.* **65**, 3068-3075.
- Kjellén, L. (1985). A hypothesis accounting for the effect of the host cell on neutralization-resistant virus. *J. Gen. Virol.* **66**, 2279-2283.
- Klasse, P. J., and Moore, J. P. (1996). Quantitative model of antibody- and soluble CD4-mediated neutralization of primary strains and T-cell line-adapted strains of human immunodeficiency virus type 1. *J. Virol.* **70**, 3668-3677.
- Klenk, H.-D., and Rott, R. (1988). The molecular basis of influenza virus pathogenicity. *Adv. Virus Res.* **34**, 247-281.

- Klimov, A.L., Rocha, E., Hayden, F.G., Shult, P.A., Roumillat, L.F., and Cox, N.J. (1995). Prolonged shedding of amantadine-resistant influenza A viruses by immunodeficient patients: detection by polymerase chain reaction-restriction analysis. *J. Infect. Dis.* **172**: 1352
- Kobasa, D., Kodihalli, S., Luo, M., Castrucci, M. R., Donatelli, I., Suzuki, Y., and Kawaoka, Y. (1999). Amino acid residues contributing to the substrate specificity of the influenza A virus neuraminidase. *J. Virol.* **73**, 6743-6751.
- Kobayashi, M., Toyoda, T., and Ishihama, A. (1996). Influenza virus PB1 protein is the minimal and essential subunit of RNA polymerase. *Arch. Virol.* **141**, 525-539.
- Koff, W. C., and Knight, V. (1979). Inhibition of influenza virus uncoating by rimantidine hydrochloride. *J. Virol.* **31**, 261-263.
- Korte, T., Ludwig, K., Booy, F. P., Blumenthal, R., and Herrmann, A. (1999). Conformational intermediates and fusion activity of influenza virus haemagglutinin. *J. Virol.* **73**, 4567-4574.
- Kretzschmar, E., Bui, M., and Rose, J. K. (1996). Membrane association of influenza virus matrix protein does not require specific hydrophobic domains or the viral glycoproteins. *Virol.* **220**, 37-45.
- Krug, R. M., and Etkind, P. R. (1973). Cytoplasmic and nuclear specific proteins in influenza virus infected MDCK cells. *Virol.* **56**, 334-348.
- Kühn, L. C., and Kraehenbuhl, J.-P. (1981). The membrane receptor for polymeric immunoglobulin is structurally related to secretory component. *J. Biol. Chem.* **256**, 12490.
- Lafferty, K. J. (1963b). The interaction between virus and antibody. II Mechanism of the reaction. *Virol.* **21**, 76-90.
- Lamarre, A., and Talbot, P. J. (1995). Protection from lethal coronavirus infection by immunoglobulin fragments. *J. Immunol.* **154**, 3975-3984.
- Lamb, R. A., and Choppin, P. W. (1976). Synthesis of influenza viral proteins in infected cells: translation of viral polypeptides, including three P polypeptides, from RNA produced by primary transcription. *Virol.* **74**, 504-519.
- Lamb, R. A., and Lai, C. J. (1982). Spliced and unspliced messenger RNAs synthesised from cloned influenza virus M DNA in SV40 vector: expression of the influenza membrane protein (M1). *Virol.* **123**, 237-256.
- Lamb, R. A., and Choppin, P. W. (1983). The gene structure and replication of influenza virus. *Ann. Rev. Biochem.* **52**, 467-506.
- Lamb, R. A., Zebedee, S. L., and Richardson, C. D. (1985). Influenza M2 protein is an integral membrane protein expressed on the infected-cell surface. *Cell* **40**, 627-633.

- Lamb, R. A., and Krug, R. M. (1996) "Orthomyxoviridae : The viruses and their replication", Third ed., Vol. 1. Lippencott - Raven, Philadelphia.
- Lambkin, R. L. (1994) "The selection of influenza A virus escape mutants by antiserum," Ph.D. Dissertation, Univ. of Warwick.
- Lambkin, R., and Dimmock, N. J. (1995). All rabbits immunized with type A influenza virions have a serum antibody haemagglutination-inhibition antibody response biased to a single epitope in antigenic site B. *J. Gen. Virol.* **76**, 889-897.
- Laver, W. G., and Valentine, R. C. (1969). Morphology of the isolated haemagglutinin and neuraminidase sub-units of influenza virus. *Virol.* **38**, 105-119.
- Lazarowitz, S. G., Compans, R.W., Choppin, P.W. (1971). Influenza virus structural and non-structural proteins in infected cells and their plasma membranes. *Virol.* **46**, 830-843.
- Lazarowitz, S. G., and Choppin, P. W. (1975). Enhancement of the infectivity of influenza A and B viruses by proteolytic cleavage of the hemagglutinin polypeptide. *Virol.* **68**, 440-454.
- Le Comte, J., and Oxford, J. S. (1981). Detection of antigenic variation of influenza A matrix protein by a competitive radioimmunoassay. *J. Gen. Virol.* **57**, 403-408.
- Lee, J., and Lentz, B. R. (1997). Evolution of lipidic structures during model membrane fusion and the relation of this process to cell membrane fusion. *Biochem* **36**, 6251-6259.
- Lentz, M. R., Webster, R. G., and Air, G. M. (1987). Site-directed mutation of the active site of influenza neuraminidase and implications for the catalytic mechanism. *Biochem* **26**, 5321-5358.
- Li, M. L., Ramirez, B. C., and Krug, R. M. (1998). RNA-dependent activation of primer RNA production by influenza virus polymerase : different regions of the same protein subunit constitute the two required RNA-binding sites. *EMBO J.* **17**, 5844-5852.
- Licheng, S., Summers, D. F., Peng, Q., and Galarza, J. M. (1995). Influenza A virus polymerase subunit PB2 is the endonuclease which cleaves host cell mRNA and functions only as a trimeric enzyme. *Virol.* **208**, 38-47.
- Lindau, M., and Almers, W. (1995). Structure and function of fusion pores in exocytosis and ectoplasmic membrane fusion. *Curr. Op. Cell Biol.* **7**, 509-517.
- Liu, C. G., Eichelberger, M. C., Compans, R. W., and Air, G. M. (1995). Influenza type A virus neuraminidase does not play a role in viral entry, replication, assembly, or budding. *J. Virol.* **69**, 1099-1106.
- Lu, Y., Qian, X.-Y., and Krug, R. M. (1994). The influenza virus NS1 protein: a novel inhibitor of pre-mRNA splicing. *Genes Dev.* **8**, 1817-1828.

- Lu, Y., Wambach, M., Katze, M. G., and Krug, R. M. (1995). Binding of the influenza virus NS1 protein to double-stranded RNA inhibits the activation of the protein kinase that phosphorylates the eLF-2 translation initiation factor. *Virology* **214**, 222-228.
- Luo, G., Chung, L., and Palese, P. (1993). Alterations of the stalk of the influenza virus neuraminidase: deletions and insertions. *Virus Research* **29**, 141-153.
- Marsh, M. (1984). The entry of animal viruses into cells by endocytosis. *Biochemistry Journal* **218**, 1-10.
- Marsh, M., and Helenius, A. (1989). Virus entry into animal cells. *Advances in Virus Research* **36**, 107-151.
- Martin, K., and Helenius, A. (1991a). Nuclear transport of influenza virus ribonucleoproteins: the viral matrix protein (M1) promotes export and inhibits import. *Cell* **67**, 117-130.
- Martin, K., and Helenius, A. (1991b). Transport of incoming nucleocapsids into the nucleus. *Journal of Virology* **65**, 232-244.
- Masurel, N., and Marine, W. M. (1973). Recycling of Asian and Hong Kong influenza A virus hemagglutinins in man. *American Journal of Epidemiology* **97**, 44-49.
- Matlin, K. S., Reggio, H., Helenius, A., and Simons, K. (1981). Infectious entry pathway of influenza virus in a canine kidney cell line. *Journal of Cell Biology* **91**, 601-613.
- Matrosovich, M., Zhou, N., Kawaoka, Y., and Webster, R. (1999). The surface glycoproteins of H5 influenza viruses isolated from humans, chickens, and wild aquatic birds have distinguishable properties. *Journal of Virology* **73**, 1146-1155.
- Mbawuike, I. N., Pacheco, S., Acuna, C. L., Switzer, K. C., Zhang, Y., and Harriman, G. R. (1999). Mucosal immunity to influenza without IgA: an IgA knockout mouse model. *Journal of Immunology* **162**, 2530-2537.
- McInerney, T. L., McLain, L., Armstrong, S. J., and Dimmock, N. J. (1997). A human IgG1 (b12) specific for the CD4 binding site of HIV-1 neutralizes by inhibiting the virus fusion entry process, but b12 Fab neutralizes by inhibiting a post-fusion event. *Virology* **233**, 313-326.
- McKimm-Breschkin, J. L., McDonald, M., Blick, T. J., and Colman, P. M. (1996). Mutation in the influenza virus neuraminidase gene resulting in decreased sensitivity to the neuraminidase inhibitor 4-guanidino-Neu5Ac2en leads to instability of the enzyme. *Virology* **225**, 240-242.
- McKimm-Breschkin, J. L., Sahasrabudhe, A., Blick, T. J., McDonald, M., Colman, P. M., Hart, G. J., Bethell, R. C., and Varghese, J. N. (1998). Mutations in a conserved residue in the influenza virus neuraminidase active site decreases sensitivity to Neu5Ac2en-derived inhibitors. *Journal of Virology* **72**, 2456-2462.

- McLain, L., and Dimmock, N. J. (1989). Protection of mice from lethal influenza by adoptive transfer of non-neutralizing haemagglutination-inhibiting IgG obtained from the lungs of infected animals treated with defective-interfering virus. *J. Gen. Virol.* **70**, 2615-2624.
- McLain, L., and Dimmock, N. J. (1994). Single- and multi-hit kinetics of immunoglobulin G neutralization of human immunodeficiency virus type 1 by monoclonal antibodies. *J. Gen. Virol.* **75**, 1457-1460.
- Meier-Ewert, H., and Compans, R. W. (1974). Time course of synthesis and assembly of influenza virus proteins. *J. Virol.* **14**, 1083-1091.
- Melikyan, G. B., Niles, W. D., and Cohen, F. S. (1993a). Influenza virus haemagglutinin-induced cell-planar bilayer fusion - quantitative dissection of fusion pore kinetics into stages. *J. Gen. Physiol.* **102**, 1151-1170.
- Melikyan, G. B., Niles, W. D., Peeples, M. E., and Cohen, F. S. (1993b). Influenza haemagglutinin-mediated fusion pores connecting cells to planar membranes - flickering to final expansion. *J. Gen. Physiol.* **102**, 1131-1149.
- Melikyan, G. B., White, J. M., and Cohen, F. S. (1995). GPI-anchored influenza hemagglutinin induces hemifusion to both red blood cell and planar bilayer membranes. *J. Cell Biol.* **131**, 679-691.
- Mellman, I. (1996). Endocytosis and molecular sorting. *Ann. Rev. Cell Dev. Biol.* **12**, 575-625.
- Mena, I., Jambrina, E., Albo, C., Perales, B., Ortín, J., Arrese, M., Vallejo, D., and Portela, A. (1999). Mutational analysis of influenza A virus nucleoprotein : identification of mutations that affect RNA replication. *J. Virol.* **73**, 1186-1194.
- Metzger, H. (1978). The IgE-mast cell system as a paradigm for the study of antibody mechanisms. *Immunol. Revs.* **41**, 186.
- Millar, B. M. G., Calder, L. J., Skehel, J. J., and Wiley, D. C. (1999). Membrane fusion by surrogate receptor-bound influenza haemagglutinin. *Virol.* **257**, 415-423.
- Miller, N., and Hutt-Fletcher, L. M. (1988). A monoclonal antibody to glycoprotein gp85 inhibits fusion but not attachment of Epstein-Barr virus. *J. Virol.* **62**, 2366-2372.
- Mims, C. A., and White, D. O. (1984) "Viral pathogenesis and immunology". Blackwell Scientific Publications, Oxford.
- Mitchell, G. F. (1979). Responses to infection with metazoan and protozoan parasites in mice. *Adv. Immunol.* **28**, 451.
- Mitnaul, L. J., Castrucci, M. R., Murti, K. G., and Kawaoka, Y. (1996). The cytoplasmic tail of influenza A virus neuraminidase (NA) affects NA incorporation into virions, virion morphology, and virulence in mice but is not essential for virus replication. *J. Virol.* **70**, 873-879.

- Morris, S. J., Sarkar, D. P., White, J. M., and Blumenthal, R. (1989). Kinetics of the pH-dependent fusion between 3T3 fibroblasts expressing influenza hemagglutinin and red blood cells. Measurement by dequenching of fluorescence. *J. Biol. Chem.* **264**, 3972-3978.
- Moser, M. R., Bender, T. R., Margolis, H. S., Noble, G. R., Kendal, A. P., and Ritter, D. G. (1979). An outbreak of influenza aboard a commercial airliner. *J. Epidemiol.* **110**, 1-6.
- Mozdzanowska, K., Furchner, M., Washko, G., Mozdzanowska, M., and Gerhard, W. (1997). A pulmonary influenza virus infection in SCID mice can be cured by treatment with hemagglutinin-specific antibodies that display very low virus-neutralizing activity in vitro. *J. Virol.* **71**, 4347-4355.
- Mozdzanowska, K., Maiese, K., Furchner, M., and Gerhard, W. (1999). Treatment of influenza virus-infected SCID mice with non-neutralizing antibodies specific for the transmembrane proteins matrix 2 and neuraminidase reduces the pulmonary virus titre but fails to clear the infection. *Virol.* **254**, 138-146.
- Mukaigawa, Y., and Nayak, D. P. (1991). Two signals mediate nuclear localization of influenza virus (A/WSN/33) polymerase basic protein 2. *J. Virol.* **65**, 245-253.
- Murphy, B. R., Nelson, D. L., Wright, P. F., Tierney, E. L., Phelan, M. A., and Chanock, R. M. (1982). Secretory and systemic immunological response in children infected with live attenuated influenza A virus vaccines. *Infect. Immun.* **36**, 1102-1108.
- Murphy, B. R., and Clements, M. L. (1989). The systemic and mucosal immune response of humans to influenza virus A. *Curr. Topics Microbiol. Immunol.* **146**, 107-116.
- Murphy, B. R., and Webster, R. G. (1996) "Orthomyxoviruses", Third ed., Vol. 1. Lippencott - Raven, Philadelphia.
- Murti, K. G., and Webster, R. G. (1986). Distributions of hemagglutinin and neuraminidase on influenza virions as revealed by electron microscopy. *Virol.* **149**, 36-43.
- Murti, K. G., Brown, P. S., Bean, W. J., and Webster, R. G. (1992). Composition of the helical internal components of influenza virus as revealed by immunological labeling/electron microscopy. *Virol.* **186**, 294-299.
- Nakagawa, Y., Kimura, N., Toyoda, T., Mizumoto, T., Ishihama, A., Oda, K., and Nakada, S. (1995). The RNA polymerase PB2 subunit is not required for replication of the influenza virus genome but is involved in capped mRNA synthesis. *J. Virol.* **69**, 728-733.
- Nakagawa, Y., Oda, K., and Nakada, S. (1996). The PB1 subunit alone can catalyze cRNA synthesis, and the PA subunit in addition to the PB1 subunit is required for viral RNA synthesis in replication of the influenza virus genome. *J. Virol.* **70**, 6390-6394.

- Nakajima, K., Desselberger, U., and Palese, P. (1978). Recent human influenza A (H1N1) viruses are closely related to strains isolated in 1950. *Nature (Lond.)* **274**, 334-339.
- Nath, S. T., and Nayak, D. P. (1990). Function of two discrete regions is required for nuclear localization of polymerase protein basic protein 1 of A/WSN/33 influenza virus (H1N1). *J. Virol.* **10**, 4139-4145.
- Nermut, M. V., and Frank, H. (1971). Fine structure of influenza A2 (Singapore) as revealed by negative staining, freeze-drying and freeze-etching. *J. Gen. Virol.* **10**, 37-51.
- Neumann, G., Castrucci, M. R., and Kawaoka, Y. (1997). Nuclear import and export of influenza virus nucleoprotein. *J. Virol.* **71**, 9690-9700.
- Nieto, A., de la Luna, S., Bárcena, J., Portela, A., and Ortín, J. (1994). Complex structure of the nuclear translocation signal of influenza virus polymerase PA subunit. *J. Gen. Virol.* **75**, 29-36.
- Niles, W. D., and Cohen, F. S. (1993). Single event recording shows that docking onto receptor alters the kinetics of membrane fusion mediated by influenza hemagglutinin. *Biophys. J.* **65**, 171-176.
- Nishikawa, F., and Sugiyama, T. (1983). Direct isolation of H1N2 recombinant virus from a throat swab etc. *J. Clin. Microbiol.* **18**, 425-427.
- Nisonoff, A., Hooper, J. E., and Spring, S. B., Eds. (1975a) "The Antibody Molecule". Academic Press Inc. New York, .
- Nunes-Correia, I., Ramalho-Santos, J., Nir, S., and Pedroso de Lima, M. C. (1999). Interactions of influenza virus with cultured cells: detailed kinetic modeling of binding and endocytosis. *Biochem* **38**, 1095-1101.
- Ohizumi, Y., Suzuki, H., Matsumoto, Y.-I., Mashuo, Y., and Numazaki, Y. (1992). Neutralizing mechanisms of two human monoclonal antibodies against human cytomegalovirus glycoprotein 130/55. *J. Gen. Virol.* **73**, 2705-2707.
- Oi, V. T., Vuong, T. M., Hardy, R., Reidler, J., Dengl, J., Herzenberg, L. A., and Stryer, L. (1984). Correlation between segmental flexibility and effector function of antibodies. *Nature (Lond.)* **307**, 136-140.
- O'Neill, R. E., Jaskunas, R., Blobel, G., Palese, P., and Moroianu, J. (1995). Nuclear import of influenza virus RNA can be mediated by viral nucleoprotein and transport factors required for protein import. *J. Biol. Chem.* **270**, 22701-22704.
- O'Neill, R. E., Talon, J., and Palese, P. (1998). The influenza virus NEP (NS2 protein) mediates the nuclear export of viral ribonucleoproteins. *EMBO J.* **17**, 288-296.

- Osiowy, C., and Anderson, R. (1995). Neutralization of respiratory syncytial virus after cell attachment. *J. Virol.* **69**, 1271-1274.
- Otto, M., Günther, A., Fan, H., Rick, O., and Huang, R. T. C. (1994). Identification of annexin 33kda in cultured cells as a binding protein of influenza virus. *FEBS Letts.* **356**, 125-129.
- Outlaw, M. C. (1989) "Neutralization of influenza virus on respiratory epithelial cells," Ph.D. Dissertation, Dept. Biological Sciences, Univ. of Warwick.
- Outlaw, M. C., Armstrong, S. J., and Dimmock, N. J. (1990). Mechanisms of neutralization of influenza virus vary according to IgG concentration. *Virol.* **178**, 478-485.
- Outlaw, M. C., and Dimmock, N. J. (1990). Mechanisms of neutralization of influenza virus on mouse tracheal epithelial cells by mouse monoclonal polymeric IgA and polyclonal IgM directed against the viral haemagglutinin. *J. Gen. Virol.* **71**, 69-76.
- Outlaw, M. C., and Dimmock, N. J. (1993). IgG-neutralization of type A influenza viruses and the inhibition of the endosomal fusion stage of the infectious pathway. *Virol.* **195**, 413-421.
- Padlan, E. A. (1994). Anatomy of the antibody molecule. *Mol. Immunol.* **31**, 169-217.
- Pak, C. C., Krumbiegel, M., and Blumenthal, R. (1994). Intermediates in influenza virus PR/8 hemagglutinin-induced membrane fusion. *J. Gen. Virol.* **75**, 395-399.
- Palese, P., Tobita, K., Ueda, M., and Compans, R. W. (1974). Characterization of temperature sensitive influenza virus mutants defective in neuraminidase. *Virol.* **61**, 397-410.
- Palese, P., and Young, J. F. (1982). Variation of influenza A, B and C viruses. *Science* **215**, 1468-1478.
- Palladino, G., Mozdzanowska, K., Washko, G., and Gerhard, W. (1995). Virus-neutralizing antibodies of immunoglobulin G (IgG) but not of IgM or IgA isotypes can cure influenza virus pneumonia in SCID mice. *J. Virol.* **69**, 2075-2081.
- Palokangas, H., Metsikkö, K., and Väänänen, K. (1994). Active vacuolar H⁺ATPase is required for both endocytic and exocytic processes during viral infection of BHK-21 cells. *J. Biol. Chem.* **269**, 17577-17585.
- Parham, P. (1983). On the fragmentation of monoclonal IgG1, IgG2a, and IgG2b from BALB/c mice. *J. Immunol.* **131**, 2895-2902.
- Parren, P. W. H. I., Mondor, I., Naniche, D., Ditzel, H. J., Klasse, P. J., Burton, D. R., and Sattentau, Q. J. (1998). Neutralization of human immunodeficiency virus type 1 by antibody to gp120 is determined primarily by occupancy of sites on the virion irrespective of epitope specificity. *J. Virol.* **72**, 3512-3519.

- Patterson, S., and Oxford, J. S. (1986). Early interactions between animal viruses and the host cell: relevance to viral vaccines. *Vaccine* **4**, 78-89.
- Patterson, S., Gross, J., and Oxford, J. S. (1988). The intracellular distribution of influenza virus matrix protein and nucleoprotein in infected cells and their relationship to haemagglutinin in the plasma membrane. *J. Gen. Virol.* **69**, 1859-1872.
- Perales, B., and Ortin, J. (1997). The influenza A virus PB2 polymerase subunit is required for the replication of viral RNA. *J. Virol.* **71**, 1381-1385.
- Petri, T., and Dimmock, N. J. (1981). Phosphorylation of influenza virus nucleoprotein *in vivo*. *J. Gen. Virol.* **57**, 185-190.
- Pinto, L. H., Holsinger, L. J., and Lamb, R. A. (1992). Influenza virus M2 protein has ion channel activity. *Cell* **69**, 517-528.
- Plotch, S. J., and Krug, R. M. (1977). Influenza virion transcriptase: synthesis *in vitro* of large polyadenylic acid-containing complementary RNA. *J. Virol.* **21**, 24-34.
- Plotch, S. J., Bouloy, M., and Krug, R. M. (1979). Transfer of 5' terminal cap of a globin mRNA to influenza viral complementary RNA during transcription *in vitro*. *Proc. Natl. Acad. Sci. USA* **76**, 1618-1622.
- Plotch, S. J., Bouloy, M., Ulmanen, I., and Krug, R. M. (1981). A unique cap (m⁷GpppXm)-dependent influenza virion endonuclease cleaves capped mRNAs to generate the primers that initiate viral mRNA transcription. *Cell* **23**, 847-858.
- Pons, M. W., Schulze, I. T., and Hirst, G. K. (1969). Isolation and characterization of the ribonucleoprotein of influenza virus. *Virology* **39**, 250-259.
- Pons, M. W. (1971). Isolation of influenza virus ribonucleoprotein from infected cells. Demonstration of the presence of negative-stranded RNA in viral RNP. *Virology* **46**, 149-160.
- Possee, R. D., Schild, G. C., and Dimmock, N. J. (1982). Studies on the mechanism of neutralization of influenza virus by antibody: evidence that neutralizing antibody (anti-haemagglutinin) inactivates influenza virus by inhibiting virion transcriptase activity. *J. Gen. Virol.* **58**, 373-386.
- Poumbourios, P., Brown, L., White, D. O., and Jackson, D. C. (1990). The stoichiometry of binding between monoclonal antibody molecules and the hemagglutinin of influenza virus. *Virology* **179**, 768-776.
- Pritchett, T. J., and Paulson, J. C. (1989). Basis for the potent inhibition of influenza virus infection by equine and guinea pig α_2 -macroglobulin. *J. Biol. Chem.* **264**, 9850-9858.
- Pritchett, T. J., Brossmer, R., Rose, U., and Paulson, J. C. (1987). Recognition of monovalent sialosides by influenza virus H3 hemagglutinin. *Virology* **160**, 502-506.

- Pritlove, D. C., Poon, L.M., Fodor, E., Sharps, J., and Brownlee, G.G. (1998). Polyadenylation of influenza virus mRNA transcribed in vitro from model virion RNA templates: requirement for 5' conserved sequences. *J. Virol.* **72**, 1280-1286.
- Pritlove, D. C., Poon, L. L. M., Devenish, L. J., Leahy, M. B., and Brownlee, G. G. (1999). A hairpin loop at the 5' end of influenza A virus virion RNA is required for synthesis of poly(A)⁺ mRNA in vitro. *J. Virol.* **73**, 2109-2114.
- Privalsky, M. L., and Penhoet, E. E. (1977). Phosphorylated protein components present in influenza virions. *J. Virol.* **24**, 401-405.
- Privalsky, M. L., and Penhoet, E. E. (1981). The structure and synthesis of influenza virus phosphoproteins. *J. Biol. Chem.* **256**, 5368-5376.
- Prokudinakantorovich, E. N., and Semenova, N. P. (1996). Intracellular oligomerization of influenza virus nucleoprotein. *Virol.* **223**, 51-56.
- Puri, A., Booy, F. P., Doms, R. W., White, J. M., and Blumenthal, R. (1990). Conformational changes and fusion activity of influenza virus hemagglutinin of the H2 and H3 subtypes: effects of acid pretreatment. *J. Virol.* **64**, 3824-3832.
- Qian, X.-Y., Alonso-Capien, F., and Krug, R. M. (1994). Two functional domains of the influenza virus NS1 protein are required for regulation of nuclear export of mRNA. *J. Virol.* **68**, 2433-2441.
- Qiu, Y., and Krug, R. M. (1994). The influenza virus NS1 protein is a poly(A)-binding protein that inhibits nuclear export of mRNAs containing poly(A). *J. Virol.* **68**, 2425-2432.
- Qiu, Y., Nemeroff, M., and Krug, R. M. (1995). The influenza virus NS1 protein binds to a specific region in human U6 snRNA and inhibits U6-U2 and U6-U4 snRNA interactions during splicing. *RNA* **1**, 304-316.
- Rees, P. J., and Dimmock, N. J. (1981). Electrophoretic separation of influenza virus ribonucleoproteins. *J. Gen. Virol.* **53**, 125-132.
- Reginster, M., and Nermut, M. V. (1976). Preparation and characterization of influenza virus cores. *J. Gen. Virol.* **31**, 211-220.
- Reid, A. H., Fanning, T. G., Hultin, J. V., and Taubenberger, J. K. (1999). Origin and evolution of the 1918 "Spanish" influenza virus hemagglutinin gene. *Proc. Natl. Acad. Sci. USA* **96**, 1651-1656.
- Richardson, J. C., and Akkina, R. K. (1991). NS2 protein of influenza virus is found in purified virus and phosphorylated in infected cells. *Arch. Virol.* **116**, 69-80.
- Richman, D. D., Hostetler, K. Y., Yazaki, P. J., and Clark, S. (1986). Fate of influenza A virion proteins after entry into subcellular fractions of LLC cells and the effect of amantadine. *Virol.* **151**, 200-210.

- Rieber, E. P., Federle, C., Reiter, C., Krauss, S., Gürtler, L., Eberle, J., Deinhardt, F., and Riethmüller, G. (1992). The monoclonal CD4 antibody M-T413 inhibits cellular infection with human immunodeficiency virus after viral attachment to the cell membrane: an approach to postexposure prophylaxis. *Proc. Natl. Acad. Sci. USA* **89**, 10792-10796.
- Rigg, R. J., Carver, A. S., and Dimmock, N. J. (1989). IgG-neutralized influenza virus undergoes primary, but not secondary uncoating *in vivo*. *J. Gen. Virol.* **70**, 2097-2109.
- Roberts, P. C., Lamb, R. A., and Compans, R. W. (1998). The M1 and M2 proteins of influenza A virus are important determinants in filamentous particle formation. *Virol.* **240**, 127-137.
- Robinson, J. H., Easterday, B. C., and Tumova, B. (1979). Influence of environmental stress on avian influenza virus infection. *Avian. Dis.* **23**, 346-353.
- Rocha, E., Cox, N.J., Black, R.A., Harmon, M.W., Harrison, C.J., Kendal, A.P. (1991). Antigenic and genetic variation in influenza A (H1N1) virus isolates recovered from a persistently infected immunodeficient child. *J. Virol.* **65**, 2340-2350.
- Roehrig, J. T., Hunt, A. R., Kinney, R. M., and Mathews, J. H. (1988). *In vitro* mechanisms of monoclonal antibody neutralization of alphaviruses. *Virol.* **165**, 66-73.
- Rogers, G. N., and Paulson, J. C. (1983). Receptor determinants of human and animal influenza virus isolates: differences in receptor specificity of the H3 hemagglutinin based on species of origin. *Virol.* **127**, 361-373.
- Rogers, G. N., Paulson, J. C., Daniels, R. S., Skehel, J. J., Wilson, I. A., and Wiley, D. C. (1983). Single amino acid substitutions in influenza haemagglutinin change receptor binding specificity. *Nature (Lond.)* **304**, 76-78.
- Rogers, G. N., Daniels, R. S., and Skehel, J. J. (1985). Host-mediated selection of influenza virus receptor variants. Sialic acid α 2,6 gal-specific clones of A/duck/Ukraine/1/63 revert to sialic acid α 2,3 gal-specific wildtype *in ovo*. *J. Biol. Chem.* **260**, 7362-7367.
- Rohm, C. et al. (1996). Characterization of a novel influenza hemagglutinin, H15: criteria for determination of influenza A subtypes. *Virol.* **217**, 508-516.
- Roitt, I., Brostoff, J., and Male, D., Eds. (1993) "Immunology", 3rd ed. Mosby, London.
- Rota, P. A., Rocha, E. P., Harmon, M. W., Hinshaw, V. S., Sheerar, M. G., Kawaoka, Y., Cox, N. J., and Smith, T. F. (1989). Laboratory characterization of a swine influenza virus isolated from a fatal case of human influenza. *J. Clin. Microbiol.* **27**, 1413-1416.
- Ruggeri, F. M., and Greenberg, H. B. (1991). Antibodies to the trypsin cleavage peptide VP8* neutralize rotavirus by inhibiting binding of virions to target cells in culture. *J. Virol.* **65**, 2211-2219.

- Ruigrok, R. W. H., Calder, L., and Wharton, S. A. (1989). Electron microscopy of the influenza virus submembranal structure. *Virology* **173**, 311-316.
- Ruigrok, R. W. H., Hirst, E. M. A., and Hay, A. J. (1991). The specific inhibition of influenza A virus maturation by amantadine: an electron microscopic examination. *J. Gen. Virol.* **72**, 191-194.
- Ruigrok, R. W. H., and Baudin, F. (1995). Structure of influenza virus ribonucleoprotein particles. II Purified RNA-free influenza virus ribonucleoprotein forms structures that are indistinguishable from the intact influenza ribonucleoprotein particles. *J. Gen. Virol.* **76**, 1009-1014.
- Russell, P. H. (1984). Newcastle disease virus: the effect of monoclonal antibody in the overlay on virus penetration and the immunoselection of variants. *J. Gen. Virol.* **65**, 795-798.
- Sahasrabudhe, A., Lawrence, L., Epa, V. C., Varghese, V. N., Colman, P. M., and McKimm-Breschkin, J. L. (1998). Substrate, inhibitor, or antibody stabilizes the Glu 119 Gly mutant influenza virus neuraminidase. *Virology* **247**, 14-21.
- Sanz-Ezquerro, J. J., de la Luna, S., Ortín, J., and Nieto, A. (1995). Individual expression of influenza virus PA gene induces degradation of coexpressed proteins. *J. Virol.* **69**, 2420-2426.
- Sanz-Ezquerro, J. J., Zürcher, T., de la Luna, S., Ortín, J., and Nieto, A. (1996). The amino terminal one-third of the influenza virus PA protein is responsible for the induction of proteolysis. *J. Virol.* **70**, 1905-1911.
- Sanz-Ezquerro, J. J., Fernández-Santarén, J., Sierra, T., Aragón, T., Ortega, J., Ortín, J., Smith, G. L., and Nieto, A. (1998). The PA influenza virus polymerase subunit is a phosphorylated protein. *J. Gen. Virol.* **79**, 471-478.
- Sato, S. B., Kawasaki, K., and Ohnishi, S.-I. (1983). Hemolytic activity of influenza virus hemagglutinin glycoproteins activated in mildly acidic environments. *Proc. Natl. Acad. Sci. USA* **80**, 3153-3157.
- Sattentau, Q. J., and Moore, J. P. (1991). Conformational changes induced in the human immunodeficiency virus glycoprotein by soluble CD4. *J. Exp. Med.* **174**, 407-415.
- Sattentau, Q. J., Moore, J.P., Vignaux, F., Traincard, F., Poignard, P. (1993). Conformational changes induced in the envelope glycoproteins of the human and simian immunodeficiency viruses by soluble receptor binding. *Virology* **67**, 7383-7393.
- Sauter, N. K., Bednarski, M. D., Wurzburg, B. A., Hanson, J. E., Whitesides, G. M., Skehel, J. J., and Wiley, D. C. (1989). Haemagglutinins from two influenza virus variants bind to sialic acid derivatives with millimolar dissociation constants: a 500-MHZ proton nuclear magnetic resonance study. *Biochem* **28**, 8388-8396.

- Scherle, P. A., Palladino, G., and Gerhard, W. (1992). Mice can recover from pulmonary influenza virus infection in the absence of class I-restricted cytotoxic cells. *J. Immunol.* **148**, 212-217.
- Schild, G. C. (1972). Evidence for a new type-specific structural antigen of the influenza virus particle. *J. Gen. Virol.* **15**, 99-103.
- Schoch, C., Blumenthal, R., and Clague, M. J. (1992). A long-lived fusion state for influenza virus-erythrocyte complexes committed to fusion at neutral pH. *FEBS Letts.* **311**, 221-225.
- Schofield, D. J. (1996) "Properties of influenza A virus-specific neutralising antibodies," Ph.D. Thesis, Dept. of Biological Sciences, Univ. of Warwick.
- Schofield, D. J., and Dimmock, N. J. (1996). Determination of affinities of a panel of IgGs and Fabs for an enveloped (influenza A) virus using surface plasmon resonance. *J. Virol. Meth.* **62**, 33-42.
- Schofield, D. J., Stephenson, J. R., and Dimmock, N. J. (1997a). High and low efficiency neutralization epitopes on the haemagglutinin of type A influenza virus. *J. Gen. Virol.* **78**, 2441-2446.
- Schofield, D. J., Stephenson, J. R., and Dimmock, N. J. (1997b). Variations in the neutralizing and haemagglutination-inhibiting activities of five influenza A virus-specific IgGs and their antibody fragments. *J. Gen. Virol.* **78**, 2431-2439.
- Scholtissek, C., van Hoyningen, V., and Rott, R. (1978a). Genetic relatedness between the new 1977 epidemic strains (H1N1) of influenza and human influenza strains isolated between 1947 and 1957 (H1N1). *Virol.* **89**, 613-617.
- Scholtissek, C., Rohde, W., von Hoyningen, V., and Rott, R. (1978b). On the origin of human influenza virus subtypes H2N2 and H3N2. *Virol.* **87**, 13-20.
- Scholtissek, C., Burger, H., Bachmann, P. A., and Hannoun, C. (1983). Genetic relatedness of haemagglutinins of the H1 subtype of influenza A viruses isolated from swine and birds. *Virol.* **129**, 521-523.
- Schroeder, C., Ford, C. M., Wharton, S. A., and Hay, A. J. (1994). Functional reconstitution of influenza virus M2 protein expressed by baculovirus: evidence for proton transfer activity. *J. Gen. Virol.* **75**, 3477-3484.
- Schulman, J. L., and Palese, P. (1977). Virulence factors of influenza viruses: WSN virus neuraminidase required for plaque production in MDBK cells. *J. Virol.* **24**, 170-176.
- Sha, B. D., and Luo, M. (1997). Structure and function of a bifunctional membrane: RNA-binding protein, influenza virus matrix protein M1. *Nature Struct. Biol.* **4**, 239-244.

- Shangguan, T., Siegel, D. P., Lear, J. D., Axelsen, P. H., Alford, D., and Bentz, J. (1998). Morphological changes and fusogenic activity of influenza virus haemagglutinin. *Biophys. J.* **74**, 54-62.
- Shapiro, G. I., Gurney, T., and Krug, R. M. (1987). Influenza virus genome expression: control mechanisms at early and late times of infection and nuclear-cytoplasmic transport of virus-specific RNAs. *J. Virol.* **61**, 764-773.
- Shapiro, and Krug (1988). Influenza virus RNA replication *in vitro*: synthesis of viral template RNAs and virion RNAs in the absence of added primer. *J. Virol.* **62**, 2285-.
- Shi, L. C., Galarza, J.M., and Summers, D.F. (1996). Recombinant-baculovirus-expressed PB2 subunit of the influenza A virus RNA polymerase binds cap groups as an isolated subunit. *Virus Res.* **42**, 1-9.
- Shimizu, K., Iguchi, A., Gomyou, R., and Ono, Y. (1999). Influenza virus inhibits cleavage of the pre-mRNAs at the polyadenylation site. *Virol.* **254**, 213-219.
- Shortridge, K. F., Zhou, N. N., Guan, Y., Gao, P., Ito, T., Kawaoka, Y., Kodihalli, S., Krauss, S., Markwell, D., Murti, K. G., Norwood, M., Senne, D., Sims, L., Takada, A., and Webster, R. G. (1998). Characterisation of avian H5N1 influenza viruses from poultry in Hong Kong. *Virol.* **252**, 331-342.
- Siegel, D. P. (1993). Energetics of intermediates in membrane fusion: comparison of stalk and inverted micellar intermediate mechanisms. *Biophys. J.* **65**, 2124-2140.
- Simons, K., and Garoff, H. (1980). The budding mechanisms of enveloped animal viruses. *J. Gen. Virol.* **50**, 1-21.
- Skehel, J. J., and Schild, G. C. (1971). The polypeptide composition of influenza A viruses. *Virol.* **44**, 396-408.
- Skehel, J. J. (1972). Polypeptide synthesis in influenza virus-infected cells. *Virol.* **49**, 23-36.
- Skehel, J. J. (1973). Early polypeptide synthesis in influenza virus-infected cells. *Virol.* **56**, 394-399.
- Skehel, J. J., Bayley, P. M., Brown, E. B., Martin, S. R., Waterfield, M. D., White, J. M., Wilson, I. A., and Wiley, D. C. (1982). Changes in the conformation of influenza virus hemagglutinin at the low pH optimum of virus-mediated membrane fusion. *Proc. Natl. Acad. Sci. USA* **79**, 968-972.
- Skehel, J. J., Stevens, D. J., Daniels, R. S., Douglas, A. R., Knossow, M., Wilson, I. A., and Wiley, D. C. (1984). A carbohydrate side chain on hemagglutinin of Hong Kong influenza virus inhibits recognition by a monoclonal antibody. *Proc. Natl. Acad. Sci. USA* **81**, 1779-1783.

- Spruce, A. E., Iwata, A., White, J. M., and Almers, W. (1989). Patch clamp studies of single cell-fusion events mediated by a viral fusion protein. *Nature (Lond.)* **342**, 555-558.
- Spruce, A. E., Iwata, A., and Almers, W. (1991). The first milliseconds of the pore formed by a fusogenic viral envelope protein during membrane fusion. *Proc. Natl. Acad. Sci. USA* **88**, 3623-3627.
- Staudt, L. M., and Gerhard, W. (1983). Generation of antibody diversity in the immune response of BALB/c mice to influenza virus hemagglutinin. I Significant variation in repertoire expression between individual mice. *J. Exp. Med.* **157**, 687-704.
- Stegmann, T., Doms, R. W., and Helenius, A. (1989). Protein-mediated membrane fusion. *Ann. Rev. Biophysics Biophys. Chem.* **18**, 187-211.
- Stegmann, T., White, J. M., and Helenius, A. (1990). Intermediates in influenza induced membrane fusion. *EMBO J.* **9**, 4231-4241.
- Stegmann, T., Delfino, J.M., Richards, F.M., Helenius, A. (1991). The HA2 subunit of influenza hemagglutinin inserts into the target membrane prior to fusion. *J. Biol. Chem.* **266**, 18404-18410.
- Stegmann, T. (1993). Influenza hemagglutinin-mediated membrane fusion does not involve inverted phase lipid intermediates. *J. Biol. Chem.* **268**, 1716-1722.
- Stegmann, T., and Helenius, A. (1993) Influenza virus fusion: from models towards a mechanism. In "Viral fusion mechanisms" (J. Bentz, Ed.), pp. 89-111. CRC Press: Boca Raton, Florida.
- Stegmann, T., Bartoldus, I., and Zumbunn, J. (1995). Influenza hemagglutinin-mediated fusion: influence of receptor binding on the lag phase preceding fusion. *Biochem* **34**, 1825-1832.
- Steineke-Gröber, A., Vey, M., Angliker, H., Shaw, E., Thomas, G., Roberts, C., Klenk, H.-D., and Garten, W. (1992). Influenza virus hemagglutinin with multibasic cleavage site is activated by furin, a subtilisin-like endoprotease. *EMBO J.* **11**, 2407-2414.
- Steinhauer, D. A. (1999). Role of hemagglutinin cleavage for the pathogenicity of influenza virus. *Viol.* **258**, 1-20.
- Subbarao, K., Klimov, A., Katz, J., Regnery, H., Lim, W., Hall, H., Perdue, M., Swayne, D., Bender, C., Huang, J., Hemphill, M., Rowe, T., Shaw, M., Xu, X., Fukuda, K., and Cox, N. (1998). Characterisation of an avian influenza A (H5N1) virus isolated from a child with a fatal respiratory illness. *Science* **279**, 393-396.
- Sugita, A., Yoshioka, Y., Itamura, S., Kanegae, Y., Oguchi, K., Gojobori, T., Nerome, K., and Oya, A. (1991). Molecular evolution of haemagglutinin genes of H1N1 swine and human influenza A viruses. *J. Mol. Evol.* **32**, 16-23.

- Sugrue, R. J., Bahadur, G., Zambon, M. C., Hall-Smith, M., Douglas, A. R., and Hay, A. J. (1990a). Specific structural alteration of the influenza haemagglutinin by amantadine. *EMBO J.* **9**, 3469-3476.
- Sugrue, R. J., Belshe, R. B., and Hay, A. J. (1990b). Palmitoylation of the influenza A virus M2 protein. *Viol.* **179**, 51-56.
- Suñé, C., Jiménez, G., Correa, I., Bullido, M. J., Gebauer, F., Smerdou, C., and Enjuanes, L. (1990). Mechanisms of transmissible gastroenteritis coronavirus neutralization. *Viol.* **177**, 559-569.
- Sweet, C., and Smith, H. (1980). Pathogenicity of influenza virus. *Microbiol. Rev.* **44**, 303-330.
- Tamura, M., Webster, R. G., and Ennis, F. A. (1991). Antibodies to HA and NA augment uptake of influenza A viruses into cells via Fc receptors. *Viol.* **182**, 211-219.
- Tashiro, M., and Rott, R. (1996). The role of proteolytic cleavage of viral glycoproteins in the pathogenesis of influenza virus infections. *Sem. Virol.* **7**, 237-243.
- Tatulian, S. A., Hinterdorfer, P., Baber, G., and Tamm, L. K. (1995). Influenza hemagglutinin assumes a tilted conformation during membrane fusion as determined by attenuated total reflection FTIR spectroscopy. *EMBO J.* **14**, 5514-5523.
- Tatulian, S. A., and Tamm, L. K. (1996). Reversible pH-dependent conformational change of reconstituted influenza hemagglutinin. *J. Mol. Biol.* **260**, 312-316.
- Taylor, H. P., and Dimmock, N. J. (1985a). Mechanism of neutralization of influenza virus by secretory IgA is different from that of monomeric IgA or IgG. *J. Exp. Med.* **161**, 198-209.
- Taylor, H. P., and Dimmock, N. J. (1985b). Mechanisms of neutralization of influenza virus by IgM. *J. Gen. Virol.* **66**, 903-907.
- Taylor, H. P., Armstrong, S. J., and Dimmock, N. J. (1987). Quantitative relationships between an influenza virus and neutralizing antibody. *Viol.* **159**, 288-298.
- Tiffany, J. M., and Blough, H. A. (1970). Estimation of the number of surface projections on myxo- and paramyxoviruses. *Viol.* **41**, 392-394.
- Topham, D. J., Tripp, R. A., Hamilton-Easton, A. M., Sarawar, S. R., and Doherty, P. C. (1996a). Quantitative analysis of the influenza virus-specific CD4+ T cell memory in the absence of B cells and Ig. *J. Immunol.* **157**, 2947-2952.
- Topham, D. J., Tripp, R. A., Sarawar, S. R., Sangster, M. Y., and Doherty, P. C. (1996b). Immune CD4+ T cells promote the clearance of influenza virus from major histocompatibility complex class II -/- respiratory epithelium. *J. Virol.* **70**, 1288-1291.

- Toyoda, T., Kobayashi, M., and Ishihama, A. (1996). Molecular dissection of influenza virus RNA polymerase PB1 subunit alone is able to catalyze RNA synthesis. *Virus Genes* **12**, 155-163.
- Tse, F. W., Iwata, A., and Almers, W. (1993). Membrane flux through the pore formed by a fusogenic viral envelope protein during cell fusion. *J. Cell Biol.* **121**, 543-552.
- Tsurudome, M., Glück, R., Graf, R., Falchetto, R., Schaller, U., and Brunner, J. (1992). Lipid interactions of the haemagglutinin HA2 NH2-terminal segment during influenza virus-induced membrane fusion. *J. Biol. Chem.* **267**, 20225-20232.
- Ugolini, S., Mondor, I., Parren, P. W. H. I., Burton, D. R., Tilley, S. A., Klasse, P. J., and Sattentau, Q. J. (1997). Inhibition of virus attachment to CD4+ target cells is a major mechanism of T cell line-adapted HIV-1 neutralization. *J. Exp. Med.* **186**, 1287-1298.
- Ulmanen, I., Broni, B., and Krug, R. M. (1981). Role of two of the influenza virus core P proteins in recognising cap 1 structures (m7GpppNm) on RNAs and in initiating viral RNA transcription. *Proc. Natl. Acad. Sci. USA* **78**, 7355-7359.
- Ulmanen, I., Broni, B. A., and Krug, R. M. (1983). Influenza virus temperature-sensitive cap (m7GpppNm)-dependent endonuclease. *J. Virol.* **45**, 27-35.
- Underdown, B. J., and Schiff, J. N. (1987). Immunoglobulin A: strategic defence initiative at the mucosal surface. *Ann. Rev. Immunol.* **4**, 389-417.
- Varghese, J. N., Laver, W. G., and Colman, P. M. (1983). Structure of the influenza virus glycoprotein antigen neuraminidase at 2.9Å resolution. *Nature (Lond.)* **303**, 35-40.
- Varghese, J. N., Epa, V.C., Colman, P.M. (1995). Three-dimensional structure of the complex of 4-guadino-NeuSAc2en and influenza virus neuraminidase. *Protein. Sci.* **4**, 1081-1087.
- Vey, M., Orlich, M., Adler, S., Klenk, H. D., Rott, R., and Garten, W. (1992). Hemagglutinin activation of pathogenic avian influenza viruses of serotype H7 requires the protease recognition motif R-X-K/R-R. *Virol.* **188**, 408-413.
- Viitala, J., and Järnefelt, J. (1985). The red cell surface revisited. *TIBS* **10**, 392-395.
- Vogle, U., Kunerl, M., and Scholtissek, C. (1994). Influenza A virus late mRNAs are specifically retained in the nucleus in the presence of a methyltransferase or a protein kinase inhibitor. *Virol.* **198**, 227-233.
- von Itzstein, M., Wu, W. Y., Kok, G. B., Pegg, M. S., Dyason, J. C., Jin, B., Phan, T. V., Smythe, M. L., White, H. F., Oliver, S. W., Colman, P. M., Varghese, J. N., Ryan, D. M., Woods, J. M., Bethell, R. C., Hotham, V. J., Cameron, J. M., and Penn, C. R. (1993). Rational design of potent sialidase-based inhibitors of influenza virus replication. *Nature (Lond.)* **363**, 418-423.

- Vrijzen, R., Mosser, A., and Boeyé, A. (1993). Postadsorption neutralization of poliovirus. *J. Virol.* **67**, 3126-3133.
- Wagner, D. K., Clements, D. L., and Murphy, B. R. (1987). Analysis of immunoglobulin responses after administration of live and inactivated influenza A vaccine indicates that nasal wash immunoglobulin G is a transudate from serum. *J. Clin. Microbiol.* **25**, 559-562.
- Wakefield, L., and Brownlee, G. G. (1989). RNA-binding properties of influenza virus matrix protein M1. *Nucl. Acids Res.* **17**, 8569-8580.
- Wang, C., Lamb, R. A., and Pinto, L. H. (1994). Direct measurement of the influenza A virus M2 protein ion channel activity in mammalian cells. *Virology* **205**, 133-140.
- Wang, E., Wolf, B. A., Lamb, R. A., Choppin, P. W., and Goldberg, A. R. (1976) The presence of actin in enveloped viruses. In "Cold Spring Harbor Symposium on Cell Motility" (R. Goldman, T. Pollard, and J. Rosenbaum, Eds.), Vol. 3, pp. 589-598. Cold Spring Harbor Laboratory: Cold Spring Harbor, N.Y.
- Wang, M.-L., Skehel, J. J., and Wiley, D. C. (1986). Comparative analyses of the specificities of anti-influenza hemagglutinin antibodies in human sera. *J. Virol.* **57**, 124-128.
- Wang, P., Palese, P., and O'Neill, R. E. (1997). The NPI/NPI-3 (karyopherin α) binding site on the influenza A virus nucleoprotein NP is a nonconventional nuclear localization signal. *J. Virol.* **71**, 1850-1856.
- Weber, F., Kochs, G., Gruber, S., and Haller, O. (1998). A classical bipartite nuclear localisation signal on Thogoto and influenza A virus nucleoproteins. *Virology* **250**, 9-18.
- Weber, T., Paesold, G., Mischler, R., Semenza, G., and Brunner, J. (1994). Evidence for H⁺-induced insertion of influenza HA2 N-terminal segment into viral membrane. *J. Biol. Chem.* **269**, 18353-18358.
- Webster, R. G., Campbell, C. H., and Granoff, A. (1971). The *in vivo* production of 'new' influenza viruses. I Genetic recombination between avian and mammalian viruses. *Virology* **44**, 317-328.
- Webster, R. G., and Laver, W. G. (1980). Determination of the number of nonoverlapping antigenic areas on Hong Kong (H3N2) influenza virus hemagglutinin with monoclonal antibodies and the selection of variants with potential epidemiological significance. *Virology* **104**, 139-148.
- Webster, R. G., Laver, W. G., Air, G. M., and Schild, G. C. (1982). Molecular mechanisms of variation in influenza viruses. *Nature (Lond.)* **296**, 115-121.
- Webster, R. G., Brown, L. E., and Laver, W. G. (1984). Antigenic and biological characterization of influenza virus neuraminidase (N2) with monoclonal antibodies. *Virology* **135**, 30-42.

- Webster, R. G., and Rott, R. (1987). Influenza virus A pathology: the pivotal role of the haemagglutinin. *Cell* **50**, 665-666.
- Webster, R. G., Bean, W. J., Gorman, O. T., Chambers, T. M., and Kawaoka, Y. (1992). Evolution and ecology of influenza A viruses. *Microbiol. Rev.* **56**, 152-179.
- Webster, R. G. (1998). Influenza : An emerging disease. **4 (Special issue)**, 436-441.
- Weis, W., Brown, J. H., Cusack, S., Paulson, J. C., Skehel, J. J., and Wiley, D. C. (1988). Structure of the influenza haemagglutinin complexed with its receptor, sialic acid. *Nature (Lond.)* **333**, 426-431.
- Wells, M. A., Albrecht, P., and Ennis, F. A. (1981). Recovery from a viral respiratory tract infection. I Influenza pneumonia in normal and T cell-deficient mice. *J. Immunol.* **126**, 1036-1041.
- Wharton, S. A., Skehel, J. J., and Wiley, D. C. (1986). Studies of influenza virus hemagglutinin-mediated membrane fusion. *Viol.* **149**, 27-35.
- Wharton, S. A., Belshe, R. B., Skehel, J. J., and Hay, A. J. (1994). Role of virion M2 protein in influenza virus uncoating: specific reduction in the rate of membrane fusion between virus and liposomes by amantadine. *J. Gen. Virol.* **75**, 945-948.
- Wharton, S., Calder, L. J., Ruigrok, R. W. H., Skehel, J. J., Steinhauer, D. A., and Wiley, D. C. (1995). Electron microscopy of antibody complexes of influenza virus haemagglutinin in the fused pH conformation. *EMBO J.* **14**, 240-246.
- White, J., Kartenbeck, J., and Helenius, A. (1982a). Membrane fusion activity of influenza virus. *EMBO J.* **1**, 217-222.
- White, J., and Wilson, I. A. (1987). Anti-peptide antibodies detect steps in a protein conformational change: low pH activation of the influenza virus hemagglutinin. *J. Cell Biol.* **105**, 2887-2896.
- Whittaker, G., Kemler, I., and Helenius, A. (1995). Hyperphosphorylation of mutant virus matrix protein, M1, causes its retention in the nucleus. *J. Virol.* **69**, 439-445.
- Whittaker, G., Bui, M., and Helenius, A. (1996). Nuclear trafficking of influenza virus ribonucleoproteins in heterokaryons. *J. Virol.* **70**, 2743-2756.
- WHO Memorandum (1980). A revision of the system of nomenclature for influenza viruses. *Bull. WHO* **58**, 585-591.
- Wiley, D. C., Skehel, J. J., and Waterfield, M. (1977). Evidence from studies with a chemical cross-linking reagent that the haemagglutinin of influenza virus is a trimer. *Viol.* **79**, 446-448.
- Wiley, D. C., Wilson, I. A., and Skehel, J. J. (1981). Structural identification of the antibody-binding sites of Hong Kong influenza haemagglutinin and their involvement in antigenic variation. *Nature (Lond.)* **289**, 373-378.

- Wiley, D. C., and Skehel, J. J. (1987). The structure and function of the hemagglutinin membrane glycoprotein of influenza virus. *Ann. Rev. Biochem.* **56**, 365-394.
- Wilson, I. A., Skehel, J. J., and Wiley, D. C. (1981). Structure of the haemagglutinin membrane protein of influenza virus at 3 Å resolution. *Nature (Lond.)* **289**, 366-373.
- Wilson, I. A., and Cox, N. J. (1990). Structural basis of immune recognition of influenza virus hemagglutinin. *Ann. Rev. Immunol.* **8**, 737-771.
- Wilson, I. A., and Stanfield, R. L. (1993). Antibody-antigen interactions. *Current Opinion in Structural Biology* **3**, 113-118.
- Winter, G., Field, S., and Brownlee, G. G. (1981). Nucleotide sequence of the haemagglutinin gene of influenza virus H1 subtype. *Nature (Lond.)* **292**, 72-75.
- Wohlfart, C. (1988). Neutralization of adenoviruses : kinetics, stoichiometry and mechanisms. *J. Virol.* **62**, 2321-2328.
- Wolff, T., O'Neill, R. E., and Palese, P. (1998). NS1-binding protein (NS1-BP): a novel human protein that interacts with the influenza A virus nonstructural NS1 protein is relocalized in the nuclei of infected cells. *J. Virol.* **72**, 7170-7180.
- Wrigley, N. G. (1979). Electron microscopy of influenza virus. *Brit. Med. Bull.* **35**, 35-38.
- Wunderli-Allenspach, H., Günthert, M., and Ott, S. (1993). Inactivation of PR8 influenza virus through the octadecylrhodamine B chloride membrane marker. *Biochem* **32**, 900-907.
- Yasuda, J., Nakada, S., Kato, A., Toyoda, T., and Ishihama, A. (1993). Molecular assembly of influenza virus: association of the NS2 protein with virion matrix. *Virol.* **196**, 249-255.
- Ye, Z., Baylor, N. W., and Wagner, R. R. (1989). Transcription-inhibition and RNA-binding domains of influenza A virus matrix protein mapped with anti-idiotypic antibodies and synthetic peptides. *J. Virol.* **63**, 3586-3594.
- Yewdell, J. W., Webster, R. G., and Gerhard, W. U. (1979). Antigenic variation in three distinct determinants of an influenza type A haemagglutinin molecule. *Nature (Lond.)* **279**, 246-248.
- Yewdell, J. W., Gerhard, W., and Bächli, T. (1983). Monoclonal anti-hemagglutinin antibodies that detect irreversible alterations that coincide with the acid activation of influenza virus A/PR/8/34-mediated hemolysis. *J. Virol.* **48**, 239-248.
- Yoden, S., Kida, H., and Yanagawa, R. (1985). Is bivalent binding of monoclonal antibodies to different antigenic areas on the hemagglutinin of influenza virus required for neutralization of viral infectivity? *Arch. Virol.* **85**, 209-216.

- Yoden, S., Kida, H., Kuwabara, M., and Webster, R. G. (1986). Spin-labelling of influenza virus hemagglutinin permits analysis of the conformational change at low pH and its inhibition by antibody. *Virus Res.* **4**, 251-261.
- Yoshimori, T., Yamamoto, A., Moriyama, Y., Futai, M., and Tashiro, Y. (1991). Bafilomycin A1, a specific inhibitor of vacuolar-type H⁺-ATPase, inhibits acidification and protein degradation in lysosomes of cultured cells. *J. Biol. Chem.* **266**, 17707-17712.
- Yoshimura, A., Kuroda, K., Kawasaki, K., Yamashina, S., Maeda, T., and Ohnishi, S.-I. (1982). Infectious cell entry mechanism of influenza virus. *J. Virol.* **43**, 284-293.
- Zebedee, S. L., and Lamb, R. A. (1988). Influenza A virus M2 protein: monoclonal antibody restriction of virus growth and detection of M2 in virions. *J. Virol.* **62**, 2762-2772.
- Zhang, J., and Lamb, R. A. (1996). Characterization of the membrane association of the influenza virus matrix protein in living cells. *Virology* **225**, 255-266.
- Zheng, H., Lee, H. A., Palese, P., and García-Sastre, A. (1999). Influenza A virus RNA polymerase has the ability to stutter at the polyadenylation site of a viral RNA template during RNA replication. *J. Virol.* **73**, 5240-5243.
- Zhirnov, O. P. (1990). Solubilization of matrix protein M1/M from virions occurs at different pH for orthomyxo- and paramyxoviruses. *Virology* **176**, 274-279.
- Zhou, Y., König, M., Hobom, G., and Neumeier, E. (1998). Membrane-anchored incorporation of a foreign protein in recombinant influenza virions. *Virology* **246**, 83-94.
- Zimmerberg, J., Blumenthal, R., Curran, M., Sarkar, D., and Morris, S. (1994). Restricted movement of lipid and aqueous dyes through pores formed by influenza hemagglutinin during fusion. *J. Cell Biol.* **127**, 1885-1894.
- Zvonarjev, A. Y., and Ghendon, Y. Z. (1980). Influence of a membrane (M) protein on influenza A virus transcriptase *in vitro* and its susceptibility to rimantadine. *J. Virol.* **33**, 583-586.